

IGNEOUS AND METAMORPHIC GEOCHEMISTRY
OF MULL LAVAS

by

Marjorie Ann Morrison

A thesis submitted for the degree of
Doctor of Philosophy in the University of London

Department of Geology,
Imperial College of Science and Technology,
Prince Consort Road,
London S.W.7.
1979.

"Rocks, like everything else, are subject to change
and so also are our views on them".

F.Y. Loewinson-Lessing, 1936.

ABSTRACT

Multiple samples from individual, Tertiary, Mull lava flows have been analysed in order to assess the contributions of magmatic, deuteric and metasomatic processes to their compositions. With the exception of Sr, which shows limited mobility, the compositions of the lavas affected by zeolite-facies alteration appear to be pyrogenic. Local greenschist-facies alteration caused considerable bulk chemical changes but, Ti, Zr, Nb, Y, Ta, Hf and the HREE appear to have been immobile. Slight loss of P, Th, La and Ce occurred during extreme metasomatism.

The hydrothermal fluids appear to have had low $^{87}\text{Sr}/^{86}\text{Sr}$ ratios (≤ 0.7048), which rules out interaction with either, the Moinian basement or, the Tertiary plutonic rocks. Instead, the compositions of the fluids appear to have been buffered by the lavas. A model for the Mull geothermal system is presented and comparisons are made with metabasalts from other hydrothermal systems in order to elucidate the factors that control element mobility during alteration.

Comparison of the Mull lavas with those formed at other igneous centres confirms the existence of several distinct, basaltic magma types on a regional scale within the British Tertiary Igneous Province. The early major products of volcanicity were transitional basic lavas, similar in their major element chemistry to world-wide alkali basalt series. In contrast, their incompatible trace element contents bear more resemblance to olivine tholeiites and there are small but distinct differences in the relative abundances of these in the early Mull and Skye lavas.

The incompatible element abundances in the Mull and Skye lavas suggest a mantle source from which a small amount of melt ($<1\%$?) had been extracted, with the pre-Tertiary upper-mantle fusion beneath Mull slightly greater than beneath Skye. Chemical and tectonic considerations suggest this mantle was neither residual from the formation of the Archaean Lewisian complex nor, emplaced as a result of the Cenozoic rifting of the N. Atlantic. Major and trace element data for a mafic alkalic dyke of the Permian swarms which cross W. Scotland show that these had the requisite geochemical characteristics to have caused this depletion. Such dykes are more abundant in the region of Mull than Skye.

ACKNOWLEDGEMENTS

I am indebted to my supervisor, Dr. R.N. Thompson, for much helpful advice and critical encouragement throughout the course of this work.

I am grateful to the people of Mull for their kindness and hospitality during field work on the island, and in particular to Mr. and Mrs. Cattanach for delivering my samples to the Oban Ferry. Dr. R.R. Skelhorn of the City of London Polytechnic gave advice on sample localities.

Drilling of the Mull lavas was only made possible by the unremitting hard work of Dr. R.N. Thompson and Mr. D. Gidden of Imperial College, who provided most of the very necessary hard labour on site and also conveyed the equipment to and from the island. The successful recovery of the drill core represented a considerable triumph of mind over matter (and weather) on the part of all those involved. Grateful thanks are also due to Professor W.S. Mackenzie of Manchester University for making the drilling equipment available, to Mr. C. Guilford for instruction in its operation and maintenance, to the Wimpey Construction Company for the loan of core boxes, to the Department of Agriculture and Fisheries in Oban for permission to drill in Pennygown quarry and to Mr. P. Taylor for assistance in transporting the drill to the island. Considerable thanks are also due to Mr. and Mrs. M. Cooper who donated the Staffa lava sample and to Miss. L. Christie and Miss. N. Ray for collecting the Arran crinanite sample.

The E.D.S. microprobe at the Department of Mineralogy and Petrology, Cambridge University was used for the mineral analyses. This facility was kindly made available by Drs. N. Charnley and J. Long who also provided technical advice. The Sr-isotope analyses were made at the Department of Earth Sciences, Leeds University in cooperation with Dr. C.J. Hawkesworth. The rare earth element analyses and many of the trace element analyses were carried out in the Department of Geology, Bedford College. I should like to thank Dr. J.L. Gibson for making analytical facilities available and Dr. G.F. Marriner and Mr. H. Lloyd for much helpful advice and assistance in the laboratory. The remainder of the analytical work was carried out at Imperial College. The advice of Dr. G.D. Borley, Dr. R.J. Parker, Mr. P. Watkins, Mr. G. Bullen,

Dr. R.D.F. Kinghorn and Mr. M. Rahman on various aspects of this is gratefully acknowledged.

Thanks are also due to Miss. N. Hartopp for typing the manuscript and correcting numerous grammatical errors. Many of the data tables were typed by Miss. M. Jones,

This research was supported by a Natural Environment Research Council Studentship. Part of the work was presented at the IASPEI/ IAVCEI meeting in Durham, 1977. Financial support for this and for the drilling operations in Mull was provided jointly by the N.E.R.C. and Imperial College. Professor J. Sutton and Dr. G. Thomas made the financial arrangements at Imperial College.

Contents

ABSTRACT	1
ACKNOWLEDGEMENTS	2
List of Contents	4
List of Figures	7
List of Tables	10
CHAPTER ONE : GENERAL INTRODUCTION	11
1. Geological :summary of area and previous research	11
Pre-Tertiary geology	11
The Tertiary lava pile	13
Secondary alteration of the lavas	16
Timing of igneous and metamorphic events in Mull	22
Previous geochemical studies	23
2. Field relations and sample selection	27
Zeolite-facies lavas	27
Greenschist-facies lavas	28
Drill-hole in Pennygown Quarry	32
Other samples	36
CHAPTER TWO : ZEOLITE-FACIES LAVAS	37
1. Petrography	37
Magnesian basalts, LA13-15, LA16-18, LA20	39
M51-55, less-magnesian basalt	40
M1, less-magnesian basalt	41
LA7-11, less-magnesian basalt	44
M11-12, less-magnesian basalt	42
LA1-5, basaltic hawaiite	42
M5-8, hawaiite	45
2. Processes causing primary or deuteric alteration	45
Phenocryst growth and accumulation	45
Filter-pressing of residual liquids	47
3. Distribution of the secondary minerals	50
4. Intra-lava chemical variation	54
5. Copper and zinc distribution	60
6. Effects of zeolite-facies alteration on Si-saturation	63
Conclusions to chapter two	66
CHAPTER THREE: GREENSCHIST-FACIES LAVAS	68
1. Mineral transformations during greenschist-facies alteration	68
Olivine	70
Plagioclase and titanomagnetite	71

Pyroxene	77
Other phases	78
2. Vesicles, secondary mineral pods and veins	79
3. Intra-lava chemical variation	87
Mobile and immobile elements	87
Changes in oxidation state and volatile content	100
Effects of hydrothermal alteration on $^{87}\text{Sr}/^{86}\text{Sr}$ ratios	103
4. Mass balances during hydrothermal alteration	107
Major elements	107
Trace elements	117
Conclusions to chapter three	118
CHAPTER FOUR : RECONSTRUCTION OF THE MULL HYDROTHERMAL SYSTEM	120
1. Thermal gradients and water/rock ratios	120
Evidence from O-isotope studies	120
Evidence from mineral stability relationships	124
2. A hydrothermal-convection model for the Mull geothermal system	126
CHAPTER FIVE : COMPARISONS WITH ALTERED BASALTS FROM OTHER HYDROTHERMAL SYSTEMS	132
1. Eastern Iceland	132
Reykjanes flow	133
Reydarfjordur flow	133
2. Mid-Atlantic Ridge basalts	135
3. The Bhoiwada and Cliefden Outcrops	136
4. Controls on element mobility during alteration	140
5. Other Tertiary Hebridean magma types	146
CHAPTER SIX : REGIONAL GEOCHEMICAL VARIATION IN THE BRITISH TERTIARY IGNEOUS PROVINCE	150
1. Distribution of magma types within the province	152
The Skye Main Lava Series and the Mull Plateau Group	152
Skye Preshal Mhor and Mull low-alkali tholeiite basalts	161
Other magma types	163
2. Lateral heterogeneity in the Palaeocene upper-mantle beneath the Scottish Hebrides	164
Differences between Tertiary Hebridean and world-wide alkali basalts	165
Differences between the alkali basalt suites of Skye, Mull and Arran	167
3. Provenance and pre-Palaeocene chemical history of the upper- mantle beneath the British Tertiary Igneous Province	173
Permian-Tertiary basic magmatism in western Scotland	175

4. The relationship between the Tertiary igneous activity in Britain and the N. Atlantic	178
REFERENCES	181
APPENDIX I : DATA	199
I-A Sample localities	200
I-B Drill-core log	205
I-C Modal analyses	209
I-D Microprobe analyses	212
I-E Chemical analyses and C.I.P.W. Norms.	235
I-F Density data	247
APPENDIX II : ANALYTICAL TECHNIQUES	249
Sampling and sample preparation	250
Major element analyses	252
Volatile determinations	257
Trace element analyses	259
Instrumental Neutron Activation Analysis (INAA)	260
Microprobe analysis	266
Density determinations	269

List of Figures

1-1	The British Tertiary Igneous Province	12
1-2	Structural map of Mull and Morvern	15
1-3	Amygdale mineral zones of Mull and Morvern	18
1-4	Variation of $\delta^{18}\text{O}$ in the basalts with distance from the central intrusive complex	20
1-5	$\delta^{18}\text{O}$ versus age of intrusion for the plutonic rocks	20
1-6	Distribution of laumontite in the Mull lava pile	21
1-7	Veins cutting mottled lava, Pennygown Quarry	29
1-8	Mottled lava, Pennygown Quarry	29
1-9	Plan of Pennygown Quarry	30
1-10	Hydrothermally brecciated lava, Toll Doire Quarry	33
1-11	Drilling in Pennygown Quarry	33
1-12	Mottled lavas from four different flows	35
1-13	Igneous and hydrothermal breccias	35
1-14	Pyritised dyke, Pennygown Quarry	36
2-1	Magnesian basalt, LA15	43
2-2	Basaltic hawaiite, LA5	43
2-3	Hawaiite, M7	44
2-4	Altered vesicle margin from flow LA1-5	44
2-5	Altered vesicle margin, M56	49
2-6	Compositions in molar proportions of the Ca-rich zeolites and other CaAl hydrosilicates	52
2-7	$\text{Fe}_2\text{O}_3/\text{FeO}$ and MgO versus H_2O for the zeolite-facies lavas	55
2-8	Ca and Sr versus H_2O for the zeolite-facies lavas	56
2-9	Pyroxenes in the zeolite-facies lavas	59
2-10	Chondrite-normalised, rare earth patterns for M51, M53 and M56ZR	59
2-11	Cu versus Zn for the zeolite-facies lavas	61
2-12	Normative diopside-hypersthene-olivine-nepheline/quartz for the zeolite-facies lavas	65
3-1	Principal mineral transformations during greenschist-facies alteration	70
3-2	Pennygown Quarry lava-M21	72
3-3	Pennygown Quarry lava-M18	72
3-4	Pennygown Quarry lava-M16	73
3-5	Pennygown Quarry lava-M14	73
3-6	Pennygown Quarry lava-M13	74
3-7	Intensely altered basalt- M29	74
3-8	Calcite replacing plagioclase in C232a/b	76

3-9	Sediment layers infilling vesicle in M45	76
3-10	Types of vesicle infilling	80
3-11	Albite, quartz, epidote and amphibole infilling vesicle in C153	80
3-12	Secondary mineral pod in M15	82
3-13	Secondary mineral pod in M16	82
3-14	Chlorite-filled secondary mineral pod in C199	83
3-15	Chlorite-filled secondary mineral pod in M26	83
3-16	Calcite-stilbite vein	86
3-17	Laumontite-calcite-quartz vein	86
3-18	Mineralogical changes across the Pennygown Quarry lava section, M13-22	88
3-19	Chemical changes across M13-22	89
3-20	Chemical changes across the drill-core section across the Pennygown Quarry lava, C54-158	90
3-21	Chemical changes across the lower flow in the drill-core, C191-232a/b	91
3-22	Selected chondrite-normalised, rare earth pattern from M13-22	96
3-23	Chondrite-normalised, rare earth patterns from C191-232a/b	97
3-24	$\text{Fe}_2\text{O}_3/\text{FeO}$ versus H_2O for the greenschist-facies lavas	100
3-25	X-ray diffractogram showing the effects of leaching in HCl	105
3-26	SiO_2 versus Al_2O_3 for the Mull Plateau lavas	109
3-27	Distribution of the Plateau lavas on ACF and AFM diagrams	110
3-28	Distribution of the Plateau lavas on $\text{TiO}_2\text{-K}_2\text{O-P}_2\text{O}_5$ diagrams	111
3-29	Gains and losses in M13-22 during alteration	114
3-30	Normative diopside-hypersthene-olivine-nepheline/quartz-corundum in the greenschist-facies lavas	116
4-1	Alteration zones in the low-temperature geothermal areas, Iceland	122
4-2	Alteration zones in the high-temperature geothermal areas, Iceland	123
4-3	Isotherm and flow-line distributions in the Wairakei geothermal system	123
5-1	Major and trace element variations across recent and zeolitised lava flows, Iceland	134
5-2	Mass fluxes resulting from alteration of Mid-Atlantic Ridge pillow basalts	136
5-3	Chondrite-normalised, rare earth patterns for Mid-Atlantic Ridge pillow basalts	137
5-4	Chondrite-normalised, rare earth patterns for the Bhoiwada and Cliefden outcrops	139

5-5	M61, Macculloch's tree lava	147
6-1	Distribution of the various Hebridean magma types on the trace element diagrams of Floyd and Winchester (1975)	153
6-2	Distribution of the various Hebridean magma types on the trace element diagrams of Pearce and Cann (1973)	154
6-3	Distribution of the various Hebridean magma types on the $TiO_2-K_2O-P_2O_5$ diagram	155
6-4	Normative diopside-hypersthene-olivine-nepheline/quartz in basic lavas and pyroclastics from Mull and Skye	156
6-5	Sr versus $(^{87}Sr/^{86}Sr)_i$ for Mull lavas	157
6-6	Y versus Zr for the Skye Main Lava Series and the Mull Plateau Group	159
6-7	Comparison of incompatible element abundances in SMLS basalt and other lavas	166
6-8	Nb, P_2O_5 , TiO_2 and Y versus F/F+M for Palaeocene Hebridean basic rocks	169
6-9	Chondrite-normalised, rare earth patterns for SMLS and MPG basalts	170
AII-1	Ta versus Nb for the Mull lavas	258

List of Tables

1-1	Generalised Mull lava succession	14
2-1	Classification of the zeolitised lavas	38
2-2	Intra-lava variations in two magnesian basalt flows	47
2-3	X-ray data for vesicle infillings in M56 and LA19	53
2-4	Fe ₂ O ₃ contents of basalt glasses	63
2-5	Si-saturation in the zeolitised lavas	64
3-1	Mineralogy and textures of the greenschist-facies lavas	69
3-2	Correlation matrix for 15 elements in M13-22	94
3-3	Correlation matrix for 13 elements in C191-232a/b	95
3-4	Selected rare earth and trace element data for M13-22	96
3-5	Selected rare earth and trace element data for C191-232a/b	97
3-6	Rb-Sr results	104
4-1	Temperatures and water/rock ratios in the Skye hydrothermal system	122
5-1	Selected rare earth and trace element data for Mid-Atlantic Ridge basalts	137
6-1	Incompatible element abundances in Skye, Mull and Arran hawaiites	171
AII-1	Major element analyses of U.S.G.S. standard rocks	253
AII-2	Replicate major element analyses of samples using different techniques	254
AII-3	Major element analyses, figures for precision	255
AII-4	FeO, Na ₂ O determinations for standard rocks	256
AII-5	Na ₂ O determinations, figures for precision	256
AII-6	Volatile determinations	257
AII-7	Trace element analyses of standard rocks-Bedford College	261
AII-8	Trace element analyses, Bedford, figures for precision	262
AII-9	Trace element analyses of standard rocks-Imperial College	263
AII-10	Trace element analyses, Imperial, figures for precision	264
AII-11	Comparison of trace element analyses at Bedford and Imperial	264
AII-12	INAA, figures for accuracy and precision	265
AII-13	Multiple analyses of olivine probe standard	267
AII-14	Multiple analyses of jadeite probe standard	268
AII-15	Multiple analyses of Elba pyrite probe standard	268
AII-16	Density determinations for pure quartz	269

CHAPTER ONE : GENERAL INTRODUCTION

The Tertiary igneous rocks of Britain have been the subject of systematic geological investigation since the nineteenth century. The lavas of Mull are probably the most renowned, as the Mull Memoir (Bailey et.al. 1924) introduced the concepts of magma types and series; a method of comprehending igneous rocks that has remained central to petrogenetic thinking. The reputation of Hebridean lavas for being hydrothermally altered provided a considerable obstacle to their chemical study for some time. Subsequent workers described the lavas in terms of the two main basalt types recognised in the Mull Memoir - the Plateau and Non - Porphyritic Central types - and in one form or another these dominated petrogenetic ideas in the region for nearly four decades. Much recent research activity has arisen as a result of improved analytical methods and recognition that the widespread volcanism was related to the opening of the North Atlantic between the Faroe Rise and Greenland. Several new magma types have been defined on the basis of abundant chemical data but the distribution of these within the province and the extent to which they can be held to characterise it are uncertain. Relatively few new analyses of the Mull lavas have been published and as yet little attempt has been made to investigate the effects of the widespread secondary alteration on Hebridean basalts. The main objectives of this present study are : firstly, to identify the igneous and metasomatic contributions to the present compositions of the Mull lavas; secondly, using those chemical characteristics that can be considered to represent magmatic features, to compare them with lavas formed at the other Tertiary centres at an equivalent stage in their evolution. Geophysical studies of the region have been summarised recently by Bullerwell (1972) and the relationships between the igneous and tectonic activity have been reviewed by Macintyre et. al. (1975) and Bell (1976).

1. Geological summary of area and previous research.Pre - Tertiary geology

Mull lies astride the Great Glen fault and to the east of the Moine thrust which is thought to pass between Iona and the Ross of

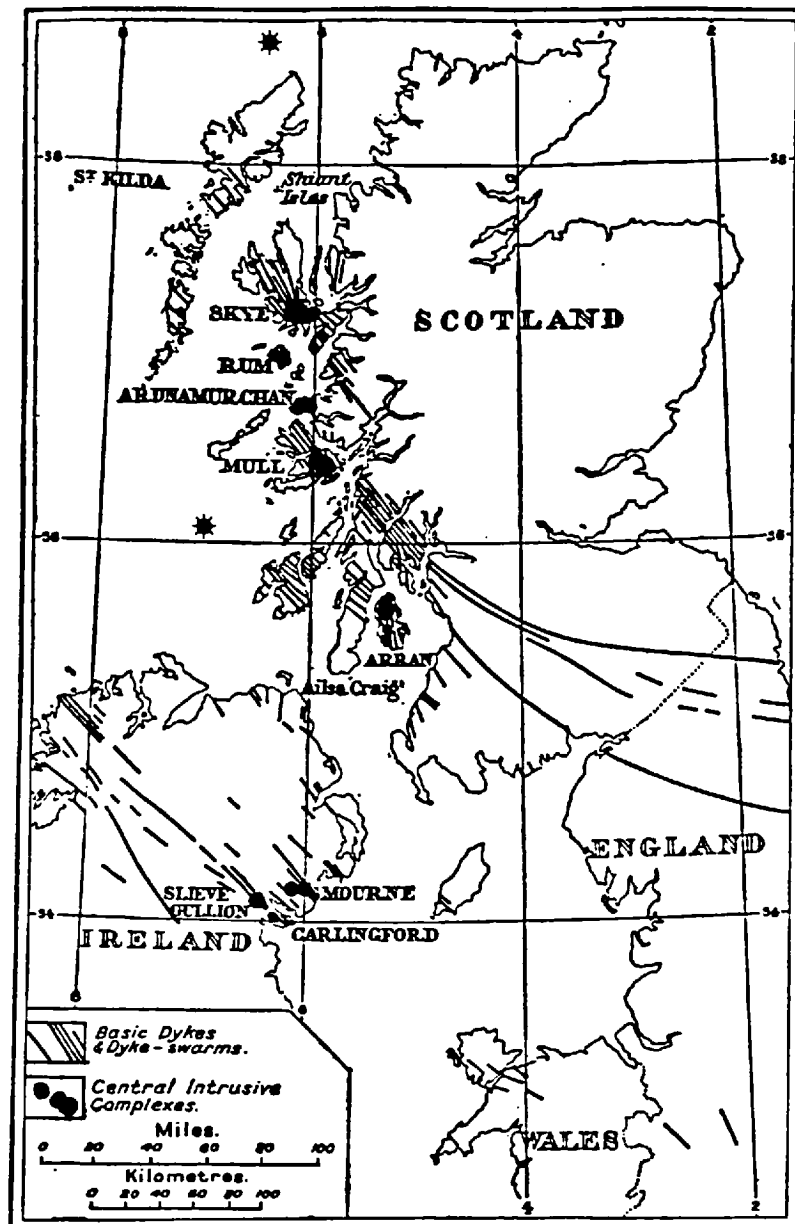


Figure 1 - 1. The British Tertiary Igneous Province
(after Richey 1961).

The stars show the Blackstones and Outer Roag centres discovered by geophysical studies. (Bullerwell 1972).

Mull. The Great Glen fault represents a line of crustal weakness that almost certainly played a part in controlling the position of the Mull igneous centre and minor displacements continued to occur along it at least until Tertiary times (Lee and Bailey 1925). The close association of these two major faults means that a wide variety of pre - Tertiary rocks are exposed in the region (Lee and Bailey op. cit.). Briefly these comprise:

- 1 The Lewisian and supposed Torridonian rocks of Iona
- 2 Moine schists and Mesozoic sediments occupying the central region between the two faults. These are presumably underlain by Lewisian gneisses but no Lewisian fragments have been found in the Tertiary vent agglomerates of Mull. Minor outcrops of other series - Upper Carboniferous strata in Morvern, Dalradian schists and Devonian lavas in the Loch Don anticline, Dalradian limestones in Lismore Island - are confined to the vicinity of the Great Glen fault.
- 3 Dalradian schists and Devonian rocks on the islands and mainland to the southeast of Mull.

The Mesozoic rocks of Mull and Morvern outcrop around the margins of the lava pile. The sequence is drastically curtailed as a result of uplift and erosion in Jurassic times. Triassic and Rhaetic deposits are succeeded directly by Upper Greensand and chalk, and the combined thickness of these groups is less than 100m. Wherever the Mesozoic and Tertiary rocks have been removed by denudation Moine schists are encountered. In both the Ross of Mull and Morvern these are intruded by Caledonian granites. In addition, one of the sparse Permian basalt - lamprophyre dyke swarms of the Scottish Highlands runs through the area surrounding Mull. The greatest concentration of these dykes, described by Bailey et al. (1924) as camptonites and related types, occurs in southeast Morvern and Lismore Island, close to the Great Glen fault. The Permian age of these swarms has been confirmed by radiometric dates ranging from 276 - 245 Ma. obtained on dykes from Mull, Coll and Orkney (Beckinsale and Obradovich 1973, Brown 1975).

The Tertiary lava pile

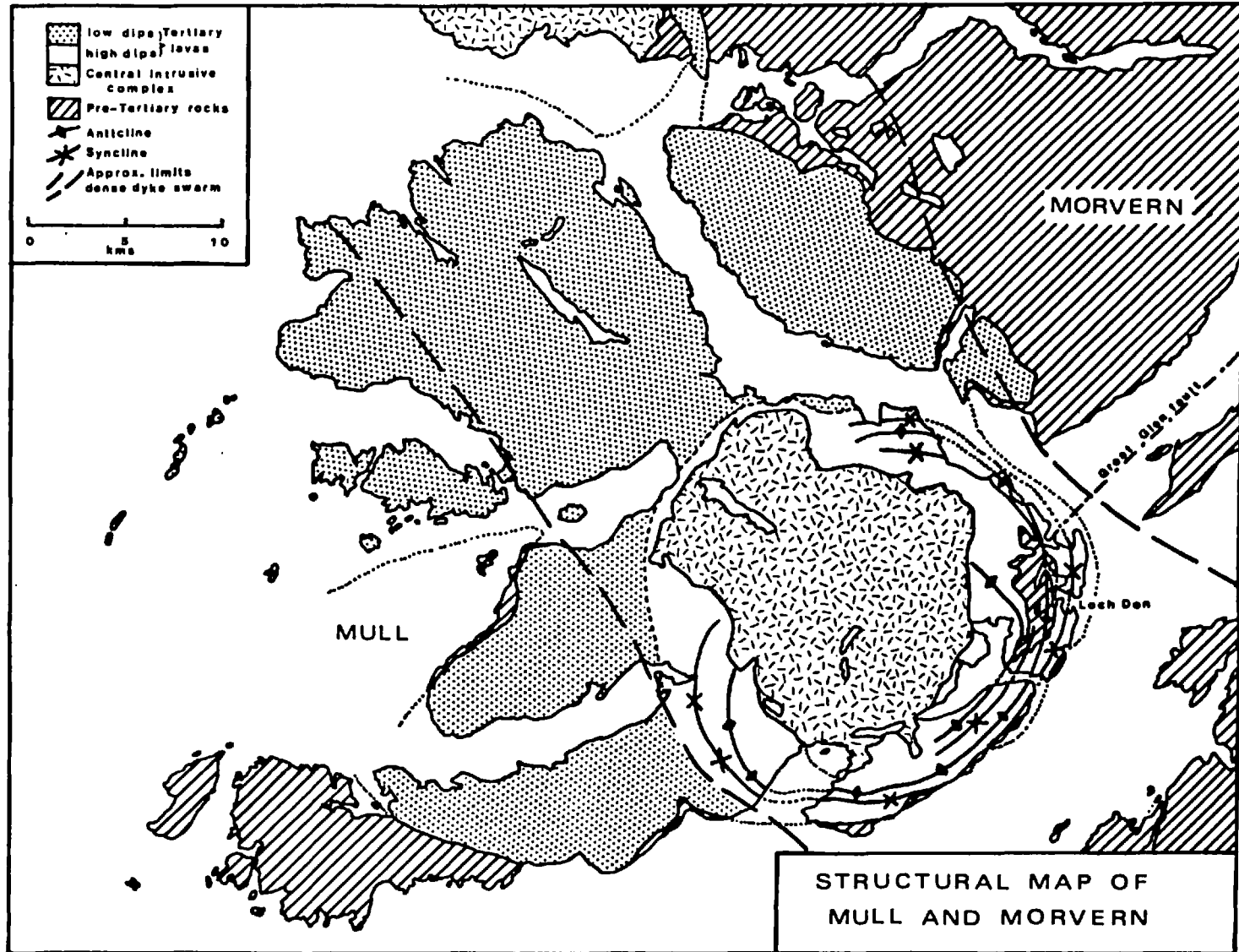
Tertiary lavas outcrop over an area of some 830 km² on Mull and Morvern. The total thickness of the succession is estimated at 1830m, although the maximum exposed in any one section (on Ben More at 970m,

the highest peak in the area) is little more than half this. The lava sequence is summarised in Table 1 - 1, details of the stratigraphy are given in the Mull Memoir (Bailey et al. 1924, pp.92-135).

Table 1 - 1 Generalised Mull lava succession
(after Bailey et al. 1924)

<u>Tertiary lavas</u>	
2. Central group 915m+. mainly ol - poor tholeiitic types	<p>Overlie Plateau Group in central and south-east Mull. Mainly preserved in subsidence caldera where three concentric zones have been recognised, pillow lavas are found in the outer and middle zones.</p> <p>f. Interior zone. The predominating Non - Porphyritic Central lavas</p> <p>e. Middle zone. Feldspar - phyrlic basalts</p> <p>d. Outer zone. Sparsly feldspar - phyrlic and aphyric lavas</p>
1. Plateau group 915m. mainly ol - rich lavas	<p>c. The Pale Suite of Ben More. 475m. in Ben More. Alkali olivine basalts with, near the base, a mugearite and feldspar - phyrlic basalt</p> <p>b. Main Suite. 475m. in Ben More. Mainly alkali olivine basalt types with some picritic and feldspar - phyrlic varieties</p> <p>a. Staffa Group. Olivine poor, often columnar basalts of very limited occurrence</p>
<u>Tertiary sediments</u>	
2. Intercalations between flows	Red boles due to subaerial weathering, rare pyroclastics, plant beds, lignites and conglomerates of SW Mull
1. Basal Deposits	<p>b. Basal mudstone - probably a lateritic ash-underlain in SE Mull by flint conglomerate</p> <p>a. Desert sands penetrating fissures in Chalk in W Mull</p>

Figure 1 - 2.



Structurally the lava pile can be divided into two sections (fig. 1 - 2) :-

1. An area of low dips comprising western and northern Mull and Morvern, made up of lavas having a dip of 5° or less.
2. A central area of steeper dips enclosing the intrusive complex in central and eastern Mull, in which the dip is more than 5° and commonly exceeds 20° . The arcuate folds in this region are concentric about the intrusive complex and are thought to have been produced at an early stage in its evolution. They post date many of the northwest - southeast trending dykes which have been deformed by these movements. (Skelhorn 1969).

The dip in the outer areas is variable and the base of the lava pile is probably a gently undulating surface, with two large shallow basins; one in north-west Mull, the axis of which is coincident with that of the dyke swarm, and the other on either side of Loch Scridain. The dips indicate that in few, if any, places does the base of the pile descend to more than 400m. below sea level. In both Morvern and Loch Scridain the lavas thin away from Mull. By combining the observed thinning rates with the thicknesses deduced from the zeolite zones, Walker (1970) made a reconstruction of the 'Mull volcano' which suggests that the lavas extended for several kilometres beyond their present day erosional remnant.

The lavas are thought to be the result of fissure eruptions from the abundant dykes. The majority of the dykes belong to the northwest - southeast trending swarm, which extends from the outer Hebrides through Mull and across northern England. The maximum crustal extension, of 10%, found in Mull as a result of their intrusion occurs on the southeast coast (Skelhorn 1969). A subsidiary branch of the regional swarm extends into Morvern where the dykes trend north - south.

Secondary alteration of the lavas

The hydrothermal alteration of the Mull lavas was first described by Bailey et al. (1924). They delineated a zone of pneumatolysis about the central complex within which no lavas with fresh olivine were found. Although the limit would appear to be based on the presence of olivine, several other criteria were also used : "Outside the limit (of pneumatolysis)... the plateau types of basalt

are apt to weather with rusty red surfaces....Inside the limit, weathering yields sombre grey and brown surfaces....Another important characteristic of the pneumatolytic core of Mull is a widespread development of albite and epidote filling vesicles and cracks". (Mull Memoir p.95).

The first systematic study was that of Walker (1970) who recognised and mapped five distinct amygdale assemblages in the lavas. Each assemblage occupies a well defined zone, named after an index mineral which it contains. Walker's mineral zones are shown in fig.1 - 3 and their assemblages listed below:

1. Carbonate assemblage: abundant calcite with aragonite (much of it pseudomorphed by calcite), dolomite rosettes, quartz and chalcedony.
2. Mesolite assemblage: mainly mesolite, thompsonite and analcite in the amygdaloidal flow tops, together with sporadic chabazite, stilbite and heulandite in the rather sparse amygdales in the flow interiors, plus occasional apophyllite, tobermorite and other calcium silicate hydrates.
3. Laumontite assemblage: the same as the mesolite assemblage but with the addition of laumontite.
4. Prehnite assemblage: prehnite present, together with the minerals of the laumontite assemblage, or with quartz, feldspar, carbonate and chlorite.
5. Epidote assemblage: epidote present, commonly associated with quartz, feldspar, chlorite, prehnite, laumontite and sporadic scolecite and lime - garnet.

The epidote and prehnite zones cut steeply across the lava stratigraphy, coincide roughly with the area of steeper dips about the central complex and appear to constitute a secondary, hydrothermal aureole enveloping it. The outer limit of the epidote zone corresponds almost exactly with the limit of pneumatolysis defined by Bailey et al. The discovery of the prehnite zone extended the known area of hydrothermal alteration a further 1 - 2 kms beyond that previously recognised. The pattern of the zeolite zones is less clear than those found in other basalt piles such as Iceland or Antrim, largely due to lack of relief, but their assemblages are almost identical. They occupy the areas of low dips and tend to be flat - lying, approximately parallel to the base of the lava pile. Accordingly, Walker ascribed their

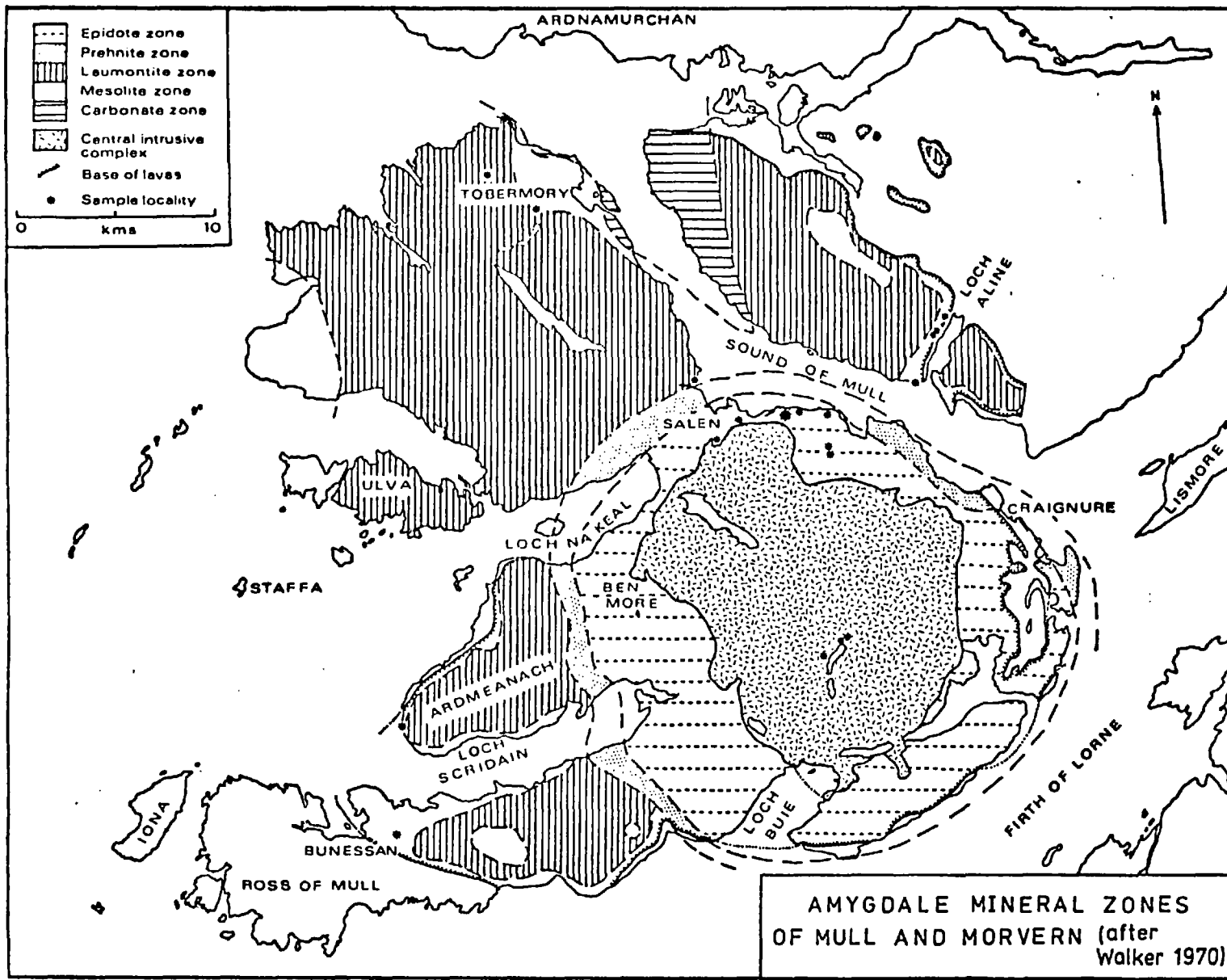


Fig 1-3

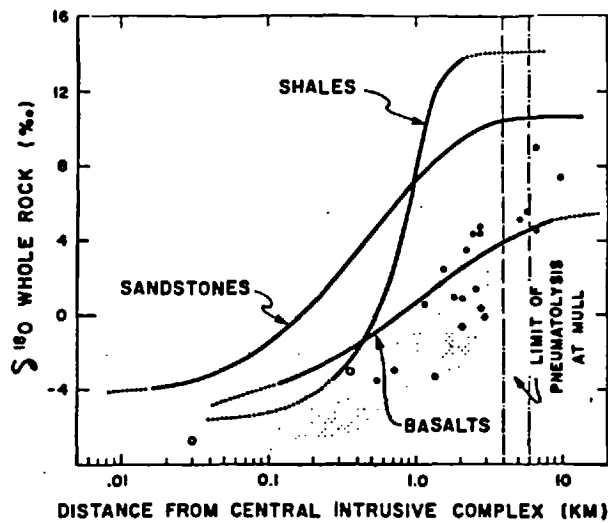
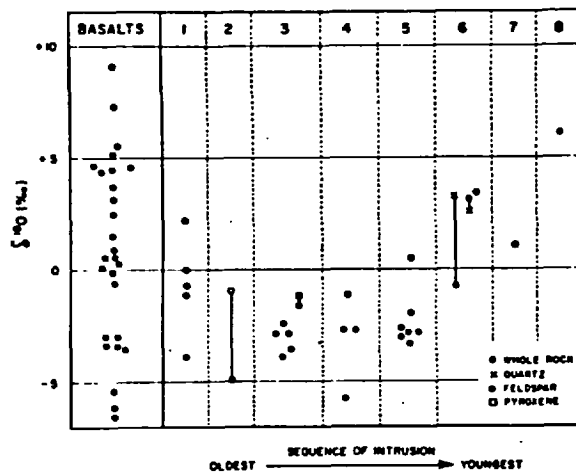
origin to the effects of low - grade burial metamorphism.

The carbonate zone of northwest Mull and Morvern extends for more than 200m. up into the lavas, but its relation to the zeolite zones is not apparent. Since, it is opposite and widens towards the large Tertiary explosive vent of Ben Hiant in Ardnamurchan, Walker suggested it defines a zone of hydrothermal alteration about this vent. For this reason the lavas within the carbonate zone were avoided when sampling for this present study.

Oxygen and hydrogen isotope studies have demonstrated that the rocks within the central aureole have undergone massive chemical exchange with heated circulating groundwaters and that similar meteoric-hydrothermal systems were established about the Tertiary intrusive centres of Skye and Ardnamurchan. (Taylor and Forester 1971, Forester and Taylor 1976). The Mull lavas exhibit systematic isotopic variation, with $\delta^{18}\text{O}$ decreasing radially inwards as the central complex is approached (fig.1 - 4). The limit of pneumatolysis coincides well with an approximate boundary between "normal" and ^{18}O -depleted rocks, all the basalts outside this limit having $\delta^{18}\text{O} > +4.9$.

The central intrusive complex: shown in figures 1 - 2 and 1 - 3 is not a single pluton but many hundreds of separate intrusions. These include a number of substantial bodies of granophyre and gabbro and a tremendous variety of dykes, cone - sheets and other small bodies. Some of the larger intrusions have their own narrow but distinct contact metamorphic aureoles but no zoning of hydrothermal minerals about any particular body was observed and accordingly Walker (1970) interpreted the distribution of the epidote and prehnite zones as constituting a hydrothermal aureole about the intrusive complex as a whole. Over twenty main episodes of intrusive activity that can be related to three distinct centres have been recognised within the complex. Forester and Taylor (1976) showed a variation of $\delta^{18}\text{O}$ with age amongst the intrusive rocks. It can be seen from fig.1 - 5 that, if their late-stage dyke sample (which was collected outside the central aureole) is discounted there is little evidence for the proposed trend.

One feature of the zeolite - zone distributions that is difficult to reconcile with a burial metamorphism model is that the higher - temperature zone, the laumontite zone, frequently lies some distance above the base of the lava pile sandwiched between two separate

Figure
1 - 4Figure
1 - 5

1 - 4 A semilogarithmic plot of $\delta^{18}\text{O}$ vs. distance from the intrusive complex. The points shown indicate basaltic country rocks lying outside the Mull plutonic complex. The curves labelled shales, sandstones and basalts represent generalised average profiles for the $\delta^{18}\text{O}$ values of these rock types around the Skye plutons.

1 - 5 $\delta^{18}\text{O}$ vs. age of intrusion for the Mull plutonic centres. Also shown are $\delta^{18}\text{O}$ for the basaltic country rocks. 8 is the NW - SE late stage dyke sample collected from outside the central aureole.

Both diagrams from Forester and Taylor (1976).

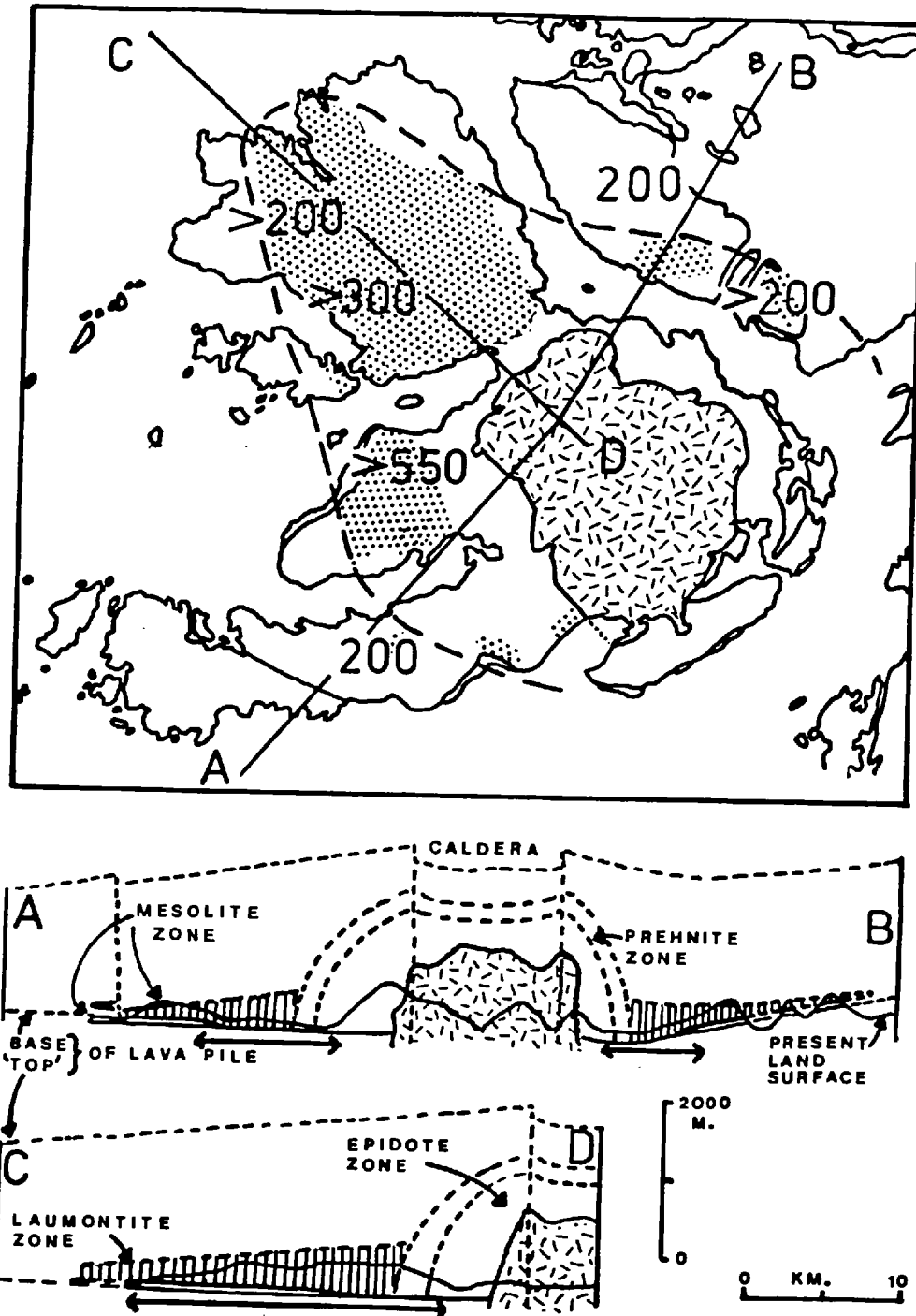


Figure 1 - 6. The stippled areas enclosed by the dashed line are the regions in which laumontite is abundant. These areas are indicated by arrows underneath the cross - sections. The figures give the available data on the thickness of the laumontite zone. (after Walker 1970).

mesolite zones, (see fig.1 - 6). Walker (1970) took no account of the relative abundance of the secondary minerals when defining the zones, using instead the appearance of an index mineral. In the outer parts of the prehnite zone this mineral coexists with the assemblage of the laumontite zone, which is gradually replaced by feldspar, chlorite and quartz adjacent to the epidote zone. Hence, the crosscutting relationship between the prehnite and laumontite zones shown in fig.1 - 6 is merely an artefact of the scheme employed by Walker. Figure 1 - 6 shows that the areas in which laumontite is particularly abundant form an additional annular zone enclosing the central complex. At least some of the zeolite zones may therefore represent a lower temperature periphery of the hydrothermal system, with the inclination of the boundaries between the zones reflecting the control exerted by the structure of the lava pile on the movement of the hydrothermal fluids. (c.f. figs.1 - 2 and 1 - 3). Significantly the region of abundant laumontite shown in fig.1 - 6 is elongated along the axis of the dyke swarm which could have provided additional pathways for the hot fluids.

This idea is not inconsistent with the oxygen isotope data. The water entering the hydrothermal - convective system is estimated by Forester and Taylor (1976) to have had initial $\delta^{18}\text{O}$ values of -11 to -12. At temperatures below 150°C not only are reaction rates slow but, these fluids would already possess the $\delta^{18}\text{O}$ values required for equilibrium with plagioclase (Taylor and Forester 1971) and hence little or no depletion would be observed. It would, however, mean that considerably greater volumes of water than those estimated from the oxygen isotope data must have circulated through the lava pile. Secondly, Walker's reconstruction of the lava pile, based on the assumption that the laumontite zone formed as a result of burial metamorphism and lay approximately 1600m. below the top of the lava pile, probably gives too large an estimate of the volume of lava extruded.

Timing of igneous and metamorphic events in Mull

Beckinsale (1974) obtained an Rb-Sr isochron for the Glen Cannel granophyre which yielded an age of 60.4 ± 1.4 Ma. This date could reflect either, the age of the intrusion or, if interaction with heated waters caused a rehomogenisation of the $^{87}\text{Sr}/^{86}\text{Sr}$ ratios of the pluton, the time at which such circulation ceased. This granophyre is related to the third and youngest of the three intrusive centres of

the Mull complex. By combining this result with the available K-Ar ages for the lavas, which cluster around 62 - 60 Ma., Beckinsale suggested that the extrusion of the lava succession as well as the entire igneous and metamorphic history of most of the Mull centre may have encompassed a period of only 1 - 2 Ma. years. 54 and 50 Ma. ages on dolerite plugs known to have been emplaced in the lavas at a later stage indicate that some igneous activity continued for several Ma. afterwards (Beckinsale 1974).

Macintyre et al. (1975) came to similar conclusions from a critical assessment of the available radiometric data for the British Tertiary Province. Using only data for which a high degree of analytical precision could be demonstrated and which were obtained on samples for which petrographic descriptions were available, allowing the elimination of any affected by secondary alteration, they demonstrated that the igneous activity was probably synchronous throughout the Province, with most of the magmatism occupying a period of 1-2 Ma. Their general geological timetable is reproduced below:

Major Phase. (c.59 Ma.) Widespread lava extrusion immediately preceding or partly coeval with, emplacement of most plutonic igneous complexes. Ubiquitous dyke intrusion throughout this stage.

Minor Phase. (c.52 Ma.) Predominately dyke intrusion with perhaps emplacement of some plutonic rocks.

The agreement between these two independent schemes is striking. Recently Fitch et al. (1978) proposed an extremely similar timetable.

The lack of any evidence for systematic magmatic migration with time precludes any origin for the province by drift in the region of a localised "mantle plume or hot - spot" and places considerable constraints on petrogenetic models.

Previous geochemical studies.

The compositions of the Mull igneous rocks were first set down in quantitative terms by Bailey et al. (1924). They recognised nine main magma types, linking those that appeared to be genetically related into magma series. Their predominating Mull Normal series comprised: firstly, the Plateau magma type; secondly, the Non - Porphyritic Central type; thirdly, the Intermediate-to-Subacid magma type (mainly minor intrusions) and fourthly, the Acid magma type (forming the granitic rocks of the central complex). The Plateau magma

type was thought to be the parental material which gave rise to the other magma types by the fractionation of olivine, augite and feldspar followed by migration of the acid residuum in large magma chambers. The problem of producing the Central lavas with Si - rich interstitial material from the Plateau type, the interstitial material of which is represented by Si - poor zeolites in the lavas, was resolved by Bailey et al. by postulating either a limited amount of crustal assimilation or, the precipitation of diverse mineral assemblages under varying conditions.

Bailey et al. (1924) recognised several variants of their basalt magma types which were usually ignored in subsequent discussions of magmatism in the Province. The petrographic similarity between the lavas of the various Tertiary centres led most workers to describe Hebridean lavas in terms of the two main groups recognised in Mull, the Plateau and Non - Porphyritic Central type, and these two names came to be used as synonyms for alkali olivine basalt and tholeiite, respectively. Notable amongst these discussions were the contributions of Bowen (1956), Kennedy (1930,1933), Tilley (1950), and Wager (1956). These discussions were nevertheless, still based to a large extent on the very limited amount of analytical data available to the authors of the Mull Memoir, many of which were analyses of altered rocks.

Published average compositions of the Mull lavas were first criticised by Daly (1933) on the grounds that "they were all more or less weathered". He concluded that the "oxide proportions in the published averages doubtless differ from those in the original magmas. Small as these differences may be, they will affect results considerably when the addition - subtraction method of discerning the process of differentiation is used". Daly's criticism is still valid today. Other than the work of Tilley and Muir (1962) little attempt has been made to establish the extent to which the compositions of these lavas have been affected by secondary alteration. Tilley and Muir reviewed the available data on Tertiary Hebridean Plateau lavas and concluded that they could all be ascribed to a ne - normative Plateau magma type, comparable to the alkali olivine basalts of Hawaii. They suggested that the appearance of hypersthene in the norms of some of these lavas was the result of hydration and

oxidation during the serpentinisation of olivine, accompanied by selective leaching. In support of this they demonstrated that unaltered pyroxene separated from a serpentinised Mull basalt was ne - normative and compositionally similar to pyroxenes in world-wide alkali basalt series, whilst the whole - rock analysis had 12% of hypersthene in its norm. This lava flow came from the Fishnish Peninsular which falls outside the zone of pneumatolysis. Nevertheless, it lies inside the prehnite zone, which was not known to exist at the time of Tilley and Muir's study. Their conclusions may not therefore be valid for other hy - normative basalts affected by a lower grade of secondary alteration. Tilley and Muir (1962) also presented a new ne - normative analysis of the Staffa lava, the type locality of the Staffa group. This was thought by Bailey et al. (1924) to be related to the central lavas, but Tilley and Muir concluded from the undersaturated composition of this flow that the Staffa group were merely pyroxene - rich variants of the Plateau lavas.

Recent studies of the Mull lavas have concentrated on samples collected from outside the central greenschist - facies zones. Fawcett (1961) described both ne- and hy - normative varieties amongst the Plateau lavas. He also recognised modal pigeonite in two tholeiitic lavas. One of these was the flow enclosing Macculloch's Tree, which was previously placed in the Staffa group by Bailey et al. (1924). Beckinsale et al. (1978) published data for twenty-one Mull lavas and plugs which are all hy- or quartz - normative. They divided these into three groups on the basis of major and trace - element compositions and $^{87}\text{Sr}/^{86}\text{Sr}$ ratios. Group 1 is an alkaline series (basalt-hawaiite-mugearite) with low initial $^{87}\text{Sr}/^{86}\text{Sr}$ ratios ≤ 0.7030 ; Group 11 is a tholeiitic series with high ($^{87}\text{Sr}/^{86}\text{Sr}$)_i ratios of about 0.7055 and the third group was thought to represent mixtures of the other two types. No petrographic descriptions of these samples have been published and their relationship to the different groups identified in the Mull Memoir is not known, other than the fact that the basic members of the Group 11 of Beckinsale et al. (1978) are all lavas placed by Bailey et al. (1924) in their Staffa group. Beckinsale et al. considered that the Group 1 and Group 11 magmas arose by the melting of a garnet lherzolite and a shallower plagioclase lherzolite source respectively.

Studies of the **Small Isles** (Ridley 1973) and Skye (Thompson et al. 1972) have revealed the presence of both ne- and hy- normative lavas amongst what are petrographically typical Plateau - type lavas. Most of the lavas described by Ridley delineated a single trend from basalt to mugearite. Thompson et al. (1972) showed that the Skye Main Lava Series basalts followed two divergent evolutionary trends; one being from the ne- normative basalt to hawaiite, mugearite and benmorite, whilst the trachytes evolved from the hy- normative basalts via a suite of previously undiscovered Si - rich, Fe - poor intermediates. Thompson (1974) suggested as a result of high pressure melting experiments that the Skye Main Lava Series ^(SMLS) magnesian basalts were formed by the partial melting of spinel lherzolite at about 60Kms. depth, with the initial melt fraction varying from approximately 5 - 10% to generate the ne- and hy- normative magmas respectively. Thompson et al. (1979) have found that the abundances of several incompatible elements correlate negatively with the degree of Si - saturation in the SMLS basalts, agreeing well with the dilution trends that would be predicted by a partial melting model.

Two other basalt magma types have been identified in Skye. A few flows of Ca - rich, alkali - poor olivine tholeiites occur at the top of the lava pile remnant intercalated with the SMLS (Thompson et al. 1972, Esson et al. 1975). Matthey et al. (1977) have shown that approximately 70% of the dykes in the regional swarm belong to this distinctive group, the Preshal Mhor magma type, and identified a third Fairy Bridge basalt type in the dyke swarm, which is so far only represented amongst the lavas by one flow. None of these basalt types can be derived from one another by the fractionation or accumulation of any of the observed phenocryst phases. The distribution of basalt types within the Province was discussed by Matthey et al. Low - alkali tholeiites similar to the Skye Preshal Mhor basalts are known to be an important component of the Mull dyke swarm and one low - alkali tholeiite lava has been found at a relatively low level in the Mull lava pile. Similar rocks have been reported from Antrim, Carlingford and Arran. Accordingly, Matthey et al. suggested that other Tertiary centres would contain a similar range of magma types to Skye. None of the other lava piles has been as extensively studied as that of Skye in recent years and hence, no overall picture of the regional geochemical variation has emerged.

2. Field Relations and Sample Selection

The unit-by-unit chemical diversity demonstrated in recent studies of unaltered basaltic lava suites (e.g., O'Nions et al. 1976, Puchelt and Emmermann 1977) and the large number of magma types identified amongst Hebridean lava piles, suggests that any attempt to study element mobility by comparing sets of analyses of relatively fresh and altered rocks will be unable to separate pyrogenic from secondary variation. Sampling was therefore aimed at collecting multiple specimens from across individual lava flows. The persistent trap featuring of the Mull lavas means that the margins of the flows which might be most affected by secondary alteration are rarely exposed. This problem is accentuated in the epidote zone as a result of tectonic and metamorphic events. The samples used in this study were obtained mainly from new roadcuttings and quarries. The localities and their relation to the secondary mineral zones are shown in fig. 1-3. Most of the lavas sampled belong to the Plateau Group of Bailey et al. (1924) as the poor and discontinuous exposure of the other lavas makes them ^{un}amenable to detailed investigation. Most of them appeared to be basalts or hawaiites, with the exception of one (M 59) which is clearly a more evolved type.

Zeolite - facies lavas

Nine lavas from the zeolite zones were sampled, and multiple samples were collected from seven of these. At all except two of the exposures (LA 1-5, LA 7-11), a red bole could be found enabling the samples to be related to their position within the flows. A distinct reddening of the soil above and below LA 7-11 coupled with step like changes in the topography suggests that this section is virtually complete. Most of the exposures were of massive, non-vesicular rock, though amygdales were more frequent near the margins. Only two of the lavas possessed what might be termed an amygdaloidal layer in which infilled vesicles make up several percent or more of the rock surface. One of these (M 51 - 55) had an amygdaloidal layer near the base from which zeolite - filled vesicle pipes penetrate vertically upwards into the flow centre for distances averaging a metre in length. Samples were taken from both these flows (M 56, LA 19) in order to investigate the chemical changes adjacent to the vesicles.

Greenschist - facies lavas

Within the greenschist - facies zones the degree of alteration could everywhere be related to the permeability of the rocks. In Pennygown Quarry, 3.5 kms. east of Salen, two lava flows and an interflow pyroclastic deposit are exposed. In the lower flow, originally an olivine - rich basalt, the top two metres are now formed of a green chlorite - rich rock which passes down into a green and grey mottled zone (figs. 1 - 7, 1 - 8). Small dark patches of less intensely altered rock appear in this zone and increase in size downwards until they coalesce and the centre of the flow is composed of uniformly dark rock. The upper flow, a plagioclase - phyrlic lava, shows a similar, but narrower, transition zone at its base. At every point around the walls of the quarry the vertical sequence - dark plagioclase - phyrlic rock, mottled zone, grey - green rock, thin tuff deposit, green chlorite - rich rock, mottled zone, dark lava - could be traced. A vertical section through the lower flow (M 13 - 22) and one across the transition zone of the upper flow (M 26 - 28) were collected.

Secondary mineral pods commonly occur in the mottled zones of both these lava flows. In the lower basalt their diameters never exceed a few centimetres and they are composed mainly of chlorite. In the upper lava they achieve diameters of up to 30 centimetres and show a series of concentric zones. Frequently, they could be seen to be surrounded by a thin halo of darker rock, 1 - 2 mm. in diameter. The smaller pods, ranging from 1 - 2 mm. to 4 or 5 cm. in diameter, appeared to consist solely of dark chlorite surrounding light chlorite, whilst the larger ones have cores of calcite and zeolites and could frequently be seen to be connected to the flow margin by thin veins of the same material. Pods at every stage of growth between these two types could be found around the walls of the quarry. They are oval in cross section and extremely regular in shape.

Thirteen separate tectonic and metamorphic events could be seen to have affected the lavas in Pennygown Quarry, most of which post-dated the alteration described above. Hydrothermal veins and a dyke that cut across the nearly horizontal zones in the upper lava flow stop abruptly at the base of this lava. The dyke could be seen in two opposite corners of the quarry but no similar intrusion in the lower lava was found. The thin tuff between the two lavas contained

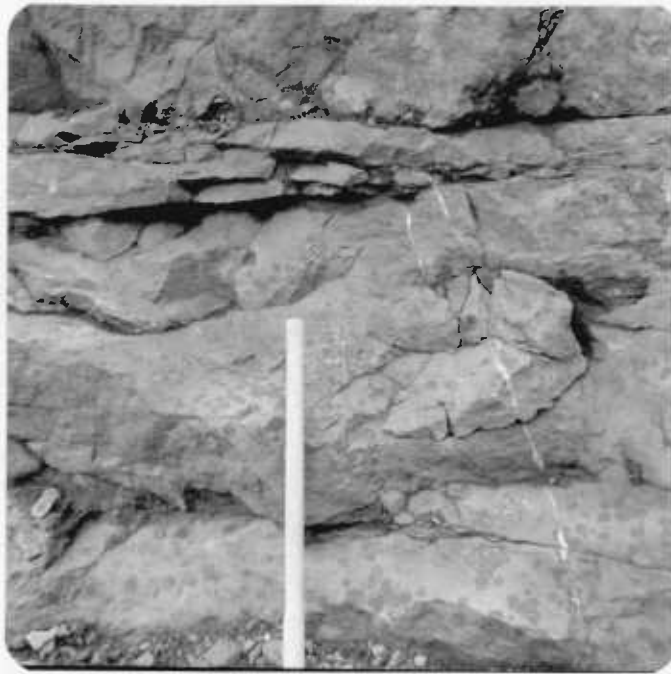


Figure 1 - 7 Transition zone in the upper margin of the olivine-rich lava Pennygown Quarry. Intensely altered chlorite-rich rock passes downwards into mottled rock with small dark patches of less altered rock that gradually increase in size. Discordant calcite veins cut the lava but these do not appear to have affected the rock immediately adjacent to them.



Figure 1 - 8 Altered lava from the centre of the mottled zone in the olivine-rich lava Pennygown Quarry.

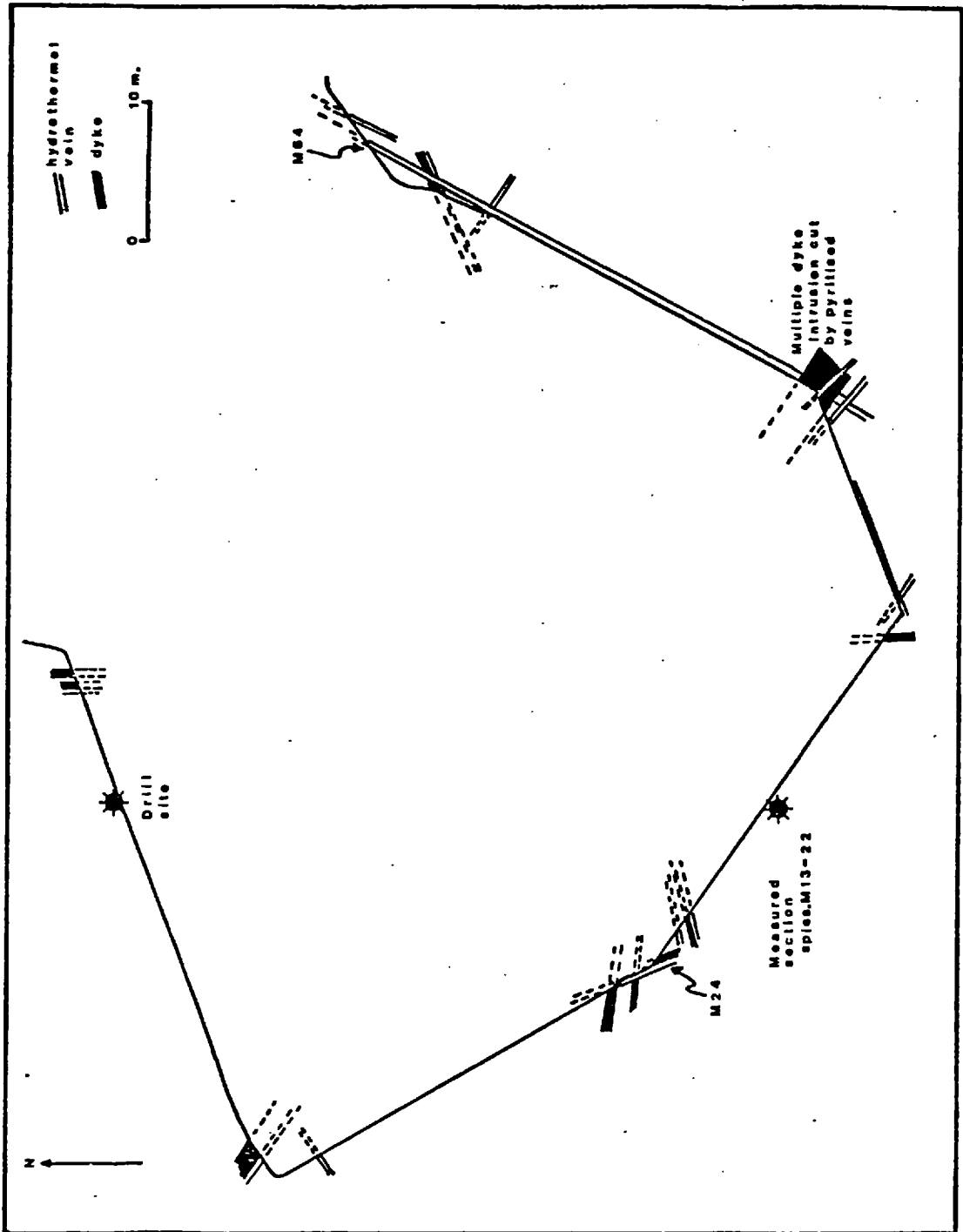


Fig. 1 - 9 Plan of Pennygown Quarry

numerous slickenslides and shear zones and considerable lateral movement must have taken place along this horizon. Other dykes and veins cutting the two lavas show no signs of being offset. The dykes all appear to be inclined, making an angle of approximately $20 - 30^{\circ}$ with the vertical and dip towards the centre of the island. They are probably cone sheets. Interestingly, the only evidence for intrusive activity observed in this region was in the quarry and no signs of these dykes could be found on the adjacent hillside. Many of the minor intrusions were cut by calcite veins, some of which were cut in turn by other intrusions. The relationship between the dykes and veins is shown on the plan of the quarry in fig.1 - 9.

Very little alteration of the lavas adjacent to these discordant veins could be seen. Even when they cut across the darker patches in the mottled zones in the lavas, and in the dykes, some of which display similar but more subdued mottling, these appear completely unaffected by them (fig.1 - 7). Thin zones of soft, intensely altered and brecciated lava debris occur around the larger veins many of which lie along the dyke/lava contacts, but the largest of these is considerably less than a metre wide. No evidence for shearing or crushing of the rock fragments in these breccias could be found and they are usually completely surrounded by a matrix of calcite or zeolites, suggesting they were supported by the fluids. The frequent penetration and brecciation of these lavas by hydrothermal veins suggests that spasmodic heating of the fluids was caused by the intrusive activity in the centre of the island. If the lavas had already been sealed and rendered impermeable by the formation of secondary minerals and the temperature of the fluids was suddenly raised, Pfluid might locally have exceeded Ptotal, causing hydrofracturing and the formation of veins and hydrothermal breccias. Samples of the veins were collected in order to investigate changes in the solution chemistry with time (M 24, M 64).

Five other lava flows were sampled in roadcuttings along the A 849 from Salen to Craignure, and one in Toll Doire Quarry $\frac{1}{2}$ km. south of Salen. Wherever the flow margins were exposed they could be seen to be more intensely altered and greener in colour than the rest of the lava. In one case an amygdaloidal bole with relict red patches was found (M 39), and a sample of a weathered flow top was

collected from the zeolitised lavas for comparison (LA 12). The lava flow exposed in Toll Doire Quarry was transected by numerous small veins, mainly along joint surfaces, though hydrofracturing and brecciation of the rock could also be seen (fig.1 - 10). This quarry is in two parts with the lava flow exposed in one part and the Toll Doire granophyre ring dyke in another part approximately 180m. away. Nowhere, however, could the junction between the granophyre and the country rocks be observed. None of these exposed vertical sections through the lavas exceeded 5 metres in length and no natural exposures of greater length could be found.

Drill - hole in Pennygown Quarry

To supplement these collections a 22 m. hole was drilled in Pennygown Quarry the following year. Core recovery of 86% was achieved. A complete log of the drill core is given in Appendix 1 and the drilling techniques are described in Appendix 11. The water needed to cool the drill bit was obtained from a shallow pool of water in the floor of the quarry. Water from this pool, which was only 2 - 3 inches in depth, was pumped down the drill rods at a pressure of 200 psi. A consistent flow back up the hole was maintained and throughout several days of almost continuous drilling the pool never dried up; clearly suggesting that the rocks are relatively impermeable and may be sealed by secondary minerals.

The top 14 m. of the drill hole transected a virtually complete section through the olivine - rich flow in the quarry. The bottom of this flow is nowhere exposed and the drilled section confirmed that the dark rock seen in the lower part of the quarry walls represented the centre of the flow. Unlike the previously sampled section, which was almost completely non - vesicular, the first few metres of the core contained several thin amygdaloidal horizons, which may represent regions where material from the flow top had been incorporated into the advancing front of the lava flow. These top few metres were light green in colour but displayed some mottling between the amygdaloidal layers. Below, these passed into a uniformly dark rock similar to that seen in the quarry. Near the base of the flow an increase in alteration was observed and it appeared to have been penetrated by a pipe amygdale similar to those seen in the zeolitised lava M 51 - 55.



Figure 1 - 10
Hydrothermally
brecciated lava,
Toll Doire Quarry.



Figure 1 - 11
Drilling in Penny-
gown Quarry. The
'milky' colouration
of the water is due
to suspended rock
flour carried back
up from the drill
hole.

The lower five metres of the core transected a plagioclase - phyrlic lava. This showed the familiar marginal transition from green to mottled to dark rock (fig.1 - 12). Small chlorite - filled pods and chlorite - lined veins which could frequently be seen to be connected were common in the upper part of the flow. The drill hole terminated in a fine - grained intrusive rock through which little penetration could be achieved. Adjacent to this, the lava had been hydrothermally brecciated and showed evidence for at least two episodes of hydrofracturing with fluidisation of the debris occurring during the second one.

The exact position and nature of the boundary between these two flows is difficult to establish because of incomplete core recovery. The plagioclase - rich flow is exposed on the beach nearby but the junction between the lavas could not be found. Above the lower five metres the core contained an igneous breccia 1½ m. thick composed of lava debris (fig.1 - 13). Some of the fragments contained plagioclase phenocrysts. This is overlain by a 1 m. thickness of mottled plagioclase - phyrlic rock, texturally similar to the lower flow and clearly different to the upper lava. Thin 1 - 2 m. flows occur elsewhere in the island, and the drill core could have transected three different flows. Alternatively, auto - intrusion and brecciation of the lower flow could have occurred during its extrusion. Phenomena of this type can be seen in several lavas in the cliffs of Mull, the most notable being the lava enclosing Macculloch's Tree. The only way of distinguishing between these two hypotheses is to establish some geochemical method of fingerprinting the lava flows.

Despite the frequent association of metal - sulphides with areas of low - grade hydrous metamorphism, these are rare in Mull. Pyrite was found in two instances both related to hydrothermal veins and to minor intrusions. Disseminated sulphides are abundant in a zone, roughly one metre wide, adjacent to a thin vein cutting a dyke in Pennygown Quarry (figs.1 - 9, 1 - 14). This dyke can be seen to post-date several of the other veins and other intrusions in the quarry and is itself a multiple intrusion containing several chilled margins. Smaller amounts of pyrite were also found in the hydrothermally brecciated lava from the base of the drill core (C 232 a/b). Local concentrations of sulphides have been found adjacent to some of the caldera ring - fractures (R.D.Beckinsale pers. comm. 1977) indicating



Figure 1 - 12 Mottled lavas from different flows. The block is from the plagioclase-phyric flow exposed in the upper part of Pennygown Quarry. The three drill core samples are from top to bottom :- olivine-rich flow in top part of drill core; thin plagioclase-phyric layer immediately above breccia; lower plagioclase-phyric lava. The drill core has a diameter of 2.5 cm.



Figure 1 - 13 Igneous and hydrothermal breccias from the top and bottom of the plagioclase-phyric lava in the drill core.

that ore - forming elements were carried by the hydrothermal fluids.

Other Samples

Five lavas not belonging to the Plateau Group were also sampled. One was the flow enclosing Macculloch's Tree (M 61) and a specimen of the Staffa lava was subsequently obtained (M 80). Three outcrops of the Non - Porphyritic Central lavas were sampled (MS 183 - 185). These outcrop in relatively low-lying areas occupied mainly by peat bogs and sections through these lavas were not exposed. One sample (M 58) was not allocated to any of the lava type divisions recognised by Bailey et al. (1924) as it was collected from a hill-top knoll south of Fishnish Peninsula, and may be a minor intrusion.



Figure 1 - 14 Disseminated pyrite surrounding a thin potassic feldspar vein cutting a dyke in Pennygown Quarry.

CHAPTER TWO : ZEOLITE FACIES LAVAS

The petrography, mineral and bulk chemistry of the zeolite- and greenschist-facies lavas are described in this and the next chapter. These observations and analyses are used to assess the extent to which these lavas have been affected by post-eruptive processes. All the mineralogical and chemical data are listed in Appendix 1. The extent to which any particular lava flow will have been affected by alteration processes will depend on a variety of factors including its initial magmatic composition and the thickness of the flow. Hence, each individual lava may have been affected to different degrees and these sections will concentrate on documenting mineralogical and chemical variations across sections through lava flows.

The processes that can cause intra-lava variation can be divided into : (1) those operating during the initial cooling or consolidation - a primary or deuteric alteration (2) those affecting the lavas after cooling - a secondary alteration (Sederholm¹⁹²⁹). This notation is used throughout this study.

The existence of several processes that can modify the compositions of the lavas make it desirable to establish or eliminate the effects of each one whenever possible. Information on the extent to which the Mull lavas may have been affected by primary or deuteric alteration has to be obtained from the zeolite-facies flows, as in many of the greenschist-facies lavas the igneous minerals have been completely or partially replaced.

1. Petrography

Petrographically the lavas from both the mesolite and laumontite zones show little evidence for secondary alteration. Their 'freshness' is emphasised by the presence of minute patches of interstitial glass in some samples. This phase has not been previously recognised in the Mull Plateau Group. The glass forms less than one percent of the groundmass in all cases, and the lavas are almost entirely holocrystalline.

Individual flows contain olivine and/or plagioclase phenocrysts in a matrix of olivine, plagioclase, poikilitic titanite, sub-

Table 2-1 Classification of the zeolitised lavas, after Thompson et al. (1972).

Sample Numbers	LA 20	LA 13-15	LA 16-18	M 1	M 51-55	LA 7-11	M 11-12	LA 1-5	M 5-8
Thorton-Tuttle Index	21.6	18.3 - 21.4	18.9 - 25.1	24.8	19.2 - 21.3	24.5 - 26.2	27.2 - 27.7	26.5 - 28.6	35.3 - 36.8
Normative Plagioclase	An 57	An 60-55	An 60-50	An 57	An 61-59	An 57-55	An 52-50	An 54-51	An 43-41
F/F+M	0.525	0.526 - 0.538	0.531 - 0.546	0.547	0.568 - 0.595	0.627 - 0.679	0.636 - 0.653	0.670 - 0.686	0.717 - 0.729
Si-Saturation	Ne	Hy	Hy	Ne	Hy	Hy	Hy	Hy	Both Ne- and Hy- normative
Phenocryst phases	olivine enclosing sparse Cr-spinels			olivine and plagioclase	almost aphyric plagioclase and a trace of olivine	olivine and plagioclase	almost aphyric olivine, plagioclase and titanomagnetite	olivine, plagioclase and titanomagnetite	
Type	magnesian basalt			less-magnesian basalt			basaltic hawaiiite	hawaiiite	

poikilitic titaniferous magnetite, traces of biotite and apatite, chlorite and zeolites. With the exception of the Staffa group and Non-Porphyrific central lavas, described in a later section, pyroxene never occurs as a phenocryst phase in these lavas. They conform well with the petrographic descriptions of this type in the Mull Memoir (Bailey et al. 1924) and to those of the early Tertiary lavas of Skye (Anderson and Dunham 1966, Thompson et al. 1972) and the Small Isles (Ridley 1973).

For descriptive and comparative purposes these lavas were subdivided using the classification procedure of Thompson et al. (1972). In this scheme constant values of Fe_2O_3 are employed to eliminate the effects of post-eruptive oxidation. Fe_2O_3 is fixed at 1.5%, if $\text{Na}_2\text{O} + \text{K}_2\text{O} < 4$, and at 2.0%, if $\text{Na}_2\text{O} + \text{K}_2\text{O} \geq 4$. This standardisation procedure was used by Thompson et al. (1972) for the Skye Main Lava Series; by Mitchell et al. (1976) for basalts dredged from the Blackstones centre and by Matthey et al. (1977) in their study of the Skye regional dyke swarm. Since many of these published analyses do not contain measured Fe_2O_3 values, the same procedure was adopted in this study for comparative purposes. The basalts were further divided into magnesian and less-magnesian varieties using their $F/F + M$ ratios and phenocryst assemblages. ($F/F + M = (\text{FeO} + \text{Fe}_2\text{O}_3) / (\text{FeO} + \text{Fe}_2\text{O}_3 + \text{MgO})$, using standard values Fe_2O_3 as defined above). The magnesian basalts have $F/F + M < 0.55$ and contain olivine and Cr-spinel. The less-magnesian basalts contain olivine and plagioclase phenocrysts and have values of $F/F + M > 0.55$. The phenocryst phases of the lavas and their classification parameters are listed in Table 2-1. The effects of zeolite-facies alteration on these parameters is discussed in a later section.

Magnesian-basalts LA 13-15, LA 16-17, LA 20

These lavas are petrographically similar. Their only phenocrysts are olivines enclosing sparse brown spinels (see fig 2-1). Al and Cr peaks were observed in the spectra obtained from the spinels with the EDS microprobe but complete analyses were not obtained, as the sections were all partially enveloped by olivine. An apparently unaltered crystal within an olivine pseudomorph in one of the green schist-facies lavas (Appendix 1-D, M 14 no.8) is an aluminous chromite, with 34% Al_2O_3 and 24.5% Cr_2O_3 . Similar Al-rich Cr spinels have been described from the lavas of Skye and the Small Isles (Thompson 1974, Ridley 1977).

The majority of the olivine phenocrysts are subhedral or rounded crystals up to 4mm in length and 2mm wide. Average grains are more equidimensional and between 1 and 0.5mm in diameter. In addition, skeletal or amoeboid crystals were observed. These show a range of sizes, up to 2mm in diameter, but never enclose a spinel phase. In several instances, notably in LA 13-15, their shapes are so intricate that only the simultaneous extinction of the crystals allow them to be distinguished from clusters of smaller olivines. Many of these skeletal olivines enclose groundmass feldspars and oxides and the areas adjacent to the larger crystals tend to be relatively poor in groundmass olivine granules.

The groundmass of the basalts consists of small olivine granules, 0.3 to 0.5mm in diameter, plagioclase laths up to 0.4mm in length, small irregularly shaped titanomagnetites and poikilitic to intergranular pyroxenes. A distinct phosphorus peak was observed in the spectra obtained from some of the pyroxenes but apatite could not be positively identified in the thin sections. The pyroxenes show a range of sizes but are smaller in the magnesian basalts than the less-magnesian basalts in which poikilocrysts 3mm or more in diameter are common. Some of the titanomagnetites contain a few thin exsolved ilmenite lamellae. No variations in the degree of deuteric oxidation were observed, either between individual samples from the same lava flow, or between different lavas. In all the lavas some secondary oxidation and maghemite formation was observed but this is usually restricted to cracks within the crystals and at their margins.

M 51-55, less-magnesian basalt

This flow has a coarse, almost doleritic texture. It is the only lava in which significant zoning of the phenocryst phases was observed and which contains no skeletal crystals. The olivine and plagioclase phenocrysts are present in approximately equal volumes. The olivines vary in size from subhedral crystals, 3mm by 2mm, to equidimensional grains, 0.5mm in diameter, that are difficult to distinguish from groundmass phases. Plagioclase occurs both as isolated phenocrysts, up to 3mm in length and 0.5mm wide, and as clusters of smaller crystals averaging 0.7mm by 0.3mm in size. Zoning in the ranges Fo88-78 and An87-50 were detected in olivine and plagioclase, respectively. The compositional range within the olivine crystals could not be fully

investigated, as the margins are partially replaced by serpentine or chlorite.

In addition to olivine, plagioclase and titanomagnetite, the groundmass contains small biotite crystals. The clinopyroxenes range up to 4mm in diameter and show an intense purple colouration at their margins. Many of the pyroxenes could be seen to enclose small apatite needles.

M 1 Less-magnesian basalt

The phenocrysts in this lava show a tendency to form small glomerophyric clusters, although isolated crystals also occur. They consist of subhedral olivines, up to 0.6mm in length and 0.2mm wide, and euhedral plagioclases showing a complete range in size from crystals measuring 0.8mm by 0.1mm to small groundmass laths, 0.2mm in length. Skeletal olivines, many of which achieve larger sizes (up to 0.8mm in diameter) than the subhedral crystals, are common. The pyroxene poikilocrysts have an average diameter of 3mm and the groundmass titanomagnetites show a subpoikilitic relationship to the other phases. This basalt lies almost on the boundary of the laumontite and prehnite zones but contains virtually no secondary minerals and cores of brown-green isotropic glass were observed inside the sparse patches of interstitial chlorite.

LA 7-11 Less-magnesian basalt

Plagioclase megacrysts, up to 4cm in length, were seen in the roadcutting in which this lava was exposed. These had a frequency of outcrop of one or two per m² and were all badly shattered as a result of the roadworks. No similar crystals were found in the thin sections of this basalt, which are almost aphyric. The sections contained up to 3% of plagioclase phenocrysts, showing a complete range of sizes from euhedral and subhedral crystals (2mm by 0.2mm) to the small groundmass laths. Many contain inclusions of olivine and opaques and in one case brown isotropic material that may be glass. The arrangement of the inclusions varies considerably; some are aligned along the axes of the crystals, whilst others show a concentric arrangement. Olivine in this lava occurs both as relatively well formed crystals, up to 0.3mm in diameter, which may be microphenocrysts and as rare skeletal or amoeboid crystals with diameters of up to 0.5mm.

The groundmass contains small randomly orientated feldspars, equidimensional olivine grains, large pyroxene poikilocrysts up to 4mm in diameter, subpoikilitic titanomagnetites, rare biotite and occasional minute sulphide blebs. The titanomagnetites tend to be concentrated into zones between the large pyroxene crystals and were never observed to be enclosed within them. Interstitial patches of chlorite occur between the feldspars, olivines and oxides in these areas. Many of these chlorite patches are concentrically zoned and some have cores of carbonate, though possible unaltered glass was observed inside a few of these. As described below, the secondary minerals are concentrated in these areas whilst olivines and feldspars enclosed by the pyroxenes appear completely unaltered. The rare sulphide grains, which have a frequency of occurrence of two or three per thin section did not appear to be associated with, or related to, any particular primary or secondary minerals.

M 11-12 Less-magnesian basalt

Like M 1, this lava shows little evidence for secondary alteration and contains relict patches of interstitial glass rimmed by chlorite. It contains subhedral to rounded olivines, up to 1.5mm in diameter, and sparse plagioclase euhedra. The groundmass consists of granular olivines, plagioclase laths, titanomagnetite, large titan-augites averaging 3mm in diameter, traces of biotite and very occasional minute sulphide blebs.

LA 1-5 Basaltic hawaiiite

Like LA 7-11, rare plagioclase megacrysts were observed in the walls of the small quarry in which this lava is exposed. Nevertheless, the thin sections appeared to be almost aphyric and the few phenocrysts are predominately plagioclases, often containing numerous inclusions. The plagioclase occurs both as glomerphyric clusters of anhedral crystals, up to 1.7mm long, and as isolated euhedral and subhedral crystals, up to 2mm in length. Sparse anhedral and skeletal olivines up to 0.3mm in diameter also occur.

The groundmass contains poikilocrysts of both clinopyroxene, up to 4mm in diameter, and titanomagnetite. The latter occur both as small crystals scattered throughout the groundmass and as larger isolated crystals, up to 0.5mm in diameter (see fig 2-2), which in reflected



Figure 2 - 1 Magnesian basalt, LA 15. The olivines show a wide range of morphologies and sizes and show little evidence for alteration. Field of view : 5mm by 3.5mm.

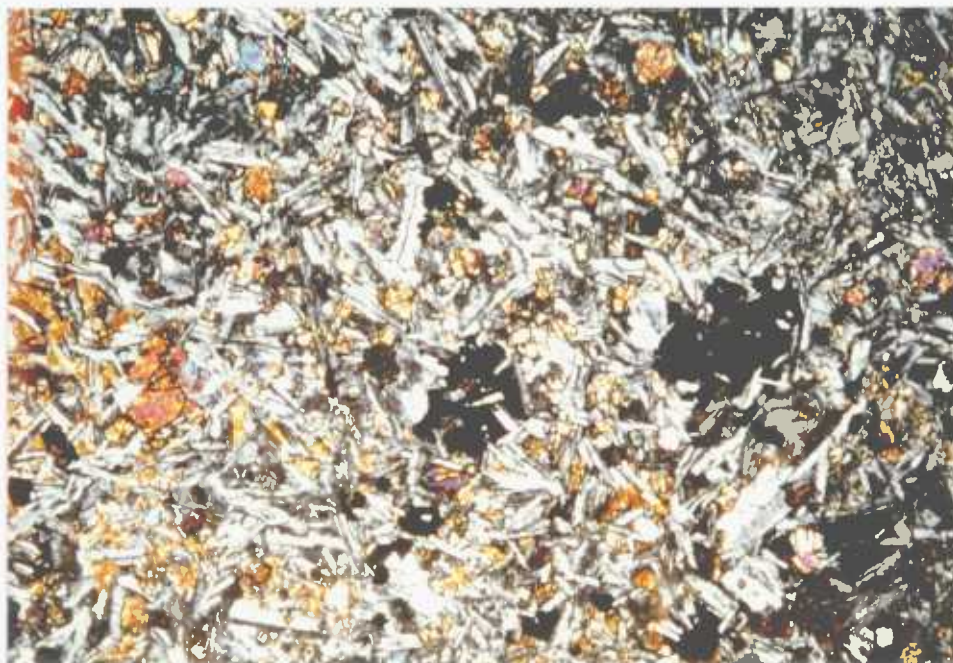


Figure 2 - 2 Basaltic hawaiite, LA 5, containing titanomagnetite poikilocrysts. Both the phenocryst and groundmass olivines appear fresh. Field of view : 3mm by 2.1mm.

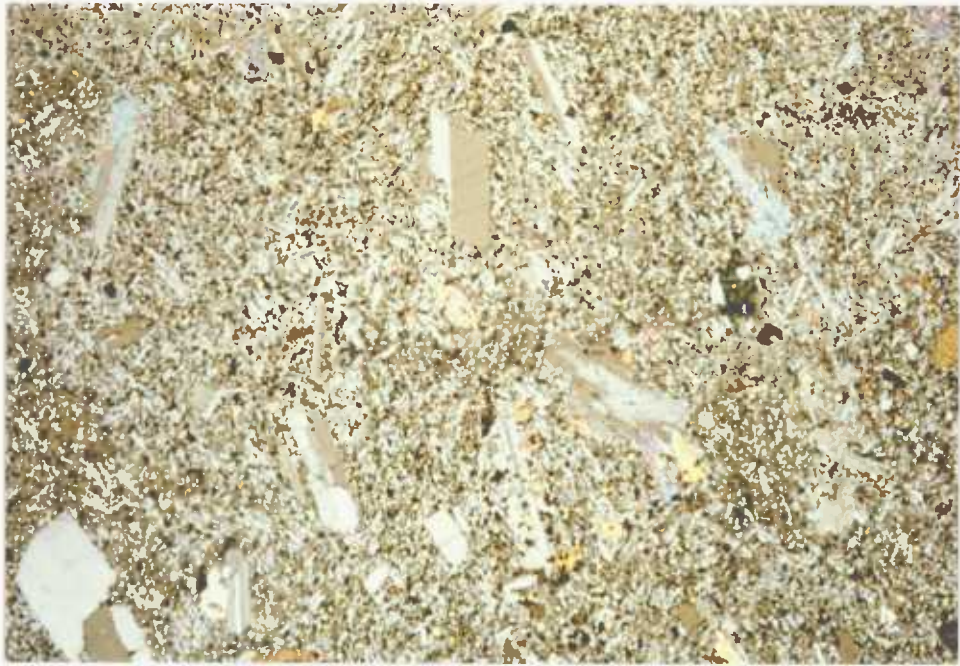


Figure 2 - 3 Hawaiite, M 7, containing fresh skeletal olivines, plagioclase phenocrysts and titanomagnetite microphenocrysts in a microcrystalline groundmass. Field of view : 4.3mm by 3mm.

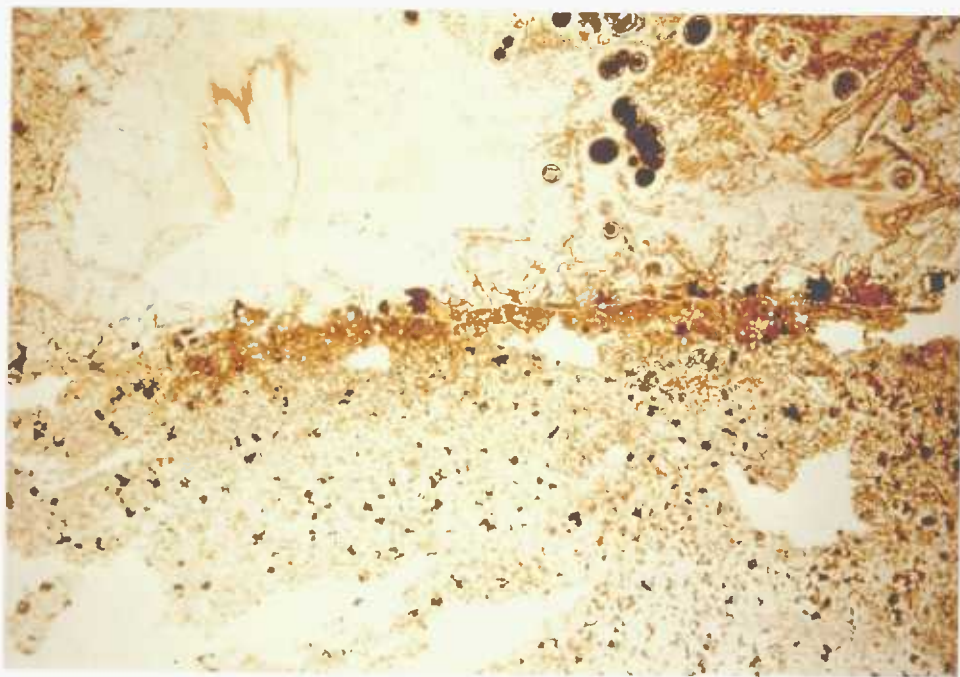


Figure 2 - 4 Vesicle margin in the basaltic hawaiite LA 1-5. Elongate plagioclases project into the vesicle which is surrounded by a thin zone of intensely altered lava.

Field of view : 11mm by 7.6mm.

light can be seen to consist of several equant patches of homogeneous titanomagnetite fringed by maghemite. Rare chlorite patches, some containing brown isotropic glass, were also recognised in the groundmass.

M 5-8 Hawaiite

Plagioclase, frequently containing inclusions of olivine and oxides, is the dominant phenocryst phase in this lava. Occasional microphenocrysts of titanomagnetite also occur. The plagioclase phenocrysts show a sub-parallel alignment and vary widely in size, reaching lengths of up to 1mm in length, and isolated crystals of olivine also occur (see fig 2-3). The groundmass is very fine grained and consists of plagioclase, titanomagnetite, olivine, small pyroxene poikilocrysts and minute irregularly distributed blebs of sulphide. No trace of interstitial glass or its alteration products could be found and all the samples of this lava appear to be virtually free of secondary minerals. M 7 is cut by a thin (0.5mm wide) calcite vein, but no replacement of the adjacent phases, including a feldspar phenocryst bisected by this vein, could be detected.

2. Processes causing primary or deuteric variation

Phenocryst growth and accumulation

The textures and crystal morphologies of these lavas indicate that many of the phenocrysts grew rapidly at relatively low pressures. The skeletal olivine phenocrysts resemble the rapid growth forms described by Drever and Johnston (1957) and numerous references to similar olivines that formed from rapidly-cooled basaltic melts can be found in the literature (e.g. Bryan 1972, Liou 1974). The relative impoverishment in groundmass olivine adjacent to the large skeletal crystals, the tendency for both olivine and plagioclase phenocrysts to enclose groundmass phases and the absence of compositional zoning in most of the phenocrysts all support this idea. Gutmann (1977) has described a suite of alkalic to transitional basalts from the Pinnacate volcanic field, Mexico, with similar textures and phenocryst assemblages to the Mull lavas discussed here. He proposed a petrogenetic model of near-surface crystallation in rising magmas for the Pinnacate lavas. Evolution of water from the melts promoted supersaturation and consequent nucleation and rapid growth of the phenocrysts. Anderson and

Wright (1972) calculated that the loss of 0.8 wt% H₂O from Kilauean lavas would induce the crystallisation of about 20% of crystals. The lavas studied by Anderson and Wright also showed a decrease in oxidation state which they related to loss of sulphur and water from the magmas prior to, and during, eruption. The presence of groundmass biotite and pegmatitic segregation veins associated with vesicles in some of the Mull lavas (described below) indicate that they were hydrous. Thompson (1974) studied a Skye hawaiite similar to M 5-8, which clearly had olivine on its natural liquidus, prior to eruption. During anhydrous melting experiments olivine was not the liquidus phase in this lava at any pressure. The groundmass titanomagnetites in the Mull lavas show little evidence of high-temperature deuteric oxidation, which argues against retention of water by the magmas during crystallisation. The textures and phenocrysts of the Plateau lavas were probably generated during low pressure processes, in a similar fashion to the Pinnacate and Hawaiian lavas discussed above.

Modal analyses (2000.pts.) for all the zeolitised lavas are listed in Appendix 1. All the large crystals regardless of their morphologies were counted as phenocrysts and variable distributions of these within a single flow were only observed in the two magnesian basalts, LA 13-15 and LA 16-18. These two lavas were thus studied in more detail to investigate whether these phenocrysts grew in situ or were accumulated within the flows during crystallisation.

LA 13-15 were collected from the lower five metres of a basalt flow exposed by a road cutting, with LA 13 being nearest to the base of the flow and LA 15 the furthest from it. LA 16-18 came from the underlying lava, which is approximately 23m thick. LA 16 and 17 came from near the upper margin and LA 18 was taken from 15m below these. The olivines in LA 15 (17% olivine 'phenocrysts') rarely contain Cr-spinel (see fig. 2-1) and show a continuous range of compositions between the large crystals and the groundmass phases of Fo₇₁₋₆₂. Cr-spinels are enclosed by many of the subhedral phenocrysts in LA 18 (14.5% olivine phenocrysts). These have compositions of Fo₈₆ whilst the other phenocrysts analysed range from Fo₈₁ to Fo₇₀. These mineralogical variations can be compared with the chemical data and densities of these samples, listed in Table 2-2. Only the apparent abundance of olivine shows any significant variation in LA 13-15,

suggesting that this is due to the growth of larger crystals away from the rapidly chilled margin. LA 18, in contrast, shows an increase in MgO, Ni, Cr and density, relative to LA 16 and 17, and a corresponding decrease in the abundance of elements that would have been excluded from the phenocryst assemblage. It therefore appears that olivine accumulation occurred within this flow.

Table 2-2 Intra-lava variation in two magnesian basalt flows.

Major element analyses were recalculated to 100% for comparative purposes. Trace elements in ppm.

	LA 13	LA 14	LA 15	LA 16	LA 17	LA 18
% olivine phenocrysts	6.75	9.30	17.00	10.00	10.38	14.48
density	2.96	2.92	2.97	2.87	2.91	2.96
MgO	11.55	12.21	11.97	10.36	10.27	12.27
Ni	354	337	328	234	223	292
Cr	785	738	783	517	501	720
SiO ₂	45.73	45.74	46.07	46.11	46.29	45.83
TiO ₂	1.55	1.53	1.55	1.66	1.70	1.60
K ₂ O	.26	.25	.27	.36	.37	.29
Zr	90	88	88	101	102	92

Filter pressing of residual liquids

Evidence for intra-lava migration of the residual melt fraction was observed in several of these lavas. Elongate crystals usually of plagioclase, frequently project into the sparse vesicles. A typical example from the basaltic hawaiite LA 1-5 is shown in figure 2-4. One thin section from the less-magnesian basalt M 1 transected three vesicles, all of which had been filled to varying degrees by minerals that were clearly liquidus phases at the time. Plagioclase laths 2mm in length project into one, the second has ingrowths of both plagioclase crystals and the third is virtually completely filled by a single large pyroxene crystal. In each case, the texture of the surrounding lava demonstrates that these were once gas-filled cavities, the shapes of which were fixed by incipient crystallisation, prior to the magma migration.

The amygdaloidal sample collected from the upper part of the magnesian-basalt LA 16-18 has olivine-free, pegmatitic segregation veins, either surrounding or associated with the vesicles. These vary from 1-5 cm in diameter. The analysed vesicle margin (LA 19 ZR) contains large prismatic clinopyroxenes, up to 0.8mm in length, sodic plagioclases (up to 0.5mm across), which contain numerous apatite needles, acicular and subhedral Fe:Ti oxides, abundant analcite, thomsonite, ankerite and chlorite. The contact (LA 19 R) between this vein and the surrounding basalt is narrow but appears to be slightly gradational, indicating that it was formed before the margin of the lava was completely crystallised. LA 19 ZR contains twice as much K_2O , P_2O_5 , Zr, Y, Rb and Nb as samples LA 16-18. It is also poor in MgO, CaO, Cr, Ni and Sr and enriched in TiO_2 and Na_2O . The chemical changes within LA 16-18 are not all strictly proportional to the variations in olivine content. LA 17 has a higher Na_2O and slightly higher T_2O content than LA 16. Migration of the residual melt phase at varying stages after the onset of groundmass crystallisation could have given rise to this difference. Accordingly intra-lava variations similar to those in LA 16-18 that cannot be directly related to the phenocryst distributions may not necessarily indicate element mobility during secondary alteration.

Segregation veins and vesicles have been described from several other basaltic lava suites. Glassy vesicle infillings have been described from the Non-porphyrific Central lavas of Mull (Bailey et al. 1924), a recent lava lake on Reunion (Upton and Wadsworth 1971) and from the Ordovician Cliefden lavas of New South Wales, Australia (Smith 1967). Pegmatitic segregations of the type seen in Mull have been described from the dykes and lavas of Skye (Harker 1904, Anderson and Dunham 1966) and from the Makaopuhi lava lake, Hawaii (Moore and Evans 1967). Although some reduction in the volume of the gas phase occupying the vesicles must occur during cooling, Smith (1967) demonstrated that this is not sufficient to explain the amount of melt migration observed. He suggested that since the Cliefden lavas were erupted into a shelving marine environment, a downslope increase in the confining pressures would have occurred, causing the necessary reduction in the gas volume. This mechanism cannot be invoked for sub-aerial lavas. The example described by Upton and Wadsworth (1971) appeared to have crystallised under a high partial pressure of oxygen.

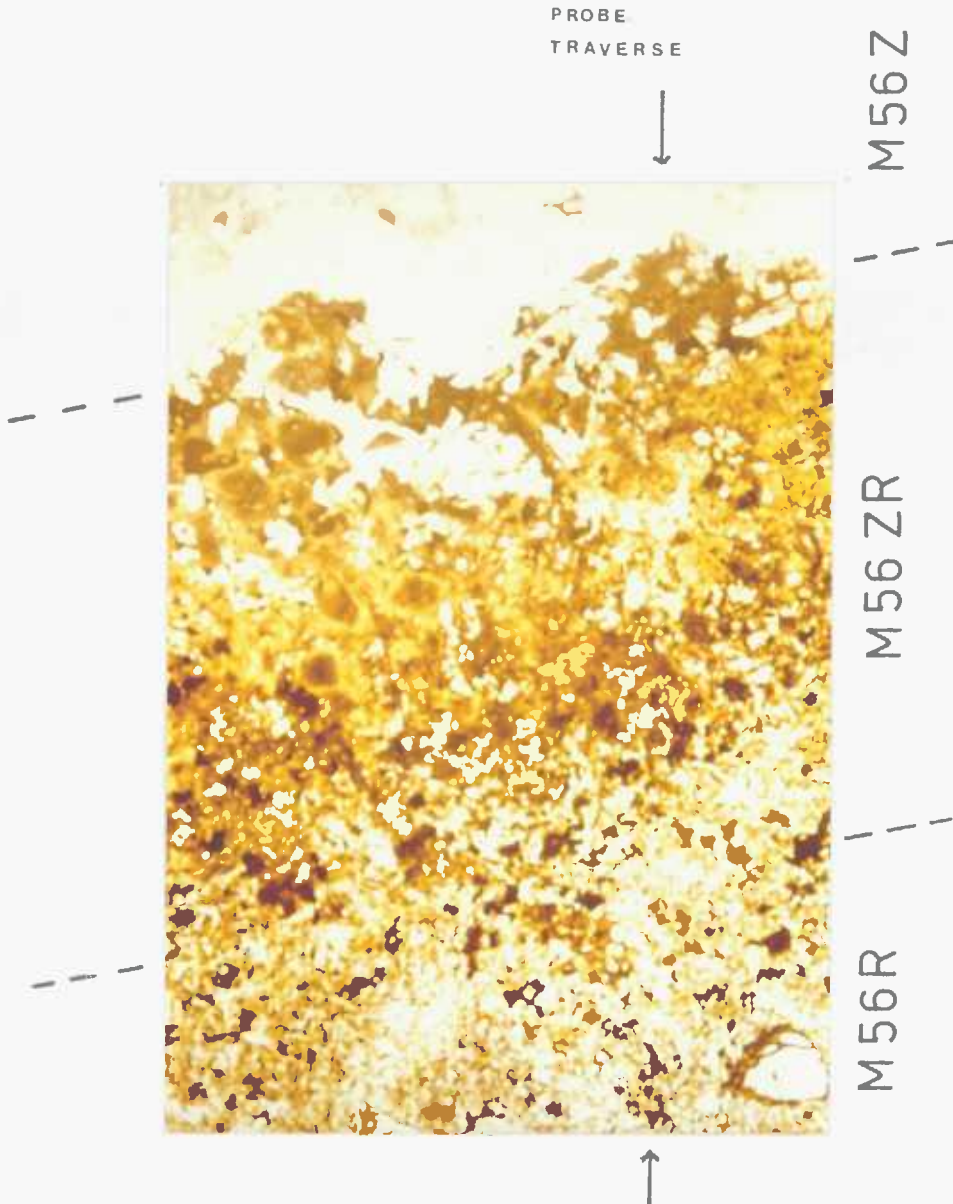


Figure 2 - 5 Altered vesicle surround M 56.
 The positions of the portions removed for analysis are indicated.
 LA 19 was sampled in a similar manner. The microprobe traverse
 discussed in the text was made across the central part of the
 section, shown by the arrows. Note the olivine phenocryst in the
 lower right which shows marginal chlorite growth only.

Field of view : 13mm by 9mm.

They proposed that water present in the vesicles dissolved in the surrounding magma, causing migration of residual silicate liquid by suction to the relatively lower pressure sites.

The groundmass titanomagnetites surrounding the vesicles in sample M 1 show no evidence for deuteric oxidation and the necessary pressure drop in this case may have been provided by diffusion or escape of the gas out of the lava. The Makaopuhi lava lake shows the same association as LA 16-18, namely olivine-free, vesicular, pegmatitic veins in the upper parts and olivine accumulation towards the base. Moore and Evans (1967) attributed the formation of these veins to filter-press action and a similar displacement mechanism is indicated for the origin of these features in the LA 16-18 flow.

3. Distribution of the secondary minerals

A clear alteration sequence can be identified in the zeolitised Mull Plateau lavas. The rare interstitial glass patches appear to have been attacked first by the hydrothermal fluids, followed by olivine and titanomagnetite and finally the plagioclases. In all the lavas extensive replacement of the primary phases was restricted to the thin zones, usually up to a centimetre across, surrounding the sparse amygdaloids. (figs 2-4, 2-5). In these zones the olivines and feldspars tend to be replaced by chlorite and zeolites. On the right hand side of fig 2-4 it can be seen that plagioclases which project into the vesicle have been partially replaced, leaving isolated feldspar fragments inside the vesicle completely surrounded by secondary minerals.

The pyroxenes in all the lavas appear to be unaltered and even ingrowths of this mineral into the vesicles show no signs of secondary mineral growth. Fawcett (1965) described small "chlorite pseudomorphs after pyroxene" in some Plateau lavas collected from outside the central zones of pneumatolysis. Nevertheless, he noted that whenever chlorite and pyroxene were adjacent the contact was sharp. The identification during the present study of small patches of interstitial glass being replaced by chlorite in some lavas suggests an alternative origin for these chlorite 'poikilocrysts'. Since the glass was initially present in small amounts in these lavas (usually <<1%), alteration of this alone is unlikely to produce significant changes in the chemistry of the lavas. In the less-magnesian basalt LA 7-11 the textural combination of large pyroxene poikilocrysts and narrow zones

between them containing glass clearly channelled the hydrothermal fluids through the lava. Alteration of the small, highly-reactive areas of glass provided a means of access for the fluids. As a result, the groundmass olivines, Fe:Ti oxides and feldspars surrounding glass patches were then attacked. A thin section of sample LA 8 shows another example of this phenomenon. Chloritisation of the olivines adjacent to a small vesicle occurs only along approximately a quarter of the vesicle margin; the rest is surrounded by pyroxene.

Apart from the scarce glass, the olivines show the most extensive replacement by secondary minerals. The dominant alteration product is a low-birefringence, pale-green, fibrous serpentine formed along cracks within the phenocrysts and replacing their margins. Secondary iron oxides were rarely observed associated with the serpentine. Many of the phenocrysts have a thin rim of brown fibrous (Fe-rich ?) serpentine. The olivines are replaced by chlorite rather than serpentine, round the margins of vesicles and in the lavas in which some alteration of the feldspars was observed. In the less-magnesian basalt LA 7-11 the small groundmass olivines between the pyroxene poikilocrysts are frequently altered and the associated feldspar laths contain numerous fine chlorite veins, which form reticulate patterns within them. Similar veining was observed in flow M 51-55 and in the magnesian basalts, but only within a few crystals. Zeolitisation of the feldspars and zeolite growth in the flow interiors is rare. Small clusters of zeolites were observed nucleated on groundmass feldspars in the magnesian basalts and zeolites occur associated with chlorite in the groundmass of M 51-55, mainly in the sample from near the base of the flow (M 51) and adjacent to the pipe vesicles (App. I-D, M 56). Similar zeolites form a thin lining of radiating crystals to the amygdales in the lavas (figs. 2-4, 2-5).

A precise identification of the zeolite species was not possible as they could not be separated for X-ray diffraction studies. A potassic variety, almost certainly phillipsite, was detected using the EDS microprobe in M 56R (the lava surrounding the pipe-vesicle section) in flow M 51-55. The others all appeared to be rich in Ca + Na and poor in K, probably thomsonite or mesolite. These are all species with relatively high Al/Si ratios, typical of those found in alkalic rocks and Si-deficient environments (Coombes et al. 1959), as are most

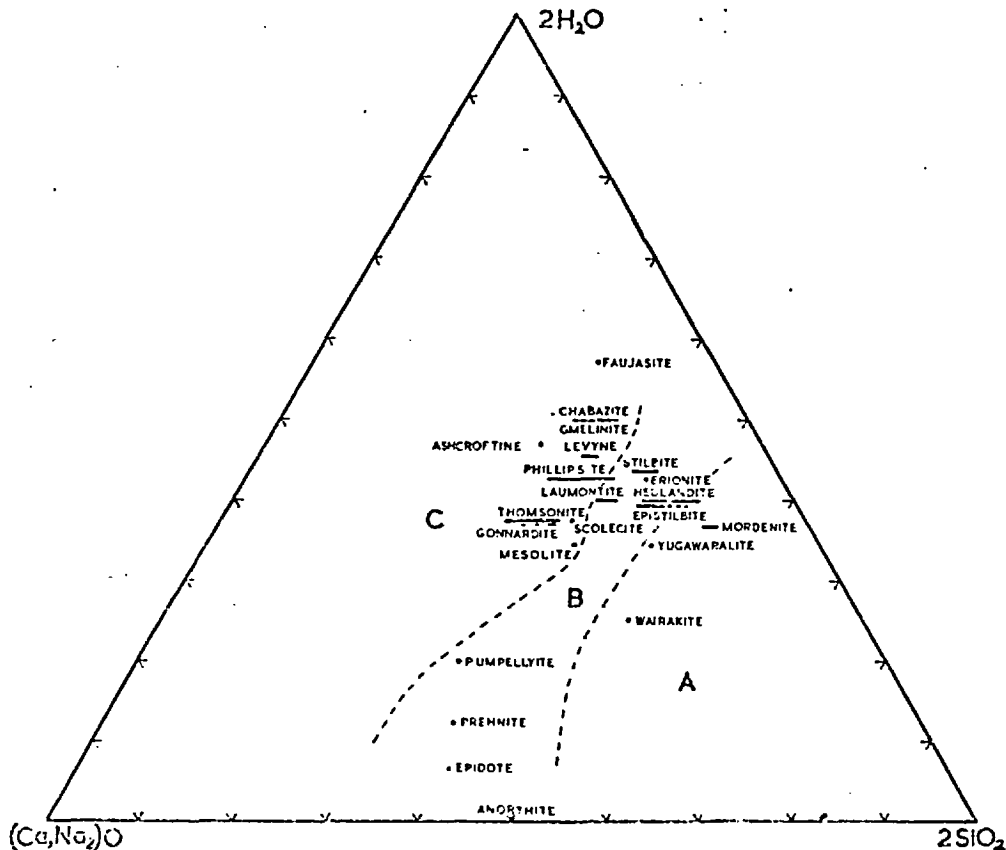


Fig 2-6 Compositions in molar proportions of Ca-rich zeolites and other Ca-Al silicates after Coombes et al.(1959).

- A - field of phases favoured by supersaturation in silica
- B - field of phases which can commonly coexist with quartz
- C - field of phases favoured by a Si-deficient environment.

of the zeolite species described from these lavas by Walker (1970). In contrast, the two amygdales separated for analysis (LA 19Z and M 56Z) are filled almost entirely by the hydrated calcium-silicate gyrolite (Table 2-3). The same mineral appears to occur in the centre of some of the other vesicles in the margins of the lavas. The other secondary minerals observed in the vesicles are chlorite and ankerite and calcite (fig 2-4), which are usually associated with the zeolites lining their margins.

In all the lavas, except the hawaiite M 5-8, some secondary oxidation of the Fe:Ti oxides was observed. The changes observed during this study are similar to those described by Ade-Hall et al. (1971) who documented the effects of hydrothermal alteration on a

Table 2-3 X-ray diffraction data for vesicle infillings
in LA 19 and M 56.

LA 19Z and M 56Z		gyrolite (Mackay+Taylor 1953)		Principal contributing reflections
d Spacing(Å)	Intensity	d Spacing(Å)	Intensity	
21.4	vs	22	vs	0006 only
10.99	s	11.0	s	000.12 only
8.36- } 7.5 } 4.76-4.67	w,d	8.4-7.4 7.4-5.4 4.75	m,d } w,d } w	band 10 $\bar{1}$ 1 11 $\bar{2}$ 1
4.20	m,s	4.20	s	
3.72-3.55 } 3.68 }	w,d s	3.72-3.45 3.65	w,d } ms }	band 20 $\bar{2}$ 1 20 $\bar{2}$ 1 000.36
3.20-3.02 } 3.16 }	w,d s	3.21-3.02 3.12	m,c } vs }	
2.8-2.6 } 2.77 }	w,d m	2.80-2.61 2.80	m,c } m,s }	band 21 $\bar{3}$ 1 000.42 21 $\bar{3}$ 1
-		2.42	w	
-		2.31-2.03 2.31	vw,d } w }	band 22 $\bar{4}$ 1, 20 $\bar{2}$ 1 21 $\bar{3}$ 1 31 $\bar{4}$ 1
?		2.17	w	
-		2.06	w	
-		1.90	w	32 $\bar{5}$ 1
1.80-1.70	w,d	1.82-1.73	vw,d }	41 $\bar{5}$ 1
1.83	m	1.82	s }	

s = strong

v = very

m = moderate

d = diffuse

w = weak

The relative intensities of the peaks were estimated by eye.

variety of oxide phases in basalts. Most of the titanomagnetites show some conversion to maghemite along cracks and around their margins (c.f. Ade-Hall et al. figs. 3a and 4a). In flow LA 7-11, the Fe:Ti oxides were never enclosed by pyroxene and are considerably altered. Many of the small crystals are extensively granulated and replaced by titanohematite or maghemite and one or two appear to show incipient haematisation of the margins (c.f. op.cit. fig 3c). Several contain relict patches of unaltered Fe:Ti oxide and in each case the sparse ilmenite lamellae appear to have been more resistant and are less altered than the associated titanomagnetite. Analyses of the oxides were recalculated on either the spinel or rhombohedral basis using the method of Carmichael (1967) and gave low totals of between 96-99%, due to the secondary oxidation. It can be seen from Appendix 1-D that the most respectable totals were obtained from the hawaiite M 7, in which little oxidation was observed, and that in each case the ilmenite lamellae gave higher totals than the titanomagnetites.

4. Intra-lava chemical variation

The whole-rock chemical analyses are listed in Appendix 1-E and examination of this shows that the individual lava flows are remarkably uniform in both their major and trace element abundances. Only the magnesian-basalt LA 16-18 (discussed above) shows variations in all the major and trace elements. Flows LA 13-15 and M 51-55 show changes of up to 60 ppm in their Sr contents and all the MFG lavas have variable $\text{Fe}_2\text{O}_3/\text{FeO}$ ratios but constant values of total iron. The largest variations in this ratio occur within the less-magnesian basalt LA 7-11, in which extensive alteration of the Fe:Ti oxides was observed. In addition, LA 7, which was collected from close to the upper margin of this lava, is enriched in Ca and depleted in Mg relative to LA 8-11.

Figure 2-7 shows that there is no correlation between $\text{Fe}_2\text{O}_3/\text{FeO}$ ratio and H_2O content in these lavas due to the fact that the principal reaction involved is oxidation rather than hydration. In the two magnesian basalts LA 13-15, LA 16-18 both $\text{Fe}_2\text{O}_3/\text{FeO}$ and H_2O increase towards the margins. Similarly, no overall correlation between Sr and H_2O contents could be found, but comparison of figures 2-7 and 2-8 shows that the marginal increase in iron oxidation and water content in LA 13-15 is accompanied by a slight decrease in Ca and Sr content,

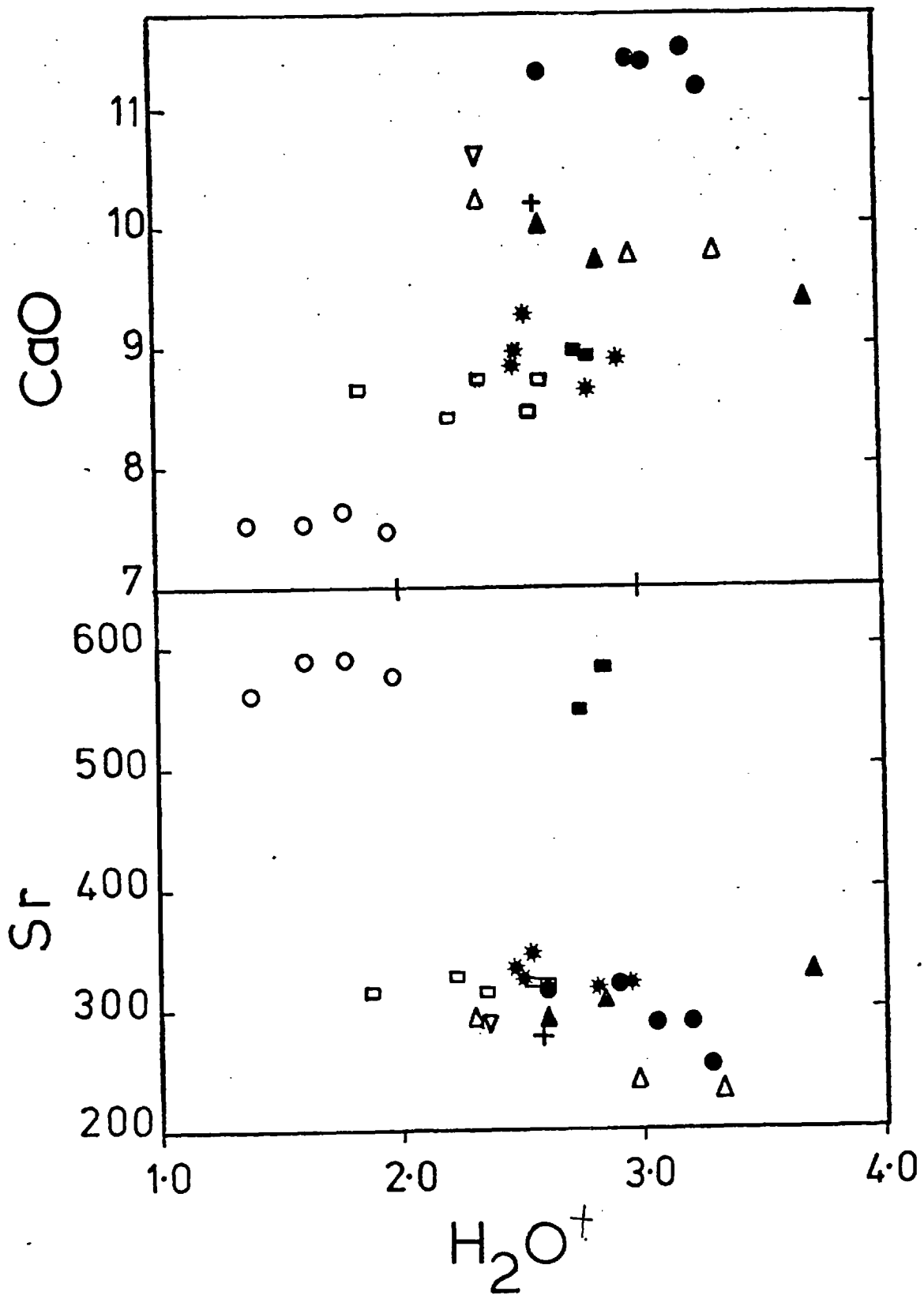


Fig 2-8 Sr and CaO versus H_2O^+ for the neolitised lavas.
 Symbols as in fig 2-7.

whilst Sr and Ca also vary together in M 51-55. The only trace element detected in significant quantities in the amygdale samples LA 19Z and M 56Z was Sr, suggesting that these variations are due to hydrothermal alteration. In each of these two lavas the changes in CaO content are slight and only just exceed the analytical uncertainties (see Appendix 11). Figures 2-7 and 2-8 also show a crude positive correlation between MgO and CaO content and H₂O in all the lavas, despite the lack of intra-lava variation of these elements. This correlation reflects the fact that the most extensive hydration preferentially affects the olivine-rich basalts.

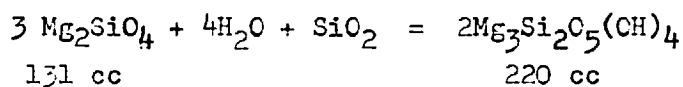
The sparse vesicles in the margin of the magnesian basalt LA 7-11 are mainly filled with Mg-rich ankerite. LA 7 is enriched in CO₂ (.43%), relative to the other samples from this lava (.21-.09% CO₂). Extensive alteration of the olivines surrounding the vesicles in LA 7 was observed, suggesting that some Mg was removed by the hydrothermal fluids during alteration. Although the groundmass feldspars in this lava are cut by small chlorite veins, the feldspars are less extensively altered than the associated olivines. Accordingly, the slightly higher CaO content of LA 7, relative to LA 8-11, might be due to the addition of calcium by the same fluids. The thin calcite vein observed cutting the hawaiite sample M 7 clearly demonstrates that some Ca was carried by these solutions.

The chemical composition of the altered basalt zone surrounding the studied vesicle in the LA 16-18 magnesian basalt flow (LA 19R and ZR) cannot be used to gain information on element mobility, as it is mainly composed of a segregation-vein. In contrast, flow M 51-55 provides suitable material for this purpose. The thin section through the pipe-vesicle margin (M 56), taken from the lower part of M 51-55, shows no textural differences from the rest of the lava. It clearly contained olivine, now pseudomorphed by chlorite (fig 2-5). A microprobe traverse was made across M 56 and the pyroxenes analysed. These are plotted in figure 2-9, together with those of the other zeolitised lavas. It can be seen that they show a similar range of compositions to those determined in sample M 55 which was collected well outside the pipe-vesicle zone. It is therefore legitimate to compare the chemical composition of M 56R and ZR with that of other parts of the M 51-55 flow, in order to assess the chemical effects of small-scale

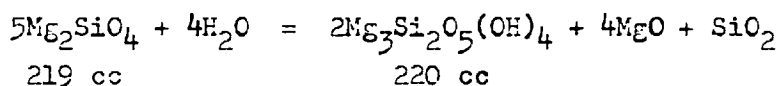
severe, zeolite-facies alteration.

Relative to M 51-55, samples M 56R and M 56ZR are slightly depleted in SiO_2 , Al_2O_3 , CaO , Na_2O and K_2O and enriched in all the other elements. Figure 2-10 shows the chondrite-normalised rare-earth patterns of M 56ZR, and M 51 and M 53, collected from the margin and centre of the lava, respectively. The REE patterns of these two samples are indistinguishable from each other. M 56ZR is slightly enriched in all the REE, relative to the other two samples. The increase in the abundances of the REE in M 56ZR is proportional to the increases in the other elements. Ratios between an average composition for M 51-55 and M 56ZR (i.e. M 56ZR/M 51-55) give values of 1.17, 1.13, 1.19, 1.15, 1.18, 1.17, and 1.15 for Ce, Yb, Hf, TiO_2 , Ni, Cr and MgO respectively. The decreases in SiO_2 , Al_2O_3 , Na_2O , CaO and K_2O are also proportional to each other, giving ratios of between 0.93 and 0.95 for M 56ZR/M 51-55. This indicates that leaching of these elements during hydrothermal alteration resulted in an apparent enrichment of the vesicle surround in less-mobile elements. The proportionality between the REE elements, TiO_2 and Mg and Ni supports the petrographic and mineralogical evidence that residual melt migration did not occur in this particular case.

The conversion of olivine to serpentine is usually expressed by a reaction of the type :-



If constant volumes are preserved during alteration then the following reaction, which does not imply the addition of extra SiO_2 , probably applies :-



The conversion of olivine to chlorite involves addition of Al, but petrographic evidence for this reaction was only observed in lavas in which associated groundmass feldspar was also altered, and up to 3% CaO was detected in chlorite replacing olivine phenocrysts (Appendix 1-D, M 55). The presence of minute chlorite veins cutting the groundmass feldspars clearly demonstrates that some of the olivine constituents were lost during alteration and chemical exchange between the igneous phases clearly occurred. Nevertheless, the constant bulk

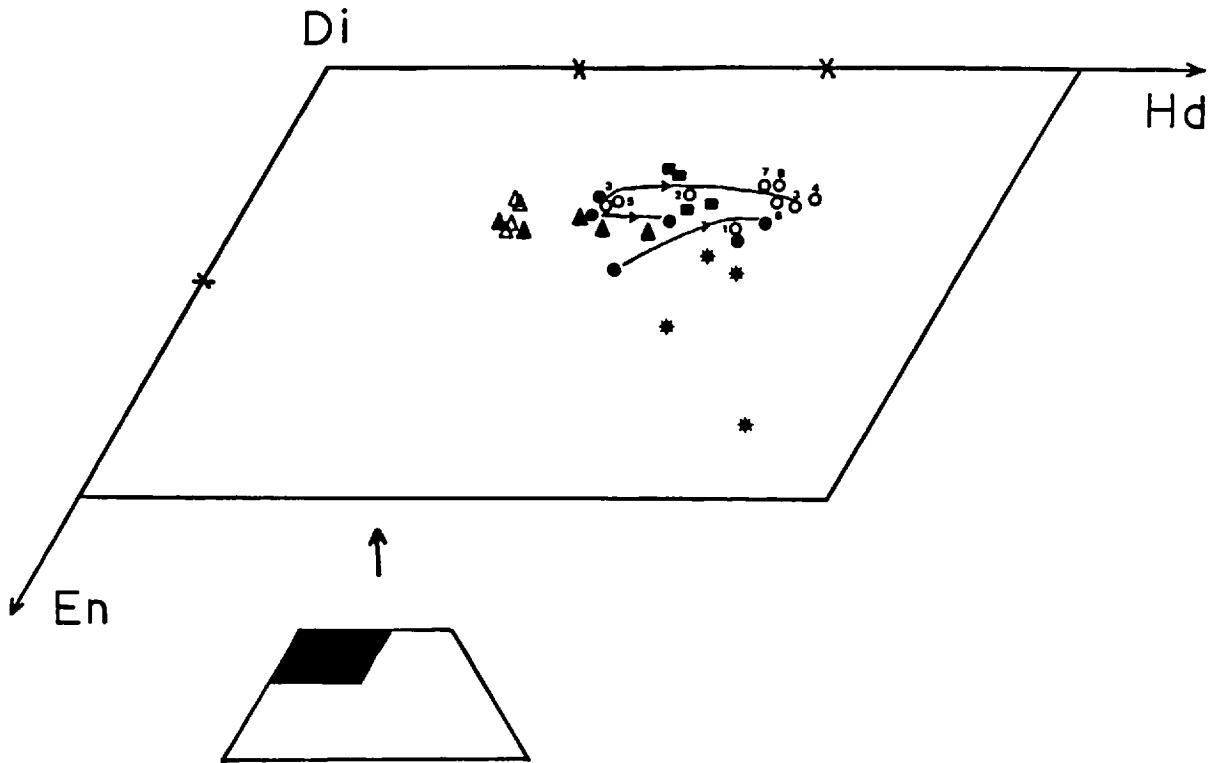


Fig. 2 - 9 Groundmass pyroxenes from the zeolitised lavas. Arrows point from cores to rims of poikilocrysts. Numbers refer to positions of crystals in traverse across M 56, 1 being 1.5cms from vesicle margin and 8 projects slightly into the vesicle.
 ▲ LA 18, △ LA 15, ● M 55, ○ M 56, ■ M 12, * LA 7.

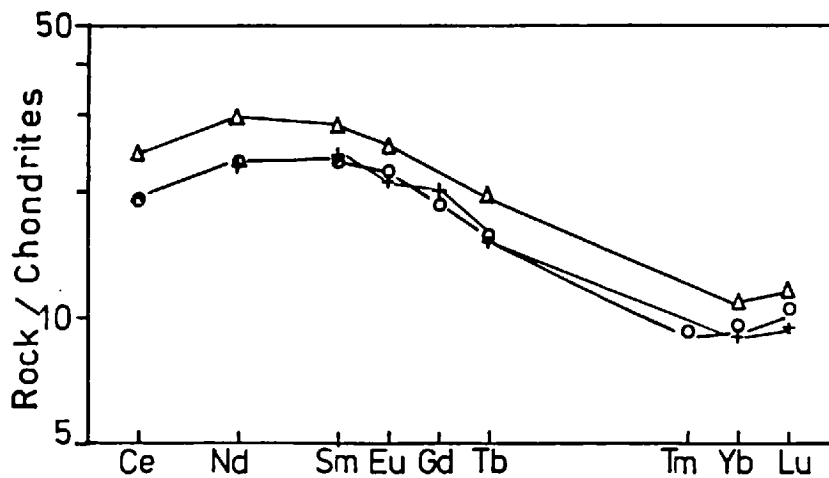


Fig. 2 - 10 Chondrite-normalised REE patterns for samples from flow M 51-55. + M 51, ○ M 53, ▲ M 56ZR.

Chemical compositions of these lavas suggests that this redistribution occurred on a scale smaller than that of the individual samples (approximately 2kgm wt.) crushed for analysis.

In contrast, the depletion in SiO_2 , Al_2O_3 , CaO , Na_2O and K_2O in M 56ZR, relative to M 51-55, suggests that the volume changes during intense alteration of this small volume of rock were accommodated by preferential migration of the feldspar constituents into the vesicle. The zeolites lining the vesicle have relative proportions of these elements similar to feldspar; the formation of thomsonite from anorthite, for example, can be expressed by a simple hydration reaction (Coombes et al. 1959). If the elements released during alteration of these relatively small basalt volumes (figs 2-4, 2-5) were consumed during the formation of zeolites lining the vesicles, then an additional source of both Ca and Si is required for the formation of the gyrolite occupying their centres.

To investigate the possibility that material may have been added to some of these lavas during alteration, Sr isotope determinations were made on some of the samples. Despite the large variations in Sr content in the magnesian basalt LA 13-15, initial $^{87}\text{Sr}/^{86}\text{Sr}$ ratios of 0.70423 ± 7 and 0.70426 ± 7 were obtained on LA 13 and LA 15, respectively. In the LA 7-11 flow LA 7, the Ca-enriched marginal sample, had $(^{87}\text{Sr}/^{86}\text{Sr})_i = 0.70433 \pm 7$, thus showing a small but significant difference from LA 9, at the centre of this flow, which has $(^{87}\text{Sr}/^{86}\text{Sr})_i = 0.70414 \pm 7$. In contrast, M 56ZR and M 56Z have $(^{87}\text{Sr}/^{86}\text{Sr})_i$ ratios of 0.70297 ± 5 and 0.70424 ± 6 , respectively. The value for M 56ZR agrees well with that of 0.70306 ± 4 obtained for this particular lava by Beckinsale et al. (1978, Table 4 sample M 168) and supports the hypothesis that the bulk of the amygdale minerals in these lavas were not derived from the lavas in which they occur.

5. Copper and zinc distribution

In contrast to the minor chemical changes discussed above, large differences in the abundance of Cu and Zn were detected within several of the zeolitised lavas. The largest variations occur in the hawaiite M 5-8, in which Cu varied from 308 to 45 ppm and Zn from 226 to 80 ppm. No correlations could be found between the Cu and Zn contents and any of the other major and trace element abundances or ratios,

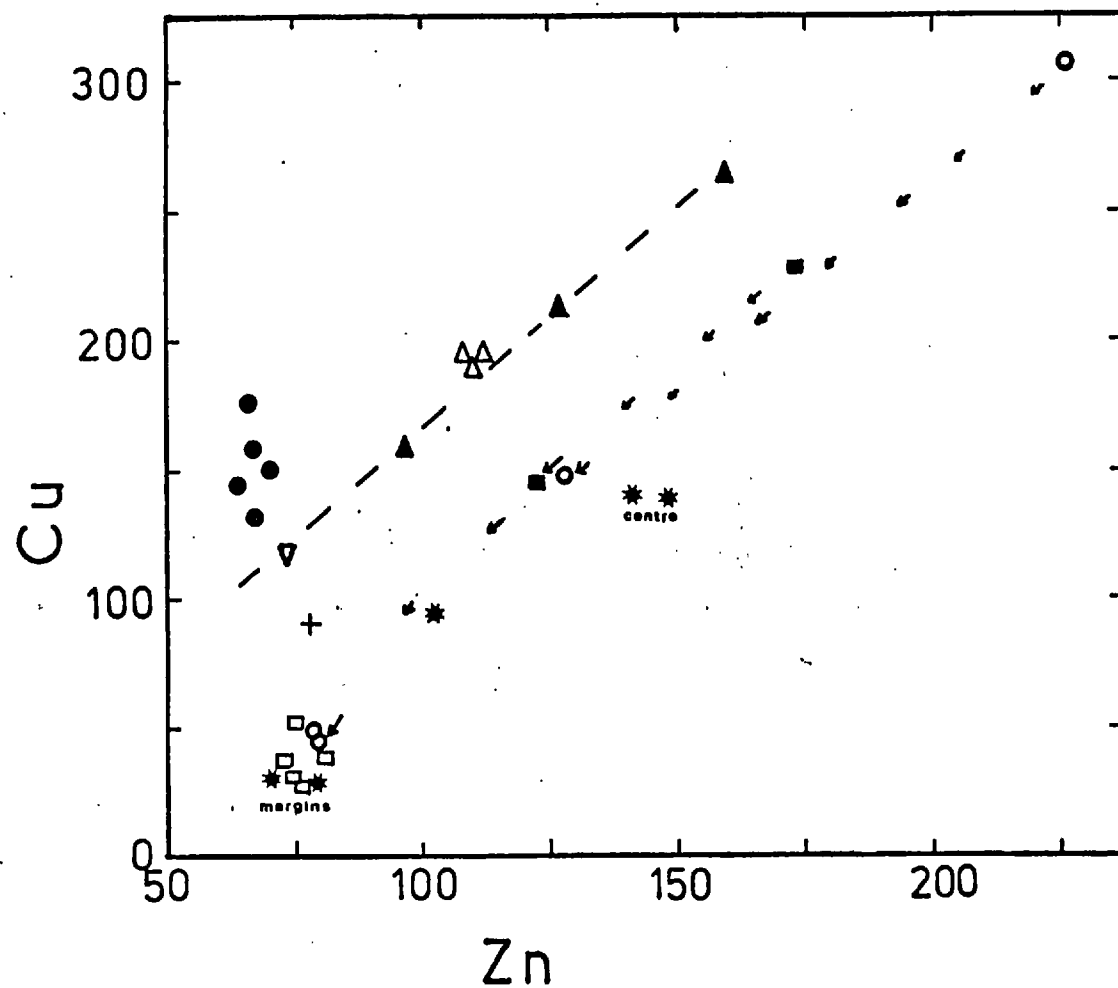


Fig 2-11 Covariance of Cu and Zn in the zeolitised lavas. Symbols as in figs 2-7 and 2-8. Arrows point from centres to margins of individual flows. See text for discussion of the dashed line.

in the MGP lavas suggesting they are due to the irregular distribution of sulphide phases within the lavas. Groundmass sulphides were observed in three of the lavas in which these variations occur, but not in the magnesian-basalts or M 51-55.

In the magnesian basalt LA 16-18 the highest concentrations of these two elements occur in LA 17 and the lowest in LA 18. On a plot of Cu against Zn (fig 2-11) these samples lie on a straight line (shown as a dashed line) which if extended passes through the origin. The other magnesian basalts lie close to, or on, the same line as samples LA 16-18. The constant Zn/Cu ratio of this flow and the evidence for both phenocryst accumulation and residual melt migration within it suggests that the Cu and Zn distributions within this particular lava may be primary.

The origin of the variable Cu and Zn contents in the other lavas is less clear. In each case the Zn/Cu ratio increases, but the overall Cu and Zn contents decrease towards the margins of the flows. Relative to LA 16-18, the altered vesicle surrounds from this flow have both higher Zn/Cu ratios and lower Zn and Cu contents. M 56R and M 56ZR are enriched in Zn, but not Cu, relative to M 51-55. Taken at face value, these data suggest that Cu and Zn were leached from the lavas during zeolitisation, with Cu being more easily mobilised than Zn. Against this must be set the fact that the largest variations occur in the hawaiite, M 5-8, and the less-magnesian basalt, M 11-12, which show virtually no petrographic alteration, whilst LA 13-15 and M 51-55 show little or no variation.

Primary groundmass sulphides are common in Tertiary Hebridean dykes but virtually unknown in lavas of similar composition (Ade-Hall and Lawley 1970). Ridley (1973) found primary pyrite and chalcopyrite in several of the Small Isles dykes, but not in any of the "obvious lava flows" (op.cit. page 3). He attributed this difference to diffusion of sulphur out of the lavas into the air. Sulphur loss from subaerial basalts is a well documented process and Anderson and Wright (1972) showed that in Kilauean lavas it caused a reduction of the margins of the Fe:Ti oxide crystals. The formation of secondary maghemite in the Mull lavas precludes any detailed studies of the primary oxidation states of the titanomagnetites, although they show little evidence for deuteric oxidation. Nevertheless, the higher Cu

and Zn contents of the lava centres could also be explained, if the saturation of the magmas in sulphur indicated by the presence of the minute blebs of sulphide observed in them, occurred when sufficient crystallisation had taken place to prevent further diffusion of volatiles out of the flows. Sulphur gradients could thus be established with the highest concentrations of sulphur occurring in the flow centres, leading to greater amounts of sulphide formation in these parts of the flows.

6. Effects of zeolite-facies alteration on Si-saturation

The secondary oxidation of the Fe:Ti oxides in these lavas causes Fe_2O_3 to vary between a maximum value of 9% in less-magnesian basalt, LA 7-11, and 1.4% in LA 20. This range can be contrasted with the Fe_2O_3 values found in fresh basalt glasses (Table 2-4). CIPW norms were calculated for the zeolite-facies lavas, using both the measured Fe_2O_3 values and standard values as proposed by Thompson et al. (1972). The results are shown in figure 2-12 and the degree of Si-saturation expressed as the percentage of normative hypersthene or nepheline listed in Table 2-5.

Table 2-4 Fe_2O_3 contents of basalt glasses.

1	2	3	4	5	6	7	8	9
1.59	1.42	2.41	1.87	1.62	1.74	1.40	1.61	1.10
Sources :								
1-7			Murata and Richter (1966)					
8			Tilley and Thompson (1970)					
9			Smithsonian Institute Standard MORB glass - USNM 113716 (Staudigel 1979)					

Tilley and Muir (1962) proposed that oxidation and selective leaching caused an increase in the degree of Si-saturation and this is borne out by the results obtained in this study. Nevertheless, few of the norms of these lavas calculated using the standard values of Fe_2O_3 are ne-normative and they show variations in the degree of Si-saturation within individual lava flows. Calculation of the norms on

a CO₂-free basis reduced both the degree of Si-saturation and the within-flow variation. The addition of CO₂ in the form of carbonate during zeolitisation clearly affects the CIPW norm. The uncertainty as to whether or not small amounts CaO have been added or removed makes the effect of this difficult to assess. LA 7-11 is the most hy-normative of all the lavas but the pyroxenes in this basalt are also less calcic than those of the other lavas (fig 2-9) suggesting this is a magmatic not a metasomatic feature.

Table 2-5 Si-saturation in the zeolitised lavas expressed as %
normative nepheline or hypersthene or quartz.

1- measured Fe₂O₃ values

2- Standard values Fe₂O₃ after Thompson et al. (1972)

3- CO₂-free basis using standard values Fe₂O₃.

Sample	1	2	3	Sample	1	2	3
LA 1	12.6 hy	6.1 hy	5.1 hy	M 1	0.3 ne	1.5 ne	-
LA 3	12.9 hy	7.9 hy	7.5 hy	M 5	7.6 hy	3.0 hy	2.1 hy
LA 5	11.8 hy	8.1 hy	7.4 hy	M 6	0.5 hy	0.5 ne	0.6 ne
LA 4	10.9 hy	7.1 hy	6.7 hy	M 7	3.9 hy	0.2 ne	0.3 ne
LA 2	9.5 hy	5.7 hy	5.4 hy	M 8	4.1 hy	0.8 hy	0.7 hy
LA 7	1.5 qtz	11.9 hy	8.5 hy	M 11	4.4 hy	1.2 hy	0.3 ne
LA 8	16.9 hy	12.1 hy	10.5 hy	M 12	6.9 hy	1.9 hy	0.8 hy
LA 9	2.4 qtz	12.5 hy	11.4 hy	M 51	4.1 hy	0.04 hy	0.2 ne
LA 10	2.9 qtz	11.6 hy	10.1 hy	M 52	4.4 hy	3.5 hy	3.0 hy
LA 11	14.5 hy	8.0 hy	7.3 hy	M 53	3.2 hy	1.0 hy	0.5 hy
LA 13	11.1 hy	9.9 hy	8.1 hy	M 54	5.5 hy	3.8 hy	3.5 hy
LA 14	11.8 hy	10.0 hy	9.4 hy	M 55	3.5 hy	0.02 hy	0.6 hy
LA 15	3.7 hy	2.5 hy	2.0 hy	LA 19R	11.5 hy	4.8 hy	-
LA 16	12.1 hy	8.1 hy	7.7 hy	LA 19ZR	10.3 hy	0.1 hy	-
LA 17	4.7 hy	1.3 hy	0.8 hy	M 56R	6.8 hy	0.01 ne	-
LA 18	9.0 hy	7.3 hy	7.2 hy	M 56ZR	11.0 hy	3.2 hy	-
LA 20	2.2 ne	2.2 ne	-				

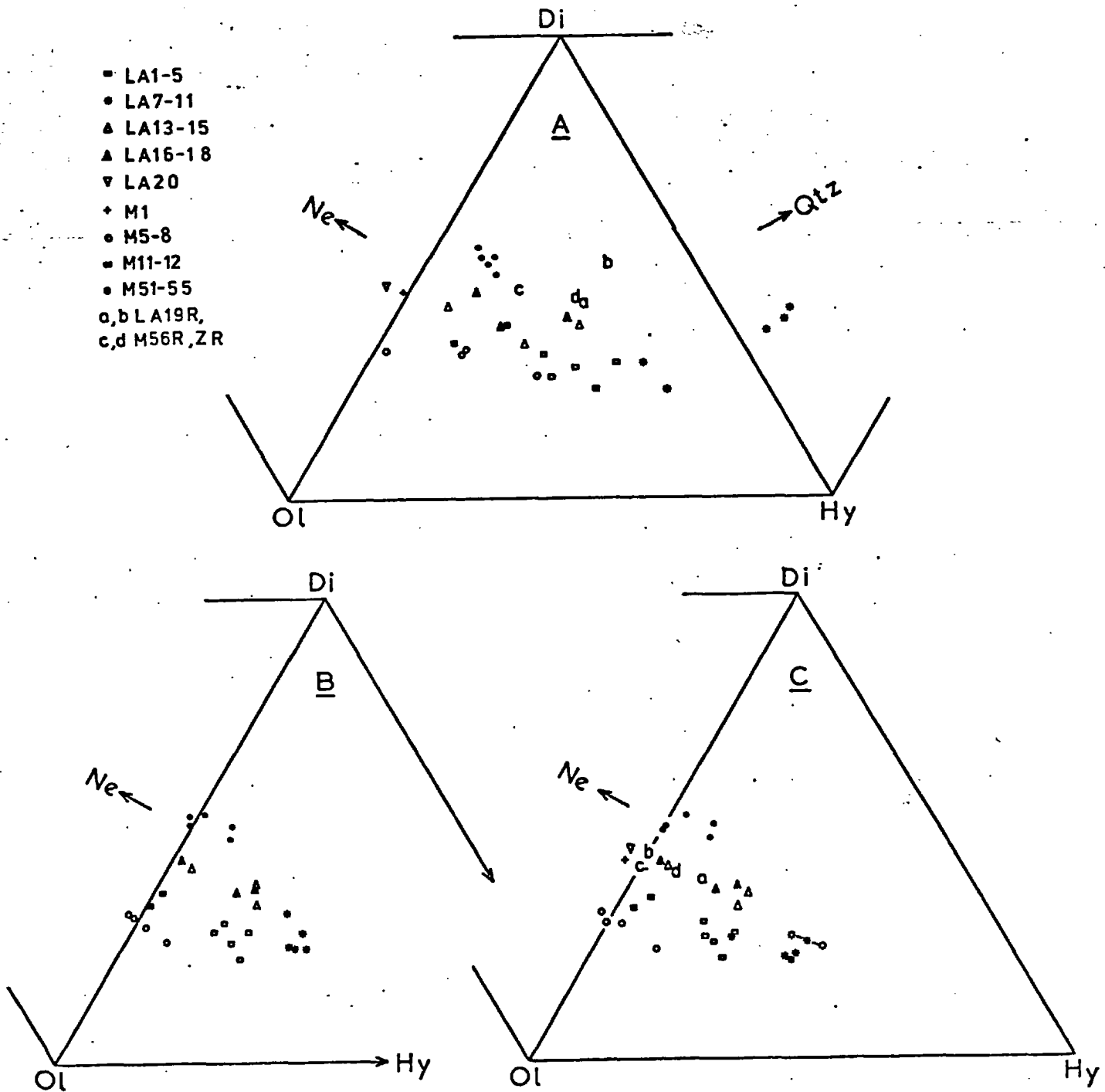


Fig 2-12 Normative diagram for the zeolitised lavas calculated as follows -

- A - using measured Fe_2O_3 values,
- B - standard Fe_2O_3 , CO_2 -free basis,
- C - standard Fe_2O_3 values.

The hollow symbols in figure 2-12c show the effect of adding and subtracting 0.05% Na₂O to the analysis of one of the lavas and shows that most of the observed intra-lava variation in Si-saturation is due to very small differences in alkali content. M 56ZR is no more hy-normative than M 51-55 and these differences within the lavas may not in fact be due to secondary processes. The largest variation in Si-saturation occurs in the magnesian basalt LA 16-18, in which both olivine accumulation and migration of the residual melt occurred, suggesting that much of the observed intra-lava variation is primary in origin.

Beckinsale et al. (1978) proposed that the zeolite-facies Mull lavas were essentially "unaltered" and that all the basalts were hy-normative. The Fe₂O₃ values recorded by Beckinsale et al. range between 1.6 and 5.8% and hence may indicate secondary oxidation. In contrast, Tilley and Muir (1962) suggested that the basalts were originally all ne-normative. The results obtained in this study suggest that the effects of secondary alteration were under-estimated and over-estimated by these authors, respectively, and that the Mull Plateau Group contains both ne- and hy- normative basalts.

Conclusions to chapter two.

1. Many, but not all, of the phenocrysts in the Mull Plateau lavas grew rapidly at low pressures in response to evolution of water from the magmas, prior to or, during eruption and emplacement. The magnesian basalts contain two generations of olivine phenocrysts - an early forsteritic one, Fo₈₆₋₈₅, enclosing Al-rich chromites and a later one of variable composition which never enclose spinels. In one massive flow olivine accumulation and concomitant upwards displacement of the residual melt occurred, but the other lava flows were unaffected by redistribution of the phenocryst phases.
2. Despite the hydrous nature of the magmas, little deuteric oxidation occurred. At a late-stage in their crystallisation the less-magnesian basalts became saturated in sulphur and sulphur gradients were established which caused groundmass sulphides to be concentrated towards the centres of the flows. These sulphides probably represent droplets of an immiscible sulphide liquid which formed at a relatively late-stage in the crystallisation of the lavas.

3. The formation and distribution of secondary minerals within the lavas was controlled by the compositions and crystallisation histories of the individual flows. The principal chemical effects of zeolite-facies alteration were hydration and oxidation. Sr shows limited mobility (<20% variation) in those flows in which some alteration of plagioclase occurred. More substantial changes are confined to within only a few mm of vesicles, where the volume changes associated with secondary mineral growth were accommodated by preferential migration of the feldspar components into the vesicles. Nevertheless, despite the varying compositions of the host lavas, the vesicle infillings in the flow margins are chemically and mineralogically similar (Table 2-3, Appendix I-E, LA 19Z and M 56Z), and most of these amygdale minerals were not derived from the basalts in which they occur. Instead the fluids which interacted with the lavas must have contained Ca and Si for which some external source is required.
4. Although secondary oxidation of the lavas caused an increase in the degree of Si-saturation, the most hy-normative flow contains the least calcic-pyroxenes and some of the variation in Si-saturation is primary in origin. The Mull Plateau Group contains both ne- and hy-normative basalts.

CHAPTER THREE : GREENSCHIST-FACIES LAVAS

The igneous mineralogy of many of the greenschist-facies lavas has been completely or partially destroyed. Nevertheless, in most lava flows, samples could be found in which the igneous textures and minerals were relatively well preserved. These show that, prior to alteration, the greenschist-facies and zeolite-facies lavas were similar petrographically. Brief descriptions of the greenschist-facies lavas are given in Table 3-1. No attempt at chemical classification was made, but they have been divided into three main types on the basis of their phenocryst assemblages which may correspond to the divisions into magnesian basalt, less-magnesian basalt and hawaiite made for the zeolite-facies lavas. Type A contains olivine and Cr-spinel, type B is plagioclase and olivine-phyric and type C contained phenocrysts of titanomagnetite in addition to olivine and plagioclase.

In three cases plagioclase phenocrysts only were identified. One of these (M 59) appears to be an evolved lava type whilst, the other two (M 47-50 and C 176) are extensively altered. In many samples from the other lava flows 'ghost' plagioclase crystals can be recognised, even when all the igneous phases have been replaced by secondary minerals. Hence, M 47-50 and C 176 may have originally contained other phenocryst phases in addition to plagioclase.

1. Mineral transformations during greenschist-facies alteration

A similar alteration sequence could be identified in the greenschist-facies to that in the zeolite-facies lavas. Fresh olivine was found only as small relict patches in one sample, M 35. One lava (M 41-46) contained unaltered plagioclases and slightly oxidised titanomagnetites but in all the other flows these two minerals have been completely or partially replaced. Unaltered pyroxene occurs in several samples and this mineral is only completely replaced in some flow margins or in highly vesicular or hydrothermally brecciated samples. The reactions appear to have been similar in most of the lavas and the chemical differences between the flows can be related to the relative abundances of the primary minerals and their alteration products. The principal mineralogical changes are summarised diagrammatically in figure 3-1. These reactions rarely appear to have reached equilibrium and considerable differences in the composition of the

Table 3-1 Mineralogy and textures of greenschist-facies lavas.

Phenocryst assemblage	Lava flow	Description
A olivine and Cr-spinel	M 13-22 & C 54-158 olivine-rich lava Pennygown Quarry.	Contained both skeletal and subhedral olivines up to 3mm diameter, the latter enclosing Al-rich chromites. Spinels and pyroxenes show little alteration throughout most of section, other phases show variable degrees replacement. Upper margin of flow has rare segregation-veins 2-3cms wide, similar but narrower 1.0-0.5cm wide structures associated with vesicles at base of flow.
B olivine and plagioclase	M 29-32 Toll Doire quarry lava	Olivines varied from 2-0.5mm diameter, plagioclases up to 2 mm by 0.5mm. All samples intensely altered, olivine pseudomorphs only recognisable in M 29, pyroxene completely replaced in M 30.
	M 34-36	Altered olivine phenocrysts up to 2mm diameter, plagioclases up to 1mm by 0.5mm. Large groundmass pyroxene poikilocrysts up to 3mm across. Titanomagnetites granulated and oxidised but sphene formation limited, consist mainly of titanohamete, maghemite, etc. One or two of the olivines in M 35 have unaltered cores.
	M 37-38	
C olivine, plagioclase & titanomagnetite	M 41-46	Fine-grained lava with plagioclases varying in size from irregular phenocrysts 0.6 by 0.1 mm to small groundmass laths. Contains small chlorite pseudomorphs after olivine microphenocrysts and oxidised titanomagnetite phenocrysts. Only slightly altered, both centre and margin of flow containing some unaltered plagioclases (An ₅₃₋₅₄).
	M 45	Intensely altered, some small relict patches pyroxene. Olivine and titanomagnetite phenocrysts barely recognisable.
	C 191-232a/b plagioclase- phyric lava in drill core	Rare, rounded plagioclase phenocrysts 4mm by 1mm, other plagioclases vary from euhedral to anhedral and are up to 2mm in diameter, some had inclusions of olivine and titanomagnetite. Had microphenocrysts of titanomagnetite (now mixtures of sphene and Fe:Ti oxides) and olivine (now chlorite). Extent alteration variable, 9 out of 14 slides examined contain relict pyroxenes.
	M 26-28	Very fine-grained and similarly texturally to M 5-8 (fig. 2-3), but had fewer phenocrysts and contained occasional rounded plagioclases up to 3mm in diameter. Relict pyroxenes recognisable in all thin sections but shows extensive alteration and contains numerous secondary mineral pods (fig 3-15)
Plagioclase and ?	M 47-50	Intensely altered lava, hydrofractured and brecciated by calcite-stilbite vein (M 49). All samples contain "ghost" plagioclases, M 47 and M 50 have relict pyroxenes.
	C 176 thin, plagioclase phyric layer above breccia in drill core	Texturally similar to C 191-232a/b, but only "ghost" plagioclases identifiable.
	M 59	Contains occasional feldspar phenocrysts up to 0.6mm in diameter. Groundmass rich in Fe:Ti oxides, many of which may be microphenocrysts, also numerous small feldspar laths and pyroxene poikilocrysts. Was either, very poor in olivine or, olivine-free.

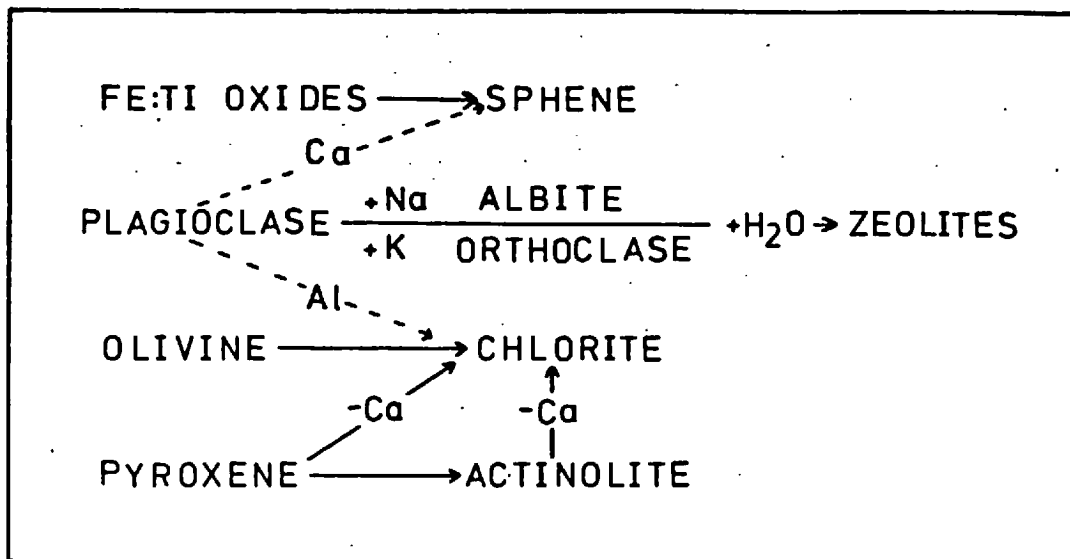


Figure 3-1 Principle mineral transformations during greenschist-facies alteration.

secondary products, even within the same thin-section, were detected by microprobe analysis.

Olivine

The dominant alteration product of olivine is chlorite but the phases actinolite, epidote, quartz, calcite and stilbite were occasionally observed within olivine pseudomorphs. Within the least altered parts of the lava flows the olivine pseudomorphs are clearly recognisable. As alteration proceeded fringes of chlorite formed on these and in some instances they coalesced to produce large patches of chlorite within which the original phenocrysts are extremely difficult to recognise. In some of the lava flows (e.g. M 29-30), in which the pyroxenes were also altered, pseudomorphs of olivine could only be recognised in one or two samples. Skeletal olivines were rarely identified in any of the lava flows but this probably reflects the greater susceptibility to alteration of crystals with a high surface area/volume ratio. Figures 3-2 to 3-6 show a sequence from the centre to the margin of the Pennygown quarry lava flow M 13-22, in

which the olivine pseudomorphs pass through all the stages described above. Figures 3-7 and 3-8 show extensively altered samples from two other lava flows (M 29-32, C 191-232a/b) in which the growth of large patches of chlorite has completely disguised the original olivines.

Within individual lava flows chlorites with a wide range of MgO/FeO ratios occur, but no distinct compositional difference could be detected between pseudomorphs of phenocrysts or groundmass olivines or between these and chlorites occupying vesicles, or secondary mineral pods (e.g. Appendix I-D, M 16 nos. 4,5; M 18 nos. 8,9). Nevertheless, the chlorites within the different lava types possess different ranges of MgO/FeO ratios. With the exception of the extensively altered marginal samples, M 13 and M 14, chlorites in the olivine and Cr-spinel bearing lava from Pennygown quarry (M 13-22, C 54-158) have MgO/FeO ratios greater than 1.2. The olivine and plagioclase-phyric lavas have chlorites with MgO/FeO ratios which vary from 0.81 to 0.70. The chlorites in the secondary mineral pods in the base of the flow M 26-28 overlying M 13-22 have MgO/FeO ratios of 0.86 to 0.83 but the values of this ratio lie between 0.68 and 0.53 in all the other lavas which contain titanomagnetite phenocrysts. These values may be contrasted with the MgO/FeO ratios of the olivines in the zeolite-facies lavas which vary from 3.51 to 0.70 in the magnesian basalts and from 0.91 to 0.60 in the hawaiites. Clearly, not only did the greenschist-facies alteration cause one or both of these elements to be mobilised within the lava flows but either MgO was lost or FeO was gained by most of the samples. The convergence of the chlorites in M 13 and base of the overlying lava towards a mean composition, despite the differences in original mineralogy between these two lavas, suggests that chemical exchange occurred between these two flows.

Plagioclase and titanomagnetite

These two minerals appear to have been stable over a similar range of conditions in most of the greenschist-facies lavas. In flow, M 41-46, many of the plagioclases are unaltered and the titanomagnetites show partial maghematisation. In the centre of the Pennygown quarry lava, M 13-22, and in the two olivine and plagioclase-phyric lavas, M 34-36 and M 37-38, many of the feldspars exhibit twinning but they all show some replacement by Na- or K- rich phases. The titanomagnetites in these particular samples are also granulated and re-



Figure 3 - 2 M 21 - Dark flow centre Pennygown Quarry lava.
The olivines have been replaced by chlorite but the individual
pseudomorphs are still recognisable. Field of view : 3mm by 2.1mm.

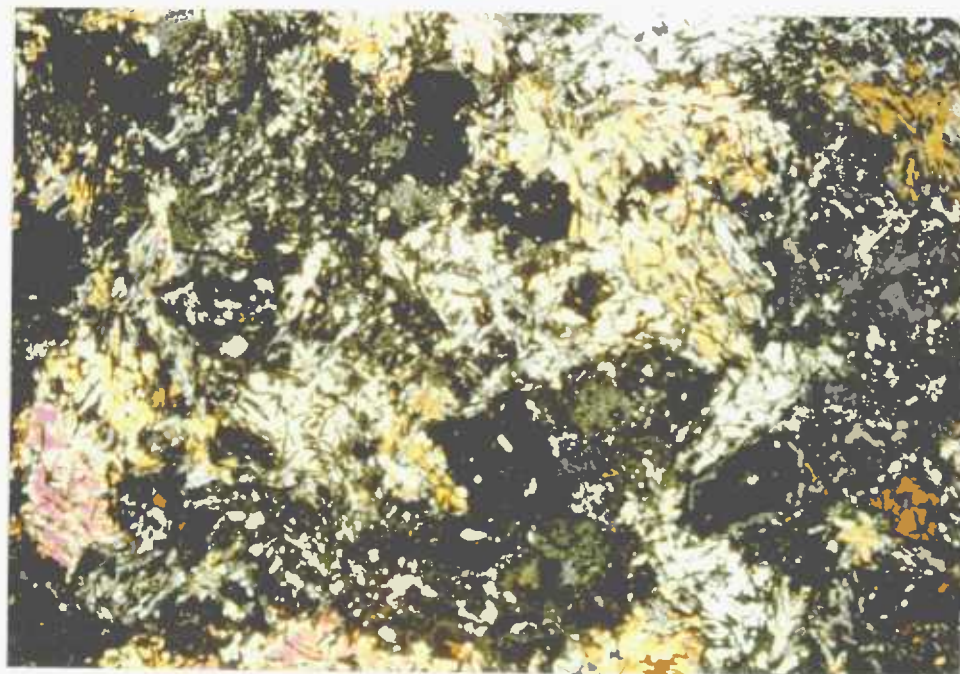


Figure 3 - 3 M 18 - Pennygown Quarry lava.
The pyroxenes show little evidence for alteration but thin over-
growths of chlorite have formed on the olivine pseudomorphs.
Field of view : 5mm by 3.5mm.



Figure 3 - 4 M 16 - Mottled Zone, Pennygown Quarry lava.
In the centre is a skeletal olivine crystal replaced by calcite
with directly below it a chlorite pseudomorph after olivine,
indicating non-equilibrium conditions.

Field of view : 5mm by 3.5mm.

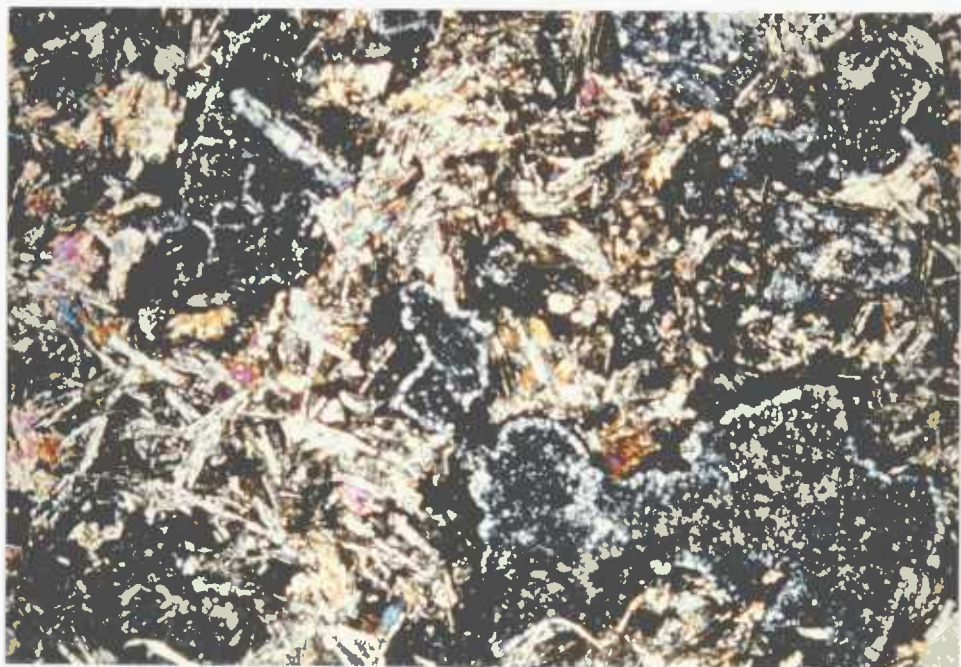


Figure 3 - 5 M 14 - Pennygown Quarry lava.

The chlorite overgrowths on the olivines have coalesced and the
original phenocrysts are no longer recognisable, but some small
relict pyroxenes still persist. Field of view : 3.4mm by 2.4mm.

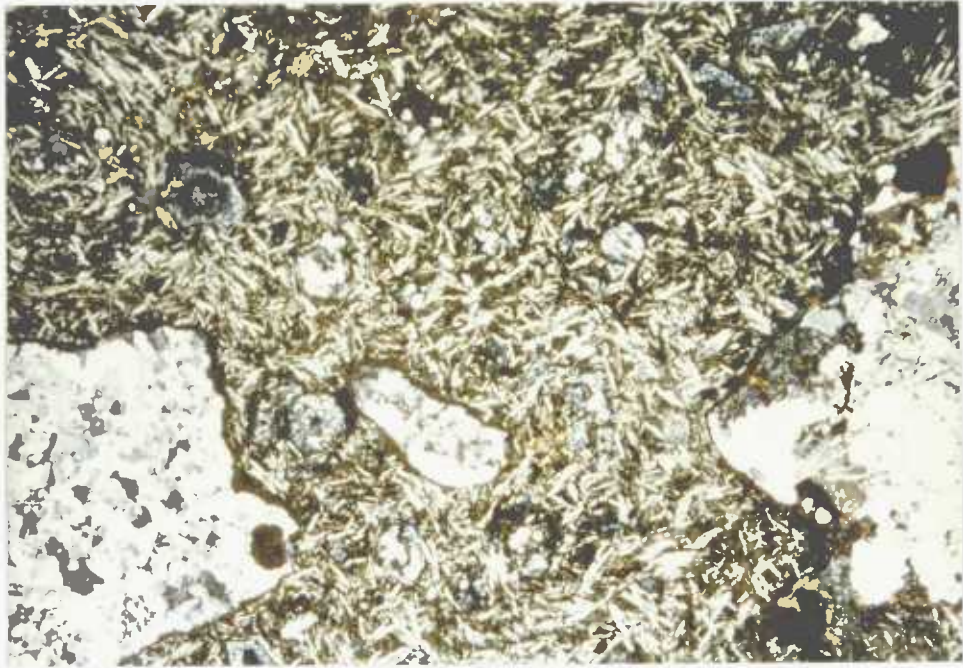


Figure 3 - 6 M 13 - Pennygown Quarry lava, contains no igneous phases but 'ghost' plagioclases are still recognisable. The disappearance of the pyroxenes coincides with the appearance of abundant secondary quartz. Field of view : 6.5mm by 4.5mm.



Figure 3 - 7 Intensely altered basaltic sample, M 29, containing relict pyroxenes, 'ghost' plagioclases and irregular patches of chlorite but no recognisable olivine pseudomorphs.

Field of view : 5mm by 3.5mm.

placed by a mixture of oxides, predominantly titanomagnetite and maghemite. In the other samples from the greenschist-facies lavas the feldspars never show twinning and contain numerous small inclusions giving them a speckled or dusty appearance (figs. 3-2 to 3-8). The inclusions, which appear to be mainly chlorite or sphene, occur in both phenocryst and groundmass feldspars and are not restricted solely to those phenocrysts that enveloped groundmass phases during their crystallisation. Chlorite inclusions are common in the A and B type lavas which were olivine-rich, whilst sphene inclusions tend to occur mainly in the C type lavas which had titanomagnetite phenocrysts. Microprobe analyses of the feldspars frequently contained a few per cent of FeO, MgO and occasionally TiO₂ (Appendix I-D; M 13 nos. 1-7, M 29 nos. 2-5). The titanomagnetite in the same samples show partial or complete replacement by sphene. The highest amounts of FeO and MgO detected in plagioclase in the zeolite-facies were 2.77% and 1.06%, respectively (Appendix I-D, LA 5 no. 7a, M 55 no. 4b), and these can be related to the presence of thin chlorite veins. In most of the feldspars in the zeolite-facies lavas, FeO rarely exceeded 1.0%, MgO was not detected and TiO₂ was below 0.2%, indicating that all these elements were mobilised, at least on a microscopic scale, during greenschist-facies alteration, and that magnesium was more mobile than iron.

Epidote was never observed replacing plagioclase during this study. Calcite pseudomorphs some of feldspars in the brecciated samples from the bottom of the drill core (fig 3-8) but the dominant alteration products of plagioclase are Na- and K- rich feldspars. A wide range of K: Na: Ca ratios was detected in the feldspars, even within the same thin section (e.g. Appendix I-D, M 13 nos. 1-7). No correlation could be found between the composition or phenocryst assemblages of the lavas and the feldspar types formed within them. Several of the analyses gave low totals, particularly those of feldspars from the hydrothermally brecciated lava from the lower part of the drill core (C 191-232a/b). Only in the phenocrysts could the individual secondary mineral species be recognised. Six different minerals - labradorite, orthoclase, epidote (apparently pseudomorphing olivine enclosed by the phenocryst), sphene (replacing oxide inclusions), laumontite and calcite - were all detected within one altered feldspar

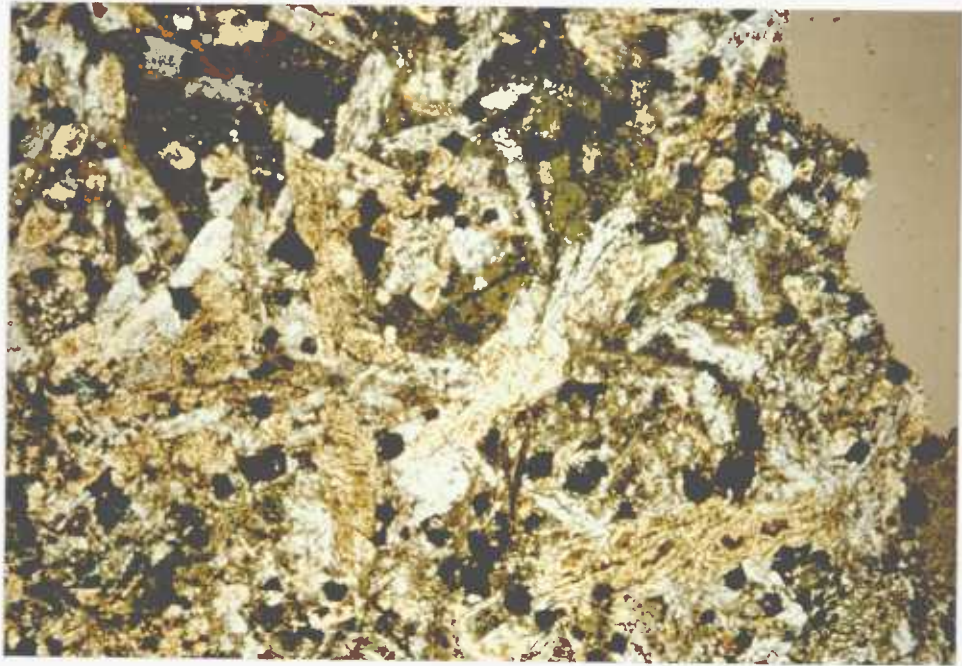


Figure 3 - 8 Calcite replacing feldspar in the hydrothermally brecciated sample C 232a/b. The speckled appearance of the feldspars is due to sphene and chlorite inclusions. Pyroxene has been completely replaced. Field of view : 5mm by 3.5mm.



Figure 3 - 9 M 45 - vesicle with sedimentary layers of chlorite cut by thin veins. The upper part is filled by epidote and chlorite and contains projections of altered basalt - indicating that some enlargement occurred. Field of view : 11.3mm by 7.8mm.

phenocryst from C 191-C 232a/b (Appendix I-D, C 212 nos.10-18). The orthoclase appeared to have replaced the labradorite and both these feldspars were then partially replaced by laumontite and calcite. The low totals of several of the feldspar analyses in these lavas indicate that similar retrogressive zeolite-growth also affected the other lava flows.

Pyroxene

In several thin sections of the Pennygown quarry lava (M 13-22, C 54-158) the pyroxenes show marginal replacement by amphibole. The amphiboles are actinolitic in composition and these marginal fringes are rarely wider than 0.05mm. The amphiboles replacing the pyroxenes in both the dark flow centre and near the margin are similar in composition. Relative to the relict pyroxenes the amphiboles are depleted in Ca and enriched in Fe, but this higher FeO content could reflect marginal zoning of the poikilocrysts, (Appendix I-D, M 14 nos.1-3, M 18 nos.1-3, 10). In many of the flows pyroxene has been replaced by chlorite, not amphibole. When amphibole did form it appears to have been less stable than chlorite. M 14 which was close to the margin of the flow M 13-22, contains 14% relict pyroxene, but only 6.6% amphibole - little more than the centre of the flow with 19-24% pyroxene and 3-6% amphibole - being rich in chlorite instead. Nevertheless, some amphibole was present in most of the samples in which the pyroxenes had been altered. In every case it was associated with quartz. The conversion of the pyroxenes to chlorite must have released both Ca and Si whilst consuming Al. The association of amphibole and quartz in pyroxene-free or pyroxene-poor samples suggests that the quartz was formed from Si released during the breakdown of the pyroxenes.

The survival of the amphiboles may be temperature dependant. Two of the lava flows (M 29-32, M 47-50) were sampled close to the Toll Doire granophyre ringdyke. At both localities the granophyre outcropped within a short distance, M 47 being collected only 10 m from one of these exposures. Both these lava flows are extensively altered and contain needles of amphibole and 'vesicle-like' structures rich in quartz and amphibole. In M 13-22 and C 54-158, the two sections through the Pennygown quarry lava, amphibole occurs in all the samples as the alteration product of pyroxene but appears to be replaced by chlorite. In the only other lava flow in which extensive

alteration of the pyroxenes was observed, C 191-232a/b, only one sample contained amphibole. The feldspars in this lava have been affected by retrogressive zeolite formation, indicating lower temperatures.

Other phases

Primary sulphides and biotite were not recognised in any of the other greenschist-facies lavas. Small grains of secondary sulphides were identified in several of the flows, inside, or adjacent to, chlorite-rich vesicles or secondary mineral pods (Appendix I-D, M 13 no.15, M 16 nos.12-15, M 30 nos.2-4, M 48 nos.6,7). These were nucleated on and replacing small grains of secondary magnetite inside the chlorites. Relatively well formed euhedral crystals of iron-sulphides were observed in the hydrothermally brecciated lava at the base of the drill core and in a dyke in Pennygown quarry (Appendix I-D, C 232a/b nos.7-9, D 1 nos.4-7). Those appeared to be nucleated on titanomagnetite crystals. All these sulphides contained little or no zinc.

The alteration products of Cr-spinel could not be identified. No spinel phase occurs in the altered margin (M 13) of the Pennygown quarry lava M 13-22. The spinels in the other samples from this lava, including M 14, directly below M 13, appeared to be relatively unaltered, showing only a marginal decrease in reflectivity.

All the lavas discussed in this chapter lie in the epidote zone of Walker (1970). As in the zeolite-facies lavas, index minerals are rare in the flow interiors and occur mainly in the vesicles. The groundmass of several of the greenschist-facies lavas contain isolated crystals of epidote, but these did not appear to be related to any preexisting mineral phase. With the exception of the hydrothermally brecciated lava C 191-232a/b, calcite is also rare in the flow interiors being restricted mainly to vesicles and veins. The groundmass minerals in the greenschist-facies lavas appear to consist mainly of chlorite, some feldspars, numerous small grains of sphene and 'dirty mixtures' of amorphous oxides and chlorite. The mottled zones in the lavas consist of dark patches in which some Fe:Ti oxides still persist and light areas in which the oxides have been completely destroyed and replaced by sphene.

2. Vesicles, Secondary mineral pods and Veins.

The vesicles in the greenschist-facies lavas contain a wide variety of secondary minerals though chlorite is the most common. In the bottom of some of the vesicles thin 'sediment' layers occur. These layers are usually composed of chlorite but epidote and carbonate also occur (figs. 3-9, 3-10). Several vesicles in the upper flow in the drill core contained layers of chlorite which were all aligned parallel with the flow top. Those layers may have been formed from debris collapsing from the top of the vesicles or represent particulate material that was carried by the hydrothermal fluids. Although they are generally restricted to the flow margins, similar vesicle infillings can be found in the flow interiors.

Many of the vesicles are concentrically zoned, but the minerals within the zones and the sequence in which they were deposited varies considerably, even within the same lava flow. The following sequence of vesicle infillings was observed in the upper flow transected by the drill core :-

- 0 - 5m : chlorite surrounding epidote and/or albite, minor calcite (Appendix I-D, C 54)
- 5 - 6m : scarce vesicles with chlorite infillings
- 6 - 7m : chlorite surrounding albite and epidote, minor quartz and amphibole
- 7 - 9m : scarce vesicles with 'sedimentary' layers usually chlorite (fig. 3-10)
- 9 - 11m : epidote surrounding albite; epidote surrounding pumpellyite; chlorite surrounding epidote (fig. 3-10; Appendix I-D, C 130)
- 11-14m : scarce chlorite filled vesicles except at 13m where vertical train small vesicles containing quartz, epidote, amphibole and hydrogarnet occur in a pipe-like structure.

The greenschist-facies lavas tend to be intensely altered adjacent to the vesicles. Frequently, the surrounding minerals have been completely replaced and the vesicles have been enlarged by solution or brecciation at the expense of the adjacent lava. One such structure can be seen in the drill core segment shown in the centre of figure



Figure 3 - 10 Types of vesicle infillings.

C 95 - sedimentary layers of epidote, chlorite and calcite,
 C 130 - albite surrounding epidote; C 137 - mainly chlorite, albite
 and epidote; C 205 - chlorite-filled, vesicle-like structures.

The drill core diameter is 2.5cm.

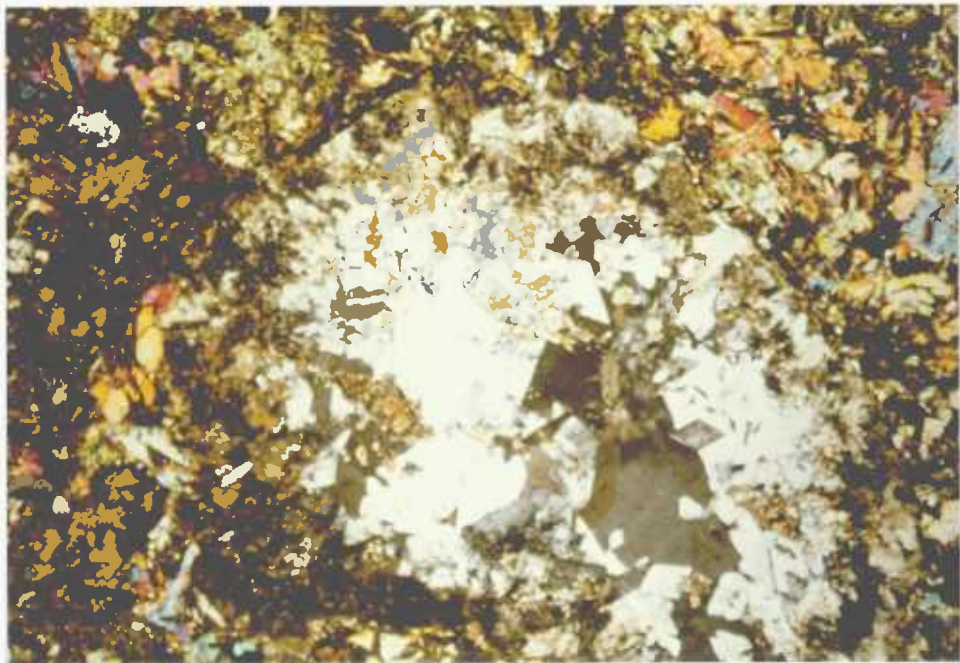


Figure 3 - 11 C 153 - small vesicle lined by albite and filled
 with quartz, epidote and amphibole. Field of view : 4.3mm by 3mm.

3-10, Dissolution of some of the basalt surrounding two vesicles has allowed them to coalesce giving rise to the single large 'vesicle' in the centre of this piece of drill core. Within the 'vesicle' is a fragment of the lava that used to divide the two amygdales from one another.

The secondary mineral pods and vesicles within individual lava flows contain the same mineral assemblages. Frequently the primary igneous minerals around the pods, especially the olivines which are most susceptible to alteration, have been pseudomorphed by secondary minerals such as calcite which are rarely found in the flow interiors. Some of the pods contain isolated crystals or fragments of less altered basalt within them. Figures 3-12 and 3-13 show secondary mineral pods from M 15 and M 16, respectively in the mottled zone of the Pennygown Quarry lava M 13-22. The pod in M 15 contains chlorite surrounding albite plates which in turn enclose calcite, epidote and a single irregularly shaped hydrogarnet crystal. The pod in M 16 consists mainly of chlorite and calcite. The contact with the surrounding lava is shown on the right hand side of figure 3-13. Unaltered pyroxene crystals can be seen projecting into the pod along this contact whilst, the centre of the pod contains unaltered pyroxene crystals fringed by amphibole. The skeletal olivine crystal pseudomorphed by calcite, shown in figure 3-4 is close to the margin of this pod which lies just outside the field of view of figure 3-4. These pods clearly formed by dissolution and replacement of the material surrounding the vesicles.

The intensely altered lavas M 29-32, M 49-50, both contain 'vesicle-like' structures with frayed margins of altered basalt. Those in M 47-50 are rich in quartz, chlorite and amphibole and contain small fragments of altered basalt. The veins in M 29-32, the Toll Doire quarry lava, contain amphibole needles, albite and quartz, and in wider veins calcite also occurs. The most altered samples from this lava have irregularly shaped segregations which contain altered basalt fragments and the same mineral assemblage - quartz, albite, calcite and amphibole - as the veins, suggesting that these apparent vesicles are also dissolution structures.

Figures 3-14 and 3-15 show two chlorite-rich pods from the lower flow in the drill core, C 191-232a/b, and the upper flow of Pennygown



Figure 3 - 12 Secondary mineral pod in M 15.
Albite enclosing calcite which in turn encloses epidote
and a single irregularly shaped hydrogrossular crystal.

Field of view : 4.3mm by 3mm.



Figure 3 - 13 Chlorite, calcite secondary mineral pod in M 16.
The centre of the pod contains amphibole-fringed, relict pyroxenes.
Similar crystals project into the pod along the right hand margin.

Field of view : 4.3mm by 3mm.

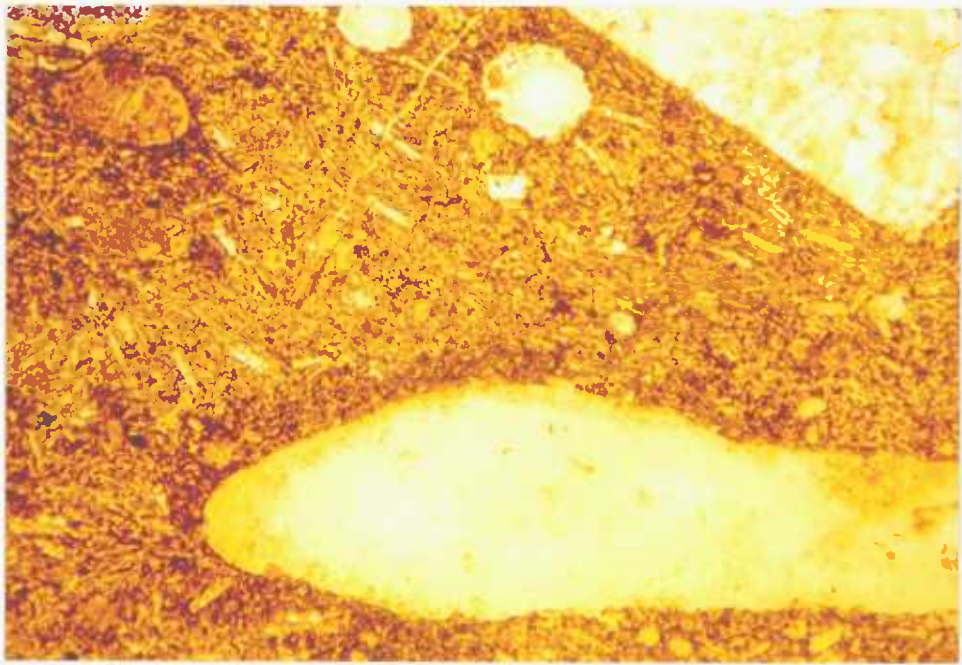


Figure 3 - 14 C 199 - chlorite-filled secondary mineral pod surrounded by dark halo of altered rock. In the upper right corner is an altered plagioclase phenocryst containing numerous small inclusions of chlorite and sphene. Field of view : 7mm by 4.9mm.

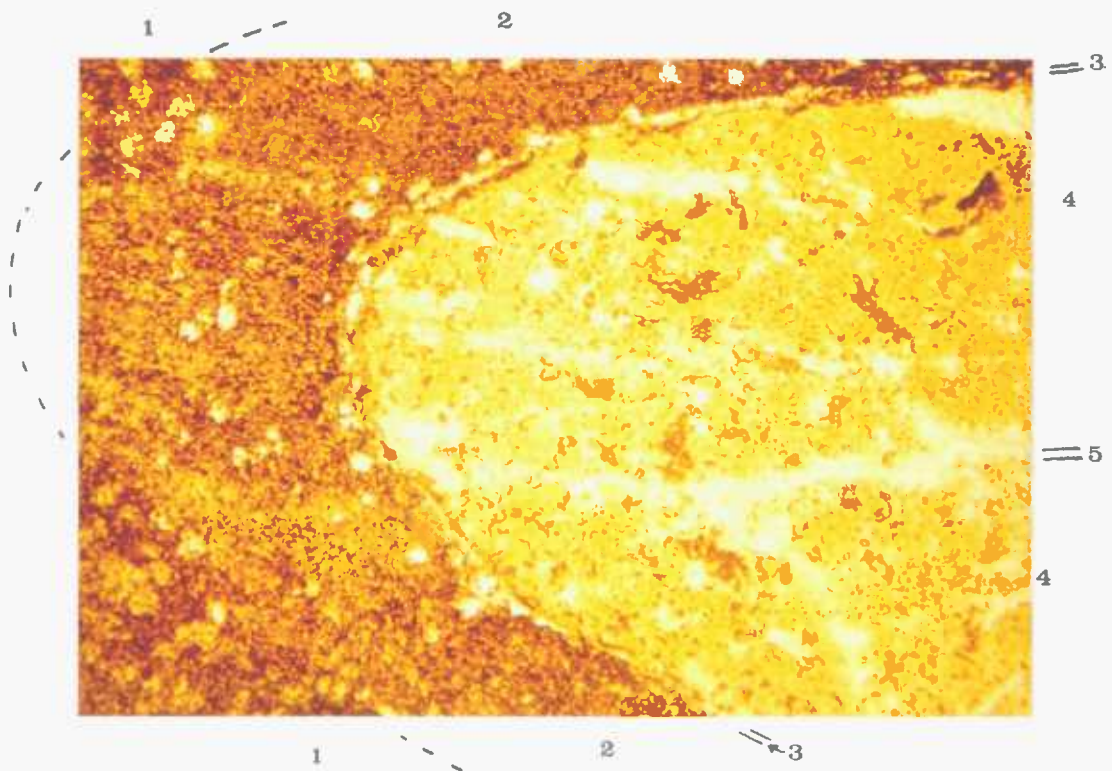


Figure 3 - 15 M 26 - chlorite filled secondary mineral pod. See text for explanation of numbers. Field of view : 10mm by 7mm.

quarry, M 26-28, respectively. Unlike the secondary mineral pods described above, these are regular in shape, resembling vesicles, and no unaltered crystals or basalt fragments were observed inside them. The pods are surrounded by haloes of intensely altered rock, rich in sphene and opaques (Appendix I-D, M 70). Several zones can be identified in the larger pods in M 26-28 and these are shown in figure 3-15. In sequence from the surrounding lava to the centre of the pod they consist of :-

- 1 - sphene and oxide-rich intensely altered lava
- 2 - blotched lava containing small segregated patches of quartz, chlorite, epidote and albite
- 3 - thin quartz-rich rim
- 4 - chlorite frequently associated with small blebs of secondary magnetite
- 5 - (in large pods only) calcite and laumontite/leonhardite, trace of albite.

The large pods in these lavas are connected to veins, those in M 26-28 are connected to the base of the lava by thin calcite-zeolite veins, and the pods in C 191-232a/b pass laterally in chlorite veins. These two lava flows are fine-grained and hence, the individual crystals have high surface area/volume ratios rendering them susceptible to alteration. These pods could thus be replacement structures produced by less selective alteration than that which occurred in flow M 13-22.

In contrast to the thin veins connected to the secondary mineral pods, the large hydrothermal veins which have frequently fractured and brecciated the green schist-facies lavas, rarely contain the same mineral assemblages as the flows they transect. Most consist of mixtures of calcite and Ca-zeolites, with or without traces of quartz and chlorite (figs. 3-16 and 3-17). Some nearly monomineralic veins of calcite or zeolite also occur, one example being the laumontite/leonhardite vein, from Pennygown quarry (M 64).

Investigations of natural geothermal systems and experimental studies have demonstrated that, in addition to temperature and pressure, the CO₂ content of the associated fluids exert strong controls on the appearance of carbonate or Ca-Al hydrosilicates (e.g. Zen

1961, Muffler and White 1969, Browne and Ellis 1970, A.B.Thompson 1971). In an H_2O-CO_2 fluid phase bearing the components for calcite, zeolite et cetera, it would be expected that at any X_{CO_2} , either calcite or zeolite could precipitate. Stable calcite-zeolite assemblages are formed only if the X_{CO_2} of the associated fluids is low or, under univariant conditions. Neither of these situations is indicated by the widespread deposition of calcite in the vesicles and secondary mineral pods and univariant conditions are only likely to be approached in closed systems. Little experimental data are available for the relevant equilibria, but the critical values of X_{CO_2} appear to be low. Liou (1971), for example, found that wairakite was not stable relative to calcite and montmorillonite at $T = 327^\circ C, P_f = 3000$ bars with $X_{CO_2} = 0.01$. Analyses of natural waters from zeolite terrains (Ellis 1959, 1963) indicates that X_{CO_2} in the fluid-phase may be of the order of 0.02. Accordingly, A.B.Thompson (1971) suggested on theoretical grounds that hydrothermal calcite-zeolite veins indicate non-equilibrium conditions. He proposed that in order to precipitate both phases from the same fluid it is essential that the carbonate is precipitated first. This would lower P_{CO_2} to the equilibrium value so that zeolite could form. If the zeolite were precipitated first, this would probably be converted to carbonate plus an aluminous phase by reaction with the H_2O-CO_2 fluid. Evidence for both these sequences can be observed in the Mull hydrothermal veins.

Figure 3-16 shows part of a calcite-stilbite vein from a hydrothermal breccia in the flow M 47-50 (Appendix I-D, M 49). The stilbite crystals are restricted to the centre of the vein, indicating later deposition. In many of the Mull hydrothermal veins, such as M 49, calcite precipitation and carbon dioxide loss will have been promoted by boiling of the fluids following hydrofracturing. In contrast, figure 3-17 shows a laumontite-calcite-quartz vein, M 24, from Penny-gown quarry in which the zeolite crystals were deposited first. The vein contains numerous small shear planes along which the calcite crystals tend to occur, suggesting they were deposited from later influxes of fluid. The calcite crystals shown in figure 3-17 are surrounded by a fringe of small, radiating, micaceous crystals which appear to have a reaction relationship with the laumontite. No positive

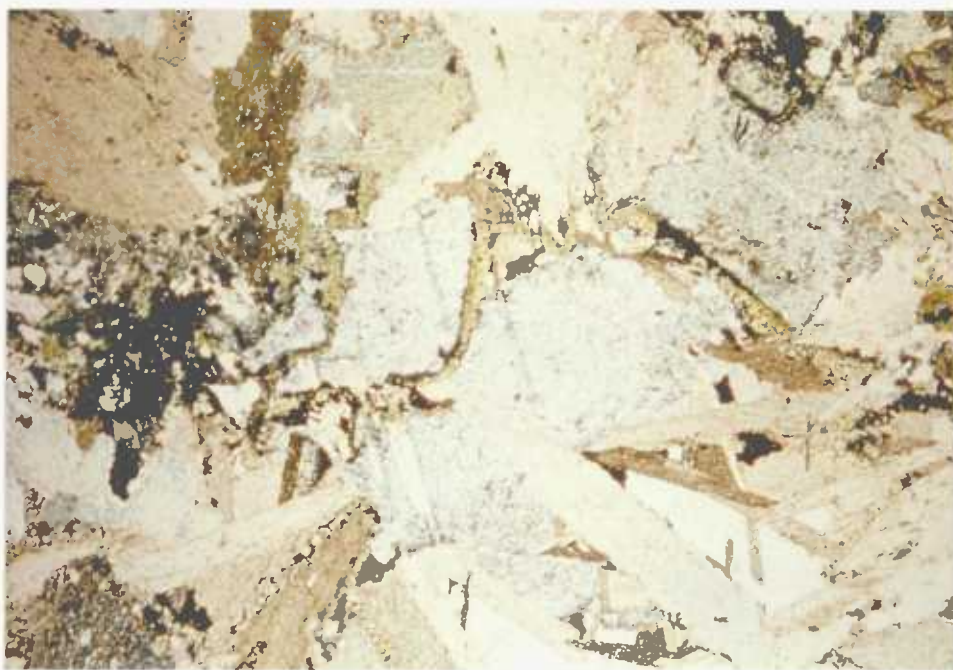


Figure 3 - 16 Central part of calcite-stilbite vein M 49.
Field of view : 4.5mm by 3.1mm.



Figure 3 - 17 Laumontite-calcite-quartz vein, M 24. The calcite is fringed by small radiating micaceous crystals which have a reaction relationship with the laumontite crystals.

identification of these radiating crystals could be made as all attempts to isolate or concentrate them for X-ray diffraction work, failed. Their optical properties are consistent with either, the calcic mica, margarite or, pyrophyllite - a relatively common phase in low-grade metasedimentary sequences. Many of the other Mull hydrothermal veins show evidence for more than one phase of fluid injection, including the hydrothermally brecciated sample, C 232a/b, from the base of the drill core.

3. Intra-lava chemical variation

The similar textures of the zeolite- and greenschist-facies lavas indicate that the hydrothermal alteration of the latter involved little change in total volume. The extensive growth of secondary minerals in the greenschist-facies lavas must, therefore, have been accommodated by considerable elemental mobility and consequent compositional changes. All the lavas show variations in oxidation state but the bulk compositional changes within several of them are small - reflecting the fact that the samples from these lava flows show similar degree of alteration. Flows M 34-36, M 37-38 and M 41-46 are only slightly altered whilst, flows M 26-28, M 29-32 and M 47-50 are extensively altered (see Table 3-1). These samples can thus provide limited information only on element mobilities during alteration. In contrast, the two sections through the Pennygown Quarry lava, M 13-22 and C 54-158, and the lower flow transected by the drill core, C 191-232a/b, show transitions from dark relatively unaltered lava to green 'spilitic' material devoid of igneous minerals. These three lava sections show variations in all the major and trace elements and the mineralogical and chemical changes across them are summarised in figures 3-18 to 3-21. It should be stressed that none of the greenschist-facies lavas contain fresh olivine (other than a trace in M 35) and in most of them some alteration of the feldspars has occurred. Hence, the nature of the chemical changes during the initial stages of the alteration cannot be established by studies of intra-lava variation alone.

Mobile and immobile elements

Comparison of figures 3-18 to 3-21 demonstrates that the chemical effects of alteration vary from flow to flow. Nevertheless,

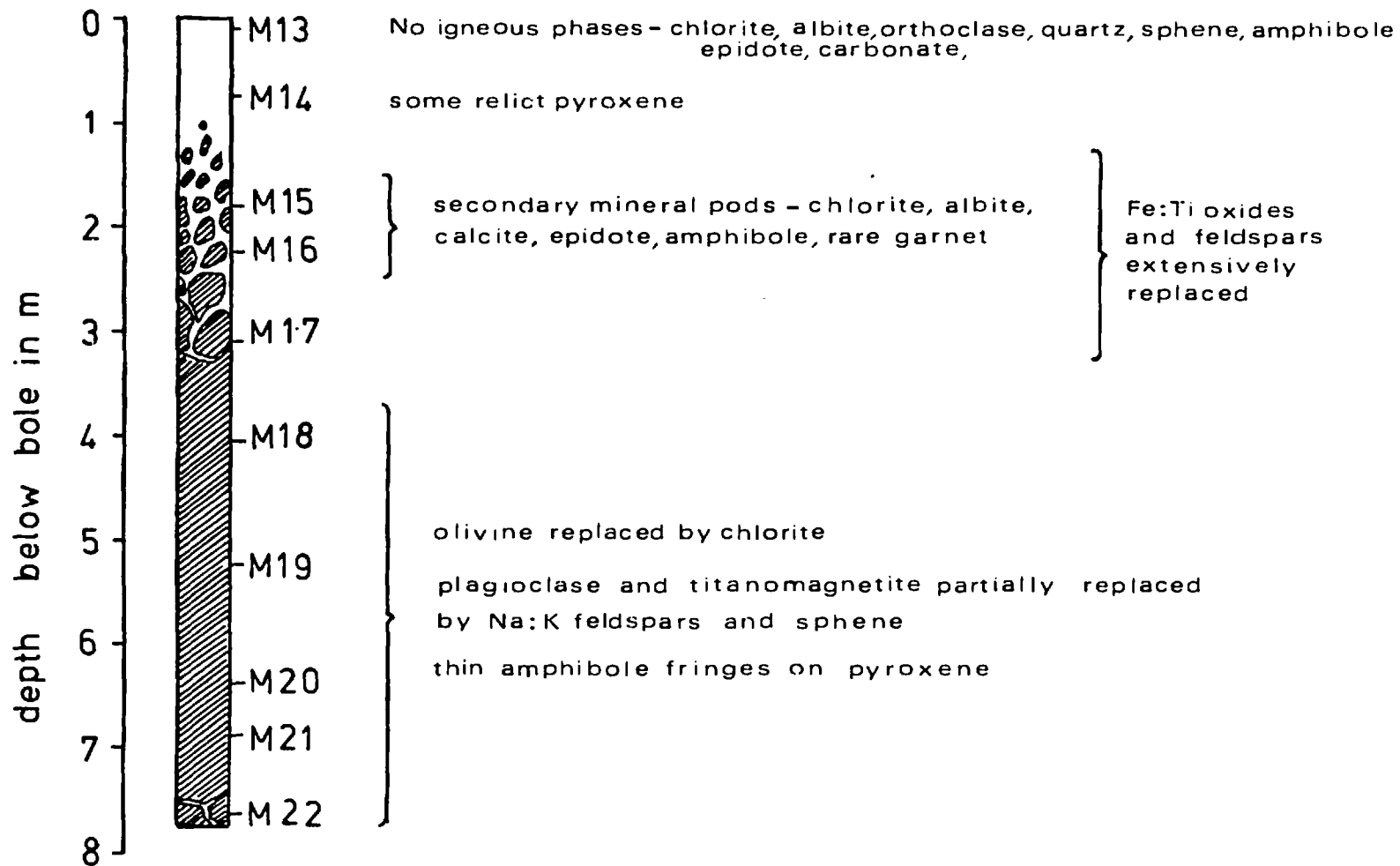


Figure 3-18 Mineralogical variation across the section M 13-22, through the Pennygown Quarry lava.

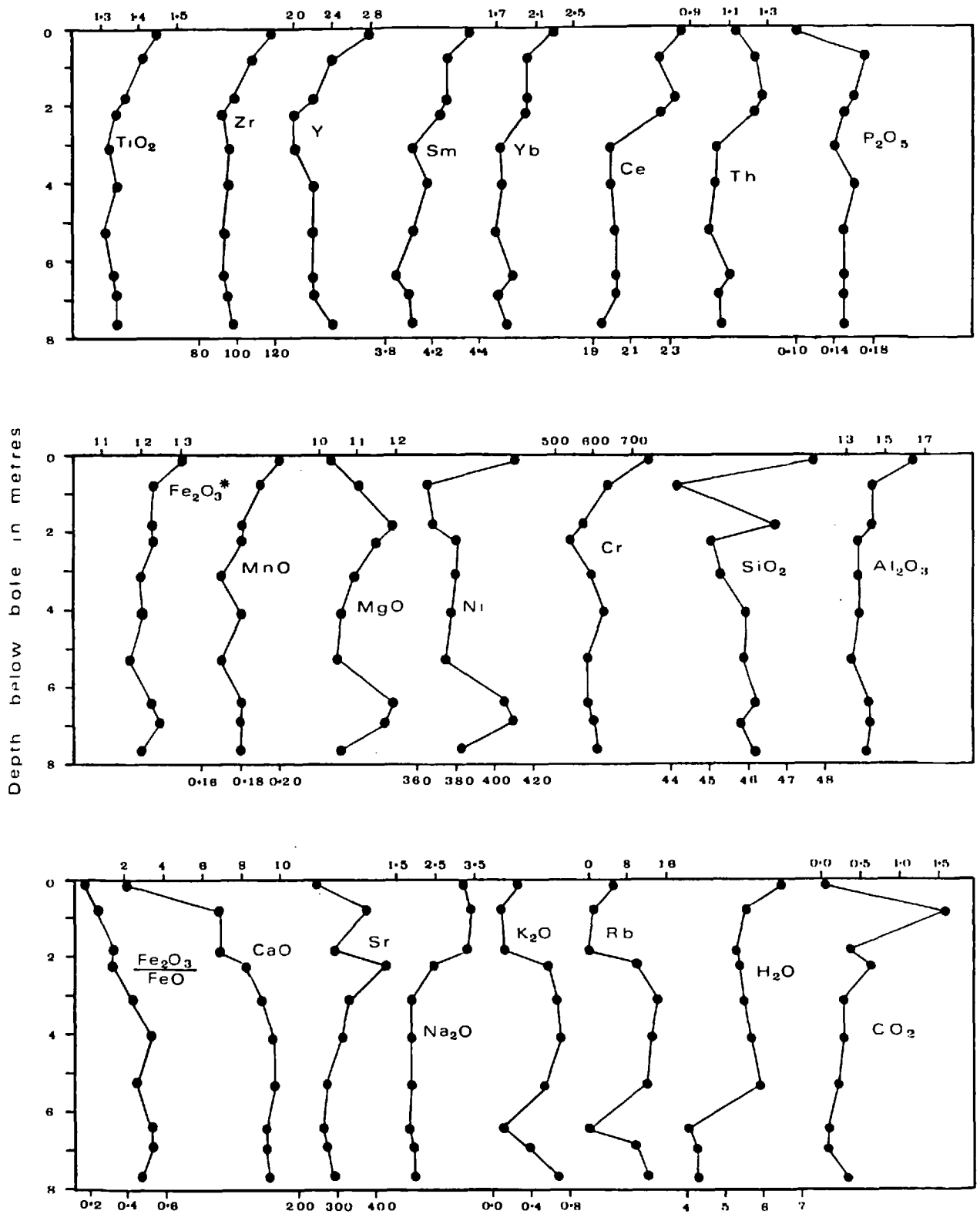


Figure 3-19 Chemical variation across M 13-22.

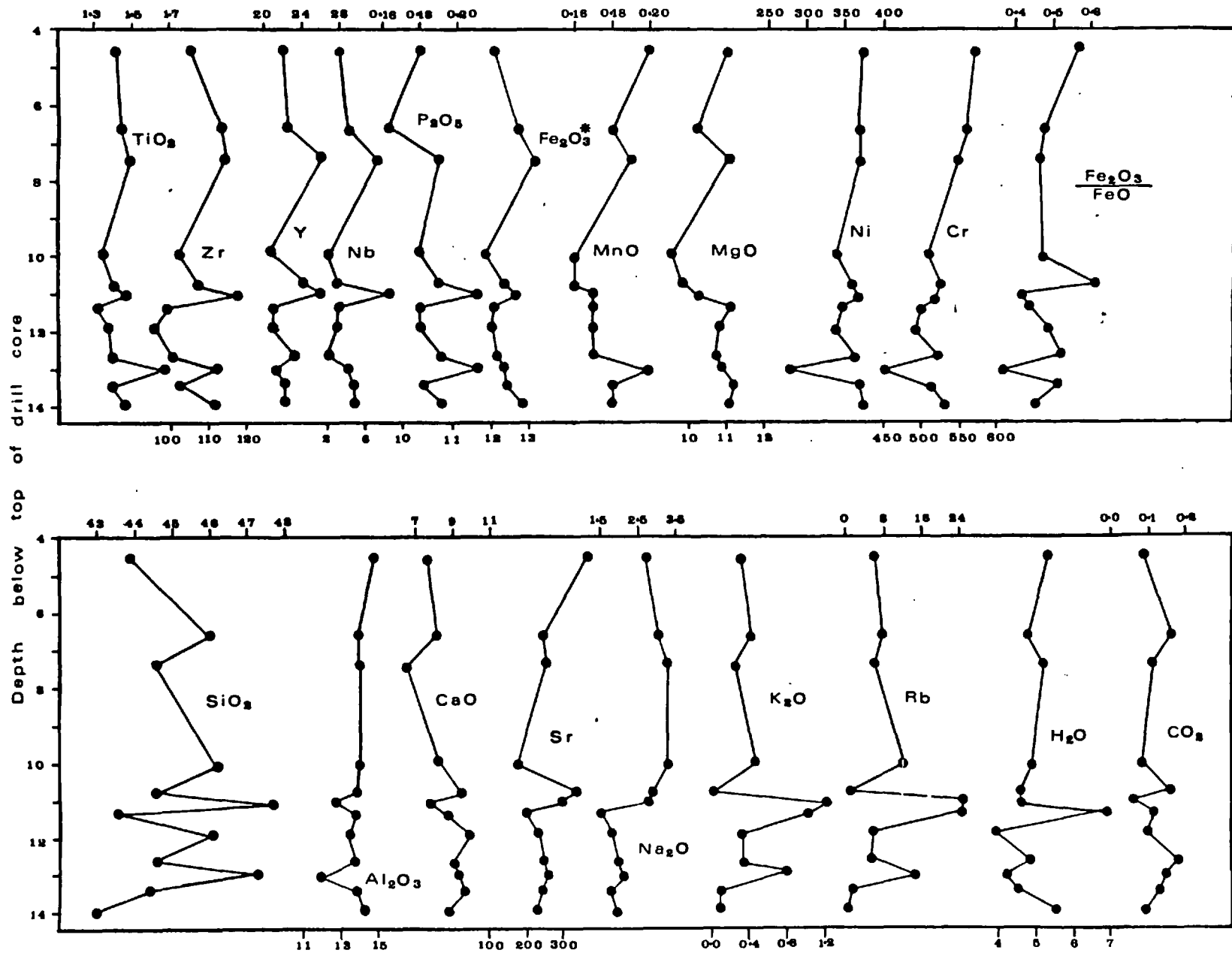


Figure 3 - 20 Chemical variation across C 54 - 158.

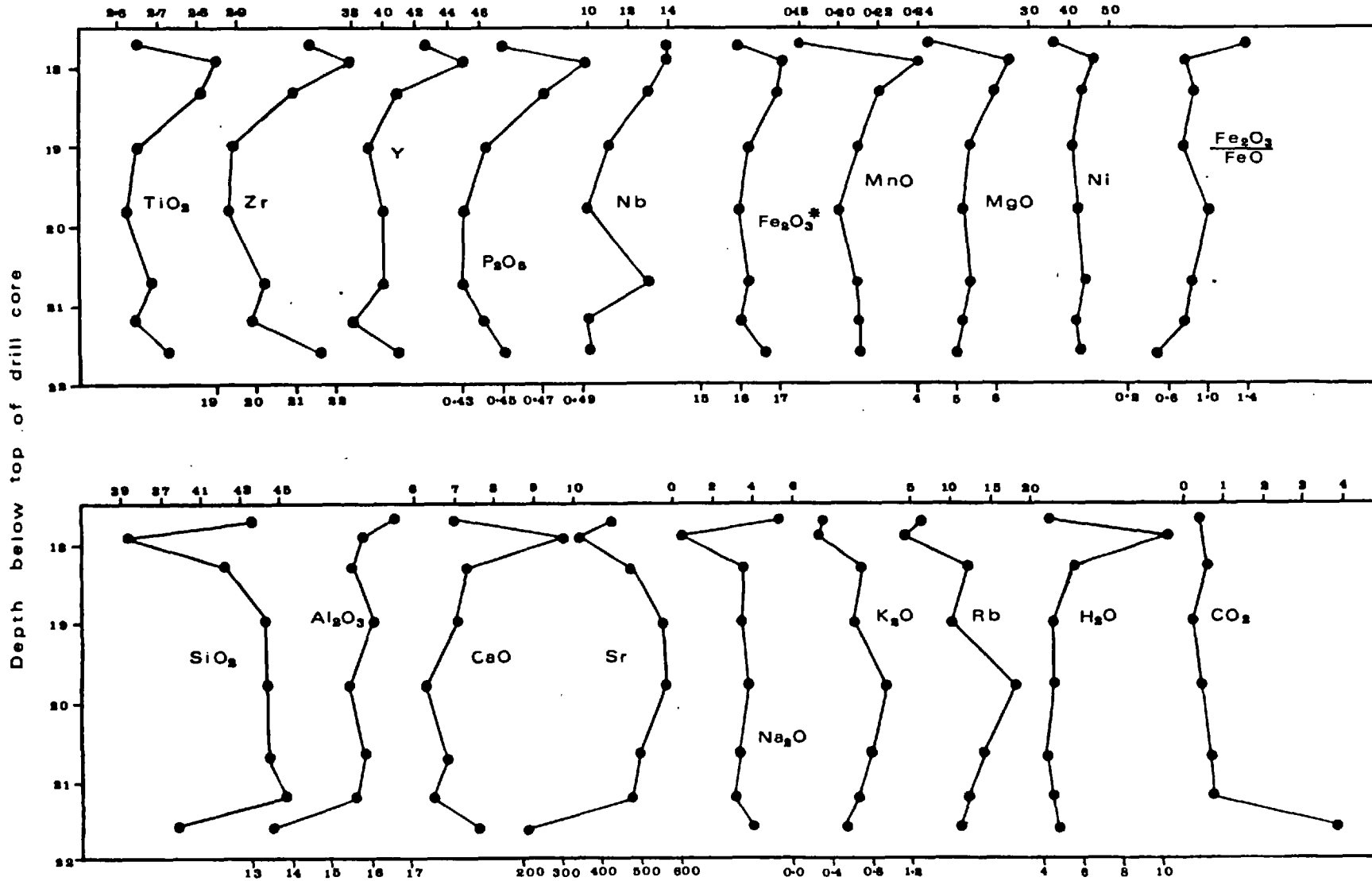


Figure 3 - 21 Chemical variation across C 191 - 232a/b.

within each lava section TiO_2 , Zr, Y, Nb, Ta, Hf and the REE show similar distributions and preserve almost constant ratios, suggesting immobility. In both M 13-22 and C 191a/b the abundances of this element group increase in the most intensely altered samples indicating that leaching of more easily mobilised elements has caused them to be concentrated in the residual material.

In M 13-22 the only secondary mineral phase that takes up significant quantities of calcium is sphene. Consequently, the progressive replacement of plagioclase and pyroxene by albite and chlorite, respectively, as the margin of this flow is approached has caused a decrease in CaO and an increase in Na_2O . The disappearance of pyroxene from the flow margin is accompanied by a sharp drop in CaO - from 6.8% in M 14 to 2.19% in M 13 - but no net increase in the chlorite content of the lava (Appendix I-C). The MgO/FeO ratios of the chlorites also decrease in the margin of the flow suggesting some leaching of Mg occurred during the alteration of the pyroxenes. Drastic loss of P_2O_5 also occurs at this point (fig. 3-19) indicating that the breakdown of the pyroxenes allowed alteration of the enclosed apatites.

A similar pattern can be recognised in the drill core section through this lava flow, C 54-158 (fig 3-20, App. I-B). The most extensively altered samples are C 54-142 from the upper vesicular part of the flow. Relative to C 145-158, they are depleted in CaO and enriched in Na_2O . The variations in C 54-158 are considerably smaller than in M 13-22, the lowest value of CaO being 6.6% in C 90, due to the deposition of the calcic phase, epidote, in the vesicles.

In contrast, progressive alteration of the flow C 191-232a/b has caused loss of K_2O , Na_2O , and SiO_2 and enrichment in CaO, MgO, MnO and Fe_2O_3^* . Loss of Al_2O_3 has also occurred in the hydrothermally brecciated sample C 232a/b. This lava flow has been affected by more than one episode of hydrothermal alteration. The plagioclases were first partially altered to Na- and K-rich feldspars and then, in all the samples except C 191, replaced by variable amounts of calcic zeolites and calcite as a result of interaction with late-stage fluids - hence

the decrease in Na_2O and K_2O . The decrease in SiO_2 coincides with the conversion of pyroxene to chlorite (fig 3-21, App. I-B). The increase in MgO and Fe_2O_3^* and the limited variations in Al_2O_3 content in these samples suggests that the formation of chlorite was accompanied by leaching of SiO_2 . Some silica will also have been lost during alteration of the alkali feldspars. In C 232a/b, which shows loss of Al_2O_3 , the feldspars are replaced by calcite (fig. 3-8). This sample shows evidence for repeated hydrofracturing and the calcite deposition indicates that the fluids had relatively high values of X_{CO_2} - resulting in preferential mobilisation of Al_2O_3 and SiO_2 .

Tables 3-2 and 3-3 are correlation matrices for selected major and trace elements from the lava flows, M 13-22 and C 191-232a/b, respectively. TiO_2 , Zr, Y, Hf and the HREE (Nd-Yb) show strong a geochemical coherence throughout the M 13-22 flow and correlate negatively with CaO - confirming the hypothesis that they were immobile during alteration. If M 13 is excluded from the calculations then the correlation coefficient between TiO_2 and P_2O_5 is 0.89 indicating that prior to the breakdown of apatite, phosphorus was also immobile. Ta, Nb, Th and Ce show similar but poorer correlations. The abundances of Ta and Nb in the Mull Plateau lavas are extremely low and small changes in their concentrations are difficult to measure. Since both these elements enter Ti sites their distributions within the flow are likely to resemble that of TiO_2 and these poorer correlation coefficients are not thought to be significant. In flow C 191-232a/b, TiO_2 , P_2O_5 , Zr and Y also behave coherently, but in this particular flow they correlate negatively with the mobile elements SiO_2 , K_2O , Rb, Na_2O and Sr and positively with CaO, Fe_2O_3^* and MgO which are clearly less mobile.

Four chondrite-normalised REE patterns from M 13-22 are shown in figure 3-22 and summarised data for the REE is listed in table 3-4. The slopes of the patterns as expressed by $(\text{Ce}/\text{Yb})_N$ are constant and there is no change in the abundance of the LREE (La and Ce) relative to the HREE, except in M 13. The Th/Yb ratio also decreases to 0.49 in M 13, whilst in the other samples this ratio varies between 0.62 and 0.58. Since La, Ce and Th will enter apatite the coincidences of these changes with the marginal decrease in P_2O_5 clearly demonstrates that

Table 3-2 Correlation matrix for fifteen major and trace elements in M 13-22.

The two values for P₂O₅ were calculated as follows : (1) including M 13; (2) excluding M 13.

	CaO	Sr	(1) P ₂ O ₅	(2) P ₂ O ₅	TiO ₂	Zr	Y	Nb	Ta	Hf	Th	Ce	Nd	Sm	Eu	Tb
CaO	1.000															
Sr	0.145	1.000														
P ₂ O ₅ (1)	0.673	0.447	1.000													
P ₂ O ₅ (2)	-0.651	0.220	—	1.000												
TiO ₂	-0.923	-0.054	-0.439	0.859	1.000											
Zr	-0.921	-0.195	-0.596	0.716	0.947	1.000										
Y	-0.827	-0.354	-0.587	0.606	0.872	0.923	1.000									
Nb	-0.484	-0.049	-0.177	0.681	0.493	0.538	0.532	1.000								
Ta	-0.506	-0.543	0.195	0.671	0.591	0.371	0.278	0.188	1.000							
Hf	-0.771	0.111	-0.123	0.636	0.753	0.616	0.492	0.178	0.892	1.000						
Th	-0.484	0.481	0.172	0.552	0.523	0.293	0.207	0.365	0.967	0.891	1.000					
Ce	-0.835	0.220	-0.276	0.564	0.771	0.639	0.503	0.071	0.829	0.974	0.469	1.000				
Nd	-0.821	0.121	-0.226	0.702	0.838	0.693	0.639	0.218	0.859	0.926	0.839	0.909	1.000			
Sm	-0.861	0.235	-0.342	0.672	0.836	0.764	0.627	0.244	0.705	0.899	0.556	0.908	0.837	1.000		
Eu	-0.957	-0.112	-0.590	0.626	0.865	0.849	0.804	0.210	0.590	0.817	0.659	0.850	0.890	0.870	1.000	
Tb	-0.914	-0.029	-0.461	0.563	0.858	0.758	0.710	0.111	0.251	0.888	0.832	0.919	0.963	0.951	0.814	1.000

Table 3-3 Correlation matrix for thirteen major and trace elements in C 191-232a/b.

	CaO	Sr	K ₂ O	Rb	Na ₂ O	SiO ₂	Al ₂ O ₃	MgO	Fe ₂ O ₃ *	P ₂ O ₅	TiO ₂	Zr	Y
CaO	1.000												
Sr	-0.554	1.000											
K ₂ O	-0.709	0.541	1.000										
Rb	-0.750	0.471	0.983	1.000									
Na ₂ O	-0.767	0.135	0.238	0.329	1.000								
SiO ₂	-0.748	0.753	0.606	-0.069	0.611	1.000							
Al ₂ O ₃	-0.073	0.494	-0.688	-0.740	0.027	0.369	1.000						
MgO	0.631	-0.027	0.002	-0.106	-0.874	-0.543	-0.985	1.000					
Fe ₂ O ₃ *	0.784	-0.492	-0.365	-0.418	-0.663	-0.976	-0.290	0.815	1.000				
P ₂ O ₅	0.873	-0.479	-0.702	-0.307	-0.624	-0.839	-0.006	0.623	0.865	1.000			
TiO ₂	0.830	-0.475	-0.466	-0.505	-0.670	-0.836	-0.155	0.782	0.976	0.919	1.000		
Zr	0.786	-0.822	-0.797	-0.746	-0.349	-0.863	-0.203	0.240	0.679	0.807	0.755	1.000	
Y	0.792	-0.615	-0.762	-0.703	-0.334	-0.844	0.012	0.216	0.582	0.761	0.668	0.894	1.000

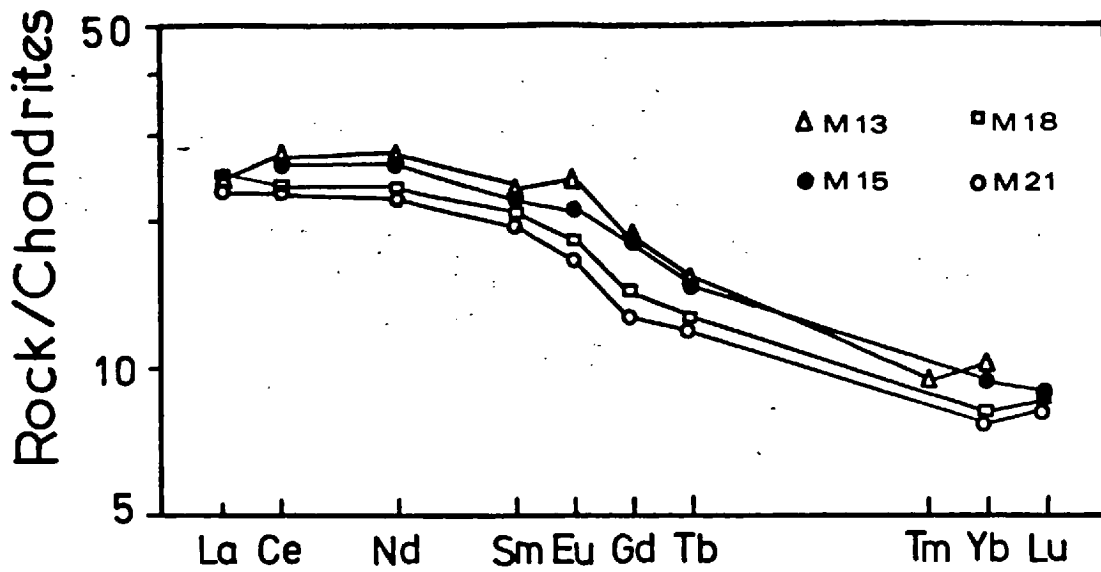


Figure 3 - 22 Chondrite-normalised REE patterns for four samples from the Pennygown Quarry lava.

Table 3 - 4 Selected rare-earth and trace element data from the section M 13 - 22 through the Pennygown Quarry lava.

Sample	Ce (ppm)	Yb (ppm)	Th (ppm)	(Ce/Yb) _N	Th/Yb
M 13	23.64	2.29	1.13	2.63±0.11	0.49
M 14	22.53	2.01	1.23	2.86±0.07	0.61
M 15	23.28	2.08	1.27	2.83±0.06	0.61
M 16	22.56	1.99	1.23	2.87±0.07	0.62
M 17	19.93	1.71	1.02	2.95±0.06	0.60
M 18	19.96	1.73	1.02	2.92±0.07	0.59
M 19	20.20	1.69	0.99	3.02±0.06	0.59
M 20	20.23	1.88	1.10	2.72±0.08	0.59
M 21	20.25	1.71	1.04	3.00±0.09	0.61
M 22	19.51	1.80	1.05	2.76±0.09	0.58

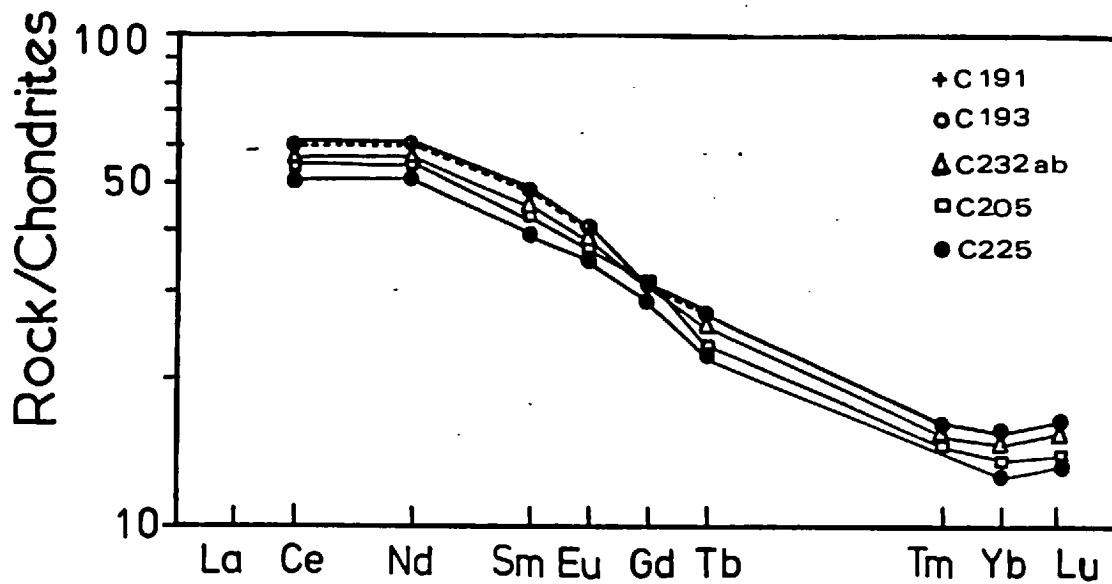


Figure 3 - 23. Chondrite-normalised REE patterns for five samples from C 191 - 232a/b, the lower flow in the drill core.

Table 3 - 5 Selected rare-earth and trace element data from C 191 - 232a/b. C 193 may have suffered slight LREE loss.

Sample	Ce (ppm)	Yb (ppm)	(Ce/Yb) _N	Th/Yb	Ta/Yb	Nb/Y
C 191	51.48	3.19	4.10 \pm 0.08	0.34	0.25	0.33
C 193	50.88	3.48	3.72 \pm 0.08	0.28	0.21	0.31
C 205	45.99	2.99	3.91 \pm 0.08	0.32	0.23	0.28
C 225	44.26	2.82	4.00 \pm 0.10	0.31	0.22	0.28
C 232a/b	49.33	3.24	3.88 \pm 0.18	0.24	0.19	0.24

they can be attributed to the breakdown of this phase in M 13. In contrast, in C 191-232a/b there is little change in $(\text{Ce}/\text{Yb})_N$ or the Th/Yb ratio despite the alteration of pyroxene in the margins of this flow (figure 3-23, table 3-5). P_2O_5 also behaves as an immobile element in all the samples from this flow, and it is evident that apatite only breaks down under conditions of extreme metasomatism. Since C 191-232a/b is more evolved than M 13-22, Ta and Nb have higher abundances in this flow. Both elements preserve relatively constant ratios with other immobile elements in C 191-232a/b (Table 3-5), suggesting that the poor correlations for Ta and Nb in M 13-22 are due to analytical problems as discussed above.

Both sphene and epidote are rare-earth acceptors. Epidote was separated from the vesicles in the drill core section, C 54-158, and analysed for REE. It contained 1.17 ppm of Ce and 0.5 ppm of Eu, but none of the other REE were detected. The presence of a trace of Ce in the vesicles supports the hypothesis that limited mobility of the LREE occurred during extreme metasomatism. The presence of Eu is also significant as M 13, which is highly reduced, contains a small positive Eu anomaly, indicating that some separation of Eu as the divalent ion occurred in the margin of the flow.

Sphene, which is present in all the greenschist-facies lavas, unlike epidote, will accept all the elements postulated to be immobile in the above discussion, except phosphorus. The fine grain size and mixed nature of the secondary minerals prevented separation of this phase for analysis. Sphene never occurs inside the secondary mineral pods and vesicles in the greenschist-facies lavas, instead the altered lava surrounding these structures is enriched in sphene (fig. 3-15, Appendix I-D, M 70). The mineralogical and chemical gradients across the secondary mineral pods will represent solubility gradients and the concentration of sphene around the margins clearly indicates that it is the principal repository for the immobile elements. In contrast, some mobility of Ti is indicated by the growth of sphene inclusions in some of the feldspars. Nevertheless, the extent to which any particular element can be considered immobile depends on the physical scale over which the chemical variation is investigated. TiO_2 and Zr, for

example, have correlation coefficients of 0.95 in M 13-22 (2 kgm samples crushed for analysis) and 0.85 in C 54-158 (samples of approximately 50 gm crushed for analysis). The data suggest that in the Mull lavas these elements were mobile on a millimetre rather than a centimetre scale.

The proportional changes in the abundances of the immobile incompatible elements mimic the changes produced by crystal-fractionation processes. This raises the possibility that some of the variations are due to variable distributions of phenocryst phases within the lava flows. In the zeolite-facies lavas this was only found to occur in the magnesian-basalts. Since unaltered Cr-spinels persist in most of the samples from the Pennygown Quarry lava, Cr should also behave as an immobile element in this flow. The element ratio Ti/Cr varies between 12 and 15 in all the samples from this lava flow except C 153v, which contains segregation vesicles and has a Ti/Cr ratio of 22. These values may be contrasted with those for the zeolite-facies lavas. Ti/Cr varies between 11 and 12 in LA 13-15, whilst in the flow LA 16-18, which does show olivine accumulation, Ti/Cr varies between 13 and 20 and rises to 38 in the segregation vein, LA 19ZR. Any variations in the phenocryst distribution within the Pennygown Quarry lava were thus small and unlikely to affect the incompatible element abundances significantly. The changes in these in the greenschist-facies lavas can clearly be ascribed to leaching processes.

These conclusions are in direct contradiction to those of Hellman et al. (1977) who stated that the preservation of nearly constant ratios by a group of elements during alteration indicated, not immobility, but rather a strong geochemical coherence during redistribution. Hellman et al. studied the REE distribution in the Cliefden outcrop - an exposure of Ordovician basalt affected by prehnite-pumpellyite facies metamorphism. Discussions of chemical variation in the Cliefden outcrop, which contains no unaltered material, are based on the assumption that it was once a homogeneous basalt lava flow (Smith 1968, Smith and Smith 1976, Hellman et al. 1977). The published description of this outcrop by Smith (1968) shows that it is texturally inhomogeneous on both a megascopic and microscopic scale. It contains numer-

ous chilled margins, poorly preserved pillows, patches of coarse grained lava, breccia zones and amygdale horizons (op.cit.figures 1 and 2, plates A to D). In addition it is a classic locality for segregation vesicles (Smith 1967). The samples used in all the studies of this exposure were small (approximately 20 cm³) and several came entirely from amygdale layers. The abundances of the incompatible elements show extremely large variations in the Cliefden outcrop - Zr, for example, varies between 20 and 159 ppm. These variations may be contrasted with the relatively small changes in abundance shown by the Mull greenschist-facies lavas, described above, and the two-fold variations in trace element concentrations between the segregation vein LA 19ZR and the adjacent lava LA 19R, described in chapter two. The resemblance of the REE distributions in the Cliefden outcrop to a fractionation trend is almost certainly more than coincidental.

Changes in oxidation state and volatile content

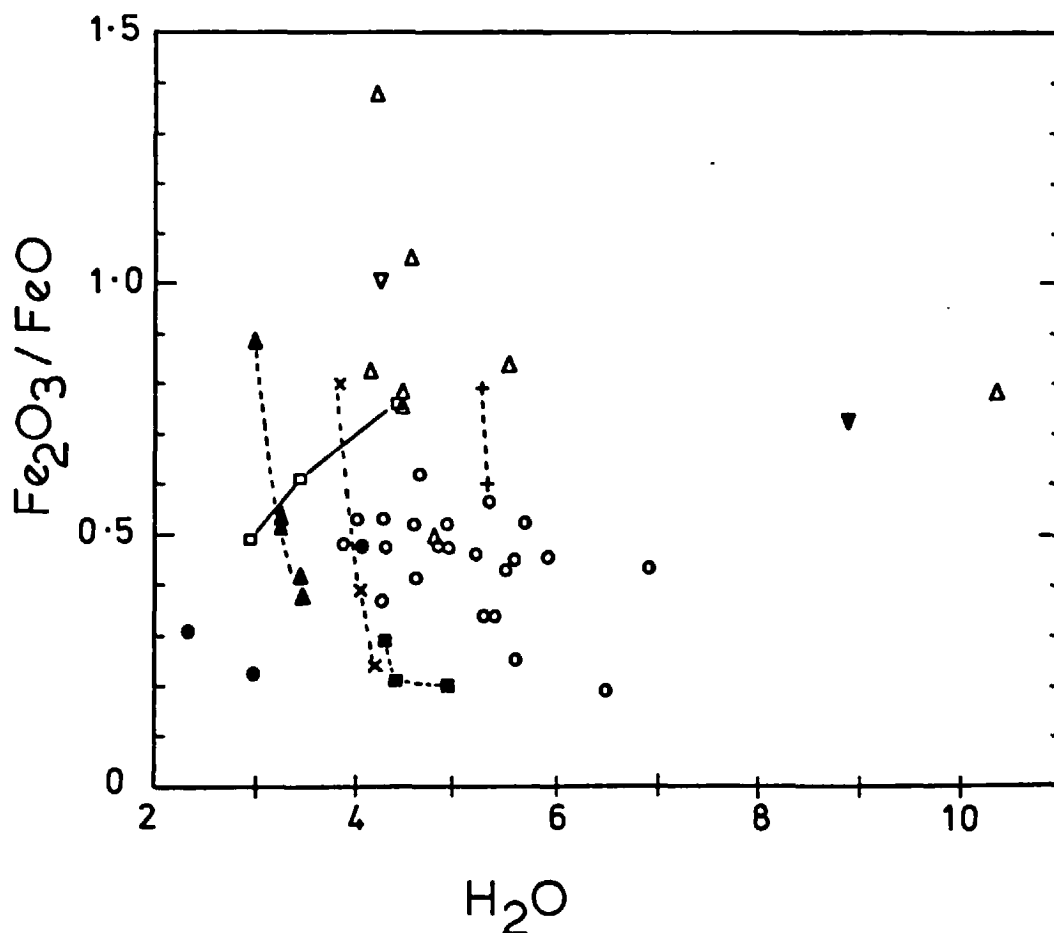


Figure 3-24 $\text{Fe}_2\text{O}_3/\text{FeO}$ versus H_2O in the greenschist-facies lavas.

○ M 13-22, □ C 54-158, ◻ M 26-28, ■ M 29-32, × M 34-36, + M 37-38
 ▲ M 41-46, ▽ M 45, ● M 47-50, ▼ C 176, △ C 191-232a/b.

The oxidation states and/or the H₂O contents are frequently used as an index of the degree of alteration in low-grade metabasalts. Figure 3-24 shows that there is no overall correlation between these two parameters in the Mull greenschist-facies lavas, although limited covariance of Fe₂O₃/FeO ratio and H₂O content does occur within some of the lava flows. Significantly, comparison of figures 3-24 and 2-7 reveals that the greenschist- and zeolite-facies lavas exhibit a similar range of oxidation states.

During hydrothermal alteration the Fe:Ti oxides were first oxidised then converted to sphene, an Fe-poor phase. In most of the lavas the only phases that take up significant quantities of iron are chlorite and amphibole, which are both ferrous ion minerals. The section M 13-22, through the Pennygown Quarry lava, shows a regular decrease in oxidation state towards the margin of the flow that can be attributed to the growth of sphene and chlorite at the expense of the Fe:Ti oxides (figs. 3-18, 3-19). The variable Fe₂O₃/FeO ratios in flows M 34-36, M 37-38, M 41-46 and M 29-30 shown in figure 3-26 can also be ascribed to the formation of sphene. M 29-32 which is extensively altered is the most reduced whilst the other three flows show only limited sphene formation.

The secondary mineral pods and vesicles tend to contain ferric ion minerals, suggesting that small variations in the water/rock ratio exerted a strong influence on the oxidation states of the lavas. In the flow M 26-28, which shows a positive correlation between Fe₂O₃/FeO ratio and H₂O content, secondary mineral pods containing chlorite and blebs of magnetite occur and the altered lava surrounding these pods contains both sphene and epidote (fig. 3-15). Similarly, epidote infills vesicles in M 45, which is oxidised (fig. 3-9). The drill core section through the Pennygown Quarry lava, C 54-158, shows little overall change in Fe₂O₃/FeO ratio as the reducing effect of chlorite and sphene formation has been offset by the deposition of epidote in the vesicles (figure 3 - 20). The marginal sample, C 191, in the flow C 191-232a/b contains epidote, and secondary mineral pods containing small blebs of magnetite occur in C 191-205. The next effect is that the upper part of this section shows little change in Fe₂O₃/FeO

ratio except in C 191 which is oxidised, whilst in the lower half of the section the growth of sphene causes reduction (fig. 3-21). Finally, the variable $\text{Fe}_2\text{O}_3/\text{FeO}$ ratios of M 47-50 reflects the presence of magnetite in vesicle-like structures in M 48.

The H_2O contents of the greenschist-facies lavas also show limited correlation with the extent of hydrothermal alteration. The lava flow M 34-36 which contains traces of unaltered olivine in one sample has higher H_2O contents than two of the samples from M 47-50 in which most of the igneous minerals have been altered. Figures 3-18 to 3-21 show that neither H_2O nor total volatile contents vary directly with the visible degree of alteration within individual lava flows.

Zeolites can contain up to 20 wt% H_2O whilst chlorite contains up to 13 wt% H_2O . In contrast, epidote and amphibole typically have no more than 3 wt% H_2O . It was shown in chapter two that the relative proportions of the igneous phases controlled the extent to which individual lavas are hydrated. Clearly, the nature of the secondary minerals replacing the primary phases is also important. This is neatly illustrated by comparison of samples C 191 and C 193 from the margin of the lower flow in the drill core. These samples show a similar degree of alteration as the pyroxenes and feldspars have been completely replaced in both of them. C 191 contains epidote and albite and has a H_2O content of 4.2% whilst, C 193 contains chlorite and zeolites and has a H_2O content of 10.3%. The higher H_2O content of M 34-36, relative to M 47-50, despite the extensive alteration of the latter flow, is due to the fact that M 34-36 contains chlorite, whilst, M 47-50 contains amphibole. The volume changes (and the degree of elemental mobility) resulting from the growth of epidote and amphibole will also be smaller than those resulting from the formation of chlorite and zeolites (c.f. C 191 and C 193 figure 3-21). Clearly, volatile contents and oxidation states cannot be used as reliable indices of alteration in a suite of lavas of initially varying compositions which have been replaced by a variety of secondary minerals.

Effects of hydrothermal alteration on $^{87}\text{Sr}/^{86}\text{Sr}$ ratios

Recent studies have demonstrated that the $^{87}\text{Sr}/^{86}\text{Sr}$ ratios of Mull lavas collected from outside the central hydrothermal aureole vary between 0.7028 and 0.7054 (Beckinsale et al. 1978, Carter et al. 1978). It therefore seems likely that the greenschist-facies lavas will also exhibit a range of $^{87}\text{Sr}/^{86}\text{Sr}$ ratios that will show no consistent relationship to the degree of alteration. Accordingly, the Sr isotope variation in the section, M 13-22, through the Pennygown Quarry lava was investigated. In addition a secondary mineral pod (M 75) that formed immediately above the base of the overlying lava, and the two discordant vein samples, M 24 and M 64, were analysed in order to determine the $^{87}\text{Sr}/^{86}\text{Sr}$ ratios of at least some of the hydrothermal fluids. The results are all listed in Table 3-5.

Within the lava flow the age corrected initial $^{87}\text{Sr}/^{86}\text{Sr}$ ratios range from 0.70519 in the least altered samples near the base of the section, to 0.70467 near the top of the flow. The Sr isotope ratios show no correlation with either the Sr or Rb distribution in the flow (fig. 3-19) but the decrease in $^{87}\text{Sr}/^{86}\text{Sr}$ corresponds with the increase in the degree of visible alteration and decrease in oxidation state towards the flow margin. $^{143}\text{Nd}/^{144}\text{Nd}$ ratios were determined on two of the samples, M 20 and M 14, using the technique described by Hawkesworth et al. (1978). In sharp contrast to their variable $^{87}\text{Sr}/^{86}\text{Sr}$ ratios, their Nd compositions are isotopically indistinguishable (M 14, 0.51265 ± 3 ; M 20, 0.51265 ± 2 ; two sigma errors).

To investigate further the Sr isotope geochemistry, pyroxene was separated from M 20 and it and some whole rock powders were subjected to leaching experiments. Leaching was carried out with 6 M HCl in sealed teflon bombs for 14 hours at 130°C (O'Nions and Pankhurst 1976). X-ray analysis of the powders before and after leaching showed marked increase in the concentrations of pyroxene and to a lesser extent plagioclase, due to the dissolution of secondary minerals such as chlorite (fig. 3-25). Analysis of the residue after leaching should thus provide $^{87}\text{Sr}/^{86}\text{Sr}$ ratios closer to the pre-alteration composition of the lava flow.

Table 3-5 Rb-Sr results.

Sample	Rb ^a	Sr ^a	Rb/Sr	$^{87}\text{Sr}/^{86}\text{Sr}^b$	$(^{87}\text{Sr}/^{86}\text{Sr})_0^c$
M 13	7.17	271	0.026	0.70486 ± 3	0.70479
M 14	1.76	375	0.005	0.70489 ± 3	0.70488
M 15	2.51	279	0.009	0.70469 ± 3	0.70467
M 16	11.8	443	0.027	0.70482 ± 3	0.70475
M 17	14.5	338	0.043	0.70496 ± 3	0.70485
M 18	15.4	310	0.050	0.70506 ± 4 (0.70519 ± 2)	0.70494
M 19	11.6	274	0.042	0.70505 ± 5 (0.70514 ± 4)	0.70495
M 20	2.62	340	0.008	0.70515 ± 2 (0.70525 ± 6)	0.70513
pyroxene	(0.26)	(51.9)	(0.005)	(0.70520 ± 2)	(0.70519)
M 21	9.08	299	0.030	0.70519 ± 3	0.70511
M 22	14.6	311	0.047	0.70531 ± 3	0.70519
	(11.6)	(129)	(0.090)	(0.70538 ± 4)	(0.70516)
M 24	2 ^x	169 ^x	0.012	0.70521 ± 6	0.70519
M 64	2 ^x	359 ^x	0.006	0.70467 ± 3	0.70466
M 65				0.70505 ± 4	
M 75A				0.70421 ± 6	
M 75B				0.70427 ± 4	

a Rb and Sr contents determined by isotope dilution ($\pm 1\%$) unless postscripted ^x which denotes XRF analysis

b present day $^{87}\text{Sr}/^{86}\text{Sr}$ ratio \pm two standard errors on the mean.
E-A, = 0.70807 ± 3 and NBS 987 = 0.71029 ± 3 during the course of this study

c Initial Sr composition calculated assuming an age of 60 m.y. and
= $1.39 \times 10^{-11} \text{ y}^{-1}$ for ^{87}Rb decay.

Results in brackets indicate that they were determined on samples which had been leached in 6m HCl (see text).

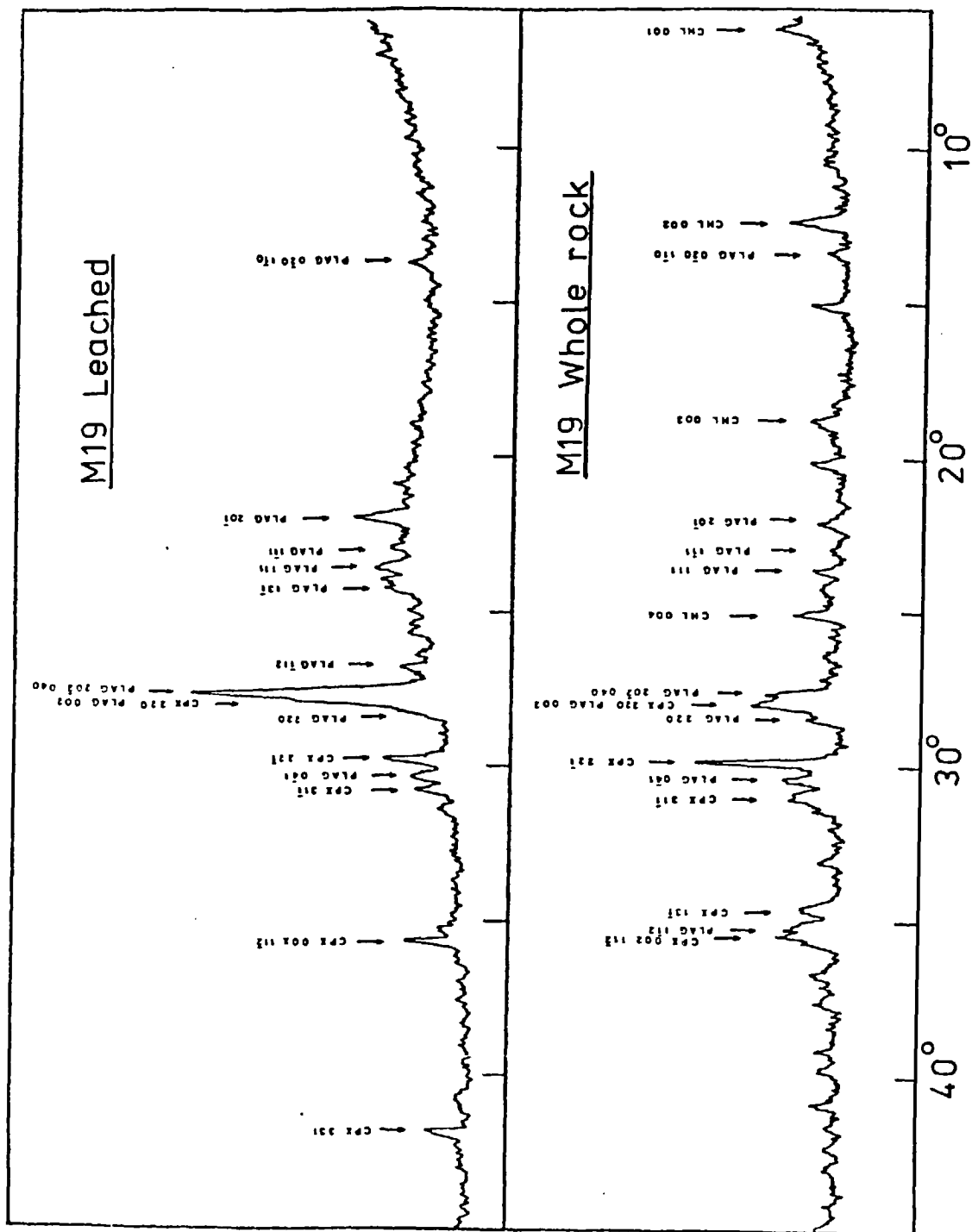


Figure 3- 25 Partial X-ray diffractogram of sample M 19 showing the effect of leaching in 6M. HCl. Cu K_{α} radiation; 1° slits; $0.5^\circ 2\theta \text{ min}^{-1}$.

The pyroxene separate has an age-corrected initial $^{87}\text{Sr}/^{86}\text{Sr}$ ratio of 0.70519, while that of the leached whole rock sample is 0.70516. Rb and Sr concentrations for the leached residues from M 18, M 19 and M 20 are not available but they all have significantly higher present day $^{87}\text{Sr}/^{86}\text{Sr}$ ratios than the unleached samples. This indicates that the altered material tends to have lower $^{87}\text{Sr}/^{86}\text{Sr}$ ratios than the fresh basalt. The leaching experiments and decrease in $^{87}\text{Sr}/^{86}\text{Sr}$ with increasing bulk rock alteration all suggest that hydrothermal alteration of this particular lava flow caused a general reduction in $^{87}\text{Sr}/^{86}\text{Sr}$. This contrasts sharply with the effects of sea water alteration as it is well documented that hydrothermal alteration of basalts on the ocean floor results in a general increase in $^{87}\text{Sr}/^{86}\text{Sr}$ ratios. (e.g. Spooner^{et al.} 1977, O'Nions et al. 1978). The composition of the leached pyroxene separate provides the best estimate of the primary composition of the magma (c.0.7052). The two $^{144}\text{Nd}/^{143}\text{Nd}$ results provide some indication that the lava was isotopically homogeneous when it cooled, and that Nd was not affected significantly by hydrothermal alteration.

The results on the main secondary minerals confirm that the fluids responsible for the alteration had low $^{87}\text{Sr}/^{86}\text{Sr}$ ratios. The secondary mineral pod from the overlying lava flow gave values of 0.70421 and 0.70427. The two vein samples, M 24 and M 64, have initial $^{87}\text{Sr}/^{86}\text{Sr}$ ratios of 0.70519 and 0.70467 ± 3 , respectively. M 65, from the intensely altered basalt surround to this vein where it cuts the Pennygown Quarry lava, has an $^{87}\text{Sr}/^{86}\text{Sr}$ ratio of 0.70505, again significantly lower than the estimated initial value for the flow of 0.7052. The veins were deposited by later stage fluids than the secondary mineral pods and the Sr isotope results could thus indicate a slight rise in the $^{87}\text{Sr}/^{86}\text{Sr}$ ratios of the fluids with time at this locality.

The low $^{87}\text{Sr}/^{86}\text{Sr}$ values of the fluids indicated by these results (≤ 0.7048) clearly rule out interaction with either Moinian basement or, Tertiary intrusives such as the Glen Cannel and Loch Usig granophyres, which have initial $^{87}\text{Sr}/^{86}\text{Sr}$ ratios of 0.7094 ± 3 and $0.7135 - 0.7162$, respectively (Pankhurst et al. 1978, Beckinsale 1974). Sources of unradiogenic Sr in the fluids are either unconfirmed but possible granulite-facies basement, or much more likely, the basalts themselves.

The Rb/Sr ratios of the two vein samples lie within the range determined for the zeolite-facies lavas, as do the $^{87}\text{Sr}/^{86}\text{Sr}$ values determined for all the secondary minerals. The data indicate that interaction of heated meteoric water with the lavas caused the chemistry of the resultant fluids to be buffered by that of the basaltic rocks. The average $^{87}\text{Sr}/^{86}\text{Sr}$ value of the lavas analysed by Beckinsale et al. (1978) and Carter et al. (1978) is 0.7035, and it is likely that the fluids in this area will have similar $^{87}\text{Sr}/^{86}\text{Sr}$ ratios. Interaction of these fluids with basalt of Sr isotope composition 0.7052 will therefore result in a reduction in $^{87}\text{Sr}/^{86}\text{Sr}$ in the more altered material (Table 3-5). Moreover, since no systematic variation in Sr content occurred within this lava section (see fig. 3-19) it would appear that Sr isotope exchange took place with little net addition or removal of Sr.

These results provide considerable constraints on models of the hydrothermal circulation 'cells'. They suggest that the Sr composition of the fluids in the basalt pile was not significantly affected by interaction with either 'old' basement (perhaps 0.5 km below the present erosion surface at this locality) or Tertiary intrusive rocks which outcrop only 1.5 km to the south. Taylor (1977) pointed out that the temperature and pressure gradients in the immediate vicinity of a magmatic intrusion would prevent hydrothermal fluids from entering it until it had undergone a considerable degree of cooling and consolidation. The large number of near vertical fractures and ringdykes around the central complex will also have served to channel the hydrothermal fluids so as to create separate circulation cells inside and outside the central complex.

4. Mass balances during hydrothermal alteration

Major elements

The extent to which elements have been added to, or subtracted from, the greenschist-facies lavas can only be fully established by comparison with the relatively unaltered zeolite-facies lavas. The A, B and C type lavas (see Table 3-1) can be compared with the magnesian basalts, less-magnesian basalts and hawaiites, respectively. Samples C 176 and M 47-50 are more problematical. The contrasting $\text{TiO}_2:\text{P}_2\text{O}_5:\text{Zr}:\text{Y}$

ratios of sample C 176 and the lower flow in the drill core, C 191-232a/b, demonstrate that the thin, plagioclase-phyric layer above the breccia zone in the drill core is a separate lava flow. C 176 and flow M 47-50 are sparsely phyric and contain recognisable plagioclase phenocrysts only, which may or may not be a result of extensive alteration. Two of the zeolite-facies lavas, LA 1-5 - the basaltic hawaiite, and LA 7-11 a less-magnesian basalt, are nearly aphyric and plagioclase is the dominant phenocryst phase in both (Appendix I-C). Their compositions may therefore, approximate to those of the precursors of C 176 and M 47-50. The compositions of the various lava types in the zeolite- and greenschist-facies zones are compared in figures 3-26 to 3-30.

Figure 3-26 shows that the greenschist-facies lavas tend to be depleted in SiO_2 , relative to the zeolite-facies lavas. Three samples, all of which contain secondary quartz, plot above the zeolite-facies lavas in figure 3-26, whilst all the rest lie close to or below them. In contrast, with exception of two samples, the overall range of Al_2O_3 contents shown by the two groups of lavas is similar. The titanomagnetite-phyric flows show some depletion in Al_2O_3 relative to the hawaiites. This group also shows the widest range of SiO_2 contents.

In figure 3-27 the two sets of lavas are compared on two sets of triangular diagrams. In each case the zeolite-facies lavas are plotted in the left hand diagram. In the ACF diagram :

$$A = \text{Al}_2\text{O}_3 + \text{Fe}_2\text{O}_3 - (\text{Na}_2\text{O} + \text{K}_2\text{O}); \quad C = \text{CaO}; \quad F = \text{FeO} + \text{MgO};$$

permutations of this diagram have been used by various authors to show bulk compositional changes in metabasalts (e.g. Jolly and Smith 1971, Humphris and G.Thompson 1978^a). It clearly shows that nearly all of the greenschist-facies lavas are depleted in CaO relative to the zeolite-facies lavas. The lavas also show variations in their A and F components on this diagram and these can be disentangled on the adjacent AFM diagram - a conventional $(\text{Na}_2\text{O} + \text{K}_2\text{O}) - (\text{Fe}_2\text{O}_3 + \text{FeO}) - \text{MgO}$ plot. The iron/magnesium ratios of the different lava types are clearly similar in both the greenschist- and zeolite-facies flows, whilst they show considerable variations in alkali content within each

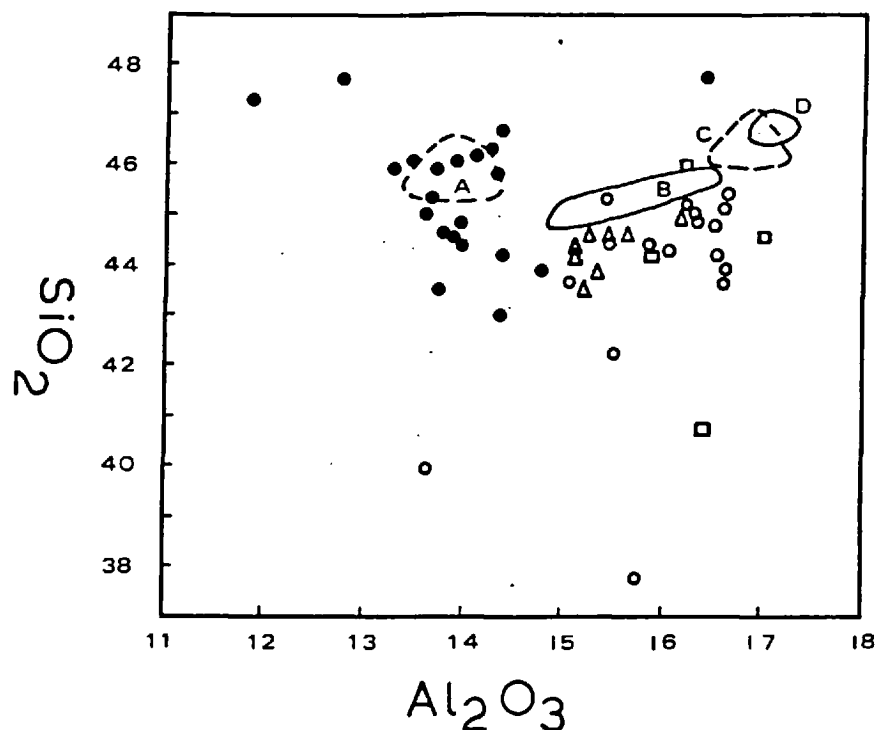


Figure 3-26 SiO₂ versus Al₂O₃ for the Plateau lavas. Zeolite-facies lavas plot in outlined fields, symbols refer to greenschist-facies lavas : A, ● - magnesian basalts; B, ▲ - less-magnesian basalts; C, □ - sparsely plagioclase-phyric lavas; D, ○ - hawaiites.

type. The mean content of the different types of greenschist-facies lavas are not however significantly different from the zeolite-facies flows.

The immobility of TiO₂ and P₂O₅ during hydrothermal alteration is clearly demonstrated in Figure 3-28 in which samples from individual lava flows lie along lines of constant TiO₂/P₂O₅ ratio, the sole exception being M 13, which has lost P₂O₅ as a result of apatite breakdown. On this diagram two of the altered flows - the Pennygown Quarry lava and the lower flow in the drill core - appear to be enriched in K₂O, relative to the zeolite-facies lavas, whilst none of them show evidence for significant depletion. Rb and Ba show similar distributions to K₂O in the altered lavas (figs. 3-19 to 3-21,); K₂O - Rb and K₂O - Ba having correlation coefficients of 0.97 and 0.83 respectively, in the Pennygown Quarry lava. The higher K₂O, Rb and Ba

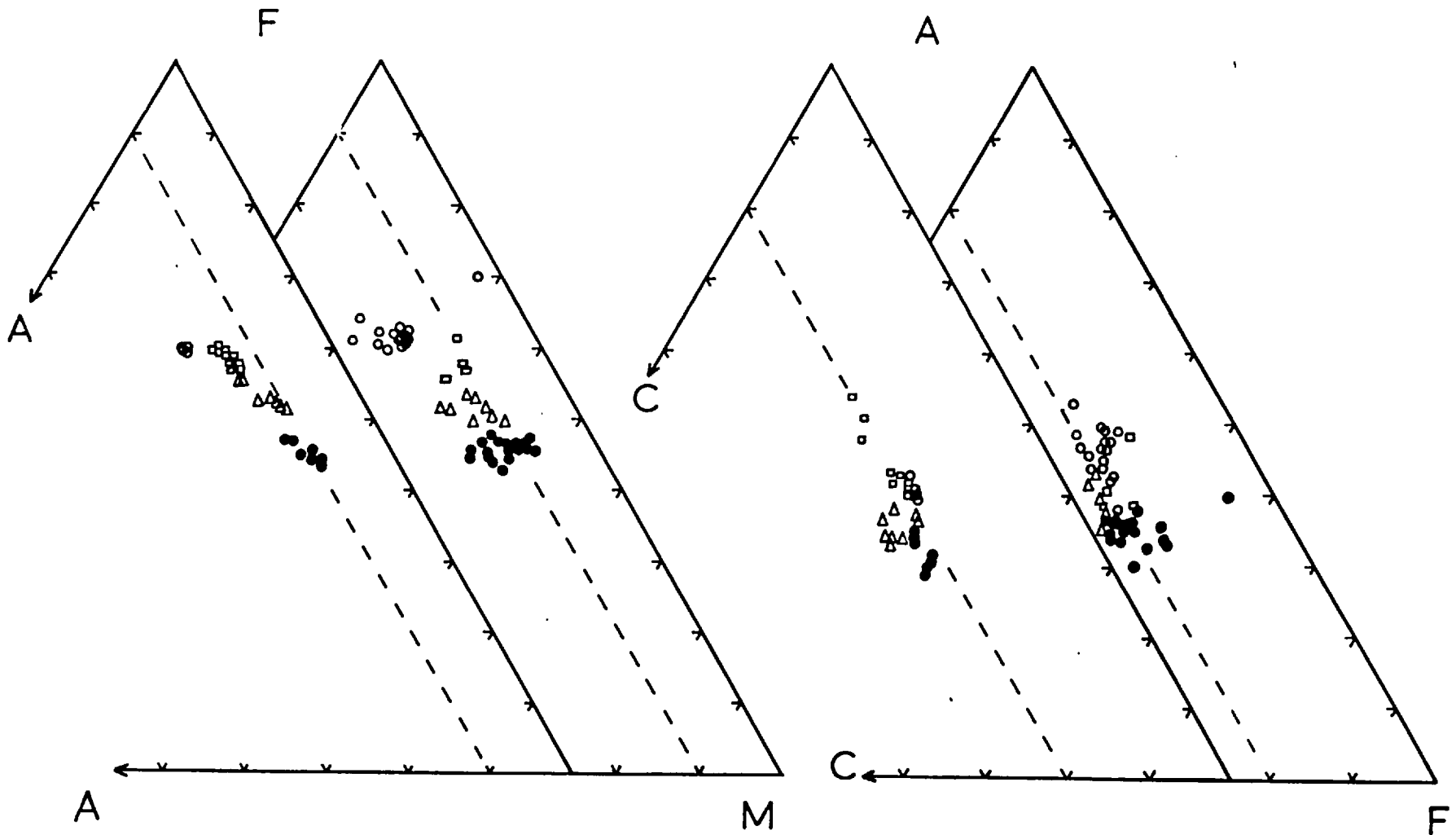


Figure 3-27 AFM and ACF diagrams.(see text for explanation). In each case the zeolite-facies lavas are plotted in the left hand diagram. Symbols as in figure 3-26.

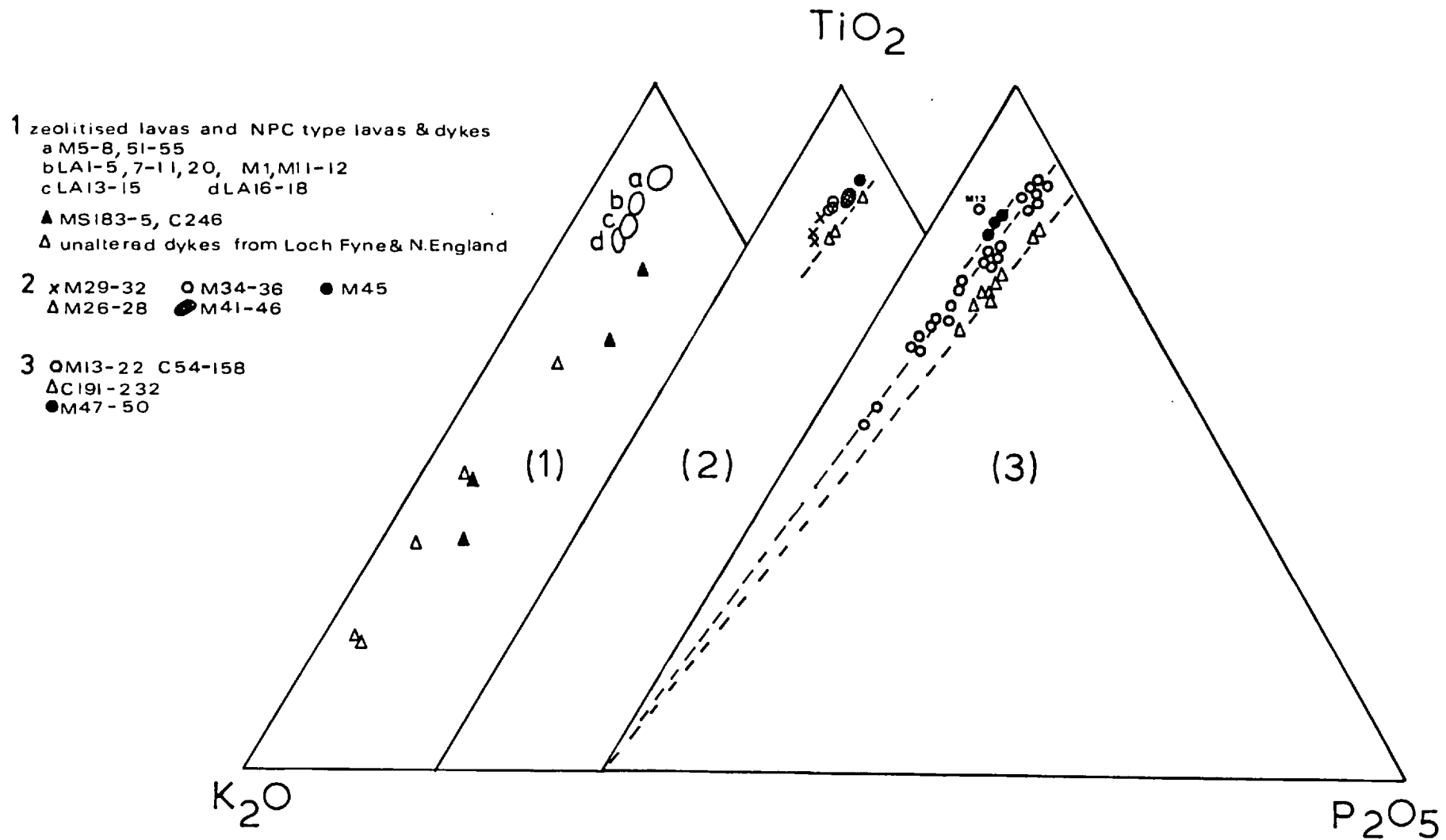


Figure 3-28 TiO₂-K₂O-P₂O₅ diagram of T.Pierce et al. (1975) showing the effect of alteration on the greenschist-facies lavas.

contents of these lavas is not a primary magmatic feature as the plagioclases in the centres of these flows have been partially replaced by K-feldspar and some additional source of these elements thus appears to be required.

One possible source is the Non-Porphyrific Central lavas which have higher K_2O contents than the Plateau Group. The Mull NPC lavas and dyke shown in figure 3-28 have also been affected by greenschist-facies, but unaltered NPC type dykes with similar K_2O contents occur in the mainland extension of the Mull regional swarm demonstrating that their high K_2O contents may be primary. (L.Nodes pers.Comm). Nevertheless, the flow C 191-232a/b shows no K_2O enrichment in the basal sample, C 232a/b, which is almost adjacent to the NPC type dyke C 246 recovered in the drill core. The $^{87}Sr/^{86}Sr$ ratios of the NPC type basalts may be higher than those of the Plateau lavas (Moorbath and Thompson 1979) and the $^{87}Sr/^{86}Sr$ ratio of the Pennygown Quarry lava was reduced during alteration. The three mugearite flows analysed by Beckinsale et al. (1978) have higher K_2O , Rb and Ba contents but lower $^{87}Sr/^{86}Sr$ ratios than many of the associated basalts. The Sr-isotope data discussed above clearly indicate that the compositions of the hydrothermal fluids were buffered by the lavas and thus the enrichment in K_2O etc. in the greenschist-facies lavas could be explained if the evolved lava types were more abundant ⁱⁿ the missing upper part of the lava pile than in the present day erosional remnant.

The only lava section in which the elemental gains and losses during alteration could be quantified was the section M 13-22, through the Pennygown Quarry lava. This section is almost completely non vesicular and hence the chemical variations across it can be attributed directly to the progressive alteration of the primary phases. The results in terms of grams of oxide lost or gained per $100cm^3$ of rock altered are shown graphically in figure 3-29. Three different calculations were performed. The dashed and dotted lines in figure 3-29 show the results obtained assuming constant volumes were maintained during alteration and using an average magnesium basalt composition and sample M 20 as the starting materials, respectively. M 20 was used as it has the lowest H_2O and highest CaO and modal pyroxene contents. The solid line shows the results obtained assuming constant TiO_2

content and again using M 20 as the starting material. The close agreement between the solid and dotted lines for all the oxides demonstrates that the constant volumes assumption is a valid one. The density data used in the calculations are all listed in Appendix I.F. Similar calculations were not performed for the other lavas as many cannot be matched up with a suitable counterpart in the zeolite-facies zones whilst, constant volume constraints cannot be applied to highly vesicular or hydrothermally brecciated samples.

Comparison of figures 3-18, 3-19 and 3-29 discloses that the alteration of plagioclase and pyroxene did result in drastic leaching of CaO and some enrichment in Na₂O. The calculation using the average magnesian basalt allows the compositional changes during the initial stages of the alteration which cannot be deduced purely from the intra-lava variation to be established. The central part of the section is depleted in SiO₂, MgO and Fe₂O₃* relative to its probable initial composition, suggesting the conversion of olivine to chlorite was accompanied by migration of the olivine components. The smaller but significant depletion in CaO, Na₂O and Al₂O₃ probably reflects the partial replacement of the plagioclase by K-feldspar. Nevertheless, Al₂O₃ and Fe₂O₃* increase in the upper parts of the flow which also shows no further net loss of MgO. The extensive breakdown of the primary phases in the flow margin released Al₂O₃ for chlorite formation which was clearly accommodated by preferential mobilisation of the feldspar components. The only oxides in which ^{the} lava flow shows a net gain are K₂O, Na₂O, H₂O and CO₂. Little corresponding increase in Na₂O occurs at the base of this lava flow (c.f. figs. 3-19 and 3-20). Significantly, the flow is overlain by an evolved Na-rich lava whilst judging by the position of sample C 176 in figures 3-27 the underlying flow was less evolved, suggesting that considerable exchange between adjacent lava flows occurred.

It is apparent from figures 3-26 and 3-27 that all the lavas, not just M 13-22, are depleted in CaO and SiO₂, but that Al₂O₃, Fe₂O₃* and MgO are considerably less affected. The extent of the compositional changes appears to have been controlled by the relative proportions of the primary phases in the lava flows. In the Pennygown Quarry lava

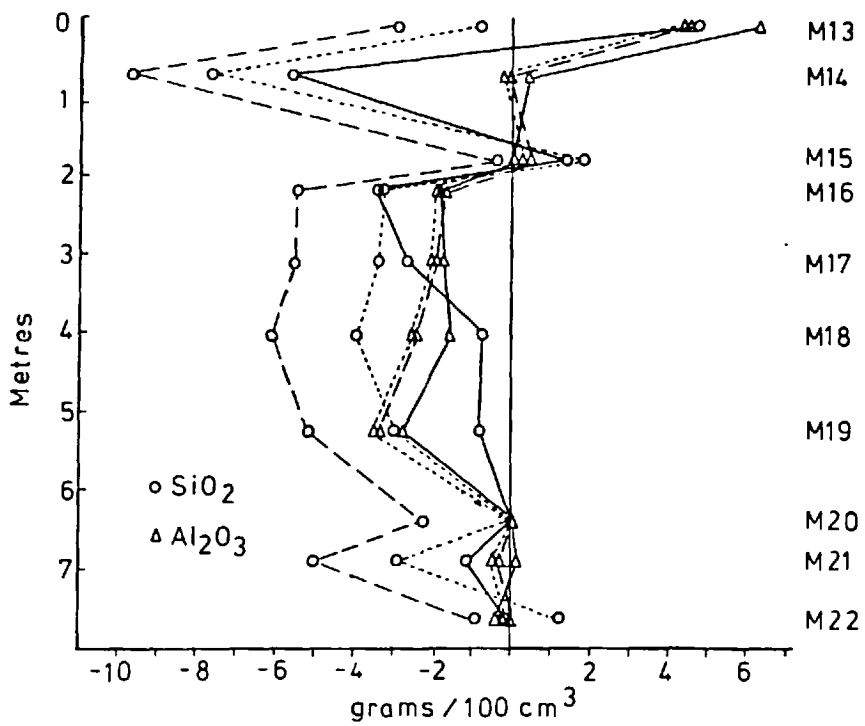
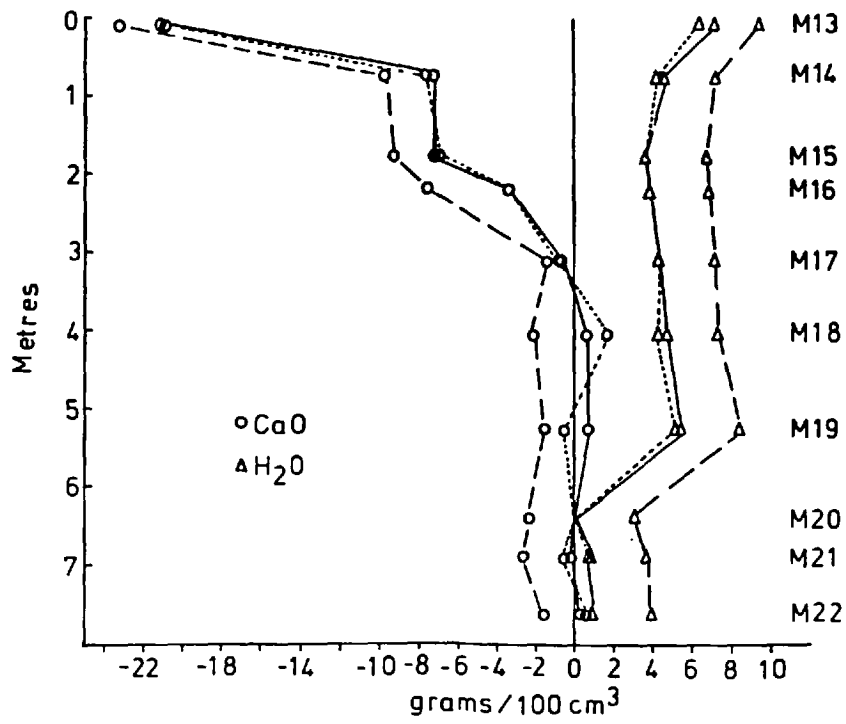


Figure 3-29 Gains (+) and losses (-) of major element oxides from the Pennygown Quarry lava flow.

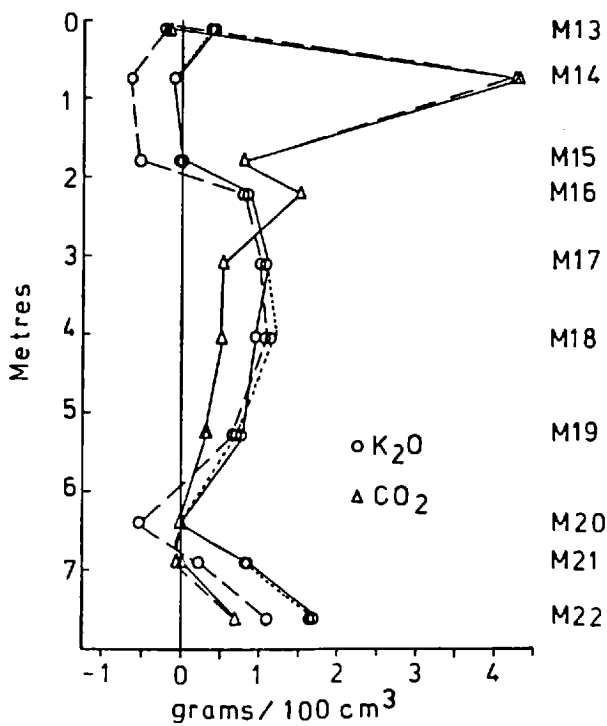
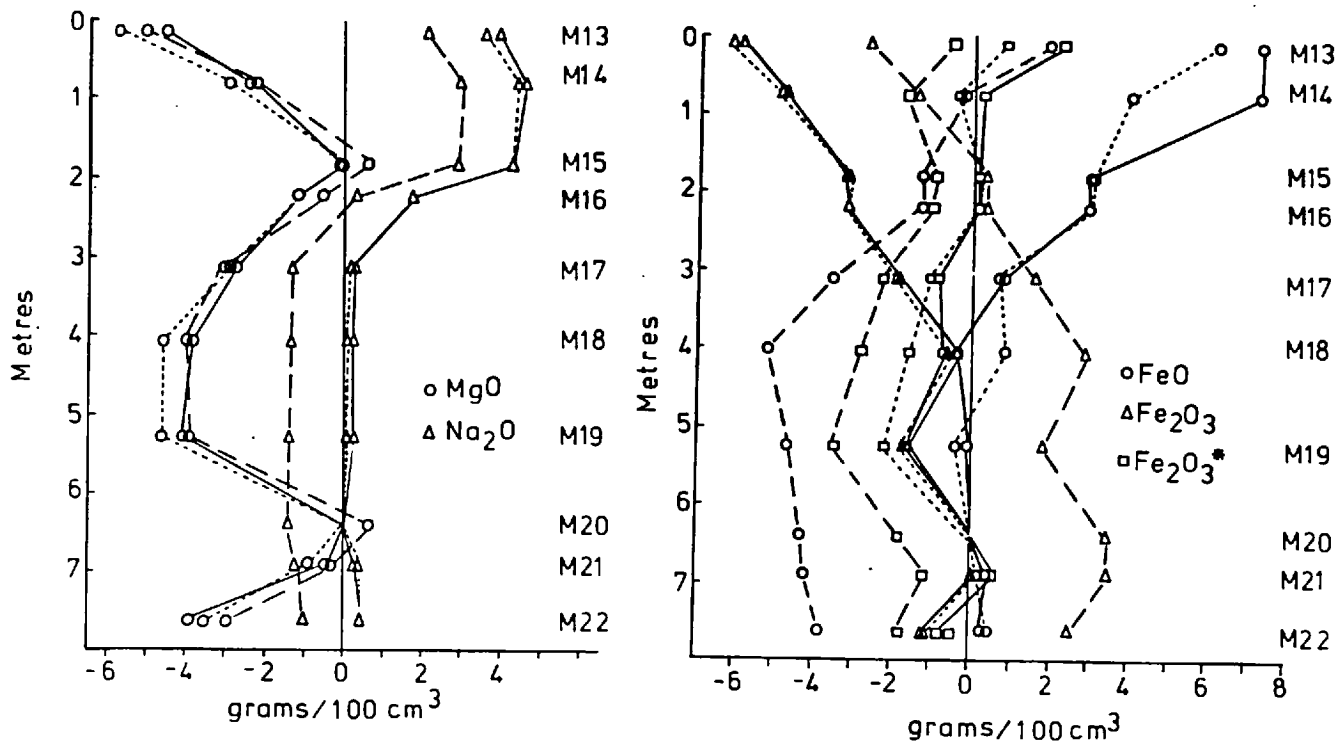


Figure 3-29 (continued).

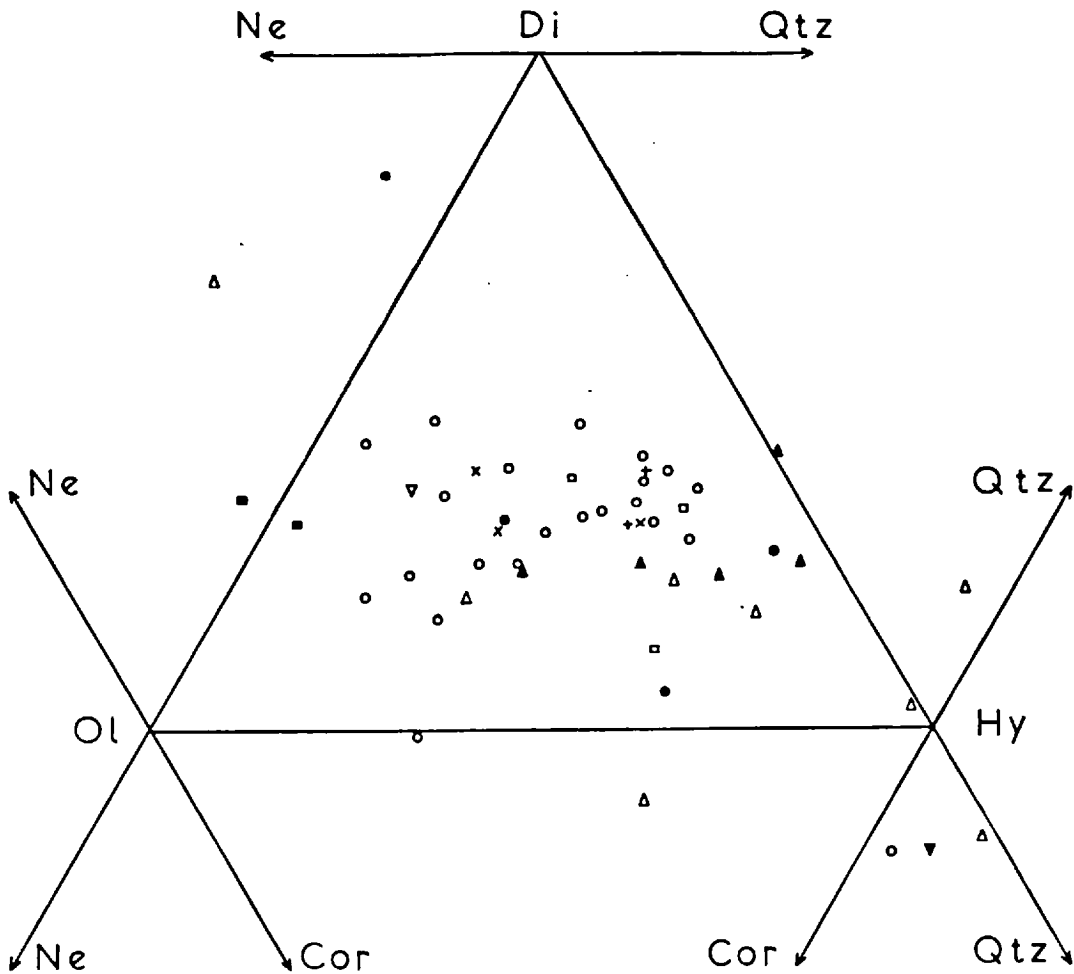


Figure 3-30

Normative quartz-diopside-hypersthene-olivine-nepheline-corundum relationships in the greenschist-facies lavas. Symbols as in figure 3-24.

which had a high proportion of mafic to felsic phases, MgO and Fe_2O_3^* were mobile and Al_2O_3 behaved as a relatively immobile element - Al_2O_3 and TiO_2 have a correlation coefficient of 0.87 in M 13-22 - suggesting most of the aluminium released by the feldspars was consumed in the formation of chlorite from olivine and pyroxene. In contrast, in C 191-232a/b, which had a relatively high proportion of felsic to mafic phases, Fe_2O_3^* and MgO were relatively immobile, whilst Al_2O_3 was mobilised (Table 3-3 and fig.3-21).

The effects of the hydrothermal alteration on the norms of the lavas is illustrated in figure 3-30. Comparison with figure 2-12 A shows that the overall range of Si-saturation shown by the zeolite- and greenschist-facies lavas is similar. The effects of leaching both Ca and Si from the lavas would thus appear to cancel each other out. Nevertheless, the net loss of CaO has caused the norms of the greenschist-facies lavas to be poor in di and rich in ol and hy relative to the zeolite-facies lavas, and the extremely Ca-depleted samples have become corundum-normative.

Trace elements

The behaviour of TiO_2 , P_2O_5 , Zr, Nb, Y, Ta, Th, Hf and the REE, which were relatively immobile, and Rb, Ba and Sr, which were mobile during alteration have all been discussed above. Cr was probably unaffected in most of the lavas. In the more-evolved lavas which contained titanomagnetite phenocrysts the abundance of this element are too low to demonstrate any unequivocal relationship with the other immobile elements and hence the Cr data for these flows should be treated with caution. Ni correlates with MgO in most of the lava flows but not in the Pennygown Quarry flow in which MgO was clearly mobilised (c.f. figures 3-19 and 3-21). The distribution of Ni within this flow also shows no correlation with the immobile trace elements indicating mobility. Nevertheless, no covariance of Ni with Cu or Zn could be detected indicating it was not taken up by secondary sulphide formation, and Ni was detected in many of the chlorites in this flow (e.g. Appendix I-D, M 13 nos.8,9). The separation of Mg and Ni in this lava thus reflects merely differing solubilities in the hydrothermal fluids.

Cu and Zn show covariance in several of the greenschist-facies lavas (M 34-36, M 26-28, M 41-46, M 37-38). The variation in these flows are similar to those in the zeolite-facies lavas discussed in chapter two. In the other lava flows both Cu and Zn varied but showed no correlation either, with each other or, with any of the other elements. In several of these lavas (M 13-22, M 29-32, M 47-50) secondary Cu sulphides were observed replacing magnetite in the vesicles and secondary mineral pods but little or no zinc was detected in these.

(e.g. Appendix I-D, M 13 no.15). The average Cu and Zn content in these flows is lower than that in the zeolite-facies lavas and it seems that some mobilisation of these elements occurred during alteration. The extent is impossible to calculate as the intra-lava variations in the zeolite-facies zones is greater than any of the inter-lava variations.

Conclusions to chapter three.

1. The hydrothermal fluids failed to achieve any significant penetration into the crystalline Moinian rocks forming the basement to the lava pile. Separate 'Circulation cells' were established inside and outside the central intrusive complex and little, or no, chemical exchange occurred between the intrusive and extrusive rocks; instead the composition of the fluids circulating within the lava pile was buffered by the lavas themselves.
2. The ratio of CO₂/H₂O in the fluid phase was low and was controlled by the mineral reactions. Additional evidence for a low partial pressure of CO₂ is furnished by the presence of sphene, rather than rutile or anatase in the flow interiors. (Schuiling and Vink 1967).
3. K, Rb, Ba, Na, Sr, Al, Mg and, to a lesser extent, Fe were redistributed within the lava pile - mainly as alkali feldspar and chlorite - whilst Ca and Si were leached and deposited in veins and vesicles - mainly as CaAl hydrosilicates, quartz and calcite. The extent of the element mobility varies from flow to flow depending on the relative proportions of mafic and felsic phases within them. Nevertheless, none of the greenschist-facies lavas can be considered to have magmatic compositions as alteration of the olivines clearly involved mobility of both Mg and Si.
4. Ti, P, Zr, Nb, Y, Ta, Hf, Th and the REE were immobile except during extreme metasomatism when apatite breakdown caused some loss of P, Th, La and Ce. Since the addition and removal of mobile elements causes changes in the concentrations of less-easily mobilised ones, ratios between these elements, but not their absolute abundances, can be considered to represent primary magmatic characteristics.

5. The greenschist-facies lavas provide a source for the Ca and Si deposited in the vesicular margins of the zeolite-facies lavas. The deduced $^{87}\text{Sr}/^{86}\text{Sr}$ ratios of the hydrothermal fluids (≤ 0.7048) is similar to that of the vesicle infilling, M 56Z, discussed in chapter two ($^{87}\text{Sr}/^{86}\text{Sr} = 0.7042$). The two analysed amygdaloidal samples, M 56 and LA 19, and the basalt flow, LA 7-11, which shows marginal enrichment in Ca and ^{87}Sr , were all collected from the lowest temperature zone - the mesolite zone. The zeolite-facies zones, therefore, were not produced by burial metamorphism, but represent a low temperature periphery to the hydrothermal system. The oxygen isotope studies of Forester and Taylor (1976) delineated only those areas in which the igneous rocks and the circulating fluids were not in isotopic equilibrium. In many areas of low-grade hydrous metamorphism, such as Mull, Sr isotope analyses of secondary minerals (or a combination of Sr and O isotope studies) may provide a more accurate geochemical method of mapping hydrothermal systems than oxygen isotope studies alone.

CHAPTER FOUR: RECONSTRUCTION OF THE MULL HYDROTHERMAL SYSTEM.

1. Thermal gradients and water/rock ratios.

In active geothermal systems pressure, temperature and solution composition are accessible to direct measurement. In fossil systems, such as Mull, these parameters can only be deduced from the mineralogical and chemical changes that have taken place in the altered rocks.

Evidence from O-isotope studies

The ^{18}O -variation in the igneous rocks of Skye has been investigated in more detail than in Mull. Nevertheless, the generalised, average profiles for the $\delta^{18}\text{O}$ values of the country rocks around the plutons in these two igneous centres are similar (fig. 1-4), and in each case the area of ^{18}O -depletion is approximately 500km^2 (Forester and Taylor 1976, 1977). Since Mull is located only 80km south of Skye and the two centres are approximately similar in age (Macintyre et al. 1975, Fitch et al. 1978), it is likely that the early Tertiary ground waters had similar $\delta^{18}\text{O}$ values in both regions. D/H analysis of altered rocks from both Skye and Mull have yielded similar δD values (Forester and Taylor 1977, Taylor and Epstein 1968) which give an estimated $\delta^{18}\text{O}_{\text{H}_2\text{O}}$ of -11 to -12 for the groundwaters initially entering the convective systems around these two igneous complexes. The Skye and Mull lavas are petrographically similar, show a similar sequence of secondary mineral zones (King 1977), and should therefore have offered approximately equal resistance to hydrothermal exchange. Accordingly, the similar radial inward depletion in ^{18}O shown by the lavas surrounding these two igneous complexes probably indicates interaction over a similar range of temperatures and water/rock ratios.

Table 4-1 gives the thermal gradients calculated by Forester and Taylor (1977) for the Skye hydrothermal system from the ^{18}O -variation shown by the country rocks. These calculations are based on several simplifying assumptions which may not be entirely realistic :-

1. The hydrothermal fluids and the rocks are assumed to have been in isotopic equilibrium. It is clear from the compositional variations detected during this study that the domain of equil-

ilibrium amongst the secondary minerals was considerably smaller than that represented by a typical thin section. Whether or not mineralogical disequilibrium necessarily implies isotopic disequilibrium is not yet clear. In both Mull and Skye the $\delta^{18}\text{O}$ values converge inwards towards an approximately constant value of -4 to -6, suggesting an approach to equilibrium in the central parts of the system(s) (fig. 1-4). In the outermost parts of the areas of ^{18}O -depletion, where both the temperatures and water/rock ratios will have been lower, this is unlikely to have been the case.

2. The calculations were made on the assumption that the complex reactions and exchanges that occurred in the lavas can be approximated by exchange between plagioclase (An_{50}) and water, since little is known of the ^{18}O -fractionation between phases such as chlorite and zeolites and water. Whilst in many cases this may be a valid assumption it is unlikely to apply to quartz-rich samples, such as M 13 from the margin of the Penny-gown Quarry flow, which will be richer in ^{18}O than samples containing little or no quartz (Taylor and Epstein 1967). During the course of this study an attempt was made to separate pairs of secondary minerals for which the ^{18}O -fractionations are known, such as quartz and feldspar, but these failed due to the fine-grained nature of the assemblages. Determinations of temperature by fluid-inclusion studies proved impossible for the same reason, as although possible inclusions were detected in several samples these were too small to allow their contents to be resolved.

In terrestrial geothermal systems the thermal gradient is constrained by the boiling point curve for water; which permits a maximum temperature of 310°C to occur at a depth of 1km in a hydrostatic pressure gradient. In systems involving downwards penetration of meteoric water, pressure on the water cannot normally exceed hydrostatic pressure so that $P_{\text{H}_2\text{O}} \approx \frac{1}{3} P_{\text{load}}$.

Studies of active geothermal systems have shown that boiling of the hydrothermal fluids causes rapid changes in pH and loss of CO_2 ,

Calculated temperatures (°C)* of oxygen isotope exchange between H₂O and basaltic country rocks and dikes, assuming closed-system convective circulation, constant water/rock ratios, and isotopic equilibrium (because of more complete equilibration at higher temperatures, and because of radial inward flow of ground water toward the central complex, the effective W/R ratios must increase inward; a realistic gradient might be given by the values enclosed by the dashed lines).

δ ₂₇ ^f	Temperature, °C					
	W/R = 0.5	W/R = 0.7	W/R = 1.0	W/R = 1.5	W/R = 2.0	W/R = 3.0
+3	103°	93°	85°	83°	85°	80°
+3.5	163°	110°	115°	110°	105°	100°
+2	270°	200°	160°	145°	135°	125°
0	710°	360°	240°	200°	180°	160°
-3	∞	∞	365°	360°	295°	245°
-5	∞	∞	∞	655°	450°	335°
-7	∞	∞	∞	∞	900°	510°

* Assuming δ₂₇^f = δ_{27(L=30)}, utilizing the following equation (i = initial value, f = final value):

$$\frac{W}{R} = \frac{+6.5 - \delta_{27}^f}{\delta_{27}^f - [\Delta - 12]}$$

where

$$+6.5 = \delta_{27}^i, \delta_{27}^i = -12$$

and

$$\Delta = 2.33 (10^6 T^{-2}) - 3.61; T \text{ is in } ^\circ\text{K (O'Neil and Taylor, 1967).}$$

Table 4 - from Forester and Taylor (1977).

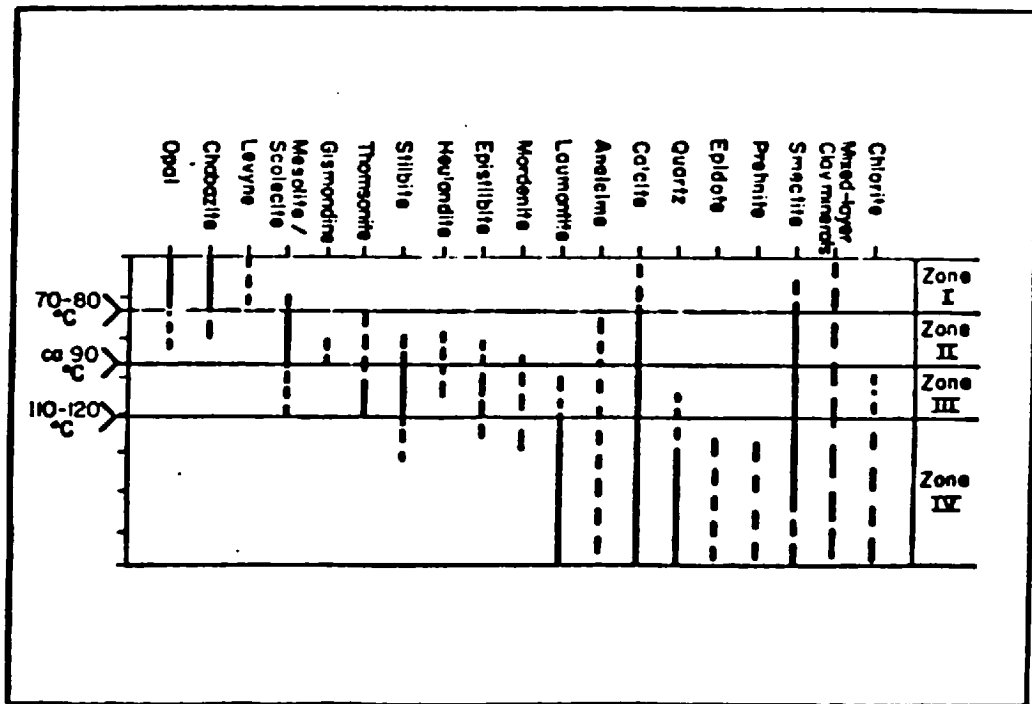


Figure 4 - 1 Alteration zones in the low-temperature geothermal areas of Iceland (from Kristmannsdottir 1975).

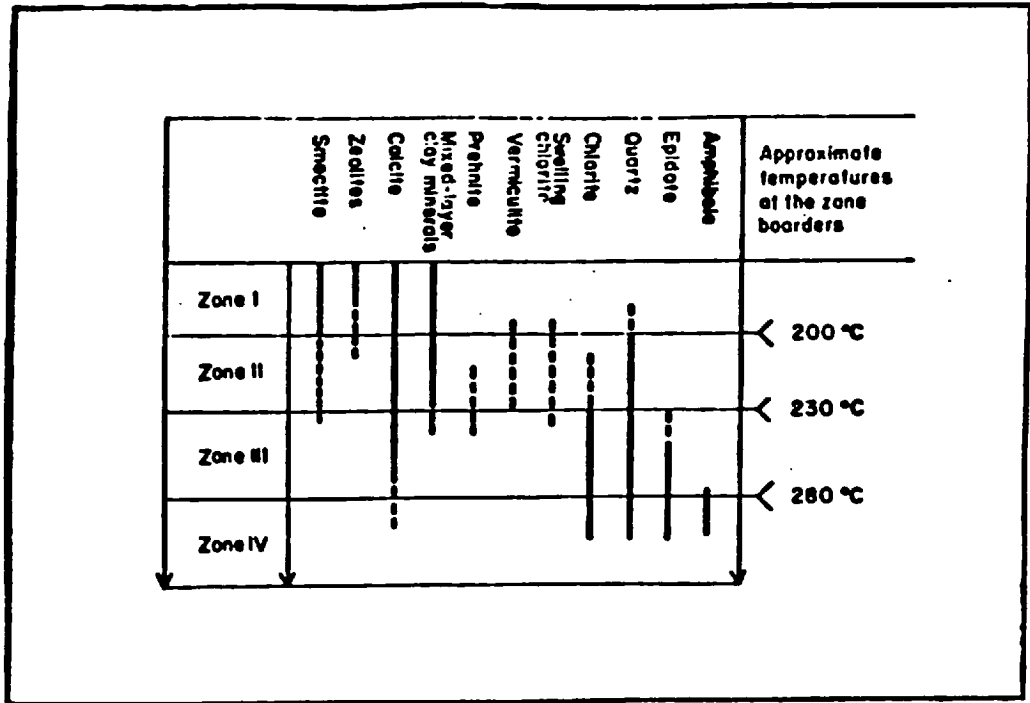
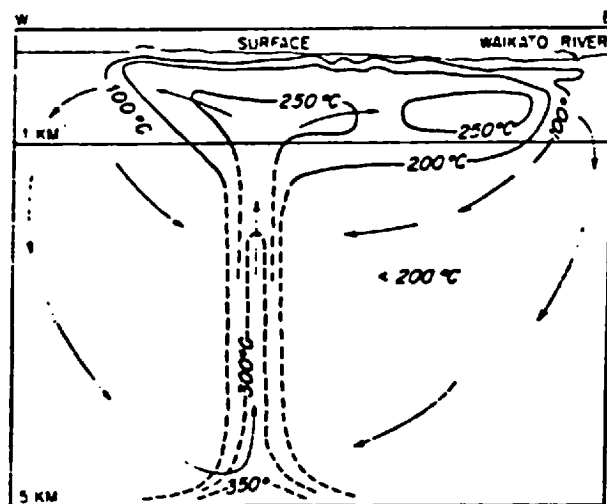


Figure 4 - 2 Alteration zones in the high-temperature geothermal areas of Iceland (from Kristmannsdottir, 1975).



Vertical section through the modern geothermal system at Wairakei, New Zealand, showing actual measured (solid lines) and estimated (dashed lines) isotherms down to a depth of 5 km beneath the surface (modified after Banwell, 1961, and Elder, 1965). The approximate flow lines of the meteoric water are shown with arrows.

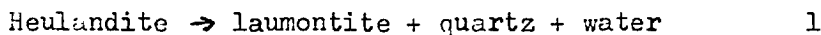
Fig. 4 - 3 from Taylor (1974).

promoting the precipitation of first calcite then silicates. (Brown and Ellis 1970, Tomasson and Kristmannsdottir 1972). The sequence of secondary mineral precipitation shown by the Mull hydrothermal veins suggests that the thermal gradients in the Mull hydrothermal system were similarly constrained by boiling of the fluids. The thermal gradient enclosed by the dashed lines in table 4-1 is thus probably far too steep. Nevertheless, the O-isotope data impose considerable limitations on temperatures and water/rock ratios in the system as the lower the temperature at which interaction took place, the higher the water/rock ratios required to produce a particular ^{18}O -depletion would be.

Evidence from mineral stability relationships.

O-isotope studies can yield little, or no, information of the thermal gradients that prevailed in the zeolite-zones, since all the lavas outside the prehnite and epidote zones have 'normal' $\delta^{18}\text{O}$ values. If the field data can be reasonably correlated with P-T diagrams, then progressive low-grade metamorphism can be calibrated. The direct application of experimental phase equilibria studies to natural assemblages is difficult. Few of the secondary mineral species found in the Mull lavas have been studied experimentally and many of the studies delineated synthesis fields rather than equilibrium boundaries. Most of these studies have been carried out on systems containing excess quartz, whilst the zeolite species found in the Mull zeolite-zones are those typical of Si-deficient environments, (fig 2-6). Furthermore, the varied secondary mineral compositions detected within individual samples cannot be considered to indicate that equilibrium was achieved. Nevertheless, the fact that the secondary mineral assemblages can be divided into a sequence of progressive zones, and that these are similar to zones described from other altered basaltic sequences (e.g. Walker 1960, Jolly and Smith 1972) argues for at least a tendency for the rocks to have approached, if not attained, phase equilibrium.

The boundary between the laumontite and mesolite zones may be approximated by the reactions :-



Analcite + quartz \rightarrow albite + water

2

Reaction (1) has been investigated by Coombs et al. (1959) and Winkler (1965). Coombs et al. suggested the equilibrium temperature for reaction (1) was 280°C at 2kb, whilst Winkler proposed a small variation about 280°C over the pressure range from 0.5 to 4kb. Reaction (2) was reversed by Campbell and Fyfe (1965) at about 190°C, 12 bars; by A.B. Thompson (1971) at 150° - 190°C, 4.5 - 2kb and by Liou (1971) at 183° - 200°C, 5 - 2kb. Problems in the direct application of the data to natural parageneses include the stoichiometry of the zeolites, the structural state of the albite, and the deviations of the activity of silica from that of quartz and the activity of H₂O from that of pure water in nature (e.g. Saha 1959, Coombs and Whetton 1967, Senderov 1965, 1968).

Most hydrothermal syntheses are carried out under conditions of $P_{H_2O} = P_{total}$, whereas in meteoric hydrothermal systems $P_{H_2O} \approx \frac{1}{2}P_{load}$. For the analcite-albite reaction considered above, Coombs et al. (1959) calculated that analcite stability would be lowered from about 280°C where $P_{H_2O} = P_{total} = 1000$ bars to only 100°C at $P_{H_2O} = \frac{1}{2}P_{total} = 1000$ bars. The same reasoning applied to the series heulandite-prehnite-epidote-anorthite suggests that each hydrous mineral is stable at much lower temperatures in a hydrothermal situation than in a regional metamorphic environment. If conditions within the rocks are osmotic, i.e. $P_{H_2O} \approx \frac{1}{2}P_{total}$, and a fissure forms and is held open for growth then whilst albite grows in the rock, analcite could form in the fissure. The large secondary mineral pods and connecting veins in the Mull lavas contain zeolites whilst the adjacent rocks usually contain feldspar, confirming that conditions during the alteration were osmotic.

Studies of contemporary geothermal areas have revealed that many of the characteristic alteration minerals are the same and appear in the same temperature range (Ellis 1967, Brown and Ellis 1970, Steiner 1967, Muffler and White 1969, Tomasson and Kristmansdottir 1972, 1974). In detail, the mineral assemblages differ due to variations in the compositions of the original rocks (e.g. Walker 1960) nevertheless, the regularity of these assemblages indicate some systematic response

of the rocks to the physical-chemical environment and therefore an approach to equilibrium - metastable or stable. In all these systems, fluid pressures are less than load pressures and the conditions are therefore equivalent to those that prevailed during the operation of the Mull hydrothermal system. The most intensively studied geothermal fields are the Icelandic geothermal areas. These have been divided into two main types (Palmason and Saemundsson 1974) :

1. - high temperature geothermal areas confined to, or on the margins of, regions of active volcanism and igneous intrusion. Typically three main secondary mineral zones can be recognised in these areas: a smectite-zeolite zone, a clay minerals-prehnite zone, and a chlorite-epidote zone.
2. - Low temperature geothermal areas located on the flanks of the active volcanic zones, or in the older parts of the lava pile. These contain a sequence of three or four distinct zeolite zones; in order of increasing temperature: the chabazite, (mesolite), stilbite and laumontite zones.

These two types of geothermal area can be considered analogous to the central greenschist-facies and surrounding zeolite-facies zones in Mull. The sequence of secondary mineral formation in the Icelandic geothermal fields and the rock temperatures at the zone boundaries are reproduced in figures 4-1 and 4-2. Comparison of these with the Mull secondary mineral zones indicates that the boundary between the mesolite and laumontite zeolite-zones corresponds to a temperature of approximately 100°C and that the prehnite/epidote zone boundary a temperature of approximately 230°C. The two flows which were sampled close to the Toll Doire granophyre ring dyke, M 47-50 and M 29-33, the Toll Doire Quarry lava, - which contain amphibole, rather than chlorite, as the alteration product of pyroxene - must have been altered at temperatures approaching 300°C. Comparison with table 4-1 suggests that the water/rock ratios varied from 3.0 or more, adjacent to the central intrusive complex, to 0.5 or less in the zeolite-zones.

2. A hydrothermal-convection model for the Mull geothermal system.

In terrestrial geothermal systems convective recirculation of

the water occurs^{as} a result of the gravitational constraint placed on the mass flux by the air/ground boundary condition. This constraint acts to retain some water in the system for periods of up to 10^4 years and the recirculation gives rise to a mushroom-shaped, high-temperature region (Elder 1965). In terrestrial systems this property dominates the isotherm distribution at high levels as can be seen from figure 4-3 which shows the measured, present-day temperature distributions in the Wairakei geothermal system, New Zealand.

The geochemical results discussed in the previous chapters indicate that the formation of both the zeolite-zones and the greenschist-facies zones can be attributed to the hydrothermal system. Support for the convective recirculation of the hydrothermal fluids is provided by the buffering of the fluid compositions by the lava pile. Comparison of figures 1-6 and 4-3 shows that the distribution of the secondary mineral zone boundaries in the Mull lava pile is similar to the isotherm distribution patterns that occur in such systems. The presence of a second mesolite zone below the higher-temperature laumontite zone, which is difficult to reconcile with a burial metamorphism model, can thus be explained by the radial inflow of cooler water at the base of the lava pile above the relatively impermeable Moine schists. Drilling in active geothermal areas in Iceland and Kamchatka as well as New Zealand has revealed the presence of similar temperature inversions at depth (Sigvaldasson 1962; Arnorsson et al. 1975, Tomasson et al. 1975, Naboko and Fiip, 1961). In these systems the main upward movement of water is localised above, or on the margins of, the active zones of volcanism, rifting and intrusion. A circulation pattern of the type shown in figure 4-3 would have been facilitated in Mull by the structure of the lava pile. The coincidence of the epidote and prehnite zones with the region of ^{18}O -depletion and steeply dipping lavas surrounding the central intrusive complex (figs. 1-2, 1-3) suggests that these mark the limit of the upward-moving portions of the meteoric-hydrothermal convective system(s) in Mull.

The low $^{87}\text{Sr}/^{86}\text{Sr}$ ratios of the hydrothermal fluids circulating

in the lava pile indicate that separate 'circulation cells' were established inside and outside the central intrusive complex. A similar situation to this exists in the present-day Reykjavik and Reykir geothermal region to the west of the active volcanic zone in southwest Iceland. Isothermal lines constructed from measurements in over 200 drillholes in this region define four areas of thermal maxima. Hydrological (Thorsteinsson and Eliasson, 1970), thermal, chemical and isotopic data (Arnason and Tomasson, 1970) indicate that these areas constitute separate circulation systems. The boundaries between the systems are formed by areas of numerous intrusions and faults. The most intensely ^{18}O -depleted rocks in Mull occur adjacent to the caldera ring fractures. It seems likely that fluid flow in the central complex was predominantly vertical being channelled along the numerous faults and intrusive contacts. The absence of any zoning of the secondary minerals about any individual intrusive body can be attributed to the sporadic nature of the intrusive activity. The emplacement of each pluton probably caused the initiation of a separate, local hydrothermal system overprinting the alteration assemblages formed by the previous system.

In contrast, fluid flow in the lava pile occurred principally along the inter-flow boundaries. The highly porous, interflow breccia zones, amygdaloidal flow margins and occasional pyroclastic deposits will have behaved as aquifers. The partially altered red bole sample, M 39, for example contains more than 15% CaO, a large proportion of which must have been deposited by the hydrothermal fluids (Appendix I-E). The geochemical results indicate that the meteoric fluids travelled distances of up to 20kms transporting Ca and Si from the epidote zone to the zeolite zones (fig. 1-3). Assuming a diameter for the area affected by hydrothermal activity of 25km, ^{and} if the effects originally extended over a vertical distance of 2kms, then up to 4000km³ of rock have been affected by interaction with meteoric fluids, and a similar volume of water must have passed through the system. This quantity of water can be accounted for by normal amounts of rainfall. If only 10 per cent of an annual rainfall of 75cm is added to the circulation

system, then given a catchment area of 2000km^2 , it would require only 10^4 years to supply the needed amounts of water.

Considerable difficulties exist in accounting for the quantities of heat necessary to drive such large convective systems. Forester and Taylor (1977) calculated that a cylindrical stock of magma contains only sufficient energy to produce a hydrothermal aureole about 0.7 stock diameters wide. This calculated value is sufficient to account for the formation of the epidote and prehnite zones, if the central intrusions are treated as a single, composite stock (see fig. 1-3), but not the zeolite-zones. The calculation assumed that the altered country rocks had been subjected to an average rise in temperature from 50° to 300°C , requiring an addition of 65 cal/g of heat throughout the alteration zone, using a specific heat of $0.25\text{ cal/g}^\circ\text{C}$. With water/rock ratios = 0.6 at least 3g of H_2O must be heated with every gram of rock, demanding an additional 85 cal/g and at least 150 cal/g for the alteration process. The maximum heat that can be liberated from a silicate melt crystallising and cooling from 1000°C to 300°C is 280 cal/g and exothermic hydration reactions in the country rocks may account for an additional 35 cal/g. The average temperature rise used by Forester and Taylor (1977) in this calculation is probably too high since it is unlikely that temperatures at any point in the system significantly exceeded 300°C . Nevertheless, this is compensated for to a certain extent as the water/rock ratios, in the central parts of the system at least, were probably considerably higher than 0.6.

The discrepancy between the calculated and observed extents of the hydrothermal systems can be explained by several factors :-

1. The intrusions do not represent a single injection of magma, but episodic additions of new magma from below.
2. The walls of Pennygown quarry contain numerous minor intrusions the surface outcrops of which could not be traced across the adjacent slopes. It seems likely that the volume of intrusions within the lava pile may thus be considerably greater than their presently mapped, areal expressions indicate.
3. Alteration of the lavas was confined predominantly to the flow

margins. Even within the central epidote zone many of the flows contain relict patches of unaltered minerals. In the zeolite-facies zones the alteration is confined mainly to within a few mm of amygdales in the flow margins. Exothermic reactions tend to be self-accelerating and once initiated will proceed ^{to completion} provided material can be supplied and removed with progress of the reaction. The mineral reactions in the centres and margins of the lava flows in the epidote zone were similar. In Pennygown quarry lava, for example, some conversion of pyroxene to amphibole could be observed in each sample from the sections through the flow. The difference between the samples was solely in the extent to which the reactions had proceeded. The similarity between the gains and losses across this flow calculated on the basis of both constant volumes and constant immobile element contents demonstrate that the assumption of constant volumes during alteration was a valid one (fig. 3-29), and growth of the secondary mineral phases was accommodated by the hydrothermal transport of material out of the lava flows. The rate controlling step in most of the alteration reactions was therefore the local water/rock ratio and rate of fluid flow. With increasing distance from the intrusive complex the lava flows show progressively less alteration and the centres of the flows were effectively by-passed by the heating effects of the hydrothermal fluids. The intrusions therefore, needed to provide only sufficient heat to alter a fraction, rather than the total volume, of lavas within the hydrothermal aureole.

The sporadic nature of the intrusive activity in the central complex means that the hydrothermal activity must also have been sporadic. The alteration of the lavas will have been accomplished by numerous, overlapping injections of meteoric fluids along the inter-flow horizons. The presence of numerous discordant hydrothermal veins and hydrobreccias indicates that at a later stage the hydrothermal activity must have become increasingly restricted and explosive in nature. This will have probably been caused by local sealing of the

escape routes for the fluids by mineral deposition in the permeable portions of the lava pile, or even by the emplacement a cross-cutting intrusive body. The lavas adjacent to these veins show little or no alteration and hence the compositions of the hydrothermal fluids will have been increasingly controlled by the intrusive rather than the extrusive rocks during this period. Possible evidence for a change in the fluid compositions with time may be provided by the two veined and pyritised samples collected from Pennygown quarry. The sulphides in the late-stage dyke sample shown in figure 1-14 are associated with veins of K-feldspar and chlorite (Appendix I-D, sample D 1). This particular secondary mineral assemblage was not observed in any of the lava flows. The general scarcity of secondary sulphides in the altered lavas can be attributed to their low initial sulphur content. The intrusive rocks in the central complex are less likely to have been affected by volatile loss during crystallisation and the sulphur necessary for the formation of these minor late-stage deposits may thus have been contributed by the plutonic rocks. As noted in chapter one, local concentrations of sulphides have been found adjacent to some of the caldera-ring fractures indicating that ore-forming elements were carried by the hydrothermal fluids in the central parts of the system.

CHAPTER FIVE: COMPARISONS WITH ALTERED BASALTS FROM
OTHER HYDROTHERMAL SYSTEMS.

In recent years the chemical changes in basaltic rocks subjected to low-grade hydrous metamorphism have been much studied. Interest has focused on element mobility and its role in geochemical mass balances (e.g. Humphris and G.Thompson 1978a) and ore-genesis (e.g. Graf 1972) and on attempts to decipher the pre-alteration history of the basalts (e.g. Condie and Barager 1974). Certain elements such as Ti, P, Zr, Nb and Y have been shown to be immobile except during extreme metasomatism (e.g. J.Pearce and Cann 1973, Herrmann et al. 1974, this study). Other elements such as Li, Sr, Rb and Ba generally appear to be mobile (e.g. Gunn and Roobol 1976, Wood et al. 1976) but as yet evidence for the mobility of other elements such as the REE and Mg, Fe and Al is controversial, (e.g. Cann 1969, Frey et al. 1974, Tanaka 1975, T.H. Pearce et al. 1977, Hellman et al. 1977, Floyd 1977). In this chapter the element mobility in the Mull Plateau lavas and basalts from other hydrothermal systems are compared in an attempt to:

- 1) elucidate the reasons why certain elements are mobile in some instances and not in others.
- 2) place constraints on the extent to which the other Tertiary Hebridean basalt magma types may have been affected by secondary alteration, as suitable material for detailed investigation could only be collected for the Mull Plateau lavas.

Only studies concerned with the chemical changes across individual eruptive units (flows or pillows) were taken from the literature.

1. Eastern Iceland.

A 10km thickness of predominantly basaltic flows is exposed in Eastern Iceland. These have been formed mainly by subaerial fissure eruptions during the separation of the European and North American lithospheric plates since approximately 14 Ma. The flows dip gently westwards and are cut by sub-horizontal zeolite-facies, amygdale mineral zones. Wood et al. (1976) studied element mobility resulting from the zeolite-facies alteration. They compared chemical variations across a post-glacial basalt on the Reykjanes Peninsula, SW Iceland, with a

zeolitised Tertiary flow from Reydarfjordur, eastern Iceland.

Reykjanes flow

This 4.5km thick basalt flow lacks a soil cover and is therefore probably no more than a few hundred years old. It contains several percent of subhedral olivine, augite and plagioclase phenocrysts with variable distributions. The groundmass consists mainly of equant granular augite intergrown with plagioclase laths, sparse subhedral Fe-Ti oxides, and rare olivine. The abundant spaces between the groundmass grains are filled with pale brown glass, which contains numerous, indeterminate 2mm opaque and translucent crystals.

Chemically the lava is a typical hy-normative olivine tholeiite with 7.6 - 8.0% MgO. A suite of twelve specimens from a vertical section through the flow revealed little variability for any elements. The slight variations that were observed could be attributed entirely to variable distributions of the phenocryst phases within the flow. The data of Wood et al. (1976) are summarised in figure 5-1. Only the chondrite-normalised patterns with the highest and lowest values of Σ REE and $(Ce/Yb)_N$ ratios are shown. It is apparent that the light rare-earth elements (LREE) show no greater variation than the heavy rare-earth elements (HREE) in this particular flow.

Reydarfjordur flow.

This 20.5m thick basalt flow is about 12 Ma old. It lies within the mesolite zone of Walker (1974). Petrographically it is similar to the Reykjanes flow and contains a few percent of olivine, augite and plagioclase phenocrysts. The groundmass is rich in granular augite, but the interstitial glass patches have been converted to a fine-grained mixture of zeolites and hydrated ferromagnesian minerals. The degree of visible alteration varies throughout the flow, being most intense in the vesicular margins. Zones with maximum alteration show complete replacement of olivine, in addition to the glass, and incipient alteration of plagioclase. The pyroxenes are unaffected by secondary alteration.

Chemically this lava is a hy-normative olivine tholeiite with 6.0 - 7.2% MgO. Wood et al. (1976) compared the chemical variation of twelve samples from a vertical section through the flow with that of

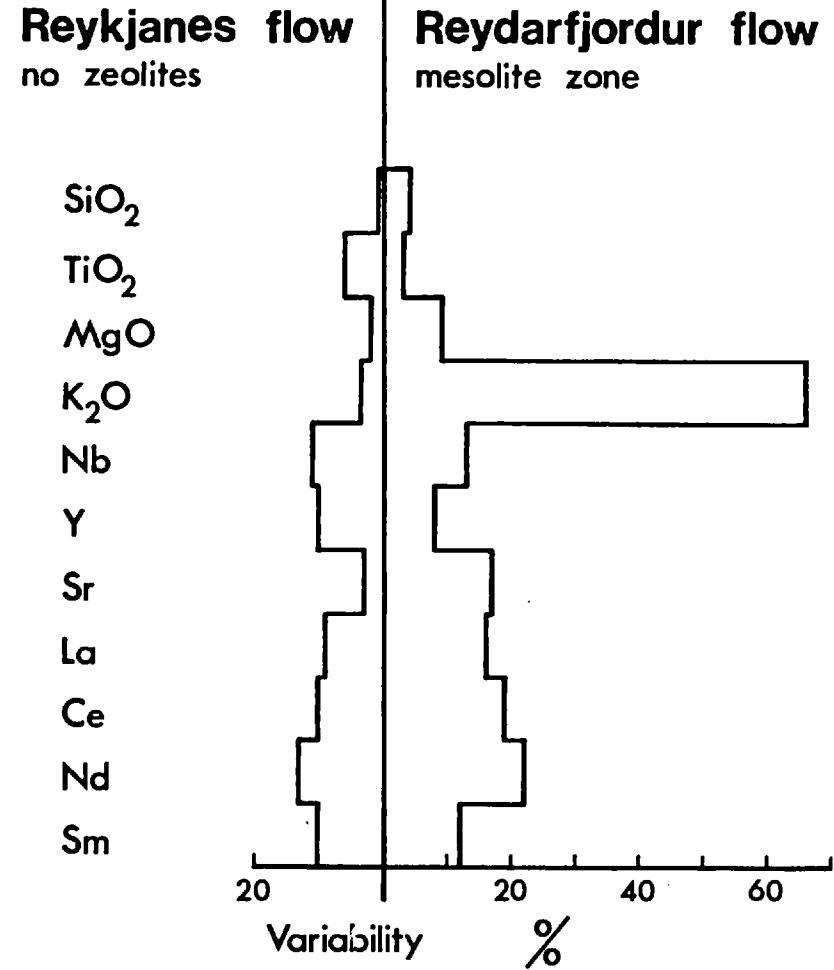
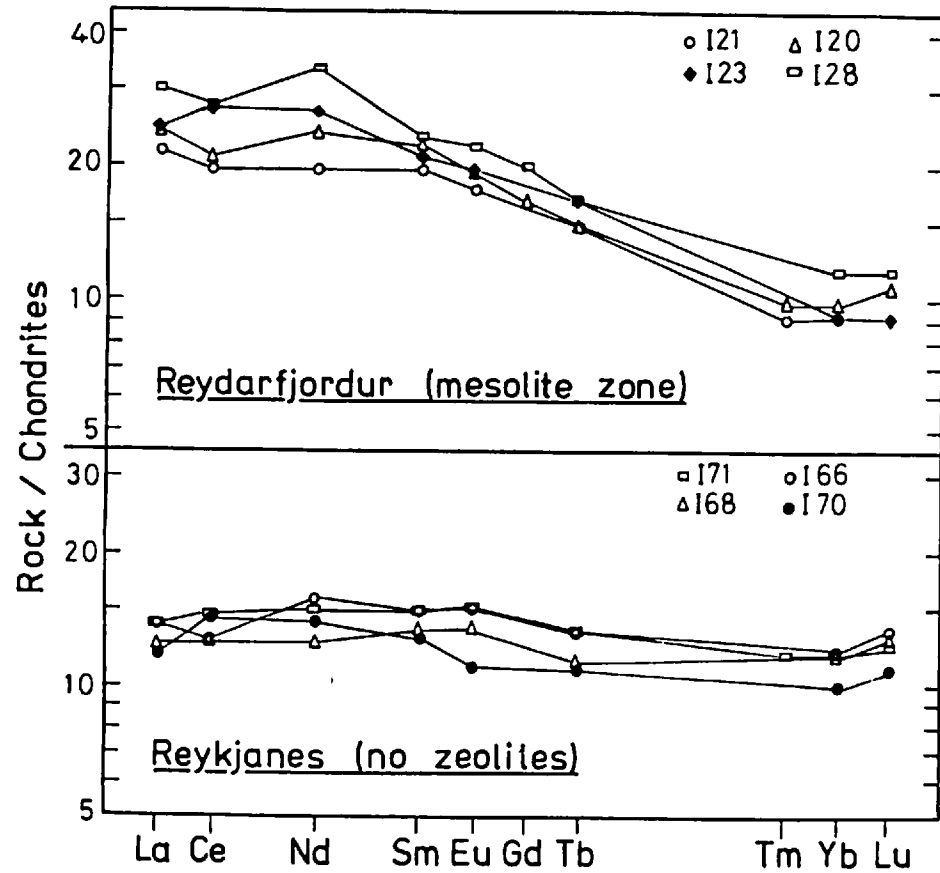


Figure 5-1 The percentage variability of major and trace elements in a recent flow from the Reykjanes Peninsula and a zeolitised flow, Reydarfjordur, eastern Iceland; and chondrite-normalised REE patterns for basalts from the two flows. (Data from Wood et al. 1976).

the Reykjanes lava and their results are summarised in figure 5-1. They found greater variability in Si, Mg, K, Rb, Sr and the LREE in the zeolitised lava flow than could be accounted for by phenocryst distribution or analytical error, indicating mobility of these elements during alteration.

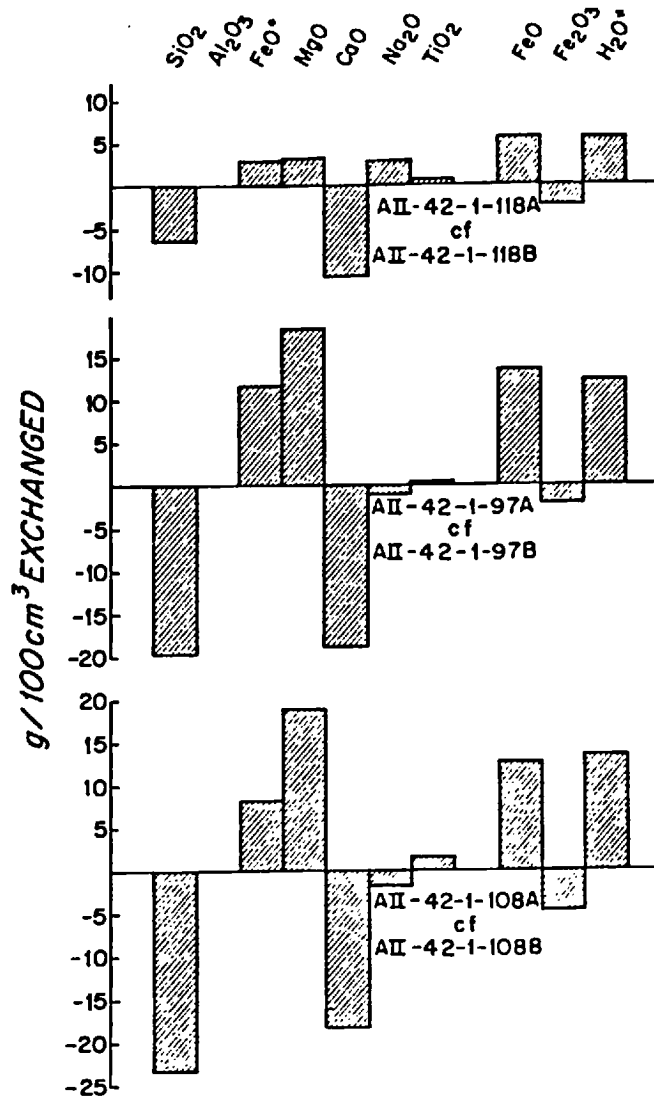
2. Mid Atlantic Ridge basalts.

Humphris and G.Thompson (1978 a,b) and Humphris et al. (1978) studied the mineralogy and chemistry of pillow lavas that show zoning due to partial replacement of the outer pillow margins by greenschist-facies assemblages during interaction with a circulating, seawater derived fluid. Only pillows dredged from the median valley were used in an attempt to ensure relatively young samples and minimise the affects of any subsequent weathering on the ocean floor. The distinct zoning displayed by these rocks allowed portions of the altered rims and relatively fresh interiors to be separated for analysis.

The interiors of the pillows consist predominantly of glass (60 - 70% by modal analysis) containing microphenocrysts and microlites of plagioclase (An_{60-70}) and rare olivine (For_{80-85}). Fine grained Fe-Ti oxides are scattered throughout the groundmass. The altered pillow rims contain the assemblage albite-actinolite-chlorite-epidote, with the dominant mineral being a ripodilitic chlorite (up to 60% by modal analysis). The outer rim of one of the most altered samples (AII-42, 1-96) is composed dominantly of quartz and chlorite with no actinolite and only 15% modal albite. In all the samples, glass is replaced by chlorite or mixtures of chlorite and actinolite. Plagioclase is albitised and in some cases altered to chlorite. Chlorite also forms pseudomorphs after olivine which are commonly associated with euhedral pyrite. The vesicles are filled with chlorite or, in the more altered samples, they are lined with quartz and then filled with chlorite.

Considerable mobility of many of the major and trace elements occurred during alteration of these pillow lavas (Humphris and G.Thompson 1978a,b; Humphris et al. 1978). Ca, Si, Cu and Sr were leached and Mg and H₂O were taken up from the circulating fluids (fig.5-2). Na, K,

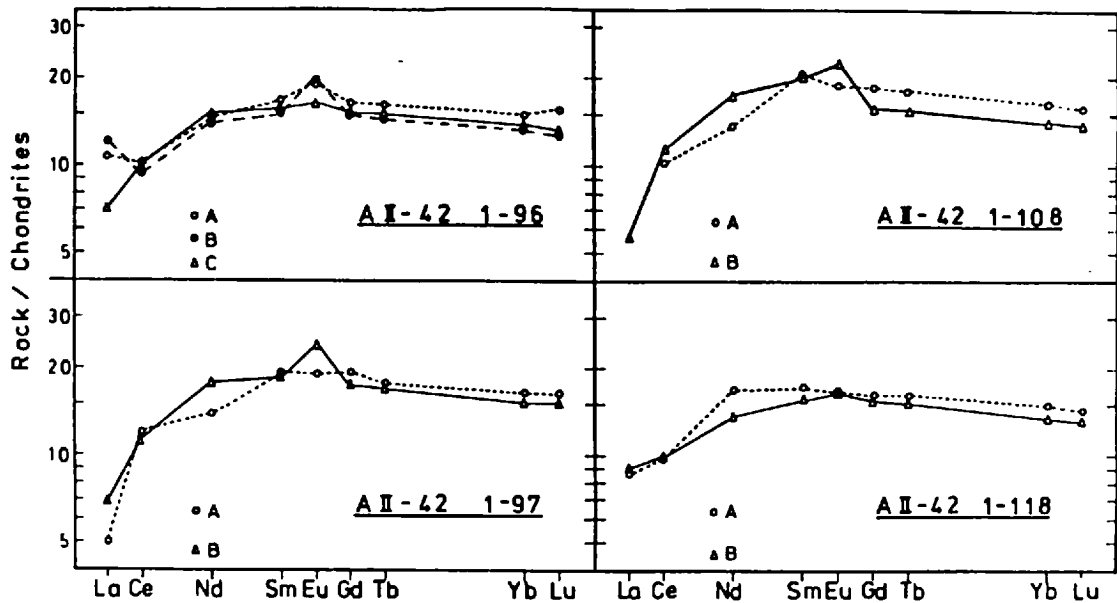
Figure 5-2
 Mass fluxes resulting
 from hydrothermal
 alteration of pillow
 basalts from the Mid
 Atlantic Ridge at 22°S.
 (From Humphris and
 G.Thompson 1978a).



Fe, Mn, B, Li, Ba, Ni, Co and the LREE were mobile but show no consistent trends. Al, Ti, Y, Zr, Cr and the HREE were immobile and hence show proportional changes in concentration (fig. 5-3, table 5-1). Some of the altered pillow margins (which are reduced relative to the 'fresh' interiors) have small positive Eu anomalies similar to that shown by the marginal sample (M 13) from the Pennygown Quarry lava (fig. 3-22).

3. The Bhoiwada and Cliefden Outcrops.

Neither of these outcrops will be described in detail as the evidence for their initial homogeneity prior to alteration is controversial.



Selected rare-earth and trace element data from partially altered pillow basalts from the Mid-Atlantic Ridge (22° S).

Sample*	Ce (ppm)	Yb (ppm)	(Ce/Yb) _N	TiO ₂ (wt.%)	Y (ppm)
AII-42 1-96A	8.77	3.27	0.68 ± 0.03	1.40	35
1-96B	8.02	2.89	0.71 ± 0.03	1.33	30
1-96C	8.57	2.96	0.73 ± 0.02	1.26	39
AII-42 1-97A	10.47	3.53	0.76 ± 0.03	1.46	40
1-97B	9.58	3.34	0.73 ± 0.04	1.37	35
AII-42 1-108A	8.88	3.42	0.66 ± 0.04	1.98	45
1-108B	9.88	3.02	0.83 ± 0.04	1.43	39
AII-42 1-118A	8.61	3.21	0.68 ± 0.04	1.53	39
1-118B	8.60	2.91	0.75 ± 0.04	1.35	38

*A, B, C: zones from a single pillow basalt, from the altered rim (A) towards the relatively fresh interior (B or C).

Figure 5-3 and Table 5-1.

Chondrite-normalised REE patterns and selected REE and trace elements for four partially hydrothermally altered pillow basalts from the Mid Atlantic Ridge. (from Humphris et al. 1978).

The Bhoiwada section has been described as exhibiting a continuous gradation from 'fresh', black, plagioclase-clinopyroxene tholeiite into a green, albite-chlorite-zeolite spilite within a single Deccan flow unit, 30m thick (Vallance 1974, Sukheswala 1974). The upper tholeiitic part consists of massive lava whilst the lower spilitic portion of the profile is pillowy at its base and is underlain by a thin layer of sediment and a sequence of amygdaloidal pillow lavas. Hellman and Henderson (1977) demonstrated that the spilite is considerably enriched in all the rare earth elements relative to the tholeiite, which they attribute to extensive mobility of the REE during alteration.

Floyd (1977) pointed out that the REE distribution in the spilite is similar to that exhibited by the more alkaline units of the Deccan basalts. Accordingly, he suggested that the Bhoiwada profile may not be a single lava flow and that the tholeiite 'top' may be a different unit to the more 'alkaline' spilite base. Although the section is described as gradational, the contact between the two portions seems sharp and there are primary textural differences between them.

The tholeiitic portion consists of coarse-grained, subophitic lava with small patches of chlorite after interstitial glass, whilst the spilite appears to have originally been a fine-grained glassy rock. (Vallance 1974, figs. 2-4; Sukheswala 1974, figs. 11, 13 and 14). Considerable support for Floyd's interpretation is provided by the fact that the two portions of the profile are separated by two layers of black siliceous material, described by Sukheswala (1974) as resembling the sedimentary matrix surrounding the underlying pillow lavas.

The REE distributions within the Bhoiwada section are shown in figure 5-4a. Patterns 1 and 2 are from the tholeiitic portion, patterns 3, 3Z and 4 from the spilite and 5 from one of the pillow lavas. The REE chondrite-normalised patterns from the two parts of profile show small parallel shifts that closely resemble those shown by the Mull lavas (figs. 3-22, 3-23) and the Mid Atlantic ridge basalts (fig. 5-3).

The Cliefden outcrop consists of a pile of basaltic flow debris and pillow lavas affected by prehnite-pumpellyite facies metamorphism (Smith 1968). Hellman et al. (1977) have described considerable mobility

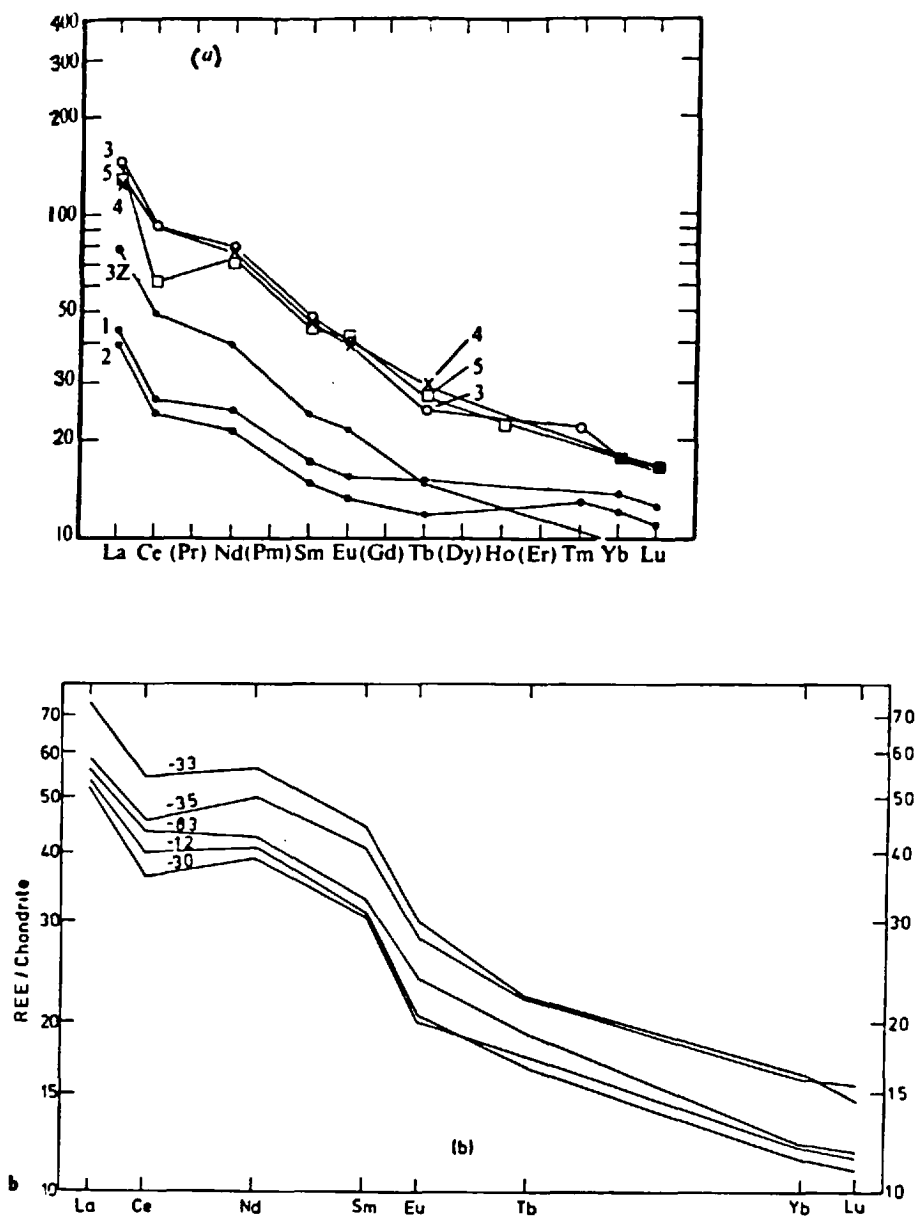


figure 5-4

- a) Chondrite normalised REE patterns from Bhoiwada, Zones 1-5
(Hellman and Henderson 1977)
- b) Selected REE patterns from the Cliefden Outcrop, NS Wales
(from Hellman et al. 1977).

of the REE and other trace elements in the outcrop during alteration. Nevertheless, it was pointed out in chapter three that much of this variation may be due to fractionation processes. Smith and Smith (1976) also considered that the trace element variation in the Cliefden Outcrop "might easily be an original magmatic spread".

The interesting feature of the Cliefden data is the simultaneous occurrence of negative Ce and Eu anomalies in the REE patterns (fig 5.4b). As Hellman et al. (1977) point out these two elements can exhibit more oxidation states than the one (i.e. 3+) commonly shown by the other REE during geological processes. It is difficult however, to envisage the formation of both anomalies by the same process. High fO_2 causes oxidation of Ce to Ce^{4+} , which will then be discriminated from incorporation into mineral lattices because of its small ionic radius; on the other hand a negative Eu anomaly can only be explained by the occurrence of Eu in the divalent state, for which rather low oxygen fugacities are required.

Hellman et al. (1977) attribute the formation of Ce anomalies to bulk loss of Ce as a result of interaction with an oxidising sea-water derived fluid. Similar anomalies have been found in altered basalts and sediments from Troodos (Robertson and Fleet, 1968) and the Shatsky Rise (Masuda, 1975). The Cliefden Outcrop has high Fe_2O_3/FeO ratios indicating oxidising conditions during alteration (Smith 1968) and hence

the negative Eu anomalies may have been an original magmatic feature. The lavas were sparsely porphyritic and contained rare phenocrysts of plagioclase and clinopyroxene. The Eu anomalies and the trace element variation could thus reflect variable degrees of plagioclase fractionation.

4. Controls on element mobility during alteration.

The metabasalts discussed here include examples of interaction with meteoric water (Mull and Iceland) and seawater (Mid Atlantic ridge and Cliefden), yet few of the differences in the chemical changes observed can be attributed to solution chemistry. The Mid Atlantic ridge basalts contain secondary pyrites and also show uptake of Mg from seawater. Humphris (1976) showed that an external source of sulphur was

required to form the pyrites and that this was probably derived from the reduction of sulphate in seawater. No additional source of iron was required as this was probably introduced to the pyrite-bearing pillows by fluids that had been enriched in Fe as a result of previous reactions. Other than these two differences the chemical changes shown by the Mull and Mid Atlantic ridge basalts during greenschist-facies alteration are extremely similar (c.f. figs. 5-2 and 3-29).

Although it is clear that greenschist-facies alteration results in more extensive replacement of the primary phases and hence, greater bulk compositional changes than zeolite-facies alteration, the degree of mobility or immobility shown by the LREE in particular cannot be related to metamorphic grade. Instead the examples discussed here suggest that the main control on potential element mobility is the igneous crystallisation of the individual lavas, in so far as this affects the relative distribution and sites of concentration of the individual elements before subsequent alteration.

The Iceland and Mull lavas may first be contrasted. The presence of augite amongst the sparse phenocrysts in the Iceland basalts indicate that this phase precipitated at liquidus or near-liquidus temperatures. In a basalt devoid of hydrous minerals, all the early crystallising phases - olivine, plagioclase and pyroxene - have partition coefficients for the REE less than one. Of these phases augite has the highest partition coefficients for the HREE (averaging 0.62 for Yb (Arth, 1976)) but low coefficients for the LREE. As Humphris et al. (1978a) point out, an Eastern Icelandic basalt crystallising augite throughout its consolidation will therefore contain a residuum chilled to glass, which is rich in total REE, and has a high LREE/HREE ratio. The two Icelandic basalts discussed here are both relatively impoverished in P and Zr (Wood et al. 1976) so that the REE-rich phases, apatite and zircon, would, if at all, precipitate very late in their consolidation. Humphris et al. (1978) could find no trace of apatite or zircon in the groundmasses or interstitial glass patches of these lavas. The glass patches are too small to allow extraction for REE analysis but are rhyolitic in composition and likely to have $(Ce/Yb)_N$ in the range 3.0 to 7.0, compared with 0.9 to 1.9 in the basaltic magmas (Humphris et al. 1978).

The phases in the eastern Iceland most readily attacked by the circulating meteoric fluids during hydrothermal alteration are first the interstitial glass and then the olivines, hence the preferential mobilisation of the LREE, Sr, Rb, K, Mg and Si.

The Plateau lavas of Mull contain no augite phenocrysts. Instead this mineral occurs as a late-stage groundmass phase in large poikilitic crystals. The restricted precipitation of augite during consolidation greatly reduces the potential of this phase to fractionate the REE in the residuum. Furthermore, the comparatively small number of augite and occasional titanomagnetite poikilocrysts in the groundmass of a given basalt volume, leave fewer intergranular spaces where residual glass pools can collect than in a comparable volume of Icelandic basalt. This in turn will restrict the opportunities for initial fluid penetration by grain-boundary diffusion. None of the Mull Plateau lavas contain more than a minute trace of glass and many appear to have been entirely holocrystalline. In the absence of abundant glass, the hydrothermal fluids attacked first the olivines, then the plagioclases. Marginal replacement only of these phases occurred during zeolite-facies alteration, hence the lack of any significant chemical changes and the REE immobility. Only when the pyroxenes broke down during greenschist-facies alteration, allowing hydrothermal attack of the enclosed apatites, did any significant mobility of P, Th and the LREE occur.

Many authors (e.g. Floyd 1977) have attempted to define alteration trends for the REE in tholeiite and alkali basalt types, because of the importance of these, and other, incompatible elements in petrogenetic modelling. Support for the contention that it is the crystallisation histories of the individual lavas, rather than their initial compositions, that determines their response to subsequent alteration may be provided by the Bhoiwada section. The upper part is nearly aphyric, containing a few plagioclase phenocrysts in an almost entirely holocrystalline, ophitic matrix that has only a trace of interstitial glass. The spilitic part of the section is fine-grained and has microphenocrysts of plagioclase and pyroxene in an originally glassy groundmass (Sukheswala 1974). Hellman and Henderson (1977) analysed two samples from the upper, tholeiitic part, which had La/Yb ratios of 5.4 and 5.5

respectively, whilst in three samples from the more 'alkaline' spilite this ratio varied between 12.4 and 14.0.

In contrast, the oceanic pillow basalts discussed here contain no augite and had high glass/crystal ratios. The microphenocrysts are predominantly plagioclase with rare olivine. Unlike the Icelandic lavas, this glass is therefore basaltic and will not have been enriched in the LREE during its crystallisation history. Hydrothermal alteration of the pillow basalts has resulted in almost complete replacement of the original mineralogy and any variation in the overall REE pattern will be controlled by the secondary minerals.

Although rock crystallisation history will control the relative availability of the elements during alteration, the nature of the secondary minerals that form must also influence the extent to which the various elements, once in solution, are reprecipitated nearby or pass out of the system. Wood et al. (1976) gave chemical data for thirteen minerals common in the amygdaloids of eastern Icelandic lavas. They comprised nine zeolites, plus apophyllite, aragonite, celadonite and chalcidony. Only the celadonite contained detectable La (> 1.0 ppm), and even in this the REE were in concentrations too low to be measured accurately. In the Bhoiwada section the local deposition of zeolites appears to have caused a dilution of the REE contents. Sample 3Z, from the spilite, analysed by Hellman and Henderson (1977), contains laumontite, quartz, prehnite filled amygdaloids, and is depleted in all the REE, relative to the other two samples, numbers 3 and 4, from this part of the profile (fig. 5-4a).

In contrast, many of the characteristic minerals of greenschist-facies assemblages - epidote, sphene, chlorite, actinolite and albite - although generally poorer in Ca and Si than their precursors, can take up the REE. In the Mull lavas the principal repository for the immobile elements appears to be sphene. The Mid Atlantic Ridge basalts described by Humphris and G.Thompson (1978a) all contain epidote, but no mention is made of the phase(s) replacing the sparse oxides in these lavas. Nevertheless, the common alteration product of the Fe-Ti oxides in ocean floor basalts subjected to greenschist-facies alteration is sphene

(e.g. Melson et al. 1968, Cann 1969, Aumento and Loncarevic 1969, Spooner and Fyfe 1973). Lambert and Holland (1974) noted that epidote is an Y-acceptor and that albite is an Y-rejector. The slight fractionation of the LREE and HREE between the cores and rims of some of the oceanic pillow lavas (fig. 5-3) could thus be due to variable distributions of the secondary phases in the different zones of the pillows. The outer margin of one of the pillows, AII - 42 1 - 96, contains 60% chlorite and is enriched in La relative to its concentration in the interior, (fig. 5-3). Humphris et al. (1978) suggested this could be due to absorption processes similar to those described in Quaternary clay-chlorite mixtures from Norway by Roaldset and Rosenquist (1971).

One of the interesting features of the REE variation in these metabasalts is the contrasting behaviour of Ce and Eu, particularly in the Mid-Atlantic Ridge and Cliefden lavas, both of which have been affected by interaction with seawater. The separate, basal pillow lava from the Bhoiwada profile also has a negative Ce anomaly (fig. 5-4a, pattern number 5). The Ce anomalies in the Cliefden basalts were attributed by Hellman et al. (1977) to interaction with an oxidising, seawater-derived fluid. Similar observations have been made for altered basalts and sediments from Troodos (Robertson and Fleet, 1976) and the Shatsky Rise (Masuda and Nagasawa, 1975). Studies of the fluids emanating from the Galapagos hydrothermal systems on the East Pacific Rise have shown that they are enriched in Eu and that reducing conditions and sulphide deposition probably prevail below the basalt/water interface (J.D. Corliss, pers. comm. 1978). The Mid-Atlantic pillow basalts discussed here are all reduced and contain secondary pyrites. Humphris and G. Thompson (1978a) showed that during alteration other pillow lavas developed oxidised epidote-rich assemblages or, chlorite-rich assemblages, devoid of pyrite. The formation of the assemblages was accompanied by loss of Fe at least some of which may have been subsequently reprecipitated as sulphides in the pyrite-bearing pillows. Spooner and his co-workers (Spooner and Fyfe, 1973; Spooner et al. 1977) have presented a hydrothermal circulation model for the ocean-floor, based on ophiolite studies, in which the diffuse, downwards penetration of oxy-

generated seawater is followed by the localised discharge of hot, metal-enriched fluids under conditions of low oxygen fugacity. The Cliefden and Mid-Atlantic Ridge metabasalts may thus represent early and late-stage alteration products, respectively, of such a system.

These various studies indicate that in some instances, low-grade zeolite-facies alteration may cause greater mobility of particular elements, such as the LREE, than greenschist-facies alteration. Nevertheless, in each case the maximum, relative movement of the LREE was small and could be related to the igneous crystallisation histories and secondary mineralogy of the individual lavas - suggesting that if these can be ascertained, the extent to which these elements can be considered to be reliable indicators of initial magmatic compositions can be determined. In each of these studies the element group Ti, Nb, Zr, Y, Ta, Hf and the HREE appeared to be immobile. It should be emphasised that all the basalts have been altered by fluids (meteoric or seawater) that have low CO₂ contents. Interaction with a CO₂-rich phase, which might occur in a mixed volcanic and sedimentary sequence, would reduce the stability fields of many of the secondary phases, such as sphene and epidote, that can take up these elements (Schuiling and Vink, 1967; A.B.Thompson, 1971). Hence, they cannot be considered to be generally immobile during any subsequent alteration.

The above discussion has been concerned mainly with the incompatible trace elements because of their petrogenetic importance. T. Pearce et al. (1977) have suggested that Fe, Mg and Al in basaltic and intermediate rocks are also little affected by alteration processes. In the eastern Icelandic basalts Mg was mobile, though only to a limited extent. Both Mg and Fe were mobile in the greenschist-facies basalts from Kull and the Mid-Atlantic ridge. In these lavas the replacement of the Al-poor phases olivine and pyroxene by chlorite (and to a lesser extent by amphibole) resulted in the uptake of any Al released during alteration of the feldspars. Nevertheless, the results obtained in this study show that the chemical changes during alteration were dependent on the relative proportions of felsic and mafic phases in the lavas, and that Al is mobile in more evolved lava types. The frequent occurrence of

the aluminous phases epidote, albite and zeolites in hydrothermal veins in altered basalt sequences also suggests their Al contents should be interpreted with caution.

5. Other Tertiary Hebridean magma types.

Recent geochemical studies of Hebridean basalts have concentrated on samples collected from outside the central zones of hydrothermal alteration. Nevertheless, many of these basalts will have been affected by low-grade, zeolite-facies alteration. The contrasting responses of the Icelandic and Mull basalts to zeolite-facies alteration discussed above indicates that the extent to which their compositions are likely to be modified depends on the crystallisation histories of the individual lavas, and in particular on the relative proportions of interstitial glass and pyroxene. With the exception of the basal "Staffa-type" discussed in more detail below, no interstitial glass has been reported from the Skye Fairy Bridge and Preshal Mhor basalts, the Skye Main Lava Series and the Small Isles lavas. The two latter groups are petrographically similar to the Mull Plateau group. It is clear from the published descriptions of these basalts (Thompson et al. 1972, Esson et al. 1975, Ridley 1973) that they have not been affected by alteration any more extensive than that exhibited by the Mull Plateau lavas from the zeolite-facies zone. Accordingly, the compositions of these basalts are probably pyrogenic.

Analyses of two lavas belonging to the Mull Staffa-type of Bailey et al. (1924) are given in Appendix I-E, - the lava enclosing Macculloch's tree (M 61) and the Staffa lava (M 80). Unlike the Plateau lavas, augite is a major phenocryst phase in this group, though the presence of modal pigeonite - mentioned by Fawcett (1961) - could not be confirmed. They contain small phenocrysts of plagioclase and augite in a groundmass of plagioclase, augite, minor olivine and Fe-Ti oxides. An originally glassy matrix is now represented by chloritic material (fig. 5-5). The augites are never poikilitic, the groundmass crystals being small and subhedral to granular. The plagioclase phenocrysts have cores of calcic bytownite. M 61, also contains rare, irregularly shaped augite and olivine phenocrysts, (fig.5-5)

and rounded clusters of plagioclase crystals with a cumulitic (?) texture which may be xenocrysts. Originally, this lava contained approximately 15 volume percent of glass, now altered to chlorite. The olivine are extensively chloritised but the plagioclases are little affected and the pyroxenes are unaltered. Hyaloclastites (some of them augite-phyric) and pillow lavas petrographically similar to the Macculloch's tree flow occur at the base of the Skye-lava pile. (Anderson and Dunham, 1966; Thompson et al. 1979).

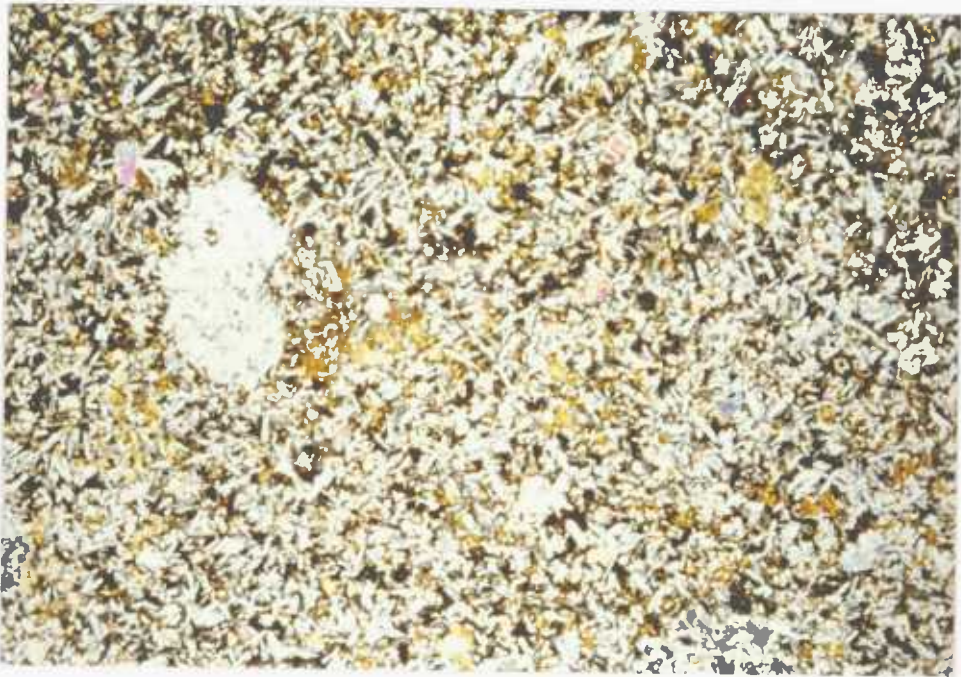


Figure 5 - 5. M 61, Macculloch's tree lava. The irregularly shaped grey crystals on the centre-left are augite phenocrysts.

Field of view 5mm by 3mm.

These lavas may be compared with the Tertiary lavas of the eastern Iceland described by Wood et al. (1976). The presence of abundant interstitial glass has rendered them more susceptible to alteration than the holocrystalline Plateau lavas, and this glass will probably have been enriched in the LREE by augite crystallisation. Preferential

alteration of the glass and olivines may have caused some mobility of Mg, Si, K, Rb, Ba and the LREE. Nevertheless, the closely similar compositions reported by Beckinsale et al. (1978) for two samples from one of the Staffa lavas (op. cit. Table 2, nos. R 68, R 69) indicates that mobility of these 'suspect' elements was small.

One sample of aphyric basalt (M 58) that does not appear to belong to any group previously discussed, was collected from a hill-top knoll south of Fishnish within the epidote zone. The outcrop is too poorly exposed to establish whether or not it is intrusive or extrusive in form. Texturally it is a holocrystalline, ophitic basalt consisting of plagioclase, clinopyroxene, titanomagnetite and minor chlorite. Some of the feldspars are dusty in appearance and show limited replacement by chlorite and sphene, but the rock is remarkably fresh in appearance. The absence of a glass phase and the growth of sphene suggests that in addition to Ti, Nb, Zr, Y, Ta and Hf, the REE are likely to have been immobile during alteration.

Chemical analyses of three representatives of the Non Porphyritic Central lavas of Mull are given in Appendix I-E (MS 183, MS 184, MS 185). They contain rare phenocrysts of plagioclase, augite and titanomagnetite in fine grained groundmass of abundant plagioclases, granules of augite, magnetite and chloritic material.

These lavas came from the epidote zone, have been extensively replaced by secondary minerals and contain thin, discontinuous veins of chlorite and calcite. The pyroxenes appear unaltered but the plagioclases have been replaced by mixtures of calcite and albite and contain numerous inclusions of sphene and chlorite. The titanomagnetite phenocrysts show marginal growth of sphene and most of the smaller granules have been completely replaced by this phase. The fine-grained groundmasses consist of a mixture of chlorite, oxides, sphene and rare crystals of calcite and epidote. Apatite was not identified. Whether or not they initially contained glass is difficult to determine but the textures would appear to indicate otherwise.

The outcrops of these lavas lie within the central intrusive complex (fig 1-3). The hydrothermal fluids circulating within this region will not have been buffered by the lavas and may have been rich in alkalis. Accordingly, their major and trace element compositions may have been substantially modified. Nevertheless, the extensive growth of sphene suggests that the element group Ti, Nb, Zr and Y will have been immobile.

CHAPTER SIX: REGIONAL GEOCHEMICAL VARIATION
IN THE BRITISH TERTIARY IGNEOUS PROVINCE.

The Tertiary igneous rocks of Britain were considered by early workers to be the remnants of a vast Thulean or Brito-Arctic province stretching from Britain to the Faroes, Iceland, Jan Mayen and Greenland, and that fragmentation and subsidence of this province led to the formation of the North Atlantic (e.g. Tyrell 1937). Subsequent reconstructions of the early Tertiary geography of the North Atlantic have considerably reduced the extent of this Thulean province - (e.g. Bott and Watts 1971). Although it is now recognised that the widespread volcanism in Britain and East Greenland was tectonically related to the opening of the N. Atlantic between Greenland and the Faroes Rise, it is equally clear that the distribution of igneous rocks within these regions cannot be explained by any simple model of sea floor spreading alone, and a large number of models of tectonomagmatic events in the region have been presented in an attempt to explain the space-time distributions of the Tertiary igneous centres (e.g. Duncan et al. 1972, Gass 1972, C. Brooks 1973, M. Brooks 1973).

Igneous activity within the British Tertiary volcanic province was predominantly basic with only minor amounts of associated acidic magmas. Geophysical studies have established that the igneous centres are underlain by cylindrical plugs of basic or ultrabasic material that extend to depths of 5-15kms or more, while the associated acid rocks rarely exceed 1000m in thickness (e.g. Roberts 1970, Bott and Tuson 1973, McQuillan et al. 1975). Localised, northwest trending dyke swarms, consisting mainly of basaltic rocks, pass through the individual centres. The dyke swarms do not appear to extend to depths of more than a few kms (Bullerwell 1972a), but they increase in intensity towards the intrusive centres, achieving crustal extensions of up to 10% (Sloan et al. 1969). The distribution of the dyke swarms implies a regional tensile stress component operating in a NE-SW direction. Palaeomagnetic studies have established that the lavas and most, but not all, of the dykes exhibit a reversed direction of magnetisation

suggesting they may have been formed within a single reversed epoch (e.g. Wilson 1970, Ade-Hall et al. 1972, Dagley and Mussett 1978). Current opinion favours the hypothesis that the onset of igneous activity within the province was contemporaneous at about 59 Ma. with most of the intrusive and extrusive activity taking place within a period of 1-2 Ma. (Beckinsale 1974, Macintyre et al. 1975, Brown and Mussett 1976, Fitch et al. 1978). The basic rocks therefore represent the products of approximately synchronous, and localised, magma generation within the Palaeocene upper mantle beneath the province. Each centre may therefore have produced magmas of slightly different composition depending on the local regime of pressure, temperature and mantle composition.

A clear picture of the distribution of basic magma types within the province is clearly essential in order to evaluate the provenance and Pre-palaeocene geochemical history of the upper mantle beneath the area. Unfortunately, few modern trace element analyses of Hebridean Tertiary basic rocks are available. Accordingly, major and trace element analyses were made of a crininite sample (MS 209) from the Dippin Head Sill. This intrusion represents the earliest emplacement of basic magma in S.Arran (Hallsall 1978) and should therefore be approximately contemporaneous with the Mull Plateau Group and the Skye Main Lava Series. In this chapter the various Mull, Skye, Arran basalts are compared in order to establish whether or not the basic magmas supplying these centres were identical. In addition to the data presented in this study published analyses from the following data sources are also used: The Skye Main Lava Series (SMLS) and a tholeiitic pillow lava from the base of the Skye lava pile, SK 965, (Thompson et al. 1972, 1979); the Skye Preshal Mhor (PMB) and Fairy Bridge (FBT) magma types (Mattey et al. 1977); an average of sixteen low alkali tholeiite dykes from the Mull regional swarm and a low alkali tholeiite lava from Mull, (MLAT) (Mattey et al. 1977, Thompson 1979). The basic lavas from Groups I, II and III of Beckinsale et al. (1978) were also used. Their group I and III lavas were all collected from Plateau Group localities (op.cit. fig 1) and hence were initially included with the Mull Plateau Group

(MPG) analyses obtained in this study. The basic members of their group II are all lavas placed by Bailey et al. (1924) in their Staffa magma type and were included with the analyses of the Staffa lava (M 80) and the McCulloch's tree lava (M 61) obtained in this study.

1. Distribution of the magma types within the province.

Several classification schemes relating basic volcanics to their magma type and tectonic setting by means of their trace element content have recently been proposed (J. Pearce and Cann 1972, 1973; T.H. Pearce et al. 1975, Floyd and Winchester 1975). The extensive secondary alteration shown by the Mull Non Porphyritic Central lavas (NPC) and the Plateau Group lavas collected from the central greenschist-facies zones, means that for these particular samples, only their immobile trace element ratios can be considered to represent magmatic characteristics. In order to include all the samples in the comparison the various magma types were plotted on the 'diagnostic' trace element diagrams of these authors (figures 6-1 to 6-3). Their distributions are discussed in more detail below.

Skye Main Lava Series and Mull Plateau Group

The Skye Main Lava Series and the Mull Plateau Group are indistinguishable on all the trace-element diagrams. The SMLS and MPG basalt also show a similar range of Si-saturation. (fig 6-4). Most of the basic members of the Small Isles lava suites analysed by Bidley (1972) also plot in the outlined field on figure 6-4, but the absence of trace element data for these lavas precludes detailed comparison. MS 209, the Arran crinanite sample, has the major-element composition of a typical nepheline-hawaiite (fig. 6-4) and similar trace element abundances to the SMLS and MPG lavas (figs. 6-1, 6-2). Comparison of figures 6-1 to 6-4 also shows that the basal "Staffa-type" lavas from both Mull and Skye (M 61, M 80, SK 965, and the Group II lavas of Beckinsale et al. (1968)) have similar trace element abundances to the SMLS and MPG basalts but substantially different major-element compositions. Beckinsale et al. (1978) claimed that their Group I and II lavas are the chemical equivalents on Mull of the ne- and hy-normative sub-

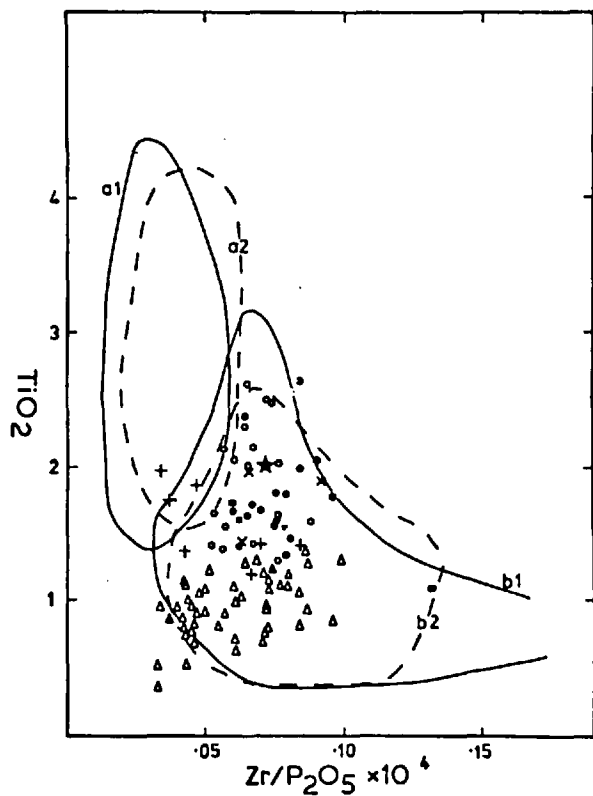
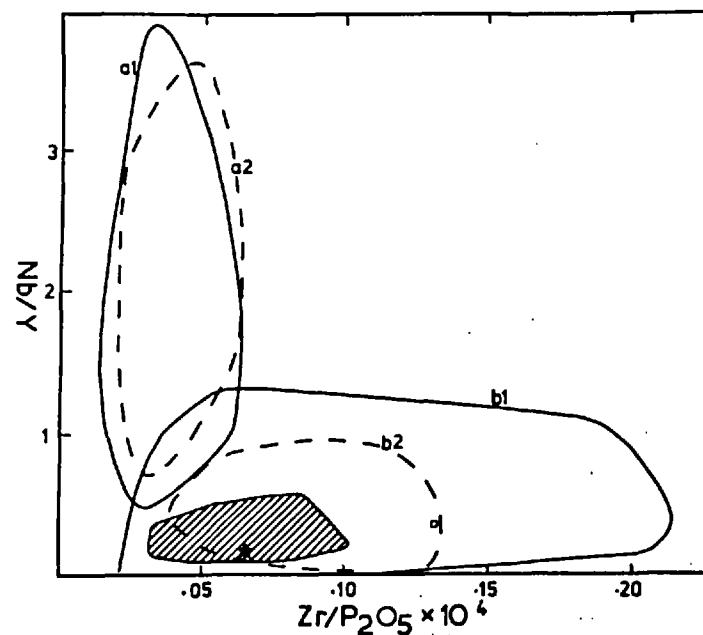
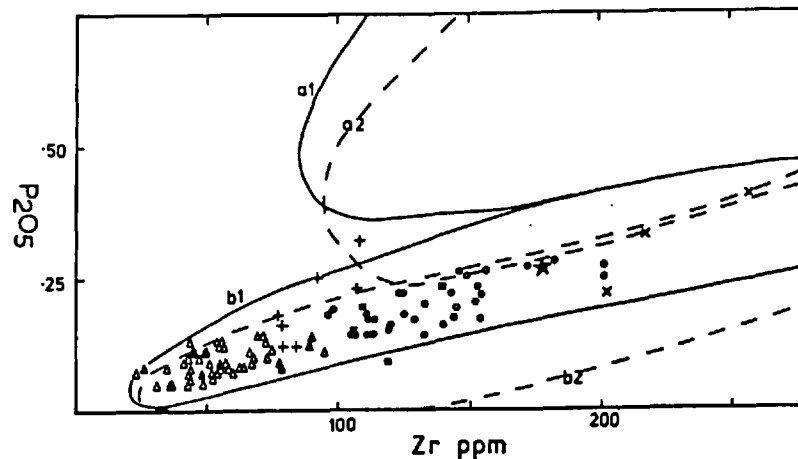


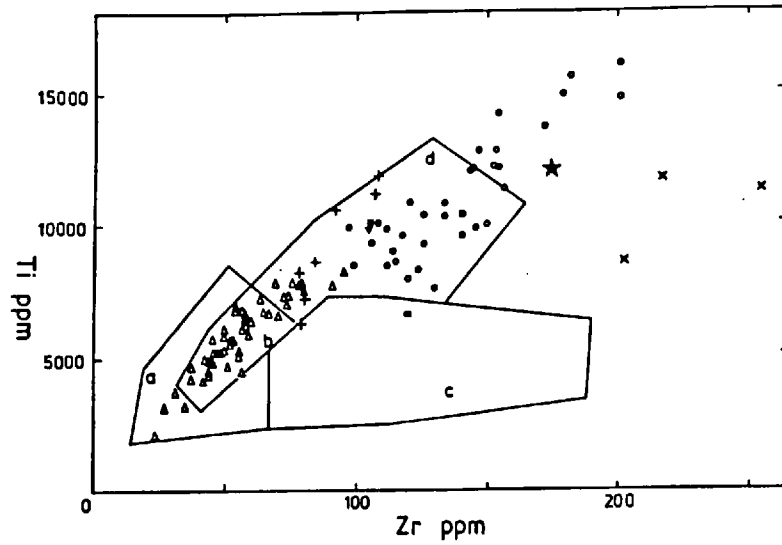
Figure 6-1

Distribution of the various Hebridean basalts on the discriminant diagrams of Floyd and Winchester (1975).

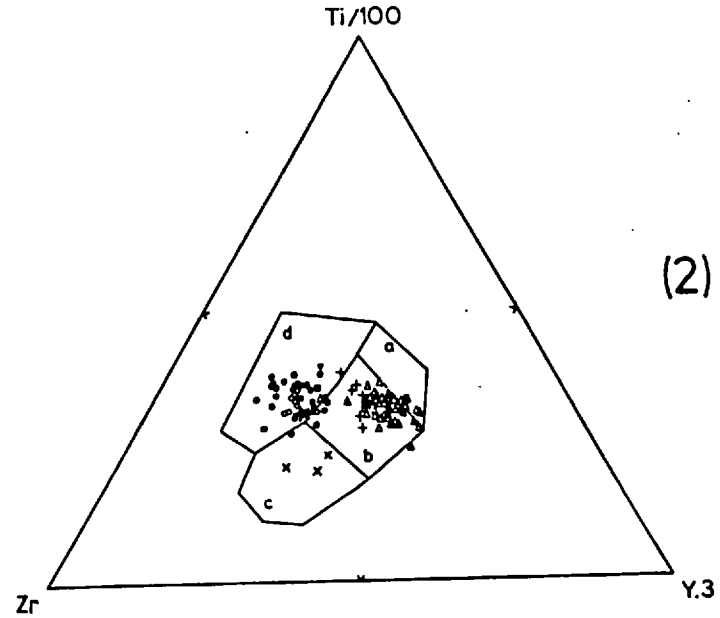
Fields: a₁ - continental alkali basalts, a₂ - oceanic alkali basalts. b₁ - continental tholeiites, b₂ - oceanic tholeiites. Symbols: o - Skye Main Lava Series; Δ - Preshal Mhor type; + - Fairy Bridge type; ◻ - SK 965; ● - Mull Plateau type; ▲ - Mull low alkali tholeiites; x - Non porphyritic central type; ■ - M 61; ▼ - M 58; ★ - MS 209.



(1)



(2)



(3)

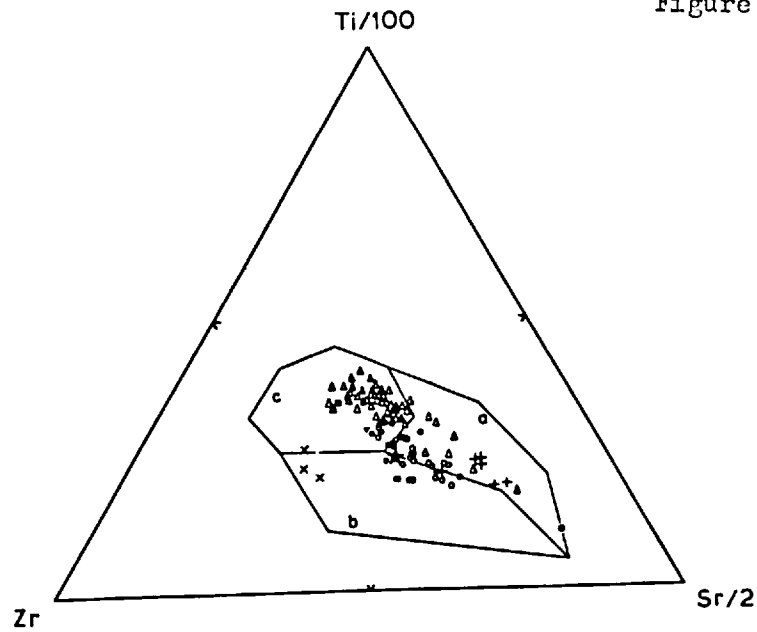


Figure 6-2 Distribution of the various Hebridean basalt types on the discriminant diagrams of J.Pearce and Cann (1973). Symbols as in previous diagram.

- Fields :
- (1) a + b = low alkali tholeiites,
c = calc alkali basalts,
d + b = ocean floor basalts
 - (2) a + b = low alkali tholeiites,
c + b = calc alkali basalts,
d = within plate basalts
 - (3) a = low alkali tholeiites,
b = calc-alkali basalts,
c = ocean-floor basalts.

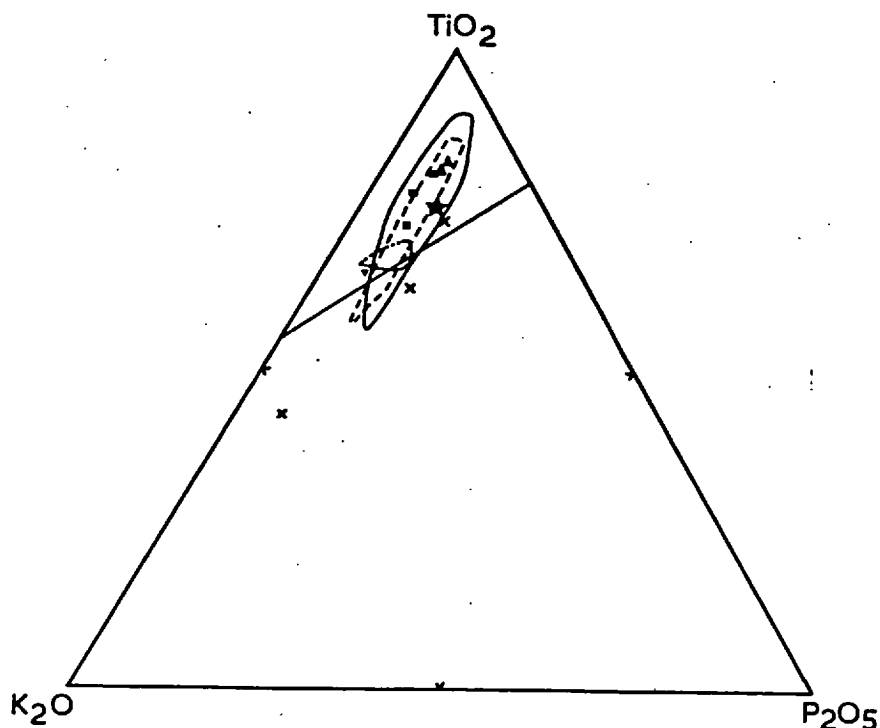


Figure 6-3.

Distribution of the various basalt types on the $\text{TiO}_2 - \text{K}_2\text{O} - \text{P}_2\text{O}_5$ diagram of T. Pearce et al. (1975). \circ Preshal Mhor magma type; \bigcirc Skye Main Lava Series and Mull Plateau Group; \cdots Skye Fairy Bridge magma type; other symbols as in previous diagrams.

divisions, respectively, of the SMLS basalts. This is clearly incorrect. The Groups I and III basalts of Beckinsale et al. plot within the outlined field of figure 6-4 and hence fall within the overall compositional range of the SMLS and MPG basalts. The major- and trace-element distributions discussed above thus support the two-fold division of the early Skye and Mull lavas made on the basis of field and petrographic data by previous workers (Bailey et al. 1924, Anderson and Dunham 1966).

Beckinsale et al. (1978) based their subdivisions of the Mull lavas on two main lines of evidence - their variable initial $^{87}\text{Sr}/^{86}\text{Sr}$ ratios, and the low Y contents of three highly evolved lavas. They claimed that the $(^{87}\text{Sr}/^{86}\text{Sr})_i$ ratios of the basalts showed no correlation with Sr content and hence represented primary magmatic characteristics of the lavas. Pb, Sr and Nd isotope studies of the Skye and

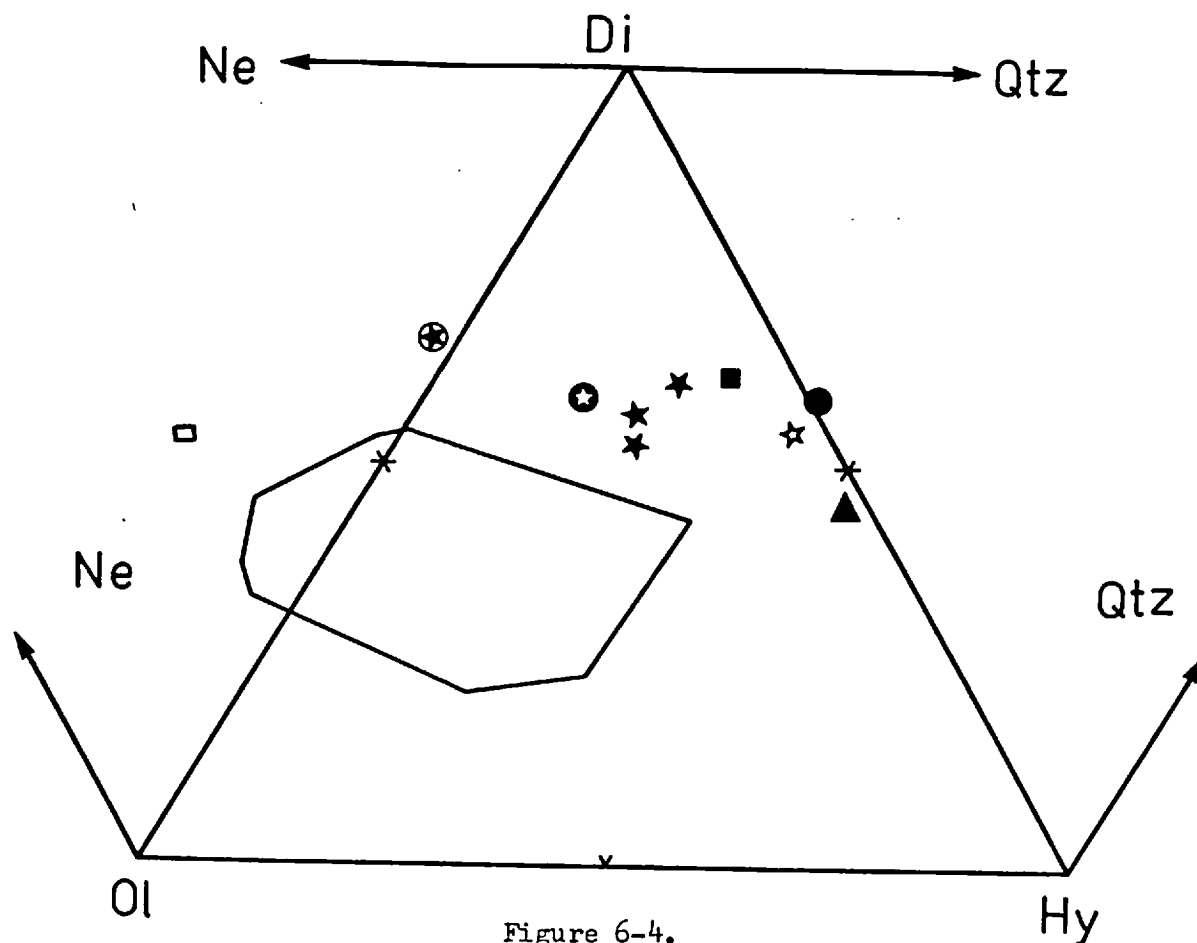


Figure 6-4.

Normative diopside-hypersthene-olivine-nepheline/quartz in basic lavas and pyroclastics from Mull, ^{Aron} and Skye. All the norms calculated with Fe_2O_3 set at 1.5%. MPG and SMLS basalts fall in the outlined field. Key to symbols: Open square MS 209. Filled stars = Mull Group II lavas of Beckinsale et al. (1978); Open star = McCulloch's Tree flow Mull, (M 61); Circled filled star = Fingal's cave flow, Staffa (Tilley and Muir 1962); Circled open star = Fingal's cave lava, this study (M 80); Filled circle = glass separated from basal tuff, NW Skye (Anderson and Dunham 1962); Filled square - basal pillow lava, NW Skye (ibid); filled triangle = basal pillow lava (SK 965), NW Skye (Thompson et al. 1979).

Mull lavas have established that they show a range of isotope ratios intermediate between those of mantle derived magmas and the Lewisian gneisses which formed the basement to these complexes (Moorbath and Welke, 1968, Carter et al. 1978, Moorbath and Thompson 1979). The Sr

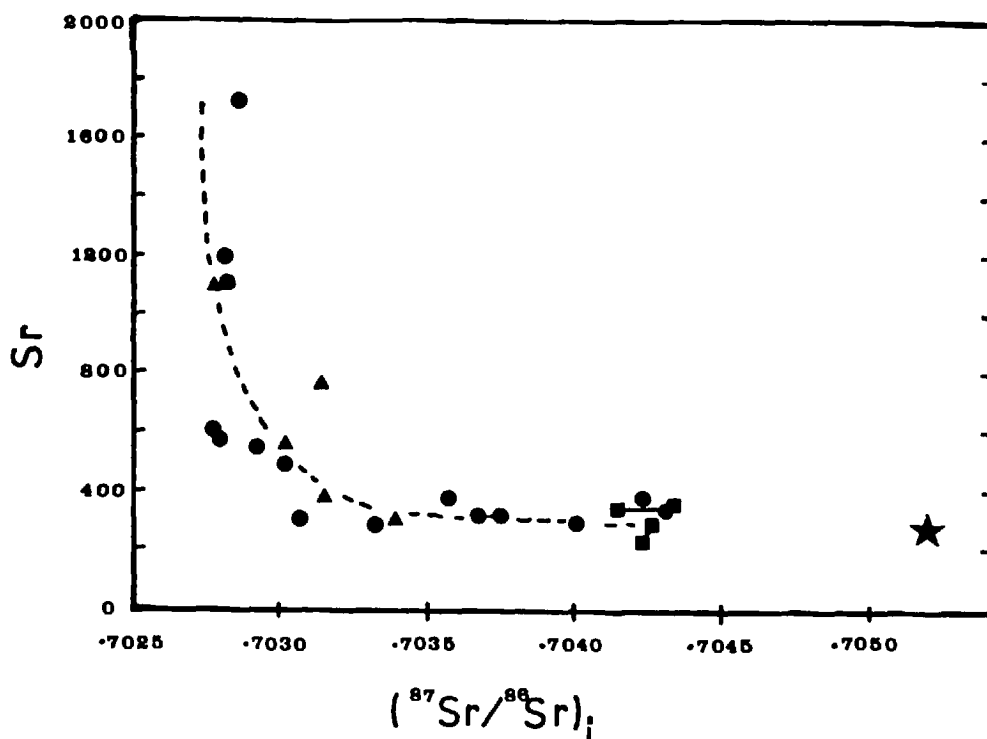


Figure 6-5.

Sr versus initial $^{87}\text{Sr}/^{86}\text{Sr}$ ratios for Mull lavas.

Data sources: ● - Groups I and III lavas of Beckinsale et al. (1978);
 ▲ - Carter et al. (1978); ■ Moorbath and Thompson (1979);
 ★ - deduced initial composition of Pennygown Quarry lava (this study).

and $(^{87}\text{Sr}/^{86}\text{Sr})_i$ ratios of the MPG lavas and Groups I and III of Beckinsale et al. are plotted against each other in figure 6-5 and it is clear from this that there is a correlation between these two parameters indicating that the lavas have been affected by crustal contamination. Significantly, the contamination curve shown in figure 6-5 is extremely similar to that obtained for the SMLS by Moorbath and Thompson (1979).

The effects of bulk contamination on the Skye and Mull basalts was modelled by Morrison et al. (1979). Their results indicated that it was impossible to produce magmas with the minor and trace-element contents of the SMLS and MPG lavas by incorporating small amounts of suitable contaminant materials (Lewisian gneiss and/or a Skye granite showing cotectic melting at upper crustal pressures) in the basalts.

Further, Moorbath and Thompson (1979) could find no correlation between either SiO_2 content or Si-saturation and $(^{87}\text{Sr}/^{86}\text{Sr})_i$ ratios in the Skye basalts. The range of isotopic compositions shown by these lavas would thus appear to be the result of selective element movements which are discussed in more detail by Moorbath and Thompson (1979).

Geochemical and melting studies suggest that the Skye Main Lavas Series magnesian basalts were formed by the partial melting of a spinel lherzolite at about 60kms depth, with the degree of initial melt fraction varying from approximately 5-10% to generate the ne- and hy-normative magmas, respectively. Ti, Zr, P, Hf and the middle rare earth elements correlate negatively with Si-saturation in the SMLS basalts agreeing with the dilution trends which would be predicted from a partial melting model. The less-incompatible elements Y and Yb show smaller concentration ranges due to their partial retention in upper mantle diopside (Thompson 1974, Thompson et al. 1979). The nearly identical Si-saturation ranges and trace element abundance ranges in the SMLS and MPG suggest the latter were produced by similar degrees of partial melting. The more alkalic Arran crinanite sample (MS 209) may have been generated from basic magma produced by a slightly smaller degree of partial melting. This is reinforced by their petrographic similarity and the presence of Al-rich chromites similar to those crystallised in high-pressure experiments, in the SMLS and MPG basalts (Thompson 1974).

Thompson (1974) suggested that the SMLS less-magnesian basalts and hawaiites were produced by the high-pressure fractionation of olivine, plagioclase and aluminous subcalcic augite in the lowermost crust and uppermost mantle. Concordant, independent, numerical models of this process have been provided by major and trace element data (Thompson 1974, Thompson et al. 1979). The small number of evolved rocks analysed during the course of this study precludes any detailed consideration of their genesis. Nevertheless, the Mull hawaiites, including those of Beckinsale et al. (1968), and the Arran crinanite sample, MS 209, plot close to the Skye hawaiites along the fractionation trend for the SMLS lavas on the Y-Zr diagram shown in figure 6-6. The

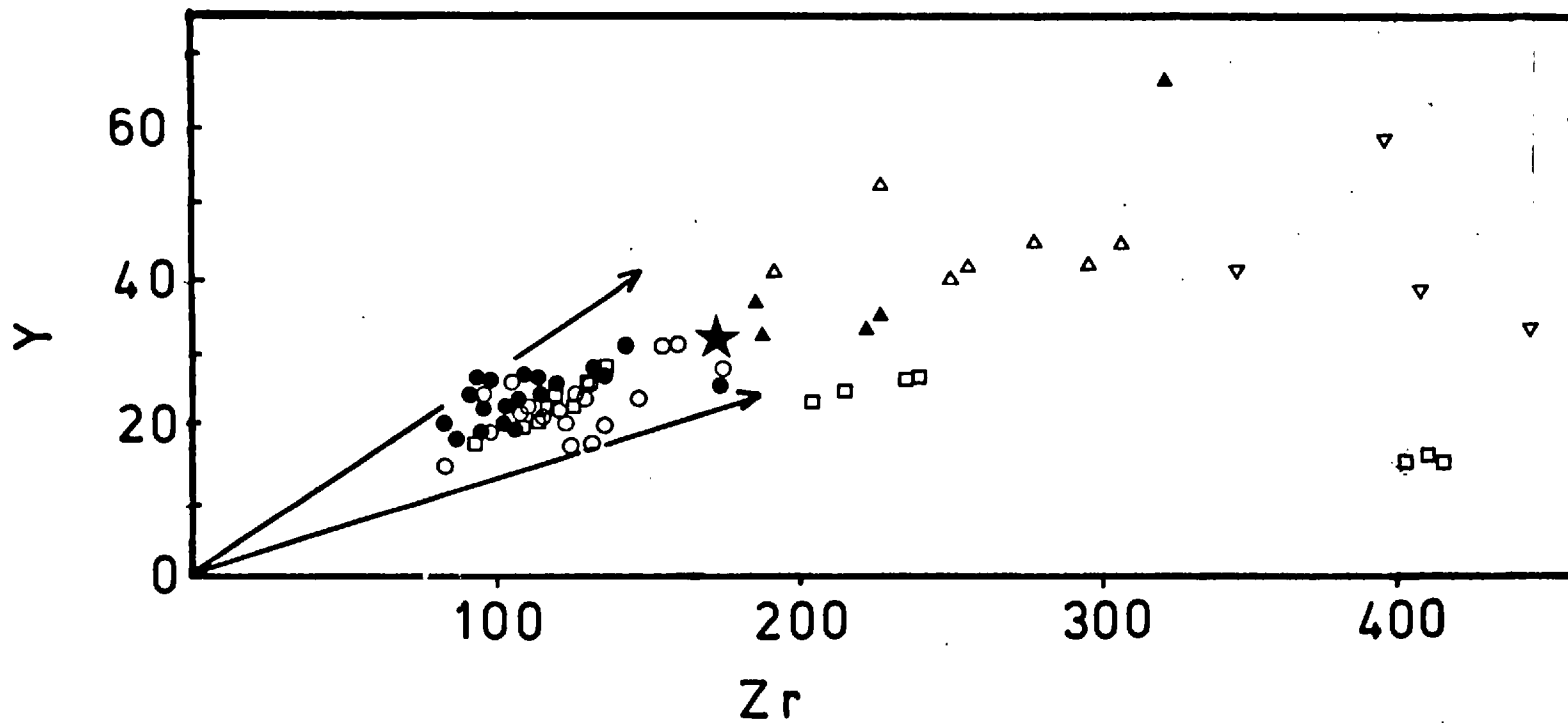


Figure 6-6 Y versus Zr for Skye Main Lava Series and Mull-Plateau Group.

SMLS: o - basalts, Δ-hawaiites, ▽ Benmorites, Mugearites and trachyte

MPG: ● - basalts, ▲-hawaiites and M 59. ★ MS 209

□ - Group I and III lavas of Beckinsale et al.(1978).

three low-Y lavas of Beckinsale et al. (1978) plot in the lower right hand corner of figure 6-6. It is clear from their evolved compositions, particularly their low Ni and Cr contents (op.cit. Table 1), that these lavas cannot be primary magmas and must have been affected by some degree of fractional crystallisation. No basic magmas with very low-Y contents have been reported from the British Tertiary Province. Thompson et al. (1979) showed that the SMLS benmorites and low-Fe intermediate and trachyte lavas have low Y, Yb, Zr, and Hf contents as a result of zircon fractionation (see fig. 6-6). Other REE-bearing phases such as apatite also become important in controlling the fractionation trends of these lavas. It seems likely that the three low Y samples of Beckinsale et al. could have been similarly produced by extensive fractionation of the MPG magmas.

Beckinsale et al. (1978) suggested the Palaeocene upper mantle beneath Mull (and by implication beneath Skye also) was vertically inhomogeneous. The discussion above indicates that their Group I and Group III subdivisions are based on parameters reflecting crustal rather than mantle processes. Several lines of evidence suggest that the differences between the SMLS and MPG basalts and the basal 'Staffa-type' lavas may also be due to crustal processes. The most notable features of those distinctive, local, basal lavas are as follows :-

1. Relative to the SMLS and MPG lavas they are volumetrically insignificant, representing less than 1% of the total lava succession in both islands (Bailey et al. 1924, Anderson and Dunham 1966).
2. They were erupted only at the onset of volcanic activity.
3. The relative abundances of most of the incompatible and rare earth elements in these lavas fall within the range shown by the SMLS and MPG basalts but they have significantly higher K, Rb and Ba contents and higher initial $^{87}\text{Sr}/^{86}\text{Sr}$ ratios (figs. 6-1, 6-2; Appendix I-E, N 61, 80; Beckinsale et al, 1978, Thompson et al. 1979, Moor bath and Thompson 1979).
4. Their normative di-rich compositions relative to the SMLS and MPG basalts. It is also apparent from figure 6-4 that these di-

rich rocks exhibit a wide-range of Si-saturation.

5. Augite is a phenocryst phase in these basal lavas whilst in none of the SMLS and MPG basalts was augite a near-liquidus phase.

The petrography and major element compositions of these basal volcanics suggest they approach low-pressure olivine-plagioclase-augite-liquid cotectic equilibria in the natural basalt system. In contrast, the compositions of the SMLS and MPG basalts are related to high pressure (> 10 kb) cotectics (Thompson 1974). It seems likely that small batches of basic magma which were halted prior to eruption in the K, Rb and Ba-rich and high $^{87}\text{Sr}/^{86}\text{Sr}$ environment of the amphibolite-facies Lewisian gneisses of the upper crust (Carter et al. 1978) will possess higher values of these parameters than subsequent magma batches which ascended more rapidly through the crust.

Skye Preshal Mhor and Mull low-alkali tholeiite basalts.

These two magma types show identical distributions on the various trace element diagrams in figures 6-1 and 6-2. On all except the Nb/Y - Zr/P₂O₅ plot (fig. 6-1), they occupy different regions to the SMLS and MPG lavas. The Skye Preshal Mhor basalts are characterised by high CaO contents (11-13%), low total alkali contents, low abundances of the large-ion lithophile elements and a light rare earth depleted chondrite-normalised pattern ($\text{Ce}/\text{Yb}_N < 1.0$). The Mull low alkali tholeiite dykes show similar major and trace element contents but no rare earth element data are available for them (Mattey et al. 1977). MS 133, the MLAT lava sample has a LREE depleted pattern (Thompson 1979). Skelhorn et al. (1979) have shown that the chilled margin of the Ben Buie gabbro in Mull shows the distinctive chemical characteristics of the Preshal Mhor magma type.

Dykes of the PMB magma type comprise more than 70% of the total regional dyke swarm of Skye and have been injected within a relatively narrow zone that defines the axis of maximum crustal extension for the swarm as a whole (Mattey et al. 1977). Lavas of this type are rare in Skye other than a few flows intercalated with the SMLS at the top of the

lava pile (Thompson et al. 1972, Esson et al. 1975). Unless the PMB dykes failed to reach the surface to form flows, lavas of this type must have been abundant in the upper, now eroded parts of the Skye lava pile.

Low alkali tholeiite dykes form a substantial proportion of the Mull regional dyke swarm (Lamacraft 1979). Since the Ben Buie gabbro also appears to belong to this distinctive magma type this clearly suggests that the MLAT magmas were similarly emplaced at the climax of crustal extension and that lavas of this type were also common in the upper part of the Mull lava pile. At this point the analogy breaks down as the MPG are overlain by the Non-Porphyrific central lavas. On the various trace element plots in figures 6-1 and 6-2 these lavas form a distinct group, plotting in totally different areas to the other magma types on all except the Nb/Y - Zr/P₂O₅ plot. On the Ti/100 - Zr - Y.3 and Ti/100 - Zr - Sr/2 diagrams of J.Pearce and Cann (1973) (fig. 6-2) they lie in the 'calc-alkali' fields. The NPC lavas, though undoubtedly tholeiitic, would thus appear from these diagrams, to belong to yet another distinct magma type.

The reason that the NPC lavas plot in the 'calc-alkali' fields is they possess distinctly higher Zr and only slightly higher TiO₂ contents to the other magma types (Appendix I-E). A high Zr/TiO₂ ratio is often an indicator of magmatic differentiation and these lavas do contain titanomagnetite phenocrysts. Although their major element compositions have probably been substantially modified by secondary alteration they all possess low MgO contents (4.5 to 3.0%) (Appendix I-E). This raises the possibility that they may be evolved members of the MLAT magma type. In the regional swarms dykes of more evolved compositions tend to be restricted to the vicinity of the Tertiary centres, (Skelhorn 1969, Matthey et al. 1979) and the practice in recent geochemical studies of only using samples collected from outside the central zones of hydrothermal alteration, may have introduced a systematic bias into the data. L.Nodes (pers.comm. 1978) has found that the Mull NPC lavas show a wider range of trace element abundances than the three samples discussed here. Whether or not these belong to the MLAT magma type cannot yet be determined without further

study and by means of rare earth element data in particular.

The SMLS and PMB lavas have similar relative abundances of the ultra-incompatible elements such as La and Ta (Thompson et al 1979). Accordingly, Thompson et al. have proposed that the PMB magmas originated from a further melting increment of the lherzolite mantle volume that had previously produced the SMLS basalts (with inefficient melt extraction); leaving a final harzburgitic residuum. Other possible models fail to explain the interstratification of the SMLS and PMB lavas and the appearance of the Preshal Mhor magma type at the climax of crustal extension in the dyke swarm. Although many of the Tertiary Hebridean rocks show isotopic evidence for crustal contamination, Moorbath and Thompson (1979) have found that the lowest initial $^{87}\text{Sr}/^{86}\text{Sr}$ ratios in both the SMLS and PMB lavas are identical, which supports the single mantle source model. Clearly, a similar scenario could be adapted to explain the genesis of the Mull low alkali tholeiites.

Other magma types.

The Skye Fairy Bridge basalts form a tight cluster on each of the diagrams in figures 6-1 to 6-3. On the P_2O_5 - Zr and Ti - Zr diagrams they fall between the SMLS and PMB; on the TiO_2 - Zr/ P_2O_5 and Ti/100 - Zr - Sr/2 diagrams they overlap the SMLS but are totally separate from the PMB; on the Ti/100 - Zr - Y.3 plot they plot close to the PMB and are completely distinct from the SMLS. M 58, the basalt sample collected from the hill top knoll, south of Fishnish Peninsula in Mull, plots close to the Skye FBT basalts in every case. SK 971, the lava flow from the type FBT locality in Skye has a slightly LREE-enriched chondrite-normalised pattern with $\text{Ce}/\text{Yb}_\text{N} = 1.7$ (Thompson et al. 1979). M 58 has a very similar REE pattern, also with a $\text{Ce}/\text{Yb}_\text{N}$ ratio of 1.7 (Appendix I-E). Dykes with similar trace and rare earth element abundances to M 58 occur in the mainland extension of the Mull regional dyke swarm (L.Nodes pers.comm. 1978). Nevertheless, these two basalt types also show some compositional dissimilarities. The FBT contain both ne- and hy- normative types and like the SMLS and MPG can be described as transitional basalts. M 58 contains no modal olivine

and has a distinctly tholeiitic major element composition (Appendix I-E).

The FBT have similar relative abundances of the ultra-incompatible elements such as La/Ta to the SMLS and PMB lavas, as do M 58, MS 133, the Mull low alkali tholeiite lava flow, and the MPG (Thompson et al. 1979, Thompson 1979, Appendix I-E this study). A dynamic or continuous melting model, of the type proposed by Thompson et al. (1979) for the SMLS and PMB lavas, can also generate magmas with similar incompatible element abundances to the FBT (and M 58): either by a slightly higher degree of partial fusion and melt extraction during the initial melting or, by the extraction of a smaller melt fraction than that required to produce the PMB during a subsequent melting increment.

Basalts with the distinctive major element chemistry of the PMB magma type have been reported from Arran, Carlingford and Antrim (Mattey et al. 1977) but no trace element data are available for these rocks. Some low alkali tholeiite dykes have been found in the Arran regional dyke swarm (L.Nodes pers. comm. 1978). Mitchell et al. (1976) have reported analyses of eight basalts dredged from the Blackstones igneous centre. Four of these samples (72/7/18, 75/3/1, 75/5/8, 75/5/9) have transitional major element compositions whilst the other four have high CaO contents and are tholeiitic (72/7/1, 72/7/11, 75/3/2, 75/5/7). On the trace element diagrams of J.Pearce and Cann (1973) these basalts show similar distributions to the FBT and PMB magma types of Skye (Mitchell et al. Fig.3). Nevertheless, the absolute trace element abundances and K₂O contents of these basalts do not fall within the compositional range of the Skye basalt types. More data, and particularly more REE analyses, are needed in order to establish whether or not the various basic magma types within these centres can be considered comparable to those recognised in Skye as suggested by Mattey et al. (1977).

2. Lateral heterogeneity in the Palaeocene upper mantle beneath the Scottish Hebrides.

The overlapping chemistry of the various Skye, Mull and Arran

basalt types demonstrates that these centres produced a series of compositionally similar (though not necessarily identical) basic magma types. The Skye Main Lava Series, the Mull Plateau Group and the Arran crinanites represent the early major products of vulcanicity at these centres and can thus be used to monitor the composition and variability of their Palaeocene upper mantle-source regions. Accordingly, these basalts are compared in more detail in this section.

Differences between Tertiary Hebridean and world-wide alkali basalt suites.

The early lavas of the British Tertiary Province have traditionally been regarded as one of the world's most typical examples of an alkali basalt suites (e.g. Kennedy 1933, Tilley 1950, Wager 1956, Coombs and Wilkinson 1969, Carmichael et al. 1974). The SMLS and MPG both contain ne- and hy-normative types and are possibly best classified as transitional basalts. Nevertheless, it can be seen from fig. 6-1 that their trace element contents bear more resemblance to those of olivine tholeiites. MS 209, the Arran crinanite sample, has the major element composition of a typical nepheline-hawaiite (Appendix I-E) and similar trace element abundances to the SMLS and MPG (figs. 6-1, 6-2, and 6-6). Durant (1978) noted a similar discrepancy between the major and trace element compositions of Hebridean alkali basalts in his study of the Islay and Jura dyke swarms.

The magnitude of this incompatible-element depletion in the Tertiary Hebridean basalts, relative to other alkali basalt suites can be seen from figure 6-7. The rare-earth and other incompatible-element contents of representative world-wide samples, taken from the literature, are normalised on this diagram to their abundances in the average composition of the SMLS less-magnesian basalts. Since MgO is linearly related to the liquidus temperatures of basalts (Thompson 1973), constant values of this oxide were used as a criterion to select the other samples, so that only lavas at approximately comparable stages of fractional crystallisation are shown on figure 6-7. By normalising to an average SMLS composition, incorporating lavas with differing degrees of Si-saturation, the effects of variable partial melt-

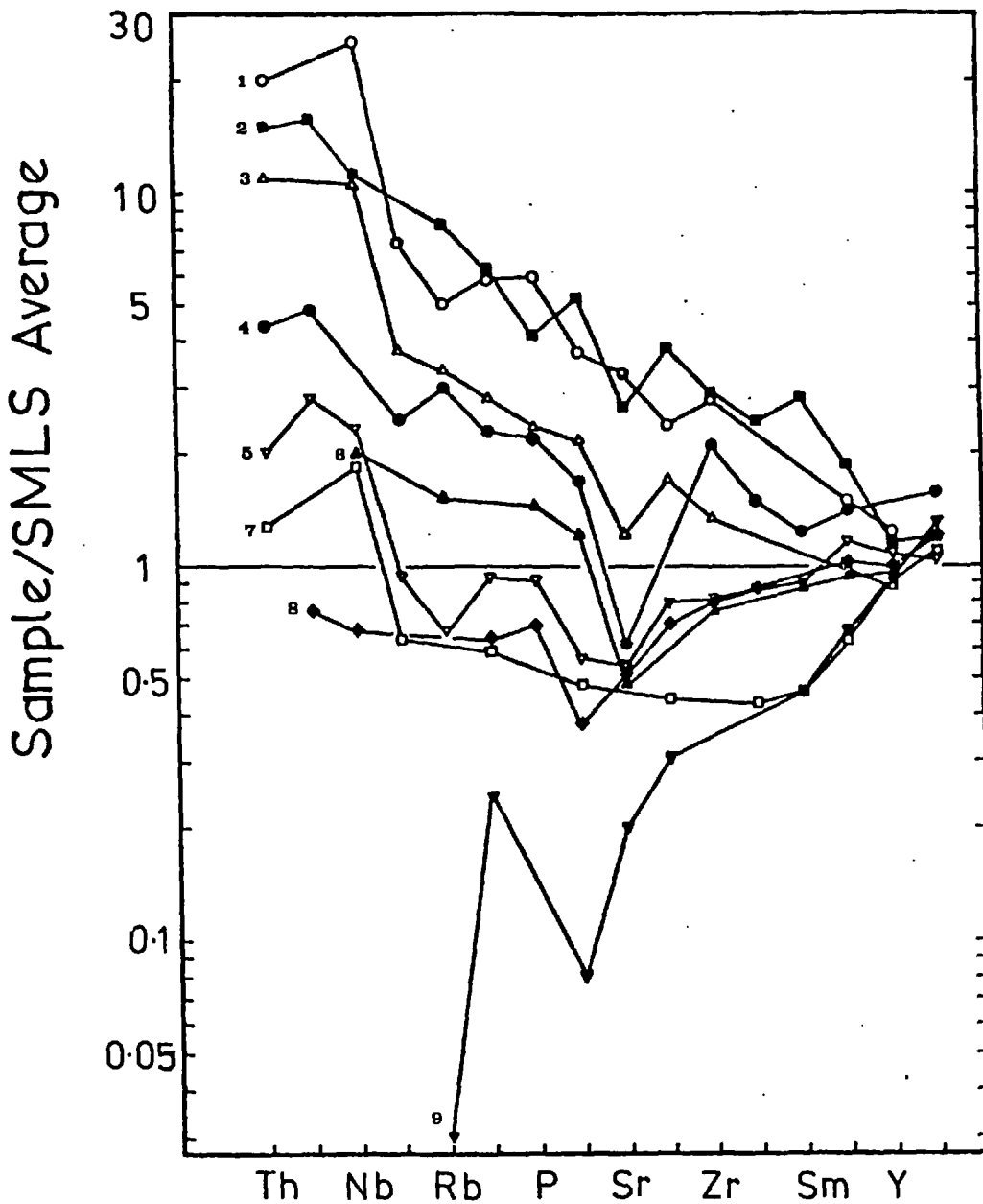


Figure 6-7 Ta La Ce K Nd Hf Ti Yb

Comparison of incompatible element abundances in SMLS basalt and other lavas. The SMLS average (MgO = 8.41%) to which the other lavas are normalized is the mean of the less-magnesian basalts (Thompson et al. 1979). MgO in the other samples ranges from 8-12 - 8.99%, except for MS 144 (7.68%) Key : 1 = nephelinite (4169), New South Wales (Kesson 1973); 2 = camptonite (MS 144), Dornie, Loch Duich (see text); 3 = alkali olivine basalt (27417), New South Wales (Kesson 1973); 4 = olivine tholeiite (72-3B), Snake River Plain (Leeman & Vitaliano 1976); 5 = olivine tholeiite (VII), eastern Iceland (Wood 1978); 6 = olivine tholeiite (AJ32), Anjouan, Comoros (Flower 1973); 7 = tholeiitic basalt glass (523 - 1GL), FAMOUS area, Mid-Atlantic-Ridge (Langmuir et al. 1977); 8 = average of MPG basalts with mean MgO (8.3%) close to SMLS average (this paper); 9 = tholeiitic basalt glass (319-21/27-30 ca), D.S.D.P. leg 34 Nazca Plate, eastern Pacific (Hart 1976). In addition, the following alkali olivine basalts plot along essentially the same line as no. 3 in the diagram : 0030436 (MgO = 8.79%), Dunedin, New Zealand (Price & Chappell 1975); M 33 (MgO = 8.42%), Madeira (Hughes and Brown 1972). A Kilauea olivine tholeiite K10037, with MgO = 8.37%, (Gunn 1971) plots close to the SMLS average.

ing during their genesis was eliminated. The trace elements are plotted from left to right along the abscissa in an empirical order of increasing abundance difference, relative both to the SMLS and to each other. The use of a vertical log-scale allows typical MORB basalts and ultra alkalic lavas to be accommodated on the same diagram.

Other than the elements K, Rb and Sr which show no regular behaviour, as noted by Kay and Gast (1973), Bougault et al. (1979) and others, the other parts of the patterns on figure 6-7 are remarkably consistent. These diverse magmas appear to be buffered to approximately constant values of Y and Yb, whilst showing systematically increasing variability in the abundances of the progressively more-incompatible elements - i.e. those with progressively lower bulk distribution coefficients between major upper-mantle minerals and basalt melt (Bougault et al. 1979). The patterns of many other samples superimpose on those plotted in figure 6-7 and are described in the legend. This consistency is remarkable in view of the fact that this diagram takes no account of differences in the mineralogy of the various mantle source regions of these lavas and the presence or absence of phases such as plagioclase or garnet.

The basalts with incompatible-element abundances most similar to the SMLS on figure 6-7 (see also legend) are the olivine tholeiites from Kilauea, Anjouan (Comores), E.Iceland and the FAMOUS area. In contrast, all the alkali basalts show progressive enrichment with increasing incompatibility in their trace-element abundances, relative to the SMLS. The abundances of Ta, La, P and Zr, in the alkali olivine basalt from New South Wales, for example, are greater than those in the average Skye basalt by factors of 10, 4, 2 and 1.5, respectively. Differences between the alkali-basalt suites of Skye, Mull and Arran.

The pattern for the Mull basalts (a mean of the samples from flows LA 7-11 and M 51-55 that has a similar MgO content to the SMLS average) lies close to that of the E.Iceland lavas on figure 6-7 and appears to show substantial depletions of the more-incompatible elements, relative to the Skye basalts. This is despite the fact, that

the nearly-identical Si-saturation ranges in the SMLS and MPG suggest they were produced by similar degrees of partial melting (see discussion above).

In figure 6-8 selected trace elements are shown plotted against $F/F+M$ for individual SMLS and MPG basalts. Unlike figure 6-7 this diagram takes no account of the effects of partial melting on the trace element concentrations, but allows the magnesian basalts to be included in the comparison. $F/F+M$ was used for the abscissa as this is the best index of fractional crystallisation in these particular rocks (Thompson et al. 1979). At similar values of $F/F+M$, the MPG show the following differences, relative to the SMLS: markedly lower abundances of the more-incompatible elements such as Nb and P; slightly lower Ti abundances; similar abundances of less-incompatible elements such as Y. These differences between the two groups are precisely those that would be predicted from the differences between their mean less-magnesian basalt compositions, shown on figure 6-7. Nevertheless, the Skye and Mull basalts do not occupy separate fields on figure 6-8 but overlap, with this overlap being greatest for the less-incompatible elements and least for the more-incompatible elements.

Chondrite-normalised rare-earth patterns for individual Mull and Skye basalts are shown in figure 6-9. All the REE patterns are sigmoidal, to varying extents. Both the SMLS and MPG contain basalts with relatively straight and strongly-curved patterns. The majority of the Skye basalts have the former type of pattern, whilst all but one of the Mull basalts have the latter type. Some of the variations in total REE content between the individual Mull and Skye basalts can be attributed to the effects of fractional crystallisation* and/or hydrothermal alteration. (Mull basalts from the greenschist-facies zones as well as the zeolite-zones were included in figure 6-9 and figure 6-10 (below) as the elements plotted in these diagrams were immobile during alteration). These processes will produce parallel shifts of the rare-earth element patterns but cannot be the cause of the variations in slopes and curvatures of the patterns. Neither can they be attributed to the variable degrees of partial melting that gave rise to the SMLS and MPG

* crystallising phases - olivine and Cr-spinel in the Mg-basalts; olivine and plagioclase in the less-Mg basalts.

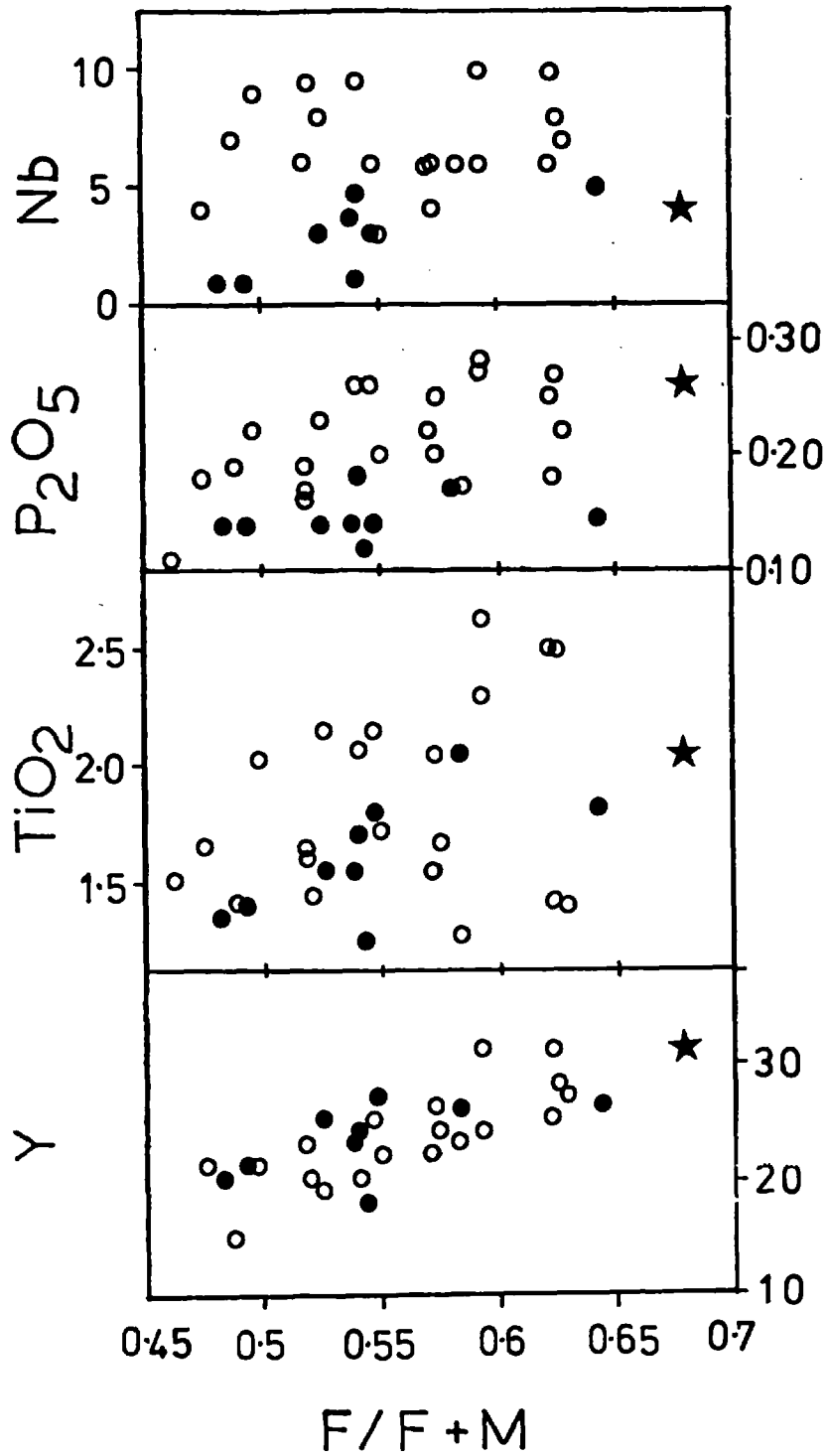


figure 6-8

Nb, P₂O₅, TiO₂ and Y versus F/F+M
 for Palaeocene Hebridean basic rocks.
 Symbols as in figure 6-1.

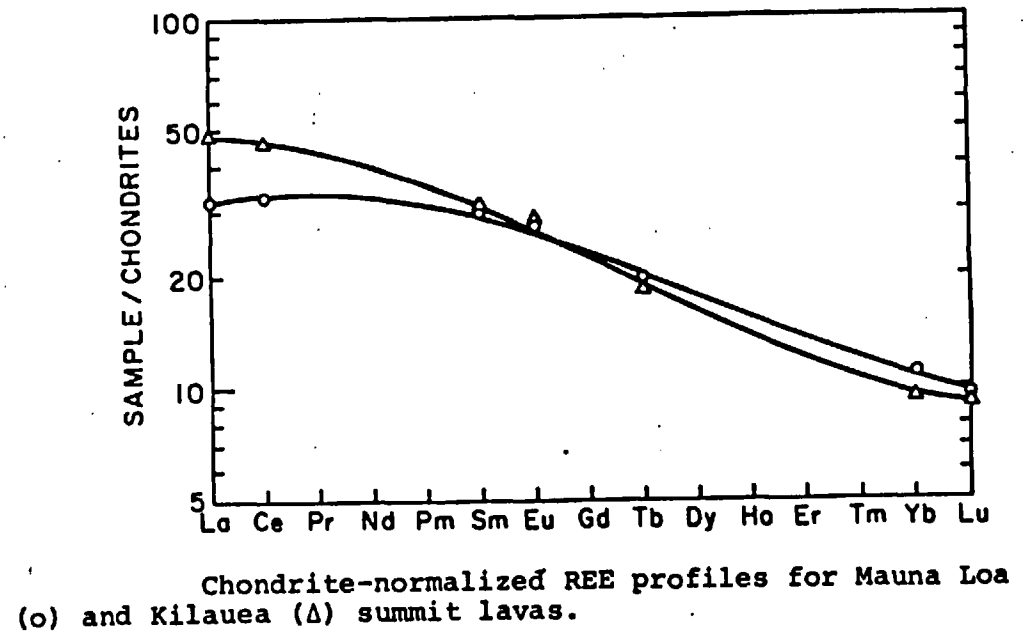
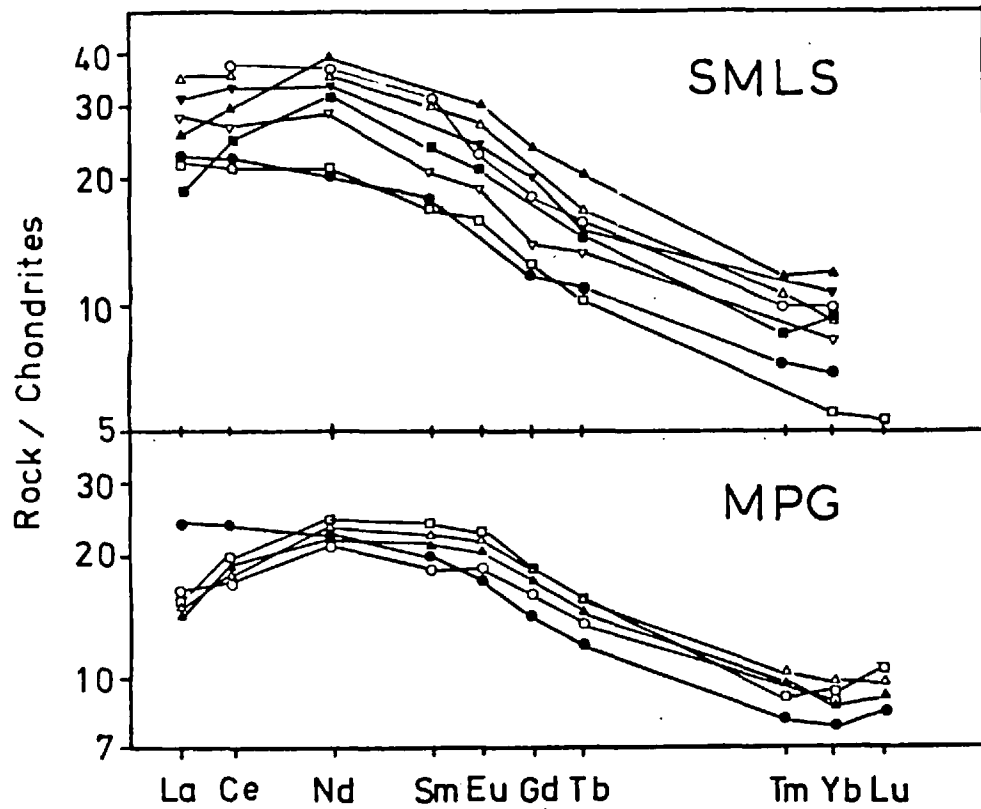


Figure 6-9 Chondrite-normalised REE patterns for representative SMLS and MPG basalts. REE profiles for Mauna Loa and Kilauea summit lavas shown for comparison from Leeman et al. (1977)

magmas, since the bulk distribution coefficients for elements such as La and Ce between major upper mantle minerals and basalt melt are so similar. Instead, the mantle sources of these basalts must have shown similar variations in the relative abundances of the REE.

The approximately constant slopes on figure 6-9 of the middle rare earths for both basalt groups allows a straight line projection to be made through the data to a point, designated Ce*, which is the value of Ce_N that would be anticipated, if the patterns showed no downwards curvature at their LREE ends. Ce*/Ce_N, is therefore an index of the depletion in the LREE relative to the MREE. Values of this ratio were calculated for all the Skye and Mull basalts REE patterns where Sm, Gd and Tb fit well to a straight line. Eu was not used as some of the basalts show small positive Eu anomalies (Thompson et al. 1979). Figure 6-10 is a plot of Ce*/Ce_N versus other ratios of more- to less-incompatible elements. These parameters show moderately good positive correlations indicating that the incompatible elements were behaving coherently in all these magmas. MS 209, the Arran crinanite sample cannot be compared directly with the Skye and Mull basalts on figure 6-7 because of its lower MgO content. In table 6-1 selected incompatible element concentrations in MS 209 are compared with ne-normative Skye and Mull hawaiites with similar F/F+M ratios. Ta, Nb and TiO₂ were excluded from the comparison as these samples contain titanomagnetite micro-phenocrysts and hence, these three elements cannot therefore be considered to have been behaving incompatibly in these particular magmas. (Thompson et al. 1979). It is apparent from Table 6-1 that MS 209 is depleted in all these elements relative to the Skye and Mull hawaiites, and hence, strongly depleted relative to world-wide nepheline hawaiites.

Table 6-1 Comparison of incompatible element concentrations in Skye/Mull/Arran hawaiites.

SK 907 is from Thompson et al.(1979).

	P ₂ O ₅	K ₂ O	Rb	Ce	Sr	Nd	Zr	Hf	Y	Yb
Skye 907	0.45	0.70	6	50.35	724	38.94	279	7.82	45	3.41
Mull M 7	0.30	0.27	3	30.57	560	29.69	230	6.07	35	2.37
Arran MS209	0.26	0.36	6	21.57	416	12.59	175	4.39	31	2.21

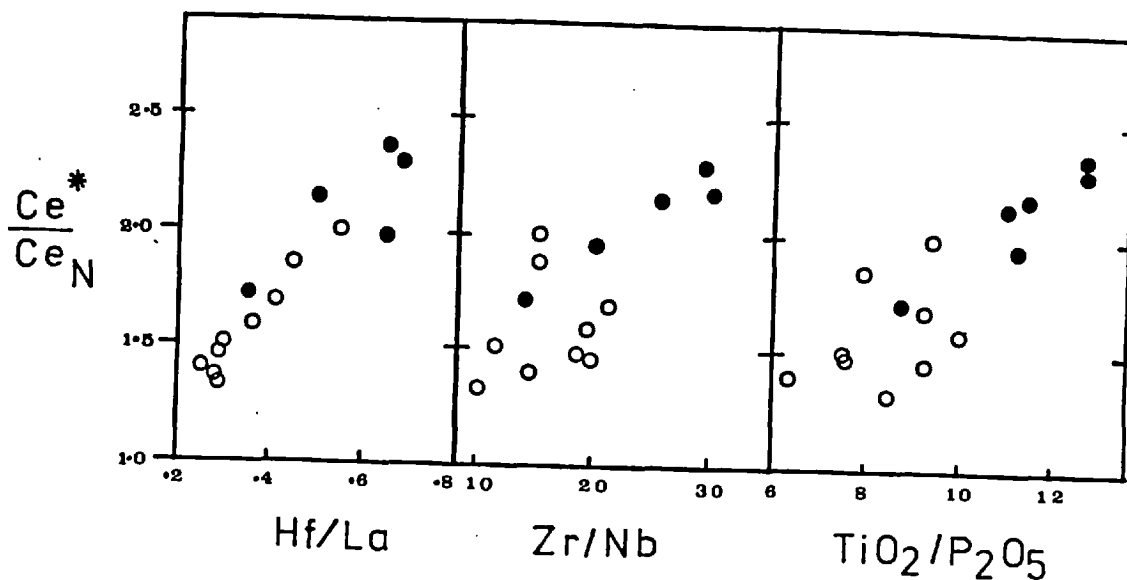


Figure 6-10.

Ce^*/Ce_N versus Hf/La, Zr/Nb and TiO_2/P_2O_5 for SMLS(o) and MPG(o) basalts.

To summarise, the incompatible element variations are interpreted as demonstrating heterogeneity in the Palaeocene upper mantle beneath Skye, Mull and Arran on two different scales:-

1. local heterogeneity beneath both Mull and Skye, on the scale of the mantle volumes involved in the production of individual magma batches
2. lateral heterogeneity on a larger scale between these igneous centres. Similar lateral heterogeneity also occurs in Hawaii where the volcano spacings are similar to the distances between the British Tertiary igneous centres (fig. 6-9).

The differences in incompatible element abundances between the SMLS and MPG are of the same type as those encountered between other members of the world-wide spectrum of basic rocks (figure 6-7). Hence, although it is not possible to prove that this variability was not caused by some obscure mantle metasomatic event, the fluid phase involved would have possessed relative abundances of the incompatible elements typical of basic magmas. This suggests that the upper mantle beneath these centres achieved its pre-Palaeocene incompatible element depletion by the extraction of a melt phase(s).

3. Provenance and pre-Palaeocene chemical history of the upper mantle beneath the British Tertiary Igneous Province.

The three most plausible ways in which the volume of upper mantle which gave rise to the Palaeocene basaltic magmatism could have gained its distinctive chemistry are discussed below.

Asthenosphere with the requisite geochemical characteristics which was previously decoupled from the sub-Scotland lithosphere, may have penetrated diapirically upwards in the Palaeocene, in response to tension associated with the opening of the North Atlantic. This leads to the somewhat defeatist conclusion that the incompatible-element depletion of this mantle volume took place at some unknown place and time by means of an unspecified process. Further, the increasing severity of this depletion with increasing distance from the initial rift position (i.e. from Skye to Mull to Arran) is the opposite relationship to that which would be predicted from published reconstructions of tectonomagmatic events in the North Atlantic (e.g. C. Brooks 1973).

Mantle accreted on to the sub-Moho lithosphere during the formation of the Archaean Lewisian complex may have been thermally reactivated during the Palaeocene. Again, the trace-element composition of this mantle volume would thus be residual from unspecified magmatic and/or metasomatic processes which took place up to 3000Ma. ago (Beckinsale et al. 1978). Moorbath and Thompson (1979) have shown that this model is not substantiated by the Nd- and Sr-isotope characteristics of the Hebridean Tertiary basalts. The complex and active Caledonian and post-Caledonian tectonomagmatic history of this region, discussed below, is difficult to reconcile with the concept of an inert Archaean lithosphere persisting beneath western Scotland until the Palaeocene.

A third possibility is that the volume of upper mantle which produced the Palaeocene magmas may have become coupled to the sub-Scotland lithosphere during the Archaean-Cenozoic time interval, and acquired its distinctive trace-element characteristics through extraction

of a melt(s) rich in the incompatible elements. The products of the following episodes of post-Lewisian pre-Tertiary magmatism are preserved in the geological record of this area : Moine (Ross of Mull), Dalradian (SW Highlands), Arenig (Arran and Southern Uplands), Devonian (widespread including Ross and Loch Don in Mull), Carboniferous (mainly in the Midland Valley but also dyke emplacement throughout the SW Highlands). Finally, Permian basaltic and lamprophyric dykes are associated with numerous lavas and plugs of this age in SW Scotland, extending to within 30kms of Arran. Similar dykes are quite abundant on the islands and Mainland around Mull whilst occurring more sparsely on and around Skye (Richey 1939 fig.5, Speight and Mitchell 1979).

A consideration of the Tertiary igneous centres in western Scotland and their relationship to the preceding tectonics and metamorphism of the Caledonian orogeny, is useful in evaluating the pre-Tertiary history of the upper mantle in this region. Skye and Rhum fall just on the foreland of the Caledonian mobile belt, whilst Ardnamurchan, Mull and Arran are just within it. Mull and Arran have areas of greenschist-facies Dalradian schists. Greenschist- and amphibolite-facies Moines outcrop on Ardnamurchan and highly metamorphosed Moines occur in western Mull. The suture line of the Caledonian Iapetus ocean may be the Highland Boundary Fault. (Lambert and Mackerrow 1976). This is straddled by the Arran igneous centre thus setting a maximum Caledonian age-limit to the sub-Arran upper mantle. Yet, the Arran crininite sample, MS 209, has similar incompatible-element abundances to the SMLS and MPG. If the suture line runs beneath the Solway Firth (Phillips et al. 1976), this is only 130kms south east of Arran and 300 kms from Skye. Even in this case the sites of subsequent western Scotland Tertiary igneous activity were close to the Caledonian lithospheric plate margin, when seen on the structural scale of present-day plate boundaries.

Subduction is commonly postulated to have occurred along a north-westerly inclined zone during the closure of the Iapetus ocean (e.g.

Phillips et al. 1976). The slab must therefore, have passed beneath at least part of western Scotland. Toksoz and Hsui (1978) have given detailed numerical modelling of how a subducting slab of oceanic lithosphere induces convection in the asthenospheric upper-mantle wedge above the subduction zone. This convecting upper mantle may in turn erode and replace the overlying lithosphere so that a back-arc basin forms. In other cases, such as the Cenozoic western USA (Scholz et al. 1971, Thompson 1977) a combination of flow induced tension and conductive heating of the stretched lithosphere leads to the formation of a magmatically active, ensialic, extensional province.

The upper Palaeozoic rift valley in the Midland valley of Scotland is a clear demonstration of post-Caledonian lithospheric extension. The abrupt change from Devonian tholeiite-rhyolite series to lower Carboniferous alkalic magmatism in Scotland resembles the Tertiary shift from calc-alkaline to alkaline magmatism in the western USA, (Christiansen and Lipman 1972). The relatively sparse occurrence of the Permian basalt-lamprophyre suite in western Scotland, indicates that the upper Palaeozoic tectomagnetic event diminished during this period, and was followed by quiescence during the Mesozoic. It therefore seems reasonable to investigate the chemistry of the Permian magmatism, the last before the Palaeocene in western Scotland.

Permian-Tertiary basic magmatism in western Scotland.

The Permian dyke swarms that pass through western Scotland show two main trends (Richey 1939). A west north west trending swarm runs through the area surrounding Mull and Ardnamurchan. In the region of Morvern and Lismore Island, immediately adjacent to the Great Glen fault, the crustal extension associated with it amounts to 3% (Speight and Mitchell 1979). A much less dense swarm trends east north east through the northern Highlands, Skye and Arisaig. Radiometric dates for members of these swarms, range from 288 to 235 Ma. (Speight and Mitchell 1979). Few chemical analyses of these dykes have been published and in particular little is known about their incompatible-trace element chemistry. A representative member of the basalt-

lamprophyre swarm which passes through Skye was therefore analysed. The results are given in Appendix I-E, sample MS 144.

This metre-wide dyke is emplaced in Lewisian gneiss on the roadside cliff of the A 871 at Dornie, opposite Eilean Donan castle, beside Loch Duich, about 8 kms east of Skye (Grid ref. NG 884-257). In thin section, it closely resembles the camptonites from Lismore and Morvern, described by Bailey et al. (1924), and those at the eastern end of the Arisaig-Loch Duich swarm, south of Loch Monar, studied by Ramsey (1955). The major element chemistry of MS 144 is very similar to that of the Loch Monar dykes (op.cit., Table 1). The abundances of the rare earth and other incompatible elements are similar to those of world-wide nephelinites (fig.6-7, Kay and Gast, 1973). D.P.Matthey (pers.comm. 1978) has found camptonite-suite dykes in Arisaig and the Sleat Peninsula, Skye with similar incompatible element abundances. It is apparent from figure 6-7 that MS 144 is enriched in the incompatible elements in approximately the same order as the SMLS and MPG are depleted, relative to the alkali olivine basalts.

The abundances of Th, Ta and Nb in the Eilean Donan Castle dyke, MS 144, suggest that the Permian and Palaeocene basic magmas of western Scotland belong to the same geochemical cycle. Inspection of figure 6-7 shows that the SMLS are depleted in these elements by a factor of two or three relative to the other incompatible elements. This results in a sharp increase in the slopes of many of the patterns of the non-Scottish rocks on the left hand side of the diagram, resulting in an apparent enrichment of these samples in Th, Ta and Nb, relative to La, Ce and Rb. The E.Iceland and FAMOUS basalts show this particularly clearly, as they are enriched in Th, Ta and Nb relative to the SMLS basalts, and depleted in all the other incompatible-elements. This can be quantified by considering the ratio La/Ta. Bougault et al. (1979) have shown that this ratio is close to 9 in basalts produced during the last few Ma. along the entire segment of the Mid Atlantic Ridge from Iceland to 36°N. This ratio ranges from 14-43 in the SMLS averaging 31. MS 144, shows a similar impoverishment in Th, Ta and Nb as the SMLS basalts. Compared to other world-wide occurrences of strongly alkalic basic rocks with similar MgO and LREE

contents, this dyke has only about half its anticipated Th, Ta and Nb (Kay and Gast 1973, Kesson 1973). The bulk distribution coefficients of the element groups Th, Ta, Nb and La, Ce and Rb between major upper-mantle mineral phases and basaltic melt are so low (≤ 0.01) (Bougault et al. 1979) that the twofold difference in the relative abundances of these groups in basic rocks from western Scotland must reflect a pre-existing feature of the chemical composition of the underlying mantle. Accordingly, this upper-mantle relative depletion in Th, Ta and Nb appears to be a pre-Permian feature of the western Scotland magmatic province.

Kay and Gast (1973) modelled the production of REE patterns very similar to that of MS 144, by approximately 1% fusion of a garnet lherzolite mantle with 4 times chondrite abundances and chondritic relative abundances of the REE, with garnet and clinopyroxene entering the melt in sub-equal proportions. The residuum was strongly depleted in the LREE. Langmuir et al. (1977) showed that the first and second melt fractions extracted from a mantle with chondritic relative abundances of the REE, had strongly LREE enriched and LREE depleted sigmoidal shaped patterns, respectively (op.cit. fig.6). Pure incremental fusion cannot produce the observed absolute abundances of these elements in the Palaeocene lavas as most of the incompatible elements would be concentrated in the first melt fraction. Langmuir et al. (1977) proposed a dynamic or continuous melting model to overcome this problem, in which a proportion of the melt was retained and contributed to the next melting episode. A similar process was proposed by Thompson et al. (1979) for the genesis of the SMLS and PMB magma types during the Palaeocene. The PMB and FBT magma types of Skye and the low alkali tholeiite lava, MS 133, and the tholeiitic basalt; M 58, from Mull also have La/Ti ratios that lie within the range 14 to 43 shown by the SMLS and MPG basalts. Hence, the process postulated for the generation of the Permian-Palaeocene basic magmas in western Scotland is similar in principle to the dynamic melting model of Langmuir et al. (1977) but with two important differences:-

1. Melting was not continuous. There were two main episodes of fusion at approximately 260 Ma. and 60 Ma. respectively.

2. During the first melting episode the ratio of extracted to retained melt was high and hence, the residual material, was strongly depleted in the more-incompatible elements. Variations in this ratio would give rise to both the local and lateral heterogeneity in the residuum indicated by the variable relative abundances of the incompatible elements in both the SMLS and MPG. Significantly, Permian basalt-lamprophyre dykes are more abundant in the region of Mull than Skye.

4. The relationship between the Tertiary igneous activity in Britain and the N. Atlantic.

The North Atlantic Ocean began to open between Greenland and the Rockall Plateau when a drastic reorientation of the rift axes occurred at about the time of magnetic anomaly 24 (Laughton 1971), 60 Ma. ago according to the time scale of Heirtzler et al. (1968). Prior to this, separation of Greenland (as part of the Laurasian plate) was taking place about a spreading axis in the Labrador sea. Around the time of anomaly 21, 53 Ma. ago on the Heirtzler et al. time scale, the rate of separation decreased and there is some evidence (from the Charlie fracture zone) suggesting a change in the relative motions of the Eurasian and North American plates (Pitman and Talwani 1972).

Recent studies of marine magnetic anomalies, and work on the Cretaceous-Tertiary boundary have led to several modifications of the magnetic reversal time scale of Heirtzler et al. (1968). LaBrecque et al. (1977) have published a new time-scale, incorporating most of these revisions, which is in reasonable agreement with the biostratigraphic ages obtained from D.S.D.P. drill holes. On this revised time scale anomaly 24 is assigned an age of approximately 56 Ma. and anomaly 21 an age of 50 Ma. Most tectonomagmatic reconstructions of events in the British Tertiary Igneous Province have been based on the apparent correlation of the major and minor phases of igneous activity in the BTIP at approximately 59 and 52 Ma., respectively, with the incidence and modification of sea-floor spreading during the early evolution of the North Atlantic (e.g. Macintyre et al. 1975, M. Brooks 1973). On the revised time-scale of LaBrecque et al. (1977) the episodes of magmatic

activity in the BTIP preceded each of the changes in spreading axes configuration.

The relationship between the BTIP centres and pre-existing lines of crustal weakness is well known: Skye, Rhum, Ardnamurchan and the Blackstones centre all lie close to the Casmusunary-Skerryvore fault; Mull lies on the Great Gaen Fault; Arran lies on or close to the Highland Boundary Fault and Lundy lies on the Sticklepath fault, a Hercynian structure reactivated in Tertiary times. Many of the structures show a close spatial relationship to areas of Permian or Permo-Carboniferous igneous activity (Richey 1939)

Gass et al. (1972) have suggested the BTIP was an abortive spreading axis, operative for a short time span. This interpretation is based partly upon the N-S alignment of many of the central igneous complexes (see fig. 1-1). Although significant tectonic activity occurred within the BTIP during the Cretaceous-Tertiary period, as George (1965) observed "the systematic form of a 'Hebridean rift' is not to be discerned from the tectonic pattern." When allowance is made for the offshore igneous centres and additional dyke-like bodies revealed by recent geophysical studies (Bullerwell 1972a,b) it is difficult to sustain a picture of a N-S alignment of the igneous centres. Instead, the dyke swarms reveal a pattern of extension fracturing in response to a regional tensile stress operating in a NE-SW direction; with the most extensive fracturing and magma emplacement occurring at points of long standing crustal weakness. Most of the basalt lavas have been extruded onto a newly uplifted and eroded land surface that testifies to a long period of late Cretaceous and early Tertiary emergence (George 1965). The approximately synchronous cessation of most of the magmatic activity within a period of 1-2 Ma. over the whole province would indicate that this stress was relieved by some major tectonic event - presumably the initiation of the split between Greenland and the Faroe rise.

The geochemical results discussed in this chapter indicate that the Palaeocene and Permian basic magmas were derived from the same mantle volumes. Accordingly, it is proposed that the BTIP basic magmas

originated from mantle diapirs emplaced as a result of the post-Caledonian lithospheric extension associated with the closure of the Iapetus Ocean, and reactivated as a result of the uplift and extension that preceded the opening of the North Atlantic.

REFERENCES

- Abbey, S., 1973. Studies in "Standard samples" of silicate rocks and minerals. Geol. Surv. Canada, paper, 73-76, 25 pp.
- Abbey, S., 1975. 1972 values for geochemical reference samples. Geochim. Cosmochim. Acta., 39, 535-537.
- Ade-Hall, J.M. and Lawley, E.A., 1970. An unsolved problem - opaque petrological differences between Tertiary basaltic dykes and lavas. Geol. J. (Special Issue), No. 2, 217-230.
- Ade-Hall, J.M., Dagley, P., Wilson, R.L., Evans, A., Smith, P., Skelhorn, R.R. and Sloan, T., 1972. A palaeomagnetic study of the Mull regional dyke swarm. Geophys. J.R. astr. Soc., 27, 517-547.
- Ade-Hall, J.M., Palmer, H.C. and Hubbard, T.P., 1971. The magnetic and opaque petrological response of basalts to regional hydrothermal alteration. Geophys. J.R. astr. Soc., 24, 137-174.
- Anderson, A.T. and Wright, T.L., 1972. Phenocrysts and glass inclusions and their bearing on oxidation and mixing of basaltic magmas, Kilauea volcano, Hawaii. Am. Mineralogist, 57, 188-216.
- Anderson, F.W. and Dunham, K.C., 1966. The geology of Northern Skye. Mem. Geol. Surv. Gt. Britain, 216 pp.
- Arnason, B. and Tomasson, J., 1970. Deuterium and chloride in geotherm-
al studies in Iceland. Geothermics, 2, Spec. issue. 1405.
- Arnorsson, S., Bjornsson, A., Gislason, G. and Gudmundsson G., 1975. Systematic exploration of the Krisuvik high-temperature area, Reykjanes Peninsula, Iceland. Proc. Second U.N. Symp. on the development and use of geothermal resources, San Francisco.
- Arth, J.G., 1976. Behaviour of trace elements during magmatic processes - a summary of theoretical models and their applications. J. Res. U.S. Geol. Surv., 4, 41-47.
- Aumento, F. and Loncarevic, B., 1969. The Mid-Atlantic Ridge near 45°N. III Bald Mountain. Can. J. Earth Sci., 6, 11-24.

- Bailey, E.B., Clough, T.C., Wright, W.B., Richey, J.E. and Wilson, G.V., 1924. Tertiary and post-Tertiary geology of Mull, Loch Aline and Oban. Mem. Geol. Surv. Scotland. 445 pp.
- Banwell, C.J., 1961. Geothermal drillholes - physical investigations. U.N.Conf. New Sources of Energy, Rome paper G 53.
- Beckinsale, R.D., 1974. Rb-Sr and K-Ar age determinations, and oxygen isotope data for the Glen Cannel granophyre, Isle of Mull, Argyllshire, Scotland. Earth Planet. Sci. Lett., 22, 267-274.
- Beckinsale, R.D. and Obradovick, J.D., 1973. Potassium-Argon ages for minerals from the Ross of Mull, Argyllshire, Scotland. Scott. J.Geol., 9, 147-156.
- Beckinsale, R.D., Pankhurst, R.J., Skelhorn, R.R. and Walsh, J.N., 1978. Geochemistry and petrogenesis of the early Tertiary lava pile of the Isle of Mull, Scotland. Contrib. Mineral. Petrol., 66, 415-427.
- Bell, J.D., 1976. The Tertiary intrusive complex on the Isle of Skye. Proc. Geol. Assoc., 87, 247-271.
- Borley, G.D., 1977. Problems of silicate analysis by X-ray fluorescence using a fusion technique and a single reference standard. Tech. Rept. No. XRF-1, Dept. of Geology, Imperial College, London, 7pp.
- Bott, M.H.P. and Tuson, J., 1973. Deep structure beneath the Tertiary volcanic regions of Skye, Mull and Ardnamurchan, north-west Scotland. Nature Phys. Sci., 242, 114-116.
- Bott., M.H.P. and Watts, A.B., 1971. Deep structure of the continental margins adjacent to the British Isles. Inst. Geol. Sci. Rept., no. 70/14.
- Bougault, M., Joron, J-L and Treuil, M. 1979. Proc. Second Ewing Symp. Am. Geophys. Union (in press)
- Bowen, N.L., 1928. The evolution of the Igneous rocks. Princeton University Press, 334 pp.
- Brooks, C.K., 1973. Rifting and doming in southern East Greenland.

- Nature Phys. Sci., 244, 23-25.
- Brooks, M., 1973. Some aspects of the Palaeogene evolution of Western Britain in the context of an underlying mantle hot spot. J.Geol. 81, 81-88.
- Brown, G.C. and Mussett, A.E., 1976. Evidence for two discrete centres in Skye. Nature, 261, 218-220.
- Brown, J.F., 1975. Potassium-argon evidence of a Permian age for the camptonite dykes : Orkney. Scott. J. Geol., 11, 259-262.
- Browne, P.R.L. and Ellis, A.J., 1970. The Ohaki-Broadlands hydrothermal area, New Zealand: Mineralogy and related geochemistry. Am.J.Sci. 269, 97-131.
- Bryan, W.B., 1972. Morphology of some quench crystals in submarine basalts. J. Geophys. Res., 77, 5812-5819.
- Bullerwell, W., 1972a. Geophysical studies relating to the Tertiary volcanic structure of the British Isles. Phil. Trans. R. Soc. Lond.A, 271, 209-215.
- Bullerwell, W., 1972b. Aeromagnetic map of Great Britain (scale 1: 625,000), sheet 1: Inst. Geol. Sci.
- Campbell, A.S. and Fyfe, W.S., 1965. Analcime-albite equilibria. Am.J.Sci. 263, 807-816.
- Cann, J.R., 1969. Spilites from the Carlsberg Ridge, Indian Ocean. J. Petrol., 10, 1-19.
- Carmichael, I.S.E., 1967. The iron-titanium oxides of salic volcanic rocks and their associated ferro-magnesian silicates. Contrib. Mineral. Petrol., 14, 36-64.
- Carmichael, I.S.E., Turner, F.J. and Verhoogen, J., 1974. Igneous petrology. McGraw-Hill, New York, 739 pp.
- Carter, S.R., Evensen, N.M., Hamilton, P.J. and O'Nions, R.K., 1978. Nd- and Sr-isotope evidence for crustal contamination of continental volcanics. Science, 202, 743-747.

- Christiansen, R.L. and Lipman, P.W., 1972. Phil. Trans. Roy. Soc. Lond. A, 271, 249-285.
- Condie, K.C. and Barager, W.R.A., 1974. Rare-earth element distributions in volcanic rocks from Archaean greenstone belts. Contrib. Mineral. Petrol., 45, 237-246.
- Coombs, D.S., Ellis, A.J., Fyfe, W.S. and Taylor, A.M., 1959. The zeolite-facies with comments on hydrothermal synthesis. Geochim. Cosmochim. Acta, 17, 53-107.
- Coombs, D.S. and Whetton, J.T., 1967. Composition of analcime from sedimentary and burial metamorphic rocks. Geol. Soc. Am. Bull., 78, 269-282.
- Coombs, D.S. and Wilkinson, J.F.G., 1969. Lineages and fractionation trends in undersaturated volcanic rocks from the East Otago Volcanic Province, New Zealand, and related rocks. J. Petrol., 10, 440-501.
- Dagley, P. and Mussett, A.E., 1978. Palaeomagnetism of the Fishnish dykes, Mull, Scotland. Geophys. J. R. astr. soc., 53, 553-558.
- Daly, R.A., 1933. Igneous Rocks and the depths of the Earth. McGraw-Hill. 598 pp.
- Drever, H.I. and Johnston, R., 1957. Crystal growth of forsteritic olivine in magmas and melts. Roy. Soc. Edinb. Trans., 63, 289-315.
- Duncan, R.A., Peterson, N and Hargreaves, R.B., 1972. Mantle plumes, movement of the European plate and polar wandering. Nature, 239, 82-86.
- Durant, G.P., 1978. The geochemistry of the Tertiary Islay and Jura dyke swarms. J. Geol. Soc. Lond., 135, 463.
- Elder, J.W., 1965. Physical processes in geothermal areas, in Terrestrial Heat Flow, Am. Geophys. Union Mon., 8, 211-239.
- Ellis, A.J., 1967. The chemistry of some explored geothermal systems. In Geochemistry of hydrothermal ore deposits. e.d. H.L. Barnes.

- New York: Holt, Rinehart and Winston. 465-514.
- Ellis, A.J., 1959. The solubility of calcite in carbon dioxide solutions. Am. J. Sci., 257, 354-365.
- Ellis, A.J., 1963. The solubility of calcite in sodium chloride solutions at high temperatures. Am. J. Sci., 261, 259-267.
- Esson, J., Dunham, A.C. and Thompson, R.N., 1975. Low-alkali, high-calcium, olivine tholeiite lavas from the Isle of Skye, Scotland. J. Petrol., 16, 488-497.
- Fawcett, J.J., 1961. Petrology of the flood basalts of the Isle of Mull, Argyllshire. Unpublished Ph.D. thesis Univ. of Manchester.
- Fawcett, J.J., 1965. Alteration products of olivine and pyroxene in basalt lavas from the Isle of Mull. Mineral. Mag., 35, 55-68.
- Fitch, F.J., Hooker, P.J., Miller, J.A. and Brerton, N.R., 1978. Glauconite dating of Palaeocene-Eocene rocks from East Kent and the time scale of Palaeogene volcanism in the North Atlantic region. J. Geol. Soc., 135, 499-512.
- Flanagan, F.J., 1973. 1972 values for international geochemical reference samples. Geochim. Cosmochim. Acta, 37, 1189-1200.
- Flanagan, F.J., 1976. 1972 compilation of data on U.S.G.S. standards. U.S. Geol. Surv. Prof. Paper, 840, 131-183.
- Flower, M.F.J., 1973. Trace element distribution in lavas from Anjouan and Grand Comore, western Indian Ocean. Chem. Geol., 12, 81-98.
- Floyd, P.A., 1977. Rare-earth element mobility and geochemical characterisation of spilitic rocks. Nature, 269, 134-137.
- Floyd, P.A. and Winchester, J.A., 1975. Magma type and tectonic setting discrimination using immobile elements. Earth Planet. Sci. Lett., 27, 211-218.
- Forester, R.W. and Taylor, H.P., 1976. ^{18}O -depleted igneous rocks from the Tertiary complex of the Isle of Mull, Scotland. Earth Planet. Sci. Lett., 32, 11-17.

- Forester, R.W. and Taylor, H.P., 1977. $^{18}\text{O}/^{16}\text{O}$, D/H and $^{13}\text{C}/^{12}\text{C}$ studies of the Tertiary igneous complex of Skye, Scotland. Am. J. Sci., 277, 136-177.
- Frey, F.A., Bryan, W.R. and Thompson, G., 1974. Atlantic ocean floor : geochemistry and petrology of basalts from legs 2 and 3 of the D.S.D.P. J. Geophys. Res., 79, 5507-5527.
- Gass, I.G. et al. 1972. Historical geology. A second level course geology. The Open University.
- George, T.N., 1965. The geological growth of Scotland. in Craig G.Y. The geology of Scotland : Oliver and Boyd Edinburgh, pp 1-48.
- Gibb, F.G.F. and Henderson, C.M.B., 1978. The petrology of the Dippin Head sill, Isle of Arran. Scott. J. Geol., 14, 1-27.
- Gordon, G.E., Randle, K., Coles, G.G., Corliss, J.B., Beeson, M.H. and Oxley, S.S., 1968. Instrumental activation analysis of standard rocks with high-resolution X-ray detectors. Geochim. Cosmochim. Acta, 32, 269-369.
- Graf, J.L., 1977. Rare earth elements as hydrothermal tracers during the formation of massive sulfide deposits in volcanic rocks. Econ. Geol., 72, 527-548.
- Gunn, B.M., 1971. Trace element partitioning during olivine fractionation of Hawaiian basalts. Chem. Geol., 8, 1-13.
- Gunn, B.M. and Roobol, M.J., 1976. Metasomatic alteration of the predominantly island arc igneous suite of the Limestone Caribbees (E.Caribbean). Geol. Rundsch., 65, 1078-1108.
- Gutmann, J.T., 1977. Textures and genesis of phenocrysts and megacrysts in basaltic lavas from the Pinacate volcanic field. Am. J. Sci., 277, 833-861.
- Halsall, T.J., 1978. The emplacement of the Tertiary dykes of the Kildonian shore, S. Arran. J.Geol.Soc. Lond., 135, 462.
- Harker, A., 1904. The Tertiary igneous rocks of Skye. Mem. Geol. Surv. Scotland.

- Hart, S.R., 1976. Deep Sea Drilling Project. Init. Rep., 34, 283-288.
- Hawkesworth, C.J., Norry, M.J., Roddick, J.C., Baker, P.E., Francis, P.W. and Thorpe, R.S., 1979. $^{143}\text{Nd}/^{144}\text{Nd}$, $^{87}\text{Sr}/^{86}\text{Sr}$ and incompatible element variations in calc-alkaline andesites and Plateau lavas from South America. Earth Planet. Sci. Lett., 42, 45-57.
- Heirzler, J.R., Dickson, G.O., Herron, E.M., Pitman, W.C. and Le Pichon, X., 1968. Marine magnetic anomalies, geomagnetic field reversals, and motions of the ocean floor and continents. J. Geophys. Res., 73, 2119-2136.
- Hellman, P.L. and Henderson, P., 1977. Are rare earths mobile during spilitisation? Nature, 267, 38-40.
- Hellman, P.L., Smith, R.E. and Henderson, P., 1977. Rare earth element investigation of the Cliefden Outcrop, N.S.W., Australia. Contrib. Mineral. Petrol., 65, 155-164.
- Herrmann, A.G., Potts, M.J. and Knake, D., 1974. Geochemistry of the rare earth elements in spilites from oceanic and continental crust. Contrib. Mineral. Petrol., 44, 1-16.
- Hughes, D.J. and Brown, G.C., 1972. Basalts from Madeira: A petrochemical contribution to the genesis of oceanic alkali rock series. Contrib. Mineral. Petrol., 37, 91-109.
- Humphris, S.E., 1976. The hydrothermal alteration of oceanic basalts by seawater. Unpublished Doctoral dissertation. Woods Hole Oceanographic Institute.
- Humphris, S.E. and Thompson, G., 1978a. Hydrothermal alteration of oceanic basalts by seawater. Geochim. Cosmochim. Acta, 42, 107-125.
- Humphris, S.E. and Thompson, G., 1978b. Trace element mobility during hydrothermal alteration of oceanic basalts. Geochim. Cosmochim. Acta, 42, 127-136.
- Humphris, S.E., Morrison, M.A. and Thompson, R.N., 1978. Influence of rock crystallisation history upon subsequent lanthanide mobility during hydrothermal alteration of basalts. Chem. Geol., 23, 125-137.

- Jolly, W.T. and Smith, R.E., 1972. Degradation and metamorphic differentiation of the Keweenaw tholeiitic lavas of northern Michigan, U.S.A. J. Petrol., 13, 273-309.
- Kay, R.W. and Gast, P.W., 1973. The rare earth content and origin of alkali rich basalts. J. Geol., 18, 653-682.
- Kennedy, W.Q., 1930. The parent magma of the British Tertiary Province. Geol. Surv. Gt. Britain, Summary of Progress II, 61-73.
- Kennedy, W.Q., 1933. Trends of differentiation in basaltic magmas. Am. J. Sci., 5th.ser., 25, 239-256.
- Kesson, S.E., 1972. The primary geochemistry of the Monaro alkaline volcanics, south eastern Australia - Evidence for upper mantle heterogeneity. Contrib. Mineral. Petrol., 42, 93-108.
- King, P., 1977. The secondary minerals of the Tertiary lavas of Northern and Central Skye - zeolite zonation patterns, their origin and formation. Unpublished Ph.D. Thesis, Univ. of Aberdeen.
- Kristmannsdottir, H., 1975. Hydrothermal alteration of basaltic rocks in Icelandic geothermal areas. Proc. second U.N. Symp. on the development and use of geothermal resources, San Francisco.
- LaBrecque, J.L., Kent, D.V. and Cande, S.C., 1977. Revised magnetic polarity time-scale for Late Cretaceous and Cenozoic time. Geology, 5, 330-335.
- Lamacraft, H., 1979. The geochemistry of the Tertiary dyke swarms of Mull, Islay and Jura. J. Geol. Soc. Lond., 136, 257-258.
- Lambert, R.St.J. and Holland, J.G., 1974. Yttrium geochemistry applied to petrogenesis utilizing calcium-yttrium relationships in minerals and rocks. Geochim. Cosmochim. Acta, 38, 1393-1414
- Lambert, R.St.J. and Mackerrow, W.S., 1976. Scott. J. Geol., 12, 271-292.
- Langmuir, C.H., Bender, J.F., Bence, A.E., Hanson, G.N. and Taylor, S.R., 1977. Petrogenesis of basalts from the FAMOUS area: Mid Atlantic Ridge. Earth Planet. Sci. Lett., 36, 133-156.
- Laughton, A.S., 1971. South Labrador Sea and the evolution of the North Atlantic. Nature, 232, 612-616.

- Lee, G.W. and Bailey, E.B., 1925. The pre-Tertiary geology of Mull, Loch Aline and Oban. Mem. Geol. Surv. Scotland.
- Leeman, W.P., Murali, A.V., Ma, M.-S and Schmitt, R.A., 1977. Mineral constitution of mantle source regions for Hawaiian basalts -- rare earth element evidence for mantle heterogeneity. in: Magma Genesis. Oregon Dept. Geol. Mineral. Ind. Bull., 96. pp 169-174.
- Leeman, W.P. and Vitaliano, C.J., 1976. Petrology of McKinney basalt, Snake River Plain, Idaho. Geol. Soc. Am. Bull., 87, 1777-1792.
- Liou, J.G., 1970. Synthesis and stability of wairakite, $\text{CaAl}_2\text{Si}_4\text{O}_{12} \cdot 2\text{H}_2\text{O}$. Contrib. Mineral. Petrol., 27, 259-282.
- Liou, J.G., 1971. Analcime equilibria. Lithos, 389-402.
- Liou, J.G., 1974. Mineralogy and chemistry of glassy basalts, Coastal range ophiolites, Taiwan. Geol. Soc. Am. Bull., 85, 1-10.
- Macintyre, R.M., McMenamin, T. and Preston, J., 1975. K-Ar results from western Ireland and their bearing on the timing and siting of Thulean magmatism. Scott. J. Geol., 11, 227-249.
- Mackay, A.L. and Taylor, H.F.W., 1953. Gyrolite. Mineral. Mag., 30, 80-91.
- Masuda, S. and Nagasawa, S., 1975. Rocks with negative cerium anomalies dredged from the Shatsky Rise. Geochem. J., 9, 227-233.
- Mattey, D.P., Gibson, I.L., Marriner, G.F. and Thompson, R.N., 1977. The diagnostic geochemistry, relative abundance and spatial distribution of high-calcium, low-alkali, olivine tholeiite dykes in the Lower Tertiary regional swarm of the Isle of Skye, N.W.Scotland. Mineral. Mag., 41, 273-285.
- Maxwell, J.A., 1968. Rock and Mineral Analyses. Wiley, Interscience. 584 pp.
- McQuillin, R., Bacon, M. and Binns, P.E., 1975. The Blackstones Tertiary igneous complex. Scott. J. Geol., 11, 179-192.
- Melson, W., Thompson, G. and Van Andel, T.H., 1968. Volcanism and metamorphism in the Mid-Atlantic Ridge, 22°N latitude. J. Geophys. Res., 75, 5925-5941.

- Mitchell, J.G., Jones, E.J.W. and Jones, G.T., 1976. The composition and age of basalts dredged from the Blackstones igneous centre, western Scotland. Geol. Mag., 113, 525-533.
- Moorbath S. and Thompson, R.N., 1979. Strontium isotope geochemistry and petrogenesis of the Early Tertiary lava pile of the Isle of Skye, Scotland, and other basic rocks of the British Tertiary Province. J. Petrol., 20, in press.
- Moorbath, S. and Welke, H., 1968. Lead isotope studies on igneous rocks from Skye, northwest Scotland. Earth Planet. Sci. Lett., 5, 217-230.
- Moore, J.G. and Evans, B.W., 1967. The role of olivine in the crystallisation of the Prehistoric Makaopuhi Lava lake, Hawaii. Contrib. Mineral. Petrol., 15, 202-223.
- Morrison, M.A., Thompson, R.N., Gibson, I.L. and Marriner, G.F., 1979. Lateral chemical heterogeneity in the Palaeocene upper mantle beneath the Scottish Hebrides. Phil. Trans. R. Soc. Lond., (in press)
- Muffler, L.J.P. and White, D.E., 1969. Active metamorphism of upper Cenozoic sediments in the Salton Sea geothermal field and the Salton Trough, south eastern California. Geol. Soc. Am. Bull., 80, 157-181.
- Murata, K.J. and Richter, D.H., 1966. Chemistry of the lavas of the 1959-60 eruption of Kilauea volcano, Hawaii. U.S. Geol. Surv. Prof. Paper., 537-A. 26 pp.
- Naboko, S.I. and PiiP, B.I., 1961, Recent metamorphism of volcanic rocks in the region of the Pauzhetsk Hot Springs (Kamchatka). Akad. Nauk. SSSR, Trudy Lab. Vulkanol., 19, 99-114.
- Norrish, K and Hutton, J.T., 1969. An accurate X-ray spectrographic method for the analysis of a wide range of geological samples. Geochim. Cosmochim. Acta, 33, 431-453.
- O'Neil, J.R., and Taylor, H.P., Jr., 1967. The oxygen isotope and cation exchange chemistry of feldspars. Am. Mineral., 52, 1414-1437.

- O'Nions, R.K., Carter, S.R., Cohen, R.S., Evenson, N.M. and Hamilton, P.J., 1978. Pb, Nd and Sr isotopes in oceanic ferromagnesian deposits and ocean floor basalts. Nature, 273, 435-437.
- O'Nions, R.K. and Pankhurst, R.J., 1976. Sr isotope and rare earth element geochemistry of D.S.D.P. leg 37 basalts. Earth Planet Sci. Lett., 31, 255-261.
- O'Nions, R.K., Pankhurst, R.J. and Gronvold, K., 1976. Nature and development of basalt magma sources beneath Iceland and the Reykjanes Ridge. J. Petrol., 17, 315-338.
- Palmason, G and Saemundsson, K., 1974. Iceland in relation to the Mid-Atlantic ridge. Ann. Rev. Earth Planet. Sci., 2, 25-50.
- Pankhurst, R.J., Walsh, J.N., Beckinsale, R.D. and Skelhorn, R.R., 1978. Isotopic and other geochemical evidence for the origin of the Loch Uisg granophyre, Isle of Mull, Scotland. Earth Planet. Sci. Lett., 38, 355-363.
- Parker, R.J., 1977. Factors affecting the quality of major element rock analysis by X-ray fluorescence combined with flux-fusion sample preparation. Tech. Rept. No, XRF - 2B, Dept of Geology, Imperial College, London. 35 pp.
- Parker, R.J., 1978. An iterative method for determining background intensities used in XRF calibration lines for flux-fusion silicate rock analysis. X-ray Spectrom., 7, 38-43.
- Parker, R.J., 1979. A computer-based system of XRF analysis and its application to a geochemical study of Vulcini volcano, central Italy. Unpublished Ph.D. Thesis., Univ. of London.
- Parker, R.J. and Willis, J.P., 1977. Programs SORT, REORD and MW for major element XRF data processing. Computers and Geosciences 3, 115-172.
- Pearce, J.A. and Cann, J.R., 1971. Ophiolite origin investigated by discriminant analysis using Ti, Zr and Y. Earth Planet. Sci. Lett., 12, 339-349.

- Pearce, J.A. and Cann, J.R., 1973. Tectonic setting of basic volcanic rocks determined using trace element analyses. Earth Planet. Lett. Sci., 19, 290-300.
- Pearce, T.H., Gormann, B.E. and Birkett, T.C., 1975. The $TiO_2-K_2O-P_2O_5$ diagram: A method of discriminating between oceanic and non-oceanic basalts. Earth Planet Sci. Lett., 24, 419-
- Pearce, T.H., Gormann, B.E. and Birkett, T.C., 1977. The relationship between major element chemistry and tectonic environment of basic and intermediate volcanic rocks. Earth Planet. Sci. Lett., 36, 121-132.
- Phillips, W.E.A., Skillman, C.J. and Murphy, T., 1976. A Caledonian plate-tectonic model. J. Geol. Soc. Lond., 132, 579-609.
- Pitman, W.C. and Talwani, M., 1972. Sea-floor spreading in the North Atlantic. Bull. Geol. Soc. Am., 83, 619-646.
- Price, R.C. and Chappell, B.W., 1975. Fractional crystallisation and the petrology of the Dunedin volcano. Contrib. Mineral Petrol., 53, 157-182.
- Puchelt, H and Emmermann, R., 1977. REE characteristics of ocean floor basalts from the Mid-Atlantic Ridge 37°N (Leg 37 D.S.D.P.). Contrib. Mineral. Petrol., 62, 43-52.
- Ramsey, J.G., 1955. A camptonitic dyke suite at Monar, Ross-shire and Inverness-shire. Geol. Mag., 92, 297-309.
- Reed, S.J.B. and Ware, N.G., 1975. Quantitative electron microprobe analysis of silicates using energy - dispersive X-ray spectrometry. J. Petrol., 16, 499-519.
- Richey, J.E., 1939. The dykes of Scotland. Trans. Edinb. Geol. Soc., 13, 393-435.
- Richey, J.E., 1961. British Regional Geology. Scotland : The Tertiary Volcanic Districts. 3rd ed. by H.M. Geol. Surv. publ. 120 pp.
- Ridley, W.I., 1973. The petrology of volcanic rocks from the Small Isles of Inverness-shire. Rept. Inst. Geol. Sci., no.73/10 55 pp.

- Roaldset, E. and Rosenquist, I. Th., 1971. Unusual lanthanide distribution. Nature Phys. Sci., 231, 153-154.
- Roberts, D.G., 1970. Recent geophysical studies on the Rockall Plateau and adjacent areas. Prec. geol. Soc. Lond. 1662. 87-93.
- Robertson, A.H.F. and Fleet, A.J., 1976. The origin of rare earths in metalliferous sediments of the Troodos Massif, Cyprus. Earth Planet. Sci. Lett., 28, 385-394.
- Routti, J.T., 1969. Sampo, a fortran IV program for the computer analysis of gamma spectra from Ge (Li) detectors, and other spectra with peaks. Amer. Govt. Rept. 19452., Univ. of California, 31 pp.
- Saha, P., 1959. Geochemical and X-ray investigation of natural and synthetic analcites. Am. Mineral., 44, 300-313.
- Scholz, C.H., Baranzangi, M. and Sbar, M.L., 1971. Geol. Soc. Am. Bull., 82, 2979-2990.
- Schuiling, R.D. and Vink, B., 1967. Stability relations of some titanium minerals. Geochim. Cosmochim. Acta., 31, 2399-2411.
- Sederholm, J.J., 1929. The use of the term "deuteric". Econ. Geol., 24 869-871.
- Senderov, E.E., 1965. Features of the conditions of zeolite formation. Geochem. Int., 2, 1143-1155.
- Senderov, E.E., 1968. Experimental study of crystallisation of sodium zeolites under hydrothermal conditions. Geochem. Int., 5, 1-12.
- Sen Gupta, J.G., 1968. Determination of fluorine in silicate and phosphate rocks, micas and stony meteorites. Anal. Chim. Acta., 42 119-125.
- Shapiro, L. and Brannock, W.W. 1975. Rapid analysis of silicate, carbonate and phosphate rocks. U.S. Geol. Surv. Bull., 1401. 76 pp.
- Sigvaldason, G.E., 1962. Epidote and related minerals in two deep geothermal drill holes, Reykjavik and Hveragerdi, Iceland. U.S. Geol. Surv. Prof. Paper. 450-E, 77-79.

- Skelhorn, R.R., Henderson, P., Walsh, J.N. and Longland, P.J.N., 1979. The chilled margin of the Ben Buie layered gabbro, Isle of Mull., Scott. J. Geol., 15, 161-167.
- Skelhorn, R.R., 1969. The Tertiary igneous geology of the Isle of Mull. Geol. Assoc. Guide No.20. 35 pp.
- Smith, R.E., 1967. Segregation vesicles in basaltic lava. Am. J. Sci., 265, 696-713.
- Smith, R.E., 1968. Redistribution of major elements in the alteration of some basic lavas during burial metamorphism. J. Petrol., 9, 191-219.
- Smith, R.E. and Smith, S.E., 1976. Comments on the use of Ti, Zr, Y, Sr, K, P and Nb in classification of basaltic magmas. Earth Planet Sci. Lett., 32, 114-120.
- Speight, J.M. and Mitchell, J.G., 1979. The Permo-Carboniferous dyke swarm of northern Argyll and its bearing on dextral displacement of the Great Glen Fault. J. Geol. Soc. Lond., 136, 3-12.
- Spooner, E.T.C., Beckinsale, R.D., England, P.C. and Seniors, A., 1977. Hydration, ^{18}O enrichment and oxidation during ocean floor hydrothermal metamorphism of ophiolitic metabasic rocks from E. Liguria, Italy. Geochim. Cosmochim. Acta, 41, 857-871.
- Spooner, E.T.C., Chapman, H.J. and Smewing, J.D., 1977. Strontium isotope contamination and oxidation during ocean floor hydrothermal metamorphism of the ophiolitic rocks of the Troodos Massif, Cyprus. Geochim. Cosmochim. Acta, 41, 873-890.
- Spooner, E.T.C. and Fyfe, W.S., 1973. Sub-sea floor metamorphism, heat and mass transfer. Contrib. Mineral. Petrol., 42, 287-307.
- Statham, P.J., 1976. A comparative study of techniques for quantitative analysis of the X-ray spectra obtained with a Si(Li) detector. X-ray Spectrom., 5, 16-28.
- Steiner, A., 1967. Clay minerals in hydrothermally altered rocks at Wairakei, New Zealand. Clays Clay Mins., 16, 193-213.
- Staudigel, H., 1979. Init. Rep. Deep Sea Drilling Project. 53, (in press).

- Sukheswala, R.N., 1974. Gradation of tholeiitic Deccan basalt into spilite, Bombay, India in Spilites and Spilitic Rocks. ed. G.C. Amstutz. Springer-Verlag. 482 pp.
- Tanaka, T., 1975. Geological significance of rare earth elements in Japanese geosynclinal basalts. Contrib. Mineral. Petrol., 52, 233-246.
- Taylor, H.P., Jr., 1977. Water/rock interactions and the origin of H₂O in granitic batholiths. J. Geol. Soc., 133, 509-558.
- Taylor, H.P., Jr., 1974. The application of oxygen and hydrogen isotope studies to problems of hydrothermal alteration and ore-deposition. Econ. Geol., 69, 843-883.
- Taylor, H.P., Jr. and Epstein, S., 1962. Relationship between ¹⁸O/¹⁶O ratios in coexisting minerals of igneous and metamorphic rocks. Geol. Soc. Am. Bull., 73, 461-86.
- Taylor, H.P., Jr. and Epstein, S., 1968. Hydrogen-isotope evidence for influx of meteoric groundwaters into shallow igneous intrusions. Geol. Soc. Am. Spec. Paper, 121, 294.
- Taylor, H.P., Jr. and Forester, R.W., 1971. Low-O¹⁸ igneous rocks from the intrusive complexes of Skye, Mull and Ardnamurchan, western Scotland. J. Petrol., 12, 465-497.
- Thompson, A.B., 1971a, Analcite-albite equilibria at low temperatures. Am. J. Sci., 271, 79-92.
- Thompson, A.B., 1971b, PCO₂ in low-grade metamorphism; zeolite, carbonate, clay mineral, prehnite relations in the system CaO-Al₂O₃-SiO₂-CO₂-H₂O. Contrib. Mineral. Petrol., 33, 145-161.
- Thompson, R.N., 1973. One-atmosphere melting behaviour and nomenclature of terrestrial lavas. Contrib. Mineral. Petrol., 45, 317-341.
- Thompson, R.N., 1974. Primary basalts and magma genesis. I. Skye, north-west Scotland. Contrib. Mineral. Petrol., 45, 317-341.
- Thompson, R.N., 1975. The 1-atmosphere liquidus fugacities of some tholeiitic, intermediate, alkalic and ultra-alkalic lavas. Am. J. Sci., 275, 1049-1072.

- Thompson, R.N., 1977. Columbia/Snake River-Yellowstone magmatism in the context of western U.S.A. Cenozoic geodynamics. Tectonophysics, 39, 621-636.
- Thompson, R.N., 1979., The British Tertiary Igneous Province: geochemistry and magma genesis. in: Igneous rocks of the British Isles, ed. D.S.Sutherland. John Wiley and sons Ltd. (in press).
- Thompson, R.N., Esson, J. and Dunham, A.C., 1972. Major element chemical variation in the Eocene lavas of the Isle of Skye, Scotland. J.Petrol., 13, 219-253.
- Thompson, R.N., Gibson, I.L., Marriner, G.F., Matthey, D.P. and Morrison, M.A., 1979. Trace-element evidence of multistage mantle fusion and polybaric fractional crystallisation in the Palaeocene lavas of Skye, N.W.Scotland. J. Petrol., 20, in press.
- Thorsteinsson, T. and Eliasson, J., 1970. Geohydrology of the Laugarnes hydrothermal system in Reykjavik. Geothermics, 2, spec.issue, 1191.
- Tilley, C.E., 1950. Some aspects of magmatic evolution. Q.J.Geol. Soc., 106, 37-61.
- Tilley, C.E. and Muir, I.D., 1962. The Hebridean Plateau magma type Trans. Edinb. Geol. Soc., 19, 208-215.
- Tilley, C.E. and Thompson, R.N., 1970. Melting and crystallisation relations of the Snake River basalts of southern Idaho, U.S.A. Earth Planet. Sci. Lett., 8, 79-92.
- Toksoz, M.N. and Hsui, A.T., 1978. Numerical studies of back-arc convection and the formation of marginal basins. Tectonophysics, 50, 177-196.
- Tomasson, J., Fridliefsson, I.B. and Stefansson, V., 1975. A hydrological model for the flow of thermal water in SW-Iceland with special reference to the Reykir and Reykjavik Thermal areas. Proc. second U.N. Symp. on the deveolopment and use of geothermal resources. San Francisco.

- Tomasson, J. and Kristmannsdottir, K., 1972. High temperature alteration minerals and thermal brines, Reykjanes, Iceland. Contrib. Mineral Petrol., 36, 123-134.
- Tyrell, G.W., 1937. Flood basalts and fissure eruptions. Volc. Bull., ser.2, 1, 89-111.
- Upton, B.G.J. and Wadsworth, W.J., 1971. Rhyodacite glass in Reunion basalt. Mineral. Mag., 38, 152-159.
- Vallance, T.G., 1974. Spilitic degradation of a tholeiitic basalt. J. Petrol., 13, 219-253.
- Wager, L.R., 1956. A chemical definition of fractionation stages as a basis for comparison of Hawaiian, Hebridean and other basic lavas. Geochim. Cosmochim. Acta, 9, 217-248.
- Walker, G.P.L., 1960. Zeolite zones and dyke distribution in relation to the structure of the basalts of eastern Iceland. J. Geol., 68, 515-528.
- Walker, G.P.L., 1970. The distribution of amygdale minerals in Mull and Morvern (western Scotland). West. Commem. Vol., pp 181-194.
- Walker, G.P.L., 1974. The structure of eastern Iceland. in: Geodynamics of Iceland and the North Atlantic area. ed. L.Kristjansson. D.Reidel, Dordrecht. pp. 177-188.
- Whipple, E.R., 1974. A study of Watson's determination of ferrous iron in silicates. Chem. Geol., 14, 223-238.
- Winkler, H.G.F., 1965. Petrogenesis of metamorphic rocks. (2nd ed.) Springer-Verlag, New York. 237 pp.
- Wilson, R.L., 1970. Palaeomagnetic stratigraphy of Tertiary lavas from Northern Ireland, Geophys. J. Roy. astr.Soc., 20, 1-9.
- Wood, D.A., 1977. The petrology and geochemistry of Tertiary lavas from Eastern Iceland. Unpubl. Ph.D. Thesis, Univ. of London.
- Wood, D.A., 1978. Major and trace element variations in the Tertiary lavas of Iceland with respect to the Iceland geochemical anomaly. J. Petrol., 19, 393-436.

- Wood, D.A., Gibson, I.L. and Thompson, R.N., 1976. Elemental mobility during zeolite-facies metamorphism of the Tertiary basalts of eastern Iceland. Contrib. Mineral. Petrol., 55, 241-254.
- Zen, E., 1961. The zeolite-facies : An interpretation. Am. J. Sci., 259, 401-409.

APPENDIX I - DATA

I - A SAMPLE LOCALITIES

<u>Samples</u>	<u>Locality</u>
LA 1 - 5	Small quarry immediately to west of pier, Loch Aline, Morvern (NM 674 443). Margins of lava flow not exposed. Sample heights above quarry floor : LA 1 0.0m; LA 3 3.4m; LA 5 4.6m; LA 2 5.5m; LA 4 6.7m. Mesolite zone.
LA 7 - 11	Cutting on west side A 884, 3km north of Loch Aline, Morvern. (NM 692 474). Flow margins not exposed but soil reddens above and below exposure and this is accompanied by step-like changes in the topography. Sample heights above base of cutting : LA 7 0.0m; LA 8 1.33m; LA 9 2.18m; LA 10 3.68m; LA 11 6.28m. Mesolite/laumontite zones.
LA 12	Roadside cutting on west side of A 884, 2km north of
LA 13 - 15	Loch Aline, Morvern (NM 683 466). Two lava flows and
LA 16 - 18	intervening red bole exposed. Samples LA 13, LA 14 and
LA 19	LA 15 collected at heights of 1.0m, 3.35m and 4.85m above junction respectively. LA 12 - sample from red bole which contains debris from both flows and varies from 1.0 to 1.5m in thickness. Base of underlying lava flow exposed in slope above north bank of Allt Achadh Forsa, 23m below red bole. Sample heights below bole : LA 16 2m; LA 17 7m; LA 18 22m. LA 19 - amygdaloidal sample from upper two metres of LA 16 - 18. Mesolite/laumontite zones.
LA 20	Cutting on west side A 884, 1km north of Loch Aline, (NM 680 458). Mesolite zone.
M 1	Massive lava flow on which remains of Aros castle stand, (NM 563 450). Laumontite zone, close to margin prehnite zone.

- M 5 - 8 Lava flow and underlying red bole exposed in small quarry on north side of Tobermory-Glengorm castle road (NM 462 563). Sample heights above bole : M 5 1.05m; M 6 2.25m; M 7 3.33m; M 8 4.16m, Laumontite zone.
- M 11 - 12 Small quarry on north side B 8073, 1.7km west of Tobermory (NM 487 545). M 11, M 12 collected 3.2 and 4.5m above red bole which is partially exposed in floor of quarry. Mesolite/Laumontite zones.
- M 51 - 55, M 56 Quarry on south side of A 849, 1.6km east of Bunnessan, (NM 395 223). Floor of quarry lies in red bole. Sample heights above red bole : M 51 0.9m; M 52 1.82m; M 53 2.55m; M 54 3.6m; M 55 4.8m, M 56 - sample from bottom metre containing part of pipe-vesicle. Mesolite zone.
- M 13 - 22 Large quarry on south side of A 849, 2.5km east of
M 26 - 28 Salen and almost opposite Pennygown Chapel (NM 607 431).
M 24, M 64 Epidote zone. Two lava flows separated by thin air-fall
Drill core tuff exposed in quarry walls. Upper flow sampled at following heights above tuff layer : M 26 0.73m; M 27 1.46m; M 28 2.00m. Lower flow sampled at following heights below tuff layer : M 13 0.1m; M 14 0.75m; M 15 1.8m; M 16 2.2m; M 17 3.1m; M 18 4.05m; M 19 5.25m; M 20 6.4m; M 21 6.9m; M 22 7.63m. See figure 1-9 for relationship between lava flows and the two vein samples M 24, M 64, and Appendix I-B for log of drill core.
- M 29 - 32 Toll Doire quarry, 1.2km south of Salen on south side B 8035 and immediately to west of Allt na Searmoin, (NM 571 418). Epidote zone. Toll Doire granophyre ring dyke exposed in south east corner of quarry, central part of hydrothermally brecciated lava flow exposed in north west part. Sample heights above floor of quarry : M 29 0.0m; M 31 2.81m; M 32 3.61m.

- M 34 - 36
M 37 - 38
M 39
- Cutting on south side A 849, 1km west of Fishnish Bay (NM 627 429). Epidote zone. Two lava flows exposed the lower one being underlain by bole that contains relict red patches (M 39). Upper flow sampled at following heights above junctions : M 34 0.2m; M 36 1.1m; M 35 2.35m. Lower flow is only 4m thick - M 37 and M 38 collected 1.2 and 2.1m above M 39, respectively.
- M 45
M 40 - 46
- Cutting on south side of A 849, 1km east of Pennygown chapel. (NM 614 432). Epidote zone. Again two lava flows exposed. M 45 collected from upper flow 0.9m above junction. Lower flow sampled at following heights below junction : M 46 0.5m; M 43 1.3m; M 42 2.75m; M 41 3.95m; M 40 5.15.
- M 47 - 50
- Cutting on south side of A 849, 1km west of turn to Glenforsa Hotel and 1.4km east of Salen (NM 583 428). Granophyre - probably part of the Toll Doire ring dyke - exposed to east of cutting. Samples collected at following distances from granophyre exposure : M 49 10m; M 48 25m; M 47 49m; M 50 71m.
- M 59
- Lava exposed in stream one third of way down hill behind Fishnish Bay, south of A 849. (NM 629 410). Epidote zone.
- M 58
- Hill top knoll, south of A 849, opposite Fishnish Bay. (NM 402 278). Epidote zone.
- M 6
- MacCullouch's tree lava, Ardmeanach Peninsula (NM 402 278). Laumontite zone.
- MS 183
- West bank of Allt Molach, a few feet above stream, two thirds of distance from new road (A 849) to Ishriff farm (NM 632 313).

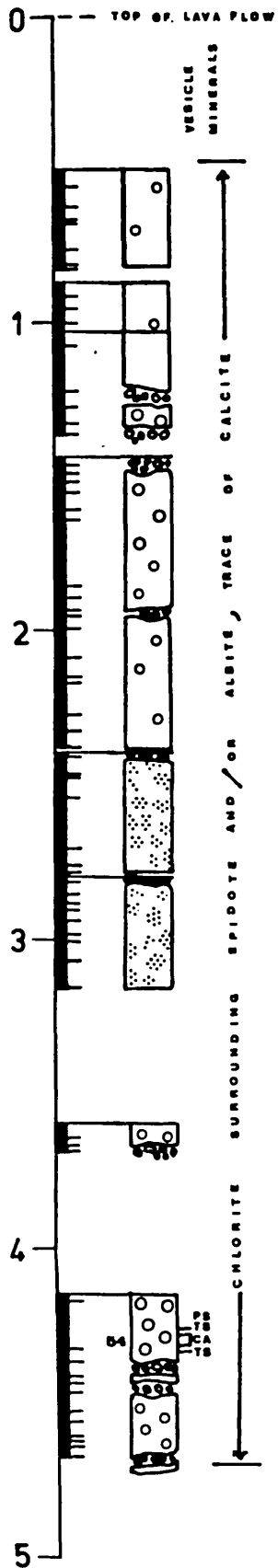
- MS 184 Cutting on new road (A 849). Top of first slope, west of point where road crosses Allt Molach. South side of road at first bend. (NM 628 312).
- MS 185 Cutting on A 849 at head of pass in Glen More. North side of road beneath intrusive sheet. May be agglomerate containing clasts of NPC lavas. (NM 619 304).

1 - B DRILL CORE LOG

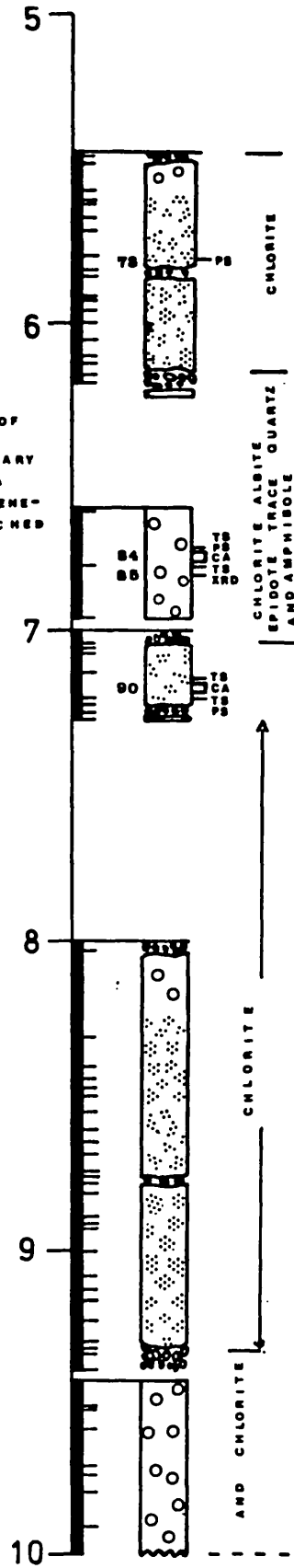
No attempt has been made to identify and draw every single piece of the core in this log. Instead, the interval occupied by each sample and the percentage recovery are shown in the left hand column; the main rock types recovered and the mineralogical variations within them are depicted in the right hand column. Rubble horizons and breaks in the section across which continuity could not be definitely established are shown diagrammatically.

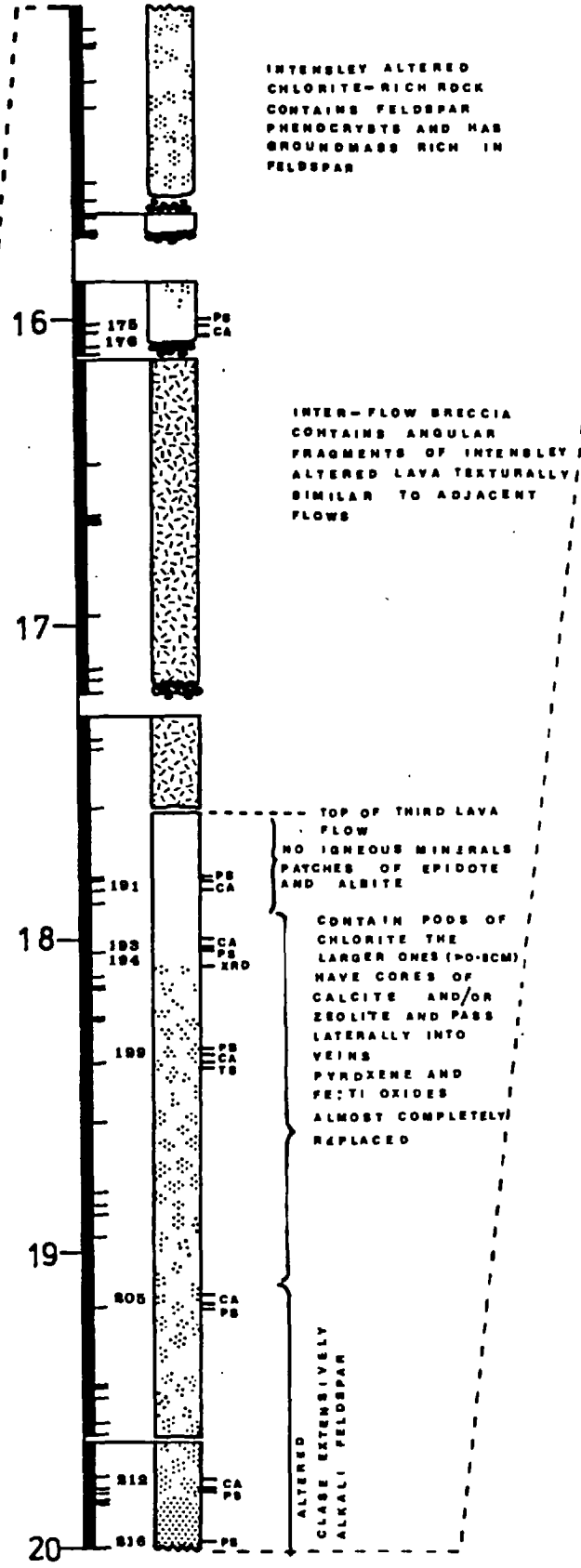
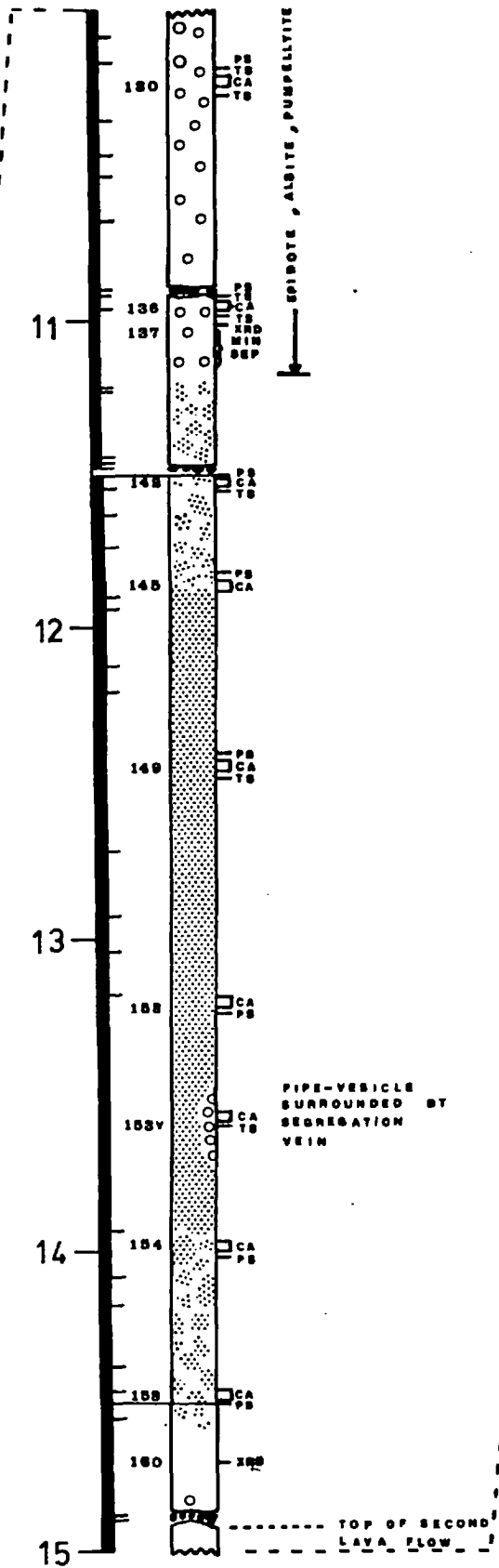
CA-chemical analysis; TS-thin section; PS- polished section;
XRD- mineral separate taken for X-ray diffraction studies

Depth below top of lava flow



REGULAR ALTERNATION OF LIGHT GREEN VESICULAR ROCK - CONTAINING NO PRIMARY MINERALS OTHER THAN A TRACE OF UNALTERED PYROXENE - AND NONVESICULAR BLOTCHED LAVA - CONTAINING SOME TITANOMAGNETITE AND PLAGIOCLASE SECTION BETWEEN 13 AND 14 M IS SIMILAR TO MIB-22





1 - C MODAL ANALYSES

Zeolite-facies lavas. Phenocryst modes

M 13-22.

Zeolite-facies lavas-phenocryst modes (2000 points).

	<u>LA 1</u>	<u>LA 2*</u>	<u>LA 3</u>	<u>LA 4</u>	<u>LA 5</u>	<u>LA 20</u>
olivine	tr	tr	0.35	0.35	0.35	12.40
plagioclase	2.00	1.55	1.65	1.90	2.00	-
titanomagnetite	-	-	-	-	-	-
groundmass	98.00	98.45	98.00	97.75	97.65	87.60

	<u>LA 7</u>	<u>LA 8</u>	<u>LA 9</u>	<u>LA 10</u>	<u>LA 11</u>	<u>M 1</u>
olivine	0.15	tr	tr	tr	tr	4.15
plagioclase	1.15	2.25	2.65	3.15	2.95	-
titanomagnetite	-	-	-	-	-	-
groundmass	98.70	97.75	97.35	96.85	97.05	94.60

	<u>LA 13</u>	<u>LA 14</u>	<u>LA 15</u>	<u>LA 16</u>	<u>LA 17</u>	<u>LA 18</u>
olivine	6.75	9.30	17.00	10.00	10.38	14.48
plagioclase	-	-	-	-	-	-
titanomagnetite	-	-	-	-	-	-
groundmass	93.25	90.70	82.85	90.00	89.62	85.52

	<u>M 5</u>	<u>M 6</u>	<u>M 7</u>	<u>M 8</u>	<u>M 11</u>	<u>M 12</u>
olivine	2.50	2.20	3.30	2.40	5.80	7.10
plagioclase	5.00	6.05	7.25	5.65	0.60	0.60
titanomagnetite	0.20	tr	0.30	tr	-	-
groundmass	92.30	91.75	89.15	91.95	93.60	92.30

	<u>M 51</u>	<u>M 52</u>	<u>M 53</u>	<u>M 54</u>	<u>M 55</u>
olivine	4.40	3.20	3.20	4.35	3.50
plagioclase	3.05	2.70	3.45	3.05	2.95
titanomagnetite	-	-	-	-	-
groundmass	92.55	94.10	93.35	91.00	93.55

* contains 0.55% unaltered glass

M 13 - 22 (4000 points).

	<u>M 13</u>	<u>M 14</u>	<u>M 15</u>	<u>M 16</u>	<u>M 17</u>
chlorite	43.00	43.83	31.15	37.12	28.59
feldspar	29.55	24.95	36.63	27.41	36.26
pyroxene	-	14.23	18.73	16.30	18.12
opaques	-	2.95	3.48	4.62	7.15
sphene	9.55	4.83	6.43	3.75	1.60
carbonate	-	0.83	0.15	4.82	2.32
amphibole	0.93	6.68	2.40	4.92	2.00
epidote	0.40	0.10	0.10	0.05	3.25
quartz	16.15	1.15	0.18	0.50	0.79
other	0.47	0.48	0.75	0.50	-
	<u>M 18</u>	<u>M 19</u>	<u>M 20</u>	<u>M 21</u>	<u>M 22</u>
chlorite	29.85	35.53	35.05	34.08	30.63
feldspar	30.98	24.20	25.30	28.63	36.00
pyroxene	19.25	21.83	23.68	19.50	16.45
opaques	9.53	11.73	11.83	12.85	9.20
sphene	3.15	3.83	tr	1.55	2.50
carbonate	0.23	0.35	tr	-	tr
amphibole	6.83	2.45	2.38	3.38	4.58
epidote	0.20	0.08	-	tr	tr
quartz	-	0.08	1.53	0.08	0.53
other	-	-	0.20	-	0.35

These figures should be considered to be approximate only. The groundmass phases have been replaced by aggregates of fine-grained minerals that are difficult to identify and impossible to count separately. Feldspar refers to the altered plagioclases plus the inclusions which are often numerous enough to cause the crystals to appear brown in colour. All the analyses listed above were obtained by counting more than one slide for each rock. Nevertheless, the presence of secondary mineral pods in the thin sections of M 16, M 17 and M 18 has caused the figures for these samples to be distorted.

I - D MICROPROBE ANALYSES.Zeolite zone rocks.

LA 5 Basaltic hawaiite
 LA 7 Less - magnesian basalt
 LA 15 Magnesian basalt
 LA 18 Magnesian basalt
 M 7 Hawaiite
 M 12 Less - magnesian basalt
 M 55 Less - magnesian basalt
 M 56 Altered vesicle surround from M 51 - 55.

Greenschist - facies zone rock.

M 13, M 14, M 15, M 16, M 18, C 54, C 130, C 158,
 M 69, all from olivine - rich flow Pennygown Quarry.
 M 70 Secondary mineral pod upper flow Pennygown Quarry.
 D 1 Pyritised dyke Pennygown Quarry
 M 29, M 30 Toll Doire Quarry lava
 M 41, M 46 Altered hawaiite
 M 48, M 49 Altered basalt and hydrothermal vein from
 same lava flow
 C 212, C 232a/b Plagioclase - rich lava from lower part
 drill core, Pennygown Quarry

- Note 1. Subscripts a,b refer to core and rim analyses
 same crystals.
2. Fe:Ti oxides recalculated using method of
 Carmichael (1967).

LA 5 - Basaltic Hawaiite.

	1	2	3	4	5	6a	6b	7a	7b	8	9a
SiO ₂	36.58	35.63	35.77	35.29	35.69	50.60	50.46	51.09	51.51	52.33	52.44
Al ₂ O ₃	-	-	.28	-	.22	29.96	30.16	28.66	28.89	29.93	29.69
Cr ₂ O ₃	-	-	-	-	-	-	-	.11	.11	-	-
FeO*	34.72	38.18	38.03	40.11	39.68	2.01	1.62	2.64	2.55	.87	1.00
MnO	.46	.52	.82	.49	.82	-	-	-	-	-	-
MgO	27.82	26.09	24.22	24.01	23.64	0.66	0.51	1.06	0.84	-	.21
NiO	-	-	-	-	-	-	-	-	-	-	-
CaO	.41	.34	.65	.42	.44	12.68	13.12	11.98	11.67	12.45	12.08
Na ₂ O	-	-	-	-	-	3.76	3.36	3.43	3.83	4.36	4.01
K ₂ O	-	-	-	-	-	-	0.07	0.09	.17	.10	.10
TiO ₂	-	.12	-	-	-	-	-	.11	-	-	-
V ₂ O ₃	-	-	-	-	-	-	-	-	-	-	-
Total	99.99	100.86	99.77	100.32	100.49	99.67	99.09	99.16	99.56	100.04	99.53

Cation proportions

	1	2	3	4	5	6a	6b	7a	7b	8	9
Basia	0 = 4	0 = 4	0 = 4	0 = 4	0 = 4	0 = 8	0 = 8	0 = 8	0 = 8	0 = 8	0 = 8
Si	1.013	0.996	1.012	1.003	1.010	2.325	2.328	2.361	2.369	2.379	2.391
Al	-	-	0.009	-	0.007	1.623	1.640	1.561	1.566	1.604	1.596
Cr	-	-	-	-	-	-	-	0.004	0.004	-	-
Fe	0.804	0.893	0.900	0.953	0.939	0.077	0.062	0.102	0.098	0.033	0.038
Mn	0.011	0.012	0.020	0.012	0.020	-	-	-	-	-	-
Mg	1.148	1.087	1.022	1.017	0.997	0.045	0.021	0.073	0.057	-	0.015
Ni	-	-	-	-	-	-	-	-	-	-	-
Ca	0.012	0.010	0.020	0.013	0.013	0.624	0.648	0.593	0.575	0.066	0.590
Na	-	-	-	-	-	0.335	0.300	0.307	0.341	0.385	0.355
K	-	-	-	-	-	-	0.004	0.005	0.010	0.005	0.006
Ti	-	0.002	-	-	-	-	-	0.004	-	-	-
V	-	-	-	-	-	-	-	-	-	-	-
Σ	2.987	3.001	2.983	2.997	2.986	5.030	5.004	5.009	5.021	5.013	4.991

Fo	58.81	Fo	54.91	Fo	53.17	Fo	51.61	Fo	51.49	An	65.11	An	68.06	An	65.51	An	62.10	An	60.86	An	62.07
Ab	34.89	Ab	31.51	Ab	33.90	Ab	36.84	Ab	38.59	Ab	37.30	Or	0.43	Or	0.59	Or	1.06	Or	0.55	Or	0.63

	9b	10a	10b	11	12	13	14	15	16	17	18
SiO ₂	54.92	52.63	52.86	52.40	51.40	32.09	32.14	30.58	1.02	.51	.64
Al ₂ O ₃	25.99	30.11	29.32	27.87	13.54	13.88	13.93	13.53	0.52	1.77	1.60
Cr ₂ O ₃	-	-	-	-	-	-	-	-	-	-	.16
FeO*	2.14	.75	1.31	2.86	26.49	25.52	24.62	25.87	48.24	67.98	66.65
MnO	-	-	-	-	.11	.21	.14	.11	.53	1.35	1.33
MgO	.58	-	-	.80	13.40	13.72	13.22	14.22	3.27	-	-
NiO	-	-	-	-	-	-	-	-	-	-	-
CaO	8.82	12.33	11.56	10.61	1.82	1.75	1.96	1.51	.33	-	.09
Na ₂ O	5.52	4.16	4.50	4.40	-	-	-	-	-	-	-
K ₂ O	.31	.15	.19	.23	-	-	-	-	-	-	-
TiO ₂	.13	-	.15	.15	-	-	-	-	43.32	24.26	25.23
V ₂ O ₃	-	-	-	-	-	-	-	-	0.36	.63	.62
Total	98.41	100.13	99.89	99.32	86.76	87.17	86.02	85.83	97.58	96.49	96.32

Cation proportions

	9b	10a	10b	11	12	13	14	15	16	17	18	
Basia	0 = 8	0 = 8	0 = 8	0 = 8	0 = 28	0 = 28	0 = 28	0 = 28	<u>Recalculated analyses.</u>			
Si	2.530	2.386	2.406	2.413	6.716	6.778	6.847	6.605	FeO	33.40	52.68	55.53
Al	1.411	1.609	1.573	1.514	3.413	3.456	3.500	3.446	Fe ₂ O ₃	16.50	17.00	14.58
Cr	-	-	-	-	-	-	-	-	Total	99.24	98.20	97.79
Fe	0.082	0.028	0.056	0.110	4.739	4.507	4.386	4.673				
Mn	-	-	-	-	0.021	0.037	0.026	0.020				
Mg	0.040	-	-	0.055	4.270	4.320	4.197	4.578				
Ni	-	-	-	-	-	-	-	-				
Ca	0.435	0.599	0.564	0.524	0.418	0.396	0.448	0.350				
Na	0.493	0.366	0.397	0.393	-	-	-	-				
K	0.018	0.009	0.011	0.014	-	-	-	-				
Ti	0.004	-	0.005	0.005	-	-	-	-				
V	-	-	-	-	-	-	-	-				
Σ	5.015	4.997	5.006	5.028	19.577	19.493	19.403	19.672				

An	46.00	An	61.51	An	57.99	An	56.33
Ab	52.05	Ab	37.59	Ab	40.89	Ab	42.21
Or	1.95	Or	0.90	Or	1.12	Or	1.46

- 1 - 5 Small anhedral olivines.
- 6 - 10 Feldspar 'phenocrysts'.
- 11 Groundmass feldspars.
- 12 - 15 Groundmass chlorites.
- 16 Exsolved ilmenite in host titanomagnetite.
- 17,18 Titanomagnetite.

LA 7 Leas - magnetian basalt.

	1	2	3	4	5	6	7	8
SiO ₂	50.48	49.53	54.46	52.59	50.56	47.31	48.91	48.54
Al ₂ O ₃	30.22	30.41	26.84	28.11	2.19	4.46	3.51	3.83
Cr ₂ O ₃	-	-	-	-	-	-	-	.12
FeO ³	1.22	1.47	2.07	2.08	11.46	11.61	11.07	14.16
MnO	-	-	-	-	.16	.18	.18	.24
MgO	.21	0.23	.90	.86	14.12	12.17	12.62	13.53
NiO	-	-	-	-	-	-	-	-
CaO	13.02	13.30	10.54	11.07	18.66	19.56	19.82	16.26
Na ₂ O	3.46	3.25	4.77	3.90	-	.64	.49	.90
K ₂ O	-	.08	.22	.15	-	-	-	-
TiO ₂	-	-	.18	.15	1.19	2.31	1.85	1.39
V ₂ O ₃	-	-	-	-	-	.17	.12	-
<u>Total</u>	<u>98.62</u>	<u>98.27</u>	<u>99.97</u>	<u>98.91</u>	<u>98.35</u>	<u>98.42</u>	<u>98.57</u>	<u>98.97</u>

Cation proportions

	1	2	3	4	5	6	7	8
Basis	0 = 8	0 = 8	0 = 8	0 = 8	0 = 6	0 = 6	0 = 6	0 = 6
Si	2.334	2.306	2.479	2.420	1.926	1.822	1.870	1.860
Al	1.647	1.669	1.440	1.525	0.098	0.203	0.158	0.173
Cr	-	-	-	-	-	-	-	0.004
Fe	0.047	0.057	0.079	0.080	0.365	0.374	0.354	0.454
Mn	-	-	-	-	0.005	0.006	0.006	0.008
Mg	0.014	0.016	0.061	0.059	0.802	0.698	0.719	0.773
Ni	-	-	-	-	-	-	-	-
Ca	0.645	0.663	0.514	0.546	0.762	0.807	0.812	0.668
Na	0.310	0.293	0.421	0.348	-	0.048	0.036	0.067
K	-	0.005	0.013	0.009	-	-	-	-
Ti	-	-	0.006	0.006	0.034	0.067	0.053	0.040
V	-	-	-	-	-	0.005	0.004	-
<u>Σ</u>	<u>4.998</u>	<u>5.009</u>	<u>5.012</u>	<u>4.991</u>	<u>3.991</u>	<u>4.031</u>	<u>4.013</u>	<u>4.045</u>
An	67.54	An 69.00	An 54.24	An 60.50	Wo 37.81	Wo 40.36	Wo 41.40	Wo 41.31
Ab	32.46	Ab 30.52	Ab 44.39	Ab 38.54	En 42.54	En 38.63	En 39.30	En 40.65
Or	0.00	Or 0.48	Or 1.37	Or 0.95	Fs 19.65	Fs 21.01	Fs 19.66	Fs 18.05

	9	10	11	12	13	14
SiO ₂	.47	.33	.50	.21	.23	.22
Al ₂ O ₃	-	.37	.59	-	-	-
Cr ₂ O ₃	-	-	-	-	-	-
FeO ³	43.86	44.57	73.59	12.63	11.47	11.14
MnO	.68	.40	.26	.84	.78	1.38
MgO	3.75	2.60	2.77	28.60	25.38	26.64
NiO	-	-	-	-	-	-
CaO	-	-	-	-	-	-
Na ₂ O	-	-	-	7.43	13.15	10.76
K ₂ O	-	-	-	-	-	-
TiO ₂	49.00	47.40	13.84	-	-	-
V ₂ O ₃	.42	.66	.49	-	-	-
<u>Total</u>	<u>98.17</u>	<u>96.34</u>	<u>92.04</u>	<u>49.70</u>	<u>51.01</u>	<u>50.13</u>

Recalculated analyses

FeO	37.20	37.97	38.90
Fe ₂ O ₃	7.40	7.35	38.57
<u>Total</u>	<u>98.91</u>	<u>97.08</u>	<u>95.92</u>

- 1 - 4 Feldspar phenocrysts.
5 - 8 Pyroxenes.
9, 10 Ilmenite lamella in titanomagnetite.
11 Titanomagnetite showing low temperature oxidation.
12 - 15 Carbonate infilling vesicles.

LA 15 Magnesian basalt.

	1a	1b	2a	2b	3	4	5	6	7	8	9
SiO ₂	37.35	37.30	37.32	37.40	37.07	36.93	36.55	36.71	37.17	49.78	51.80
Al ₂ O ₃	-	-	-	-	-	-	-	-	-	31.16	30.14
Cr ₂ O ₃	-	-	-	-	-	-	-	-	-	-	-
FeO	25.89	28.60	26.71	27.22	28.66	29.11	31.35	32.06	32.15	-	-
MnO	.35	.37	.24	.32	.41	.39	.41	.44	.43	.51	.78
MgO	35.46	32.68	34.86	34.80	33.75	33.63	30.70	30.42	30.61	-	-
NiO	.19	-	.15	.19	.15	-	-	-	-	-	-
CaO	.36	.46	.43	.27	.36	.31	.30	.33	.35	13.64	12.61
Na ₂ O	-	-	-	-	-	-	-	-	-	3.01	3.92
K ₂ O	-	-	-	-	-	-	-	-	-	.15	.18
TiO ₂	-	.13	-	-	-	-	-	-	-	-	.12
V ₂ O ₃	-	-	-	-	-	-	-	-	-	-	-
Total	99.61	99.52	99.70	100.20	100.40	100.38	99.31	99.95	100.71	98.23	99.55

Cation proportions

	1a	1b	2a	2b	3	4	5	6	7	8	9
Basis	0 = 4	0 = 4	0 = 4	0 = 4	0 = 4	0 = 4	0 = 4	0 = 4	0 = 4	0 = 8	0 = 8
Si	0.996	1.007	0.997	0.996	0.993	0.992	1.003	1.004	1.007	2.306	2.366
Al	-	-	-	-	-	-	-	-	-	1.702	1.623
Cr	-	-	-	-	-	-	-	-	-	-	-
Fe	0.577	0.646	0.597	0.607	0.642	0.653	0.720	0.733	0.729	0.020	0.030
Mn	0.008	0.008	0.005	0.007	0.009	0.009	0.009	0.010	0.010	-	-
Mg	1.409	1.314	1.388	1.382	1.348	1.346	1.256	1.240	1.236	-	-
Ni	0.004	-	0.003	0.004	0.003	-	-	-	-	-	-
Ca	0.010	0.013	0.012	0.008	0.010	0.009	0.009	0.010	0.010	0.677	0.617
Na	-	-	-	-	-	-	-	-	-	0.270	0.347
K	-	-	-	-	-	-	-	-	-	0.009	0.011
Ti	-	0.003	-	-	-	-	-	-	-	-	0.004
V	-	-	-	-	-	-	-	-	-	-	-
Σ	3.004	2.991	3.003	3.004	3.003	3.008	2.997	2.996	2.992	4.983	4.997

Fo 70.93 Fo 67.06 Fo 69.93 Fo 69.50 Fo 67.73 Fo 67.31 Fo 63.57 Fo 62.84 Fo 62.91 An 70.81 An 63.31
Ab 28.25 Ab 35.60
Or 0.93 Or 1.10

	10	11	12	13	14	15	16	17	18	19	20
SiO ₂	51.65	57.44	56.96	51.05	49.69	50.71	49.89	.41	.34	.38	.55
Al ₂ O ₃	29.61	26.26	25.79	2.77	4.34	3.16	3.59	-	.21	2.24	2.27
Cr ₂ O ₃	-	-	-	.62	1.12	1.03	1.03	-	-	.25	-
FeO	.53	.37	.64	6.47	6.11	5.81	6.26	41.92	42.61	65.18	65.61
MnO	-	-	-	-	-	.14	-	.44	.42	1.84	1.75
MgO	-	-	-	15.31	14.44	14.74	14.73	5.09	4.63	.43	-
NiO	-	-	-	.14	-	-	-	-	-	-	-
CaO	12.11	7.73	7.47	21.25	21.39	21.43	21.60	.10	-	-	-
Na ₂ O	4.42	6.04	6.53	-	-	.44	.56	-	-	-	-
K ₂ O	.20	1.12	1.17	-	-	-	-	-	-	-	-
TiO ₂	.12	.18	.13	.80	.92	.79	.93	50.59	49.79	22.94	23.58
V ₂ O ₃	-	-	-	.19	.17	.15	-	.52	.53	1.73	1.35
Total	98.63	99.14	98.68	98.59	98.18	98.40	98.58	99.06	98.52	94.99	95.10

Cation proportions

	10	11	12	13	14	15	16	17	18	19	20
Basis	0 = 8	0 = 8	0 = 8	0 = 6	0 = 6	0 = 6	0 = 6	-	-	-	-
Si	2.379	2.600	2.599	1.911	1.869	1.902	1.875	FeO 36.33	36.50	49.76	51.24
Al	1.608	1.401	1.387	0.122	0.193	0.140	0.159	Fe ₂ O ₃ 6.20	6.79	17.14	15.86
Cr	-	-	-	0.018	0.033	0.030	0.031	99.67	99.20	96.71	96.59
Fe	0.020	0.014	0.024	0.202	0.192	0.182	0.197	-	-	-	-
Mn	-	-	-	-	-	0.004	-	-	-	-	-
Mg	-	-	-	0.854	0.810	0.824	0.825	-	-	-	-
Ni	-	-	-	0.004	-	-	-	-	-	-	-
Ca	0.598	0.375	0.365	0.853	0.862	0.862	0.870	-	-	-	-
Na	0.395	0.530	0.577	-	-	0.032	0.041	-	-	-	-
K	0.012	0.065	0.068	-	-	-	-	-	-	-	-
Ti	0.004	0.006	0.004	0.023	0.026	0.022	0.026	-	-	-	-
V	-	-	-	0.006	0.005	-	-	-	-	-	-
Σ	5.016	4.990	5.026	3.993	3.990	4.004	4.024	-	-	-	-

An 59.53 An 38.67 An 36.14 Wo 42.44 Wo 42.79 Wo 43.94 Wo 43.77
Ab 39.31 Ab 54.64 Ab 57.12 En 46.57 En 46.23 En 45.70 En 45.40
Cr 1.16 Or 6.70 Or 6.74 Fs 10.99 Fs 10.98 Fs 10.36 Fs 10.83

- 1 - 5 Olivine phenocrysts.
1b - green apparently altered rim of phenocryst.
6,7 Groundmass olivines.
8 - 12 Groundmass feldspars.
13 - 16 Pyroxenes.
17,18 Ilmenite lamellae in groundmass titanomagnetites.
19,20 Groundmass titanomagnetites.

LA 18 - Magnesian basalt.

	1	2	3	4	5	6	7	8	9	10	11	12
SiO ₂	39.98	39.66	39.14	39.35	39.31	38.45	37.64	35.75	36.65	49.42	49.99	49.46
Al ₂ O ₃	-	-	-	-	-	-	-	-	1.46	31.66	31.62	31.01
Cr ₂ O ₃	-	-	-	.15	-	-	-	-	-	-	-	-
FeO*	13.04	13.24	17.09	17.42	18.68	22.78	26.35	35.64	34.92	.97	.75	1.60
MnO	.15	.12	.18	.22	.18	.23	.33	.47	.50	-	-	-
MgO	45.79	46.20	42.69	42.87	41.46	37.94	34.92	26.07	24.28	-	-	.60
NiO	.35	.21	.16	.18	.22	-	-	-	-	-	-	-
CaO	.22	.23	.26	.32	.28	.26	.35	.45	.72	14.30	14.14	13.19
Na ₂ O	-	-	-	-	-	-	-	-	-	2.64	2.84	3.38
K ₂ O	-	-	-	-	-	-	-	-	-	-	.11	.12
TiO ₂	-	-	-	-	-	-	-	-	-	-	.14	-
V ₂ O ₅	-	-	-	-	-	-	-	-	-	-	-	-
Total	99.53	99.67	99.53	100.49	100.13	99.65	99.58	98.39	98.53	98.98	99.58	99.35

	<u>Cation proportions</u>											
Basis	0 = 4	0 = 4	0 = 4	0 = 4	5 = 4	6 = 4	7 = 4	8 = 4	9 = 4	10 = 8	11 = 8	12 = 8
Si	1.001	0.993	0.999	0.996	1.004	1.006	1.004	1.014	1.029	2.278	2.289	2.281
Al	-	-	-	-	-	-	-	-	0.048	1.721	1.707	1.686
Cr	-	-	-	0.003	-	-	-	-	-	-	-	-
Fe	0.273	0.2777	0.365	0.369	0.399	0.498	0.588	0.845	0.820	0.037	0.029	0.062
Mn	0.003	0.003	0.004	0.005	0.004	0.005	0.007	0.011	0.012	-	-	-
Mg	1.709	1.724	1.623	1.617	1.578	1.478	1.387	1.102	1.016	-	-	0.041
Ni	0.007	0.004	0.003	0.004	0.004	-	-	-	-	-	-	-
Ca	0.006	0.006	0.007	0.009	0.008	0.007	0.010	0.014	0.022	0.706	0.694	0.652
Na	-	-	-	-	-	-	-	-	-	0.236	0.252	0.302
K	-	-	-	-	-	-	-	-	-	-	0.006	0.007
Ti	-	-	-	-	-	-	-	-	-	-	0.005	-
V	-	-	-	-	-	-	-	-	-	-	-	-
Σ	2.999	3.007	3.001	3.002	2.996	2.994	2.996	2.986	2.947	4.979	4.982	5.031

Fo 86.22 Fo86.13 Fo81.65 Fo81.43 Fo79.82 Fo74.80 Fo70.25 Fo56.59 Fo55.34 An75.00 An72.84 An67.81
 Ab25.00 Ab26.48 Ab31.46
 Or - Or 0.68 Or 0.73

	13	14	15	16	17	18	19	20	21	22	23	24
SiO ₂	53.62	50.74	50.22	51.13	49.99	50.09	40.49	40.08	1.006	.41	2.17	1.09
Al ₂ O ₃	27.26	2.36	3.46	3.11	3.64	2.46	28.76	29.15	.84	-	2.56	1.95
Cr ₂ O ₃	-	.32	.23	.71	1.13	-	-	-	-	-	-	-
FeO*	1.66	7.85	8.48	6.13	6.39	9.53	.46	.17	52.28	43.21	61.92	63.12
MnO	-	.20	.15	.15	.16	.21	-	-	.65	.45	2.38	2.83
MgO	.88	14.39	13.79	15.25	14.64	13.55	-	-	2.91	3.42	.27	-
NiO	-	-	-	-	-	-	-	-	-	-	-	-
CaO	10.61	21.31	21.03	21.38	21.28	20.76	11.10	11.28	.19	-	.34	.16
Na ₂ O	4.66	-	.38	-	-	-	3.92	3.99	-	-	-	-
K ₂ O	.28	-	-	-	-	-	-	-	-	-	-	-
TiO ₂	.18	1.01	1.65	.79	.83	1.60	-	-	39.04	50.66	24.94	25.09
V ₂ O ₅	-	.14	.11	.13	.13	0.11	-	-	.58	.36	1.01	1.02
Total	99.15	98.30	99.15	98.78	98.19	98.30	84.72	84.66	97.49	98.49	95.58	95.26

	<u>Cation proportions</u>						<u>Recalculated analyses</u>				
Basis	13 = 8	14 = 6	15 = 6	16 = 6	17 = 6	18 = 6	21	22	23	24	
Si	2.458	1.918	1.882	1.907	1.883	1.907	FeO	30.21	39.50	53.11	51.14
Al	1.473	0.105	0.153	0.137	0.161	0.110	Fe ₂ O ₃	24.52	4.11	2.80	13.31
Cr	-	0.010	0.007	0.021	0.034	-		99.94	98.89	96.84	96.59
Fe	0.064	0.248	0.266	0.191	0.201	0.303					
Mn	-	0.006	0.005	0.005	0.005	0.007					
Mg	0.060	0.811	0.770	0.848	0.822	0.768					
Ni	-	-	-	-	-	-					
Ca	0.521	0.863	0.844	0.855	0.859	0.847					
Na	0.414	-	0.028	-	-	-					
K	0.016	-	-	-	-	-					
Ti	0.006	0.029	0.046	0.022	0.023	0.046					
V	-	0.004	0.003	0.004	0.004	0.003					
Σ	5.014	3.924	4.004	3.990	3.994	3.991					

An 54.77 Wo43.05 Wo42.79 Wo42.63 Wo42.55 Wo42.30
 Ab 43.53 En43.34 En42.34 En46.60 En45.92 En41.10
 Or 1.70 Fa13.61 Fa14.87 Fa10.77 Fa11.53 Fa16.58

- 1 - 7 Olivine phenocrysts
 1 - 4 all enclosing spinels.
 7 "altered" olivine appears to be chloritised.
 8,9 Groundmass olivines. Both green coloured appear chloritised.
 10 - 13 Groundmass feldspars.
 14 - 18 Pyroxenes.
 19,20 Groundmass zeolites - probably thomsonite.
 21 - 24 Groundmass Fe:Ti oxides,
 21,22 recalculated as ilmenite,

M 7 - Hawaiite.

	1	2	3	4	5a	5b	6	7
SiO ₂	36.29	36.52	36.51	36.34	53.58	53.08	54.46	54.30
Al ₂ O ₃	-	-	-	-	28.36	29.26	29.47	28.82
Cr ₂ O ₃	-	-	-	-	-	-	-	-
FeO ^a	32.77	32.86	32.70	33.05	.46	.70	.49	.50
MnO	.53	.48	.53	.63	-	-	-	-
MgO	29.82	29.85	29.65	29.53	-	-	-	-
NiO	-	-	.15	-	-	-	-	-
CaO	.34	.29	.31	.29	10.17	11.26	11.07	10.46
Na ₂ O	-	-	-	-	5.24	4.84	4.86	5.15
K ₂ O	-	-	-	-	.10	.08	.13	.10
TiO ₂	-	-	-	-	.14	.17	-	.17
V ₂ O ₅	-	-	-	-	-	-	-	-
<u>Total</u>	<u>99.75</u>	<u>100.00</u>	<u>99.86</u>	<u>99.84</u>	<u>98.05</u>	<u>99.41</u>	<u>100.48</u>	<u>99.49</u>

Cation proportions

Basis	1 O = 4	2 O = 4	3 O = 4	4 O = 4	5a O = 8	5b O = 8	6 O = 8	7 O = 8
Si	0.999	1.002	1.004	1.001	2.464	2.419	2.446	2.461
Al	-	-	-	-	1.538	1.572	1.561	1.540
Cr	-	-	-	-	-	-	-	-
Fe	0.755	0.754	0.752	0.761	0.018	0.027	0.018	0.019
Mn	0.012	0.011	0.012	0.015	-	-	-	-
Mg	1.224	1.221	1.215	1.213	-	-	-	-
Ni	-	-	0.003	-	-	-	-	-
Ca	0.010	0.009	0.009	0.009	0.501	0.550	0.533	0.508
Na	-	-	-	-	0.467	0.427	0.427	0.453
K	-	-	-	-	0.006	0.005	0.007	0.006
Ti	-	-	-	-	0.005	0.006	-	0.006
V	-	-	-	-	-	-	-	-
<u>Σ</u>	<u>3.001</u>	<u>2.998</u>	<u>2.996</u>	<u>2.999</u>	<u>4.999</u>	<u>5.005</u>	<u>4.989</u>	<u>4.992</u>
	Fo 61.85	Fo 61.81	Fo 61.78	Fo 61.43	An 51.44 Ab 47.95 Or 0.61	An 56.00 Ab 43.53 Or 0.48	An 55.26 Ab 43.99 Or 0.75	An 52.57 Ab 46.84 Or 0.58

	8	9	10	11	12
SiO ₂	54.03	55.81	53.92	.53	1.61
Al ₂ O ₃	28.85	28.00	28.95	1.79	2.37
Cr ₂ O ₃	-	-	-	-	-
FeO ^a	.39	.37	.53	68.41	66.64
MnO	-	-	-	.55	.46
MgO	-	-	-	2.66	2.86
NiO	-	-	-	-	-
CaO	10.53	9.63	10.83	.11	.16
Na ₂ O	5.45	5.61	4.93	-	-
K ₂ O	.11	.14	.12	-	-
TiO ₂	.14	-	-	22.01	22.36
V ₂ O ₅	-	-	-	.31	.31
<u>Total</u>	<u>99.48</u>	<u>99.54</u>	<u>99.27</u>	<u>96.37</u>	<u>96.76</u>

Cation proportions

Basis	8 O = 8	9 O = 8	10 O = 8	11 Recalculated analyses.	12 Recalculated analyses.
Si	2.453	2.518	2.452	FeO 47.36	48.94
Al	1.544	1.490	1.552	Fe ₂ O ₃ 23.40	19.66
Cr	-	-	-	<u>Total</u> 98.71	<u>98.72</u>
Fe	0.015	0.014	0.020		
Mn	-	-	-		
Mg	-	-	-		
Ni	-	-	-		
Ca	0.512	0.465	0.528		
Na	0.479	0.490	0.434		
K	0.006	0.008	0.007		
Ti	0.005	-	-		
V	-	-	-		
<u>Σ</u>	<u>5.013</u>	<u>4.986</u>	<u>4.993</u>		
	An 51.33 Ab 48.06 Or 0.61	An 48.30 Ab 50.88 Or 0.82	An 54.47 Ab 44.81 Or 0.72		

- 1 - 4 Skeletal olivines.
- 5 - 9 Feldspar phenocrysts.
- 10 Groundmass feldspar.
- 11,12 Groundmass titanomagnetites.

M 12 Lens - magnesian basalt.

	1	2	3	4	5	6	7	8	9
SiO ₂	37.48	37.34	37.51	37.22	36.05	52.37	51.56	52.19	51.96
Al ₂ O ₃	-	-	-	-	-	30.62	29.84	30.16	29.05
Cr ₂ O ₃	-	-	-	-	-	-	-	-	-
FeO*	25.25	26.36	27.80	27.61	34.60	.52	1.02	.97	1.97
MnO	.31	.28	.40	.37	.47	-	-	-	-
MgO	35.82	34.95	34.25	33.68	27.99	-	-	-	.64
NiO	-	-	-	-	-	-	-	-	-
CaO	.19	.23	.23	.29	.48	12.31	12.02	12.08	11.26
Na ₂ O	-	-	-	-	-	4.02	3.94	4.02	3.94
K ₂ O	-	-	-	-	-	.17	.23	.17	.27
TiO ₂	-	-	-	-	.17	.18	-	.14	.30
V ₂ O ₃	-	-	-	-	-	-	-	-	-
Total	99.04	99.16	99.99	99.18	99.75	100.19	98.60	99.72	99.40

Cation proportions

	1	2	3	4	5	6	7	8	9
Basis	0 = 4	0 = 4	0 = 4	0 = 4	0 = 4	0 = 8	0 = 8	0 = 8	0 = 8
Si	1.000	1.000	0.998	1.004	1.002	2.370	2.376	2.377	2.383
Al	-	-	-	-	-	1.634	1.621	1.619	1.571
Cr	-	-	-	-	-	-	-	-	-
Fe	0.564	0.591	0.622	0.623	0.804	0.020	0.039	0.037	0.076
Mn	0.007	0.006	0.009	0.009	0.011	-	-	-	-
Mg	1.424	1.395	1.366	1.353	1.159	-	-	-	0.044
Ni	-	-	-	-	-	-	-	-	-
Ca	0.005	0.007	0.007	0.008	0.014	0.597	0.593	0.589	0.544
Na	-	-	-	-	-	0.353	0.352	0.355	0.350
K	-	-	-	-	-	0.010	0.013	0.010	0.016
Ti	-	-	-	-	0.003	0.006	-	0.005	0.010
V	-	-	-	-	-	-	-	-	-
Σ	3.000	3.000	3.002	2.996	2.994	4.988	4.996	4.991	5.004
	Σ Fo 71.65	Fo 70.26	Fo 68.71	Fo 68.49	Fo 59.04	An 62.21 Ab 36.76 Or 1.03	An 61.87 Ab 36.74 Cr 1.40	An 61.79 Ab 37.20 Or 1.01	An 60.19 Ab 38.09 Or 1.72

	10	11	12	13	14	15	16	17
SiO ₂	51.74	52.85	53.77	55.25	48.81	48.25	45.69	.73
Al ₂ O ₃	29.96	30.29	29.89	28.58	3.63	4.54	6.52	1.04
Cr ₂ O ₃	-	-	-	-	-	-	-	-
FeO*	.41	.44	.53	.75	8.94	9.16	9.76	66.20
MnO	-	-	-	-	.13	-	.11	1.03
MgO	-	-	-	.20	12.23	12.09	11.32	.41
NiO	-	-	-	-	-	-	-	.16
CaO	11.71	12.22	11.56	9.91	21.30	21.53	21.35	.48
Na ₂ O	4.34	4.34	4.47	5.40	.63	.62	.42	-
K ₂ O	.14	0.26	.19	.40	-	-	-	-
TiO ₂	-	.18	.13	.12	2.42	2.59	3.45	25.35
V ₂ O ₃	-	-	-	-	-	.13	-	.26
Total	98.30	100.69	100.55	100.60	98.09	98.90	98.63	95.66

Cation proportions

	10	11	12	13	14	15	16	17
Basis	0 = 8	0 = 8	0 = 8	0 = 8	0 = 6	0 = 6	0 = 6	Recalculated analysis
Si	2.384	2.382	2.418	2.480	1.866	1.833	1.752	
Al	1.627	1.610	1.585	1.512	0.164	0.203	0.294	FeO 52.50
Cr	-	-	-	-	-	-	-	Fe ₂ O ₃ 15.23
Fe	0.016	0.016	0.020	0.028	0.286	0.291	0.313	<u>97.19</u>
Mn	-	-	-	-	0.004	-	0.004	
Mg	-	-	-	0.013	0.697	0.685	0.647	
Ni	-	-	-	-	-	-	-	
Ca	0.578	0.590	0.557	0.476	0.873	0.876	0.877	
Na	0.387	0.389	0.390	0.469	0.046	0.046	0.032	
K	0.008	0.015	0.011	0.023	-	-	-	
Ti	-	0.006	0.005	0.004	0.070	0.074	0.100	
V	-	-	-	-	-	0.004	-	
Σ	5.001	5.009	4.985	5.006	4.006	4.012	4.017	
	An 59.38 Ab 39.77 Or 0.85	An 59.33 Ab 39.16 Or 1.50	An 58.14 Ab 40.70 Or 1.16	An 49.19 Ab 48.46 Or 2.36	Wo 45.20 En 38.69 Fs 16.11	Wo 44.98 En 38.61 Fs 16.41	Wo 43.62 En 37.86 Fs 18.53	

- 1 - 4 Olivine phenocrysts.
- 5 Groundmass olivine.
- 6 - 13 Feldspars
- 14 - 16 Pyroxenes.
- 17 Groundmass titanomagnetite.

M 55 - Less-Magnesian basalt.

	1a	1b	2	3	4a	4b	5a	5b	6	7
SiO ₂	40.16	38.73	39.31	39.04	46.76	48.85	46.58	55.19	46.86	46.25
Al ₂ O ₃	-	-	-	-	33.77	29.51	34.36	28.13	33.71	32.34
Cr ₂ O ₃	-	-	-	-	-	-	-	-	.13	.12
FeO ⁺	11.17	20.04	17.75	18.56	.52	2.77	0.49	.53	.49	2.18
MnO	.17	.18	.17	.26	-	-	-	-	-	-
MgO	48.14	40.60	42.31	41.91	-	.75	-	-	-	.56
NiO	.34	.16	.16	-	-	-	-	-	-	-
CaO	.32	.37	.27	.31	16.99	12.72	17.16	10.15	16.78	15.65
Na ₂ O	-	-	-	-	1.44	2.91	1.33	5.56	1.58	1.33
K ₂ O	-	-	-	-	-	.08	-	.14	-	-
TiO ₂	-	-	-	-	-	-	-	.16	-	-
V ₂ O ₃	-	-	-	-	-	-	-	-	-	-
Total	100.29	100.08	99.97	100.07	99.48	97.60	99.91	99.86	99.55	98.41

Cation proportions

Basis	1a	1b	2	3	4a	4b	5a	5b	6	7
	O = 4	O = 4	O = 4	O = 4	O = 8	O = 8	O = 8	O = 8	O = 8	O = 8
Si	0.991	0.997	1.001	0.997	2.159	2.301	2.142	2.492	2.162	2.170
Al	-	-	-	-	1.838	1.639	1.862	1.497	1.834	1.788
Cr	-	-	-	-	-	-	-	-	0.005	0.004
Fe	0.230	0.431	0.378	0.397	0.020	0.109	0.019	0.020	0.019	0.085
Mn	0.004	0.004	0.004	0.006	-	-	-	-	-	-
Mg	1.770	1.558	1.606	1.595	-	0.053	-	-	-	0.039
Ni	0.007	0.003	0.003	-	-	-	-	-	-	-
Ca	0.008	0.010	0.007	0.008	0.841	0.642	0.845	0.491	0.829	0.786
Na	-	-	-	-	0.128	0.265	0.118	0.486	0.141	0.121
K	-	-	-	-	-	0.005	-	0.008	-	-
Ti	-	-	-	-	-	-	-	0.006	-	-
V	-	-	-	-	-	-	-	-	-	-
Σ	3.009	3.003	2.999	3.003	4.986	5.014	4.986	5.001	4.990	4.994
	Fo 88.48	Fo 78.31	Fo 80.95	Fo 80.09	An 86.75	An 70.37	An 87.74	An 49.83	An 85.44	An 86.70
					Ab 13.25	Ab 29.09	Ab 12.26	Ab 49.33	Ab 14.56	Ab 13.30
					Or -	Or 0.53	Or -	Or 0.84	Cr -	Or -

	8	9a	9b	10	11	12	13	14	15	16
SiO ₂	61.89	49.48	48.04	49.99	46.50	48.96	29.31	30.28	29.24	0.58
Al ₂ O ₃	23.50	4.27	4.69	3.31	5.20	4.46	14.59	15.71	15.40	0.31
Cr ₂ O ₃	-	.25	.15	.18	-	.51	-	-	-	-
FeO ⁺	1.36	7.73	9.48	9.21	11.08	7.86	30.25	24.51	28.23	43.29
MnO	-	.14	.14	-	-	-	.19	.13	-	.50
MgO	-	13.65	12.57	13.88	11.49	13.42	9.69	11.96	11.08	2.52
NiO	-	-	-	-	-	-	-	-	-	-
CaO	4.46	21.47	20.92	19.59	20.31	21.51	1.90	3.03	2.01	.11
Na ₂ O	8.43	-	.48	.49	.39	.65	-	-	-	-
K ₂ O	.72	-	-	-	-	-	-	-	-	-
TiO ₂	.16	1.54	2.16	.93	2.71	1.73	-	-	-	51.74
V ₂ O ₃	-	.17	-	.20	.19	.13	-	-	-	.22
Total	100.51	98.81	98.53	97.78	97.86	99.23	85.92	85.63	85.06	99.26

Cation proportions

Basis	0 = 8	0 = 6	0 = 6	0 = 6	0 = 6	0 = 6	0 = 28	0 = 28	0 = 28	
Si	2.749	1.862	1.831	1.904	1.800	1.843	6.496	6.520	6.396	Recalculated
Al	1.231	0.190	0.211	0.149	0.237	0.198	3.812	3.989	3.970	analysis
Cr	-	0.007	0.004	0.006	-	0.015	-	-	-	FeO 42.09
Fe	0.050	0.243	0.302	0.293	0.359	0.248	5.605	4.414	5.164	Fe ₂ O ₃ 1.33
Mn	-	0.004	0.004	-	-	-	0.035	0.023	-	Total 99.39
Mg	-	0.766	0.714	0.788	0.622	0.753	3.199	3.839	3.612	
Ni	-	-	-	-	-	-	-	-	-	
Ca	0.212	0.866	0.854	0.799	0.842	0.868	0.450	0.700	0.470	
Na	0.725	-	0.036	0.036	0.029	0.047	-	-	-	
K	0.041	-	-	-	-	-	-	-	-	
Ti	0.005	0.047	0.052	0.027	0.079	0.049	-	-	-	
V	-	0.005	-	0.006	0.006	0.004	-	-	-	
Σ	5.013	3.990	4.018	4.007	4.014	4.024	19.597	19.485	19.612	
	An 21.68	Wo 43.09	Wo 42.82	Wo 40.65	Wo 41.96	Wo 43.96				
	Ab 74.16	En 42.99	En 40.00	En 43.25	En 37.66	En 42.18				
	Cr 4.16	Fs 14.61	Fs 17.18	Fs 16.10	Fs 20.38	Fs 13.86				

- 1 - 3 Olivine phenocrysts.
- 4 - 6 Feldspar phenocrysts.
- 4b - rim of phenocrysts showing incipient veining by chlorite and zeolites.
- 7,8 Groundmass feldspars.
- 9-12 Pyroxenes.
- 13 Interstitial groundmass chlorite.
- 14,15 Chlorite surrounding and partly replacing olivine.
- 16 Ilmenite lamella in partly oxidised titanomagnetite.

M 56 Vesicle Surround

	1	2	3a	3b	4	5	6	7	8
SiO ₂	47.75	48.62	48.80	48.36	48.89	48.05	48.15	48.00	48.76
Al ₂ O ₃	4.41	4.03	4.77	3.50	2.80	5.10	3.46	3.73	3.42
Cr ₂ O ₃	.12	.13	.60	.14	-	.62	.14	-	-
FeO ³	10.90	9.66	7.93	12.23	12.61	7.84	11.53	11.36	11.63
MnO	.14	.17	.19	.13	.21	.13	.17	-	.14
MgO	11.60	12.24	13.15	10.77	10.56	12.70	10.92	11.06	11.05
NiO	-	-	-	-	-	-	-	-	-
CaO	20.56	21.32	21.62	20.69	20.57	21.41	21.00	21.08	21.02
Na ₂ O	-	.48	-	.41	.49	-	-	.50	.42
K ₂ O	-	-	-	-	-	-	-	-	-
TiO ₂	2.36	2.35	1.62	3.05	2.79	1.96	2.64	2.56	2.48
V ₂ O ₃	.14	.27	.21	.13	.18	.24	-	.14	.16
<u>Total</u>	<u>97.98</u>	<u>99.27</u>	<u>98.88</u>	<u>99.41</u>	<u>99.09</u>	<u>98.05</u>	<u>98.01</u>	<u>98.41</u>	<u>99.09</u>

Cation proportions

	1	2	3a	3b	4	5	6	7	8
Basis	0 = 6	0 = 6	0 = 6	0 = 6	0 = 6	0 = 6	0 = 6	0 = 6	0 = 6
Si	1.840	1.845	1.842	1.851	1.879	1.829	1.862	1.850	1.867
Al	0.200	0.180	0.212	0.158	0.127	0.229	0.158	0.169	0.154
Cr	0.004	0.004	0.018	0.004	-	0.019	0.004	-	-
Fe	0.351	0.306	0.250	0.392	0.405	0.250	0.373	0.366	0.372
Mn	0.005	0.005	0.006	0.004	0.007	0.004	0.006	-	0.005
Mg	0.666	0.692	0.740	0.614	0.605	0.720	0.630	0.636	0.631
Ni	-	-	-	-	-	-	-	-	-
Ca	0.849	0.866	0.874	0.848	0.847	0.873	0.870	0.871	0.862
Na	-	0.035	-	0.031	0.036	-	-	0.037	0.031
K	-	-	-	-	-	-	-	-	-
Ti	0.068	0.067	0.046	0.088	0.081	0.056	0.077	0.074	0.071
V	0.004	0.008	0.006	0.004	0.005	0.007	-	0.004	0.005
<u>Σ</u>	<u>3.988</u>	<u>4.010</u>	<u>3.994</u>	<u>3.993</u>	<u>3.992</u>	<u>3.987</u>	<u>3.980</u>	<u>4.007</u>	<u>3.998</u>
Wo	42.21	44.11	43.26	43.66	44.09	43.48	43.92	44.55	44.28
En	37.67	38.53	42.14	34.27	33.25	41.80	35.02	35.18	34.87
Fs	20.12	17.37	14.61	22.08	22.66	14.72	21.06	20.28	20.85

	9	10	11	12	13	14
SiO ₂	47.58	39.19	38.83	46.13	39.92	54.13
Al ₂ O ₃	24.81	30.23	30.65	10.48	29.73	1.70
Cr ₂ O ₃	-	-	-	.12	-	.21
FeO ³	.14	.21	-	.24	-	.22
MgO	-	-	-	.41	-	-
NiO	-	-	-	-	-	-
CaO	7.93	12.22	12.52	28.55	11.50	33.25
Na ₂ O	-	4.02	4.06	.44	4.23	-
K ₂ O	5.08	-	-	-	-	-
TiO ₂	-	-	-	-	-	-
V ₂ O ₃	-	-	-	-	-	-
<u>Total</u>	<u>85.53</u>	<u>85.87</u>	<u>86.05</u>	<u>86.37</u>	<u>85.38</u>	<u>89.51</u>

- 1 - 8 Traverse of pyroxenes across 1.5 cm. wide altered zone around vesicle.
1 Furthest from vesicle, 8 part of vesicle edge almost completely surrounded by zeolites.
- 9 Groundmass zeolite adjacent to 3 - probably Phillipsite.
- 10 Groundmass zeolite adjacent to 5 - probably Thomsonite.
- 11 - 14 Zeolites infilling vesicle.
11,13 probably Thomsonite.
12 unknown mineral
14 gyrolite fills central part of vesicle.

	<u>M 13</u>							
	1	2	3	4	5	6	7	8
SiO ₂	58.92	63.59	65.55	60.21	65.19	64.60	62.66	28.78
Al ₂ O ₃	20.82	20.54	20.59	19.21	20.45	19.51	18.73	17.86
Cr ₂ O ₃	-	-	-	-	-	-	-	.19
FeO*	2.99	1.41	.70	2.26	.40	.30	.80	20.31
MnO	-	-	-	-	-	-	-	.23
MgO	1.46	0.70	.28	1.89	-	-	.54	19.54
NiO	-	-	-	-	-	-	-	.14
CaO	3.39	1.35	1.13	1.01	.79	.43	.17	.14
Na ₂ O	8.41	9.93	10.55	5.88	8.63	5.55	1.49	-
K ₂ O	.10	.23	-	4.98	3.39	7.25	12.79	-
TiO ₂	-	-	-	.13	-	-	.30	-
V ₂ O ₃	-	-	-	-	-	-	-	-
Total	96.10	97.74	98.80	95.77*	98.87	97.65	97.48	87.18

Cation proportions

	1	2	3	4	5	6	7	8
Basis	0 = 8	0 = 8	0 = 8	0 = 8	0 = 8	0 = 8	0 = 8	0 = 28
Si	2.753	2.875	2.914	2.838	2.926	2.963	2.946	5.929
Al	1.147	1.095	1.079	1.068	1.082	1.055	1.038	4.336
Cr	-	-	-	-	-	-	-	0.031
Fe	0.117	0.053	0.026	0.089	0.015	0.011	0.031	3.500
Mn	-	-	-	-	-	-	-	0.039
Mg	0.102	0.047	0.019	0.132	-	-	0.038	5.998
Ni	-	-	-	-	-	-	-	0.023
Ca	0.170	0.066	0.054	0.051	0.038	0.021	0.009	0.031
Na	0.762	0.870	0.909	0.537	0.751	0.494	0.136	-
K	0.006	0.013	-	0.299	0.194	0.424	0.767	-
Ti	-	-	-	0.005	-	-	0.011	-
V	-	-	-	-	-	-	-	-
Σ	5.057	5.019	5.001	5.020	5.006	4.968	4.976	19.887
An	18.11	An 6.91	An 5.61	An 5.73	An 3.88	An 2.26	An 0.95	
Ab	81.25	Ab 91.69	Ab 94.39	Ab 60.55	Ab 76.36	Ab 52.57	Ab 14.91	
Or	0.64	Or 1.40	Or -	Or 33.72	Or 19.76	Or 45.17	Or 84.14	

	9	10	11	12	13	14	15
SiO ₂	29.56	29.16	38.35	31.44	31.68	32.49	S 34.32
Al ₂ O ₃	18.69	18.41	24.17	2.62	2.74	2.98	Fe 30.83
Cr ₂ O ₃	-	-	-	-	-	-	Mn -
FeO*	19.77	20.34	11.10	1.70	1.58	1.71	Co .29
MnO	.27	.30	-	-	-	-	Cu 33.73
MgO	20.31	20.29	.28	-	-	-	Zn -
NiO	-	.14	-	-	-	-	Ni -
CaO	.09	.13	23.19	27.22	28.09	27.43	Cr -
Na ₂ O	-	-	-	-	-	-	Ti -
K ₂ O	-	-	-	-	-	-	Mg -
TiO ₂	-	-	-	33.06	33.38	32.27	Si .26
V ₂ O ₃	-	-	-	.50	.52	.51	Al -
Total	88.68	88.72	97.07	96.54	97.99	97.38	92.43

Cation proportions

	9	10	11	12	13	14
Basis	0 = 28	0 = 28	0 = 13	0 = 20	0 = 20	0 = 20
Si	5.942	5.889	3.238	4.237	4.212	4.324
Al	4.428	4.383	2.406	0.416	0.429	0.468
Cr	-	-	-	-	-	-
Fe	3.324	3.436	0.784	0.191	0.175	0.191
Mn	0.046	0.052	-	-	-	-
Mg	6.083	6.108	0.035	-	-	-
Ni	-	0.023	-	-	-	-
Ca	0.020	0.028	2.098	3.931	4.001	3.913
Na	-	-	-	-	-	-
K	-	-	-	-	-	-
Ti	-	-	-	3.350	3.337	3.232
V	-	-	-	0.054	0.055	0.055
Σ	19.844	19.919	8.561	12.178	12.209	12.182

- 1 - 7 Clouded groundmass feldspars, all except 5 and 6 appear to have inclusions of chlorite/sphere
 4 - analysis included 0.21% P₂O₅ = enclosed apatite ?
 8 Chlorite pseudomorph after olivine.
 9 - 15 All from secondary mineral pods/vesicles.
 9,10 Chlorite
 11 Epidote coexisting with 9
 12 - 14 Sphere
 15 Chalcopyrite.

M 14

	1	2	3	4	5	6	7	8
SiO ₂	49.12	51.24	50.68	64.94	27.99	29.60	.15	.27
Al ₂ O ₃	3.31	1.64	3.29	18.82	15.84	17.10	-	33.97
Cr ₂ O ₃	.27	.33	-	-	-	-	-	25.40
FeO	8.97	8.83	12.98	.41	17.86	18.07	.19	27.74
MnO	.20	.14	.36	-	.17	.22	-	.34
MgO	13.61	15.03	15.09	-	19.71	21.81	-	11.43
NiO	-	-	-	-	.13	-	-	.19
CaO	20.59	19.68	11.68	.18	.21	.20	57.42	-
Na ₂ O	.42	.41	-	3.11	-	-	-	-
K ₂ O	-	-	-	11.28	-	-	-	-
TiO ₂	1.62	.79	-	-	-	-	-	.63
V ₂ O ₃	.13	.18	-	-	-	-	-	.18
<u>Total</u>	<u>98.23</u>	<u>98.26</u>	<u>94.08</u>	<u>98.72</u>	<u>81.91</u>	<u>87.01</u>	<u>57.76</u>	<u>100.15</u>

Cation proportions

	1	2	3	4	5	6	7	8
Basis	0 = 6	0 = 6	0 = 23	0 = 8	0 = 28	0 = 28		0 = 32
Si	1.872	1.939	7.602	2.988	6.087	6.029		0.064
Al	0.149	0.073	0.581	1.021	4.059	4.107		9.664
Cr	0.008	0.010	-	-	-	-		4.848
Fe	0.286	0.280	1.628	0.016	3.248	3.079		5.600
Mn	0.006	0.004	0.046	-	0.031	0.038		0.072
Mg	0.773	0.847	3.373	-	6.386	6.620		4.112
Ni	-	-	-	-	0.023	-		0.040
Ca	0.841	0.798	1.878	0.009	0.049	0.044		-
Na	0.031	0.030	-	0.277	-	-		-
K	-	-	-	0.662	-	-		-
Ti	0.046	0.022	-	-	-	-		0.112
V	0.004	0.005	-	-	-	-		0.032
Σ	<u>4.016</u>	<u>4.009</u>	<u>15.108</u>	<u>4.971</u>	<u>19.883</u>	<u>19.917</u>		<u>24.544</u>

Wo 42.20 Wo40.54 An 0.92
 En 41.94 En44.54 Ab29.24
 Fs 15.86 Fsl4.92 Or69.84

- 1 - 2 Relict pyroxenes
 3 Amphibole fringing pyroxene
 4 Groundmass feldspar
 5 Chlorite pseudomorph after olivine
 6 Chlorite in secondary pod
 7 Calcite in secondary pod
 8 Chrome spinel inside olivine pseudomorph

M 15

	1	2	3	4	5	6	7	8	9
SiO ₂	50.59	49.36	61.53	59.45	30.23	28.47	65.25	67.05	66.16
Al ₂ O ₃	3.08	3.79	18.78	20.26	17.04	17.34	21.03	20.50	20.41
Cr ₂ O ₃	.66	.29	-	-	-	-	-	-	-
FeO ^a	7.63	8.17	2.76	2.80	16.76	16.58	-	-	-
MnO	.15	.12	-	-	.16	.13	-	-	-
MgO	14.64	13.99	2.99	3.24	22.55	21.49	-	-	-
NiO	-	-	-	-	-	-	-	-	-
CaO	20.57	20.76	3.27	1.44	.22	.30	1.64	1.06	1.01
Na ₂ O	-	.51	8.91	9.00	-	-	10.91	11.02	10.96
K ₂ O	-	-	.21	.12	-	-	-	.08	.09
TiO ₂	1.23	1.66	.53	-	-	-	-	-	-
V ₂ O ₃	-	.28	-	-	-	-	-	-	-
Total	98.55	98.93	98.97	96.31	86.95	84.32	98.84	99.70	98.63

Cation proportions

	1	2	3	4	5	6	7	8	9
Basis	0 = 6	0 = 6	0 = 8	0 = 8	0 = 28	0 = 28	0 = 8	0 = 8	0 = 8
Si	1.902	1.861	2.795	2.761	6.108	5.952	2.900	2.944	2.938
Al	0.137	0.168	1.006	1.110	4.059	4.274	1.102	1.061	1.068
Cr	0.020	0.009	-	-	-	-	-	-	-
Fe	0.240	0.258	0.105	0.109	2.832	2.899	-	-	-
Mn	0.005	0.004	-	-	0.028	0.024	-	-	-
Mg	0.820	0.786	0.203	0.224	6.789	6.695	-	-	-
Ni	-	-	-	-	-	-	-	-	-
Ca	0.828	0.839	0.159	0.072	0.046	0.067	0.078	0.050	0.048
Na	-	0.038	0.784	0.810	-	-	0.940	0.938	0.943
K	-	-	0.012	0.007	-	-	-	0.004	0.005
Ti	0.035	0.047	0.018	-	-	-	-	-	-
V	-	0.008	-	-	-	-	-	-	-
Σ	3.985	4.018	5.082	5.093	19.862	19.911	5.019	4.997	5.002
Wo		Wo	An 16.64	An 8.07			An 7.68	An 5.02	An 4.82
En		En	Ab 82.10	Ab 91.12			Ab 92.32	Ab 94.55	Ab 94.67
Fs		Fs	Or 1.26	Or 0.81			Or -	Or 0.43	Or 0.51

	10	11	12	13	14	15
SiO ₂	51.96	51.83	51.80	37.69	37.42	.27
Al ₂ O ₃	2.46	2.58	2.30	22.43	21.45	-
Cr ₂ O ₃	-	-	-	-	.13	-
FeO ^a	16.09	15.38	15.44	13.45	14.25	-
MnO	.41	.41	.55	.12	-	.13
MgO	12.51	12.54	12.98	-	-	-
NiO	-	-	-	-	-	-
CaO	12.26	12.38	12.14	22.51	23.33	55.01
Na ₂ O	-	-	.44	-	-	-
K ₂ O	-	-	-	-	-	-
TiO ₂	-	-	-	-	.25	-
V ₂ O ₃	-	-	-	-	-	-
Total	95.69	95.13	95.65	96.20	96.83	55.41

Cation proportions

	10	11	12	13	14
Basis	0 = 23	0 = 23	0 = 23	0 = 13	0 = 13
Si	7.768	7.772	7.745	3.256	3.238
Al	0.433	0.456	0.406	2.284	2.189
Cr	-	-	-	-	0.009
Fe	2.012	1.929	1.931	0.972	1.031
Mn	0.052	0.053	0.070	0.008	-
Mg	2.786	2.803	2.891	-	-
Ni	-	-	-	-	-
Ca	1.964	1.988	1.945	2.083	2.164
Na	-	-	0.127	-	-
K	-	-	-	-	-
Ti	-	-	-	-	0.016
V	-	-	-	-	-
Σ	15.015	15.000	15.115	8.602	8.647

- 1,2 Relict pyroxenes.
 3,4 Groundmass feldspar.
 3 has inclusions of sphene and chlorite
 4 has chlorite inclusions.
 5 Chlorite pseudomorph after olivine.
 6 - 15 All from same secondary mineral pod.
 6 Chlorite rim.
 7 - 9 Albite.
 10 - 12 Actinolite.
 13,14 Epidote.
 15 Calcite.

M 16

	1	2	3	4	5	6	7	8
SiO ₂	49.86	57.85	63.79	28.68	29.57	49.70	38.57	37.89
Al ₂ O ₃	3.50	22.12	20.03	17.81	17.69	4.09	21.64	23.30
Cr ₂ O ₃	.45	-	-	.21	-	-	-	-
FeO ³	7.84	1.23	.36	17.42	17.27	19.56	13.88	12.70
MnO	.20	-	-	.27	.18	.82	.11	-
MgO	14.05	1.02	0.25	21.77	22.28	10.30	.72	-
NiO	-	-	-	-	-	-	-	-
CaO	20.84	5.17	1.13	.10	.12	11.26	22.27	23.14
Na ₂ O	-	7.34	3.70	-	-	-	-	-
K ₂ O	-	.07	9.03	-	-	-	-	-
TiO ₂	1.52	.24	-	-	-	-	.21	-
V ₂ O ₃	.15	-	-	-	-	-	.20	-
Total	98.42	95.04	98.28	86.25	87.10	95.73	97.52	97.03

Cation proportions

	1	2	3	4	5	6	7	8
Basis	0 = 6	0 = 8	0 = 8	0 = 28	0 = 28	0 = 23	0 = 13	0 = 13
Si	1.883	2.715	2.929	5.885	5.985	7.565	3.286	3.232
Al	0.156	1.224	1.084	4.308	4.220	0.733	2.174	2.343
Cr	0.013	-	-	0.033	-	-	-	-
Fe	0.248	0.048	0.014	2.990	2.923	2.490	0.989	0.906
Mn	0.006	-	-	0.047	0.030	0.106	0.008	-
Mg	0.791	0.071	0.017	6.658	6.721	2.377	0.092	-
Ni	-	-	-	-	-	-	-	-
Ca	0.843	0.260	0.055	0.021	0.027	1.837	2.033	2.115
Na	-	0.668	0.329	-	-	-	-	-
K	-	0.004	0.529	-	-	-	-	-
Ti	0.043	0.009	-	-	-	-	0.013	-
V	0.005	-	-	-	-	-	0.014	-
Σ	3.987	5.000	4.958	19.94	19.905	15.068	8.609	8.596
Wo	42.08	An	27.91	An	6.07			
En	43.84	Ab	71.61	Ab	36.03			
Fs	14.08	Or	0.48	Or	57.90			

	9	10	11		12	13	14
SiO ₂	.23	2.80	.51	S	33.15	19.89	19.94
Al ₂ O ₃	-	.51	-	Fe	29.26	.67	.41
Cr ₂ O ₃	-	-	-	Mn	-	-	-
FeO ³	-	89.60	90.65	Co	.30	-	-
MnO	.11	-	-	Cu	32.83	79.25	79.60
MgO	-	-	.28	Zn	-	-	-
NiO	-	-	-	Ni	-	-	-
CaO	57.79	-	-	Cr	-	-	-
Na ₂ O	-	-	-	Ti	-	-	-
K ₂ O	-	-	-	Mg	-	-	-
TiO ₂	-	-	-	Si	.12	-	.21
V ₂ O ₃	-	-	-	Al	-	-	-
Total	58.13	92.71	91.44		95.67	99.80	100.15

- 1 Relict clinopyroxene.
 2 Groundmass plagioclase - with chlorite and sphene inclusions.
 3 Alkali feldspar adjacent to secondary mineral pod.
 4 Chlorite pseudomorph after olivine.
 5 - 15 All from secondary mineral pod.
 5 Chlorite.
 6 Actinolite.
 7,8 Epidote.
 9 Calcite.
 10,11 Fe-oxides being replaced by sulphides.
 12 - 14 Sulphides replacing 10 and 11.
 11,12,13 all from one crystal.
 11 centre
 13 margin.

M 18

	1	2	3	4	5	6	7	8	9	10	11
SiO ₂	51.97	49.83	48.90	62.99	56.77	54.33	59.58	30.44	30.47	53.67	53.72
Al ₂ O ₃	1.58	3.82	3.44	22.53	24.09	20.18	21.68	18.49	18.16	1.12	2.43
Cr ₂ O ₃	.24	.89	-	-	-	-	-	.12	-	-	-
FeO	7.86	7.04	10.13	.36	1.03	1.77	1.15	15.41	16.04	12.13	11.58
MnO	.16	.15	.19	-	-	-	-	.19	.19	.19	.29
MgO	15.23	14.41	13.13	-	.89	1.75	1.10	19.64	20.81	15.55	16.50
NiO	-	-	-	-	-	-	-	-	-	-	-
CaO	20.20	20.98	20.07	3.40	6.52	8.36	4.33	1.27	.99	12.45	11.73
Na ₂ O	-	-	.58	8.17	5.83	1.35	7.24	-	-	-	.43
K ₂ O	-	-	-	2.08	.69	1.36	.10	-	-	-	-
TiO ₂	.82	1.08	2.08	-	-	.28	-	-	-	-	-
V ₂ O ₃	-	.20	.21	-	-	-	-	-	-	-	-
<u>Total</u>	<u>98.05</u>	<u>98.40</u>	<u>98.73</u>	<u>99.53</u>	<u>95.81</u>	<u>89.73</u>	<u>95.17</u>	<u>85.56</u>	<u>86.65</u>	<u>95.11</u>	<u>96.68</u>

Cation proportions

Basis	1 0 = 6	2 0 = 6	3 0 = 6	4 0 = 8	5 0 = 8	6 0 = 8	7 0 = 8	8 0 = 28	9 0 = 28	10 0 = 23	11 0 = 23
Si	1.957	1.877	1.862	2.815	2.650	2.717	2.774	6.203	6.151	7.906	7.759
Al	0.070	0.170	0.154	1.187	1.325	1.189	1.190	4.442	4.322	0.195	0.414
Cr	0.007	0.026	-	-	-	-	-	0.020	-	-	-
Fe	0.248	0.222	0.323	0.013	0.040	0.074	0.045	2.626	2.708	1.494	1.398
Mn	0.005	0.005	0.006	-	-	-	-	0.033	0.032	0.024	0.036
Mg	0.855	0.809	0.745	-	0.062	0.130	0.077	5.965	6.262	3.414	3.552
Ni	-	-	-	-	-	-	-	-	-	-	-
Ca	0.815	0.847	0.819	0.163	0.326	0.448	0.216	0.277	0.214	1.964	1.816
Na	-	-	0.043	0.708	0.527	0.131	0.654	-	-	-	0.119
K	-	-	-	0.119	0.041	0.086	0.006	-	-	-	-
Ti	0.023	0.031	0.060	-	-	0.010	-	-	-	-	-
V	-	0.006	0.006	-	-	-	-	-	-	-	-
<u>Σ</u>	<u>3.981</u>	<u>3.992</u>	<u>4.019</u>	<u>5.005</u>	<u>4.972</u>	<u>4.787</u>	<u>4.961</u>	<u>19.566</u>	<u>19.688</u>	<u>14.997</u>	<u>15.094</u>
Wo	41.22	Wo 41.96	Wo 41.54	An 16.47	An 36.44	An 67.34	An 24.67				
En	45.37	En 45.34	En 40.56	Ab 71.54	Ab 58.95	Ab 19.66	Ab 74.68				
Fs	13.41	Fs 12.70	Fs 17.90	Or 12.00	Or 4.61	Or 13.00	Or 0.65				

1 - 3 Relict pyroxenes.
 4 - 7 Groundmass feldspars.
 8,9 Chlorite pseudomorphs after olivine.

10 Actinolite fringe on pyroxene.
 11 Actinolite replacing chlorite pseudomorph after olivine.

C 54

	1	2	3	4	5	6
SiO ₂	29.53	29.30	28.94	37.27	38.59	37.63
Al ₂ O ₃	17.62	17.02	16.49	21.76	21.10	23.30
Cr ₂ O ₃	.15	-	-	.12	-	-
FeO ³	16.96	15.96	16.26	14.65	12.88	12.79
MnO	.17	.18	.12	-	-	.13
MgO	22.30	22.13	21.79	.35	1.44	-
NiO	.14	-	.14	-	-	-
CaO	.25	.21	.26	22.47	21.66	22.93
Na ₂ O	-	-	-	-	-	-
K ₂ O	-	-	-	-	-	-
TiO ₂	-	-	-	-	-	-
V ₂ O ₃	-	-	-	-	-	-
<u>Total</u>	<u>87.10</u>	<u>84.80</u>	<u>84.01</u>	<u>96.62</u>	<u>95.67</u>	<u>96.78</u>

Cation proportions

	1	2	3	4	5	6
Basis	0 = 28	0 = 28	0 = 28	0 = 13	0 = 13	0 = 13
Si	5.977	6.059	6.065	3.230	3.331	3.221
Al	4.204	4.149	4.074	2.224	2.147	2.352
Cr	0.024	-	-	0.008	-	-
Fe	2.872	2.760	2.850	1.062	0.930	0.916
Mn	0.028	0.032	0.022	-	-	0.009
Mg	6.726	6.820	6.805	0.045	0.185	-
Ni	0.023	-	0.024	-	-	-
Ca	0.054	0.046	0.058	2.086	2.003	2.104
Na	-	-	-	-	-	-
K	-	-	-	-	-	-
Ti	-	-	-	-	-	-
V	-	-	-	-	-	-
<u>Σ</u>	<u>19.908</u>	<u>19.866</u>	<u>19.898</u>	<u>8.625</u>	<u>8.596</u>	<u>8.602</u>

- 1 Chlorite pseudomorph after olivine.
 2,3 Chlorite infilling vesicles.
 4 Epidote replacing 1.
 5,6 Epidote from centre vesicles.

C 130

	1	2	3	4	5	6	7	8
SiO ₂	.57	37.49	37.74	36.86	37.38	36.86	42.47	42.53
Al ₂ O ₃	.22	24.99	25.92	21.63	25.13	21.45	20.95	21.44
Cr ₂ O ₃	-	-	-	-	-	-	-	-
FeO ³	-	9.90	9.60	13.23	10.07	14.05	4.16	3.14
MnO	.33	-	-	-	-	-	-	-
MgO	-	-	-	-	-	-	-	-
NiO	-	-	-	-	-	-	-	-
CaO	47.34	22.57	22.38	22.42	22.44	22.41	24.95	25.14
Na ₂ O	-	-	-	-	-	-	-	-
K ₂ O	-	-	-	-	-	-	-	-
TiO ₂	-	-	-	.48	-	.12	-	-
V ₂ O ₃	-	-	-	-	-	-	-	-
<u>Total</u>	<u>48.46</u>	<u>94.94</u>	<u>95.64</u>	<u>94.62</u>	<u>95.02</u>	<u>94.89</u>	<u>92.53</u>	<u>92.25</u>

Cation proportions

	2	3	4	5	6	7	8
Basis	0 = 13	0 = 13	0 = 13	0 = 13	0 = 13	0 = 26	0 = 26
Si	3.214	3.200	3.242	3.204	3.246	7.254	7.250
Al	2.525	2.591	2.244	2.540	2.227	4.220	4.308
Cr	-	-	-	-	-	-	-
Fe	0.709	0.681	0.973	0.722	1.035	0.594	0.448
Mn	-	-	-	-	-	-	-
Mg	-	-	-	-	-	-	-
Ni	-	-	-	-	-	-	-
Ca	2.074	2.033	2.114	2.061	2.115	4.568	4.592
Na	-	-	-	-	-	-	-
K	-	-	-	-	-	-	-
Ti	-	-	0.031	-	0.008	-	-
V	-	-	-	-	-	-	-
<u>Σ</u>	<u>8.523</u>	<u>8.504</u>	<u>8.604</u>	<u>8.526</u>	<u>8.632</u>	<u>16.636</u>	<u>16.598</u>

- 1-4 All from same vesicle.
 1 Calcite
 2-4 Epidote
 5-8 All from same vesicle.
 5,6 Epidote.
 7,8 Pumpellyite.

C 158

	1	2	3	4	5
SiO ₂	31.85	30.95	29.54	29.12	56.56
Al ₂ O ₃	16.41	17.25	17.74	18.08	18.04
Cr ₂ O ₃	.11	-	-	-	-
FeO	17.31	17.75	19.39	18.82	.49
MnO	.18	.13	.32	.25	-
MgO	22.86	22.03	21.54	22.01	.50
NiO	-	-	-	-	-
CaO	.40	.38	-	.10	8.29
Na ₂ O	-	-	-	-	-
K ₂ O	-	-	-	-	-
TiO ₂	-	-	-	-	-
V ₂ O ₃	-	-	-	-	-
Total	89.10	88.48	88.52	88.37	83.88

Cation proportions

Basis	0 = 28	0 = 28	0 = 28	0 = 28
	1	2	3	4
Si	6.282	6.164	5.949	5.862
Al	3.815	4.051	4.212	4.292
Cr	0.017	-	-	-
Fe	2.856	2.956	3.265	3.169
Mn	0.030	0.023	0.054	0.042
Mg	6.719	6.537	6.463	6.605
Ni	-	-	-	-
Ca	0.084	0.080	-	0.021
Na	-	-	-	-
K	-	-	-	-
Ti	-	-	-	-
V	-	-	-	-
Σ	19.802	19.810	19.94	19.991

- 1 Chlorite pseudomorph after olivine.
- 2 Granular brown - green chlorite lining vesicle.
- 3,4 Green - brown chlorite fibres infilling vesicle.
- 5 Zeolite (probably stilbite) replacing chlorite in olivine pseudomorph.

M 69

	1	2	3	4	5	6	7	8
SiO ₂	49.21	48.30	28.74	28.93	37.48	36.30	35.83	.19
Al ₂ O ₃	2.99	3.98	17.61	17.31	12.29	3.10	5.73	-
Cr ₂ O ₃	-	.21	-	-	-	-	.17	-
FeO	12.69	10.08	16.26	15.87	13.47	24.79	21.49	.20
MnO	.20	.16	.20	.27	1.12	.44	.34	.21
MgO	11.57	13.05	23.48	22.83	-	-	-	-
NiO	-	-	-	-	-	-	-	-
CaO	19.98	19.92	.09	.21	34.04	33.23	33.29	54.44
Na ₂ O	-	-	-	-	-	-	-	-
K ₂ O	-	-	-	-	-	-	-	-
TiO ₂	2.12	2.08	-	-	-	-	.12	-
V ₂ O ₃	.25	.21	-	-	-	-	-	-
Total	99.00	98.00	86.38	85.43	98.40	97.86	96.97	55.04

Cation proportions

Basis	0 = 6	0 = 6	0 = 28	0 = 28	0 = 24	0 = 24	0 = 24
	1	2	3	4	5	6	7
Si	1.885	1.850	5.852	5.946	6.187	6.463	6.318
Al	0.135	0.180	4.228	4.195	2.392	0.651	1.191
Cr	-	0.006	-	-	-	-	0.024
Fe	0.407	0.323	2.770	2.728	1.859	3.691	3.169
Mn	0.007	0.005	0.034	0.047	0.157	0.067	0.051
Mg	0.661	0.745	7.128	6.994	-	-	-
Ni	-	-	-	-	-	-	-
Ca	0.820	0.818	0.020	0.047	6.022	6.340	6.290
Na	-	-	-	-	-	-	-
K	-	-	-	-	-	-	-
Ti	0.061	0.060	-	-	-	-	0.016
V	0.008	0.007	-	-	-	-	-
Σ	3.983	3.993	20.033	19.957	16.617	17.212	17.059

- Wo 41.21 Wo 40.31
- En 36.17 En 41.44
- Fs 22.62 Fs 18.25

- 1,2 Relict pyroxenes.
- 3,4 Chlorite lining vesicle/pod.
- 5-7 Andraditic hydrogrossulars from centre vesicle/pod.
- 8 Calcite enclosed by garnet.

M 70 - Secondary mineral pod from upper flow Pennygown Quarry.

Late pyritised dyke in Pennygown Quarry

	1	2	3	4	5	6
SiO ₂	30.55	38.08	28.21	31.10	29.46	29.09
Al ₂ O ₃	2.89	25.43	18.44	18.75	17.13	17.22
Cr ₂ O ₃	-	-	-	-	-	.11
FeO	1.61	10.36	22.04	20.66	22.17	22.36
MnO	-	.15	.40	.30	.24	.33
MgO	.21	-	18.24	17.11	18.79	18.87
NiO	-	-	-	-	-	-
CaO	27.94	23.14	.19	1.55	.17	.24
Na ₂ O	-	-	-	-	-	-
K ₂ O	-	-	-	-	-	-
TiO ₂	34.94	-	-	-	-	-
V ₂ O ₅	.34	-	-	-	-	-
<u>Total</u>	<u>98.46</u>	<u>97.16</u>	<u>87.52</u>	<u>89.47</u>	<u>87.95</u>	<u>88.22</u>

Cation proportions

	1	2	3	4	5	6
Basis	O = 20	O = 13	O = 28	O = 28	O = 28	O = 28
Si	4.052	3.200	5.843	6.218	6.059	5.983
Al	0.451	2.519	4.502	4.420	4.153	4.176
Cr	-	-	-	-	-	0.017
Fe	0.179	0.728	3.818	3.454	3.813	3.846
Mn	-	0.010	0.070	0.050	0.041	0.058
Mg	0.041	-	5.631	5.097	5.759	5.786
Ni	-	-	-	-	-	-
Ca	3.971	2.084	0.042	0.333	0.038	0.054
Na	-	-	-	-	-	-
K	-	-	-	-	-	-
Ti	3.486	-	-	-	-	-
V	0.036	-	-	-	-	-
<u>Σ</u>	<u>12.216</u>	<u>8.541</u>	<u>19.906</u>	<u>19.572</u>	<u>19.864</u>	<u>19.920</u>

- 1 - 3 Dark rock immediately adjacent to pod
 1 Granular sphene
 2 Epidote
 3 Groundmass chlorite
 4 - 6 Chlorite from pod
 4 Margin
 6 Centre

	1	2	3		4a	4b	5	6	7
SiO ₂	65.54	65.54	29.81	S	50.39	52.17	51.16	50.97	51.88
Al ₂ O ₃	18.49	18.69	16.87	Fe	46.93	47.01	46.22	46.40	46.63
Cr ₂ O ₃	-	-	-	Mn	-	-	-	-	-
FeO	-	-	23.95	Co	.66	.70	.70	.58	.55
MnO	-	-	.22	Cu	-	-	-	-	-
MgO	-	-	17.85	Zn	-	-	.21	.24	-
NiO	-	-	-	Ni	-	-	-	-	-
CaO	-	-	.61	Cr	-	-	-	-	-
Na ₂ O	-	-	-	Ti	.17	-	-	-	-
K ₂ O	16.00	16.09	-	Mg	-	-	-	-	-
TiO ₂	.13	.18	-	Si	.61	.40	.82	.70	.55
V ₂ O ₅	-	-	-	Al	-	-	-	-	-
<u>Total</u>	<u>100.16</u>	<u>100.50</u>	<u>89.30</u>		<u>98.76</u>	<u>100.29</u>	<u>99.11</u>	<u>98.90</u>	<u>99.61</u>

Cation proportions

	1	2	3
Basis	O = 8	O = 8	O = 28
Si	3.010	3.002	6.096
Al	1.001	1.009	4.066
Cr	-	-	-
Fe	-	-	4.096
Mn	-	-	0.038
Mg	-	-	5.442
Ni	-	-	-
Ca	-	-	0.133
Na	-	-	-
K	0.938	0.940	-
Ti	0.005	0.006	-
V	-	-	-
<u>Σ</u>	<u>4.954</u>	<u>4.957</u>	<u>19.870</u>

- 1,2 Orthoclase in veins associated with pyrites.
 3 Chlorite associated with 2.
 4 - 7 Pyrites disseminated in dyke adjacent to veins.
 4a/b core and rim of large crystal which appears patchy in reflected light.

Toll Doire Quarry lava.

	<u>M 29</u>					<u>M 30</u>			
	1	2	3	4	5	1	2	3	4
SiO ₂	46.15	55.92	50.61	53.84	52.48	28.12	34.50	34.36	34.49
Al ₂ O ₃	5.40	24.99	28.86	27.63	25.78	18.74	30.89	30.74	30.93
Cr ₂ O ₃	.14	-	-	-	-	-	-	-	-
FeO	11.85	.37	.84	.49	-	22.72	-	-	-
MnO	.14	-	-	-	-	.19	.35	.31	.39
MgO	10.30	-	.22	-	.12	18.49	34.37	34.44	34.24
NiO	-	-	-	-	-	.14	-	-	-
CaO	20.64	8.80	10.76	9.30	8.53	.11	-	-	-
Na ₂ O	-	6.41	2.09	5.95	2.46	-	-	-	-
K ₂ O	-	.07	4.29	-	3.76	-	-	-	-
TiO ₂	3.31	1.70	-	-	.13	.13	-	-	-
V ₂ O ₃	.29	-	-	-	-	-	.15	.19	.18
<u>Total</u>	<u>98.22</u>	<u>98.25</u>	<u>97.67</u>	<u>97.20</u>	<u>93.24</u>	<u>88.65</u>	<u>100.24</u>	<u>100.04</u>	<u>100.22</u>

Cation proportions

Basis	1	2	3	4	5	1
	0 = 6	0 = 8	0 = 8	0 = 8	0 = 8	0 = 28
Si	1.788	2.562	2.387	2.495	2.548	5.767
Al	0.247	1.350	1.605	1.509	1.476	4.531
Cr	0.004	-	-	-	-	-
Fe	0.384	0.014	0.033	0.019	0.005	3.896
Mn	0.005	-	-	-	-	0.033
Mg	0.595	-	0.016	-	-	5.651
Ni	-	-	-	-	-	0.024
Ca	0.857	0.432	0.544	0.462	0.444	0.025
Na	-	0.569	0.191	0.541	0.231	-
K	-	0.004	0.258	-	0.233	-
Ti	0.096	0.059	-	-	0.005	0.020
V	0.009	-	-	-	-	-
<u>Σ</u>	<u>3.985</u>	<u>4.991</u>	<u>5.035</u>	<u>5.026</u>	<u>4.941</u>	<u>19.947</u>

Wo 42.65 An 42.95 An 54.76 An 46.34 An 48.88
 En 34.69 Ab 56.62 Ab 19.28 Ab 53.66 Ab 25.48
 Fs 22.69 Or 0.43 Or 25.97 Or - Or 24.64

- 1 Relict pyroxene.
 2 - 5 Altered groundmass feldspars
 2 plagioclase with sphene inclusions.
 5 partially zeolitised.

- 1 Groundmass chlorite.
 2 - 4 Chalcopyrite grains in groundmass.

Altered hawaiite

	<u>M 41</u>						<u>M 46</u>				
	1	2	3	4	5	6	1	2	3	4	5
SiO ₂	53.30	53.06	53.25	48.75	31.65	1.08	53.61	53.43	54.43	32.06	0.70
Al ₂ O ₃	29.47	29.43	27.18	26.99	11.69	1.00	29.79	29.70	29.07	13.78	0.87
Cr ₂ O ₃	-	-	-	-	-	-	-	-	-	-	-
FeO	.56	.54	2.25	6.05	27.87	65.09	.84	.80	.55	25.60	64.13
MnO	-	-	-	-	.15	1.11	-	-	-	-	2.23
MgO	-	-	.33	1.91	14.90	-	-	-	-	15.18	-
NiO	-	-	-	-	-	-	-	-	-	-	-
CaO	11.67	11.67	10.99	10.24	.34	-	11.75	11.44	10.70	.78	0.24
Na ₂ O	4.63	4.44	4.53	3.29	-	-	4.62	4.97	4.93	-	-
K ₂ O	.10	.08	.14	.11	-	-	.11	.12	.10	-	-
TiO ₂	.14	-	.38	.15	-	27.87	.17	.17	-	-	27.70
V ₂ O ₅	-	-	-	-	-	.36	-	-	-	-	.34
<u>Total</u>	<u>99.86</u>	<u>99.21</u>	<u>99.04</u>	<u>97.48</u>	<u>86.61</u>	<u>96.51</u>	<u>100.89</u>	<u>100.63</u>	<u>99.78</u>	<u>87.40</u>	<u>96.21</u>

Cation proportions

	1	2	3	4	5		1	2	3	4		
Basis	0 = 8	0 = 8	0 = 8	0 = 8	0 = 28		8 = 8	8 = 8	0 = 8	0 = 28		
Si	2.417	2.419	2.452	2.327	6.817		2.410	2.409	2.460	6.732		
Al	1.575	1.582	1.476	1.519	2.969		1.578	1.578	1.548	3.411		
Cr	-	-	-	-	-		-	-	-	-		
Fe	0.021	0.021	0.087	0.241	5.021	Recalculated	0.032	0.030	0.021	4.495	Recalculated	
Mn	-	-	-	-	0.028	Analysis	-	-	-	-	Analysis	
Mg	-	-	0.022	0.136	4.784		-	-	-	4.748		
Ni	-	-	-	-	-	FeO	56.67	-	-	-	FeO	54.51
Ca	0.567	0.570	0.542	0.524	0.079	Fe ₂ O ₃	9.37	0.566	0.553	0.518	0.174	10.69
Na	0.407	0.392	0.405	0.304	-		97.46	0.403	0.434	0.432	-	97.28
K	0.006	0.004	0.008	0.006	-			0.006	0.007	0.006	-	
Ti	0.005	-	0.013	0.005	-			0.006	0.006	-	-	
V	-	-	-	-	-			-	-	-	-	
Σ	<u>4.997</u>	<u>4.988</u>	<u>5.004</u>	<u>5.063</u>	<u>19.698</u>		<u>5.000</u>	<u>5.017</u>	<u>4.985</u>	<u>19.562</u>		
	An 57.88	An 58.98	An 56.79	An 62.79			An 58.05	An 55.61	An 54.19			
	Ab 41.56	Ab 40.57	Ab 42.37	Ab 36.44			Ab 41.29	Ab 43.70	Ab 45.20			
	Or 0.56	Or 0.45	Or 0.83	Or 0.77			Or 0.65	Or 0.69	Or 0.61			

1,2 Small plagioclase phenocrysts.
 3,4 Clouded groundmass feldspars.
 4 has chlorite veins and inclusions.
 5 Chlorite pseudomorph after olivine.
 6 Groundmass titanomagnetite.

1 - 3 Small plagioclase phenocrysts.
 4 Chlorite infilling small vesicle.
 5 Groundmass titanomagnetite.

M 48 - Altered Basalt.

	1	2	3	4	5	6	7
SiO ₂	58.50	60.04	60.71	59.06	30.45	S	33.11
Al ₂ O ₃	26.24	25.64	25.01	26.00	15.23	Fe	30.43
Cr ₂ O ₃	-	-	-	-	-	Mn	-
FeO	.29	.33	.39	.28	24.40	Co	.31
MnO	-	-	-	-	.20	Cu	33.32
MgO	-	-	-	-	17.13	Zn	.23
NiO	-	-	-	-	-	Ni	-
CaO	7.34	6.67	6.18	7.21	.36	Cr	-
Na ₂ O	7.05	7.63	7.85	7.23	-	Ti	-
K ₂ O	-	-	-	-	-	Mg	-
TiO ₂	-	-	-	-	-	Si	.87
V ₂ O ₃	-	-	-	-	-	Al	.29
<u>Total</u>	<u>99.41</u>	<u>100.31</u>	<u>100.13</u>	<u>99.83</u>	<u>87.78</u>		<u>98.27</u>

Cation proportions

	1	2	3	4	5
Basis	0 = 8	0 = 8	0 = 8	0 = 8	0 = 28
Si	2.624	2.665	2.695	2.638	6.348
Al	1.388	1.342	1.309	1.369	3.743
Cr	-	-	-	-	-
Fe	0.011	0.012	0.014	0.010	4.254
Mn	-	-	-	-	0.035
Mg	-	-	-	-	5.322
Ni	-	-	-	-	-
Ca	0.353	0.317	0.294	0.345	0.080
Na	0.613	0.657	0.675	0.631	-
K	-	-	-	-	-
Ti	-	-	-	-	-
V	-	-	-	-	-
Σ	4.989	4.992	4.988	4.993	19.781
An	36.52	An32.55	An30.32	An35.35	
Ab	63.48	Ab67.44	Ab69.68	Ab64.65	
Or	-	Or	-	Or	-

- 1 - 4 Slightly clouded groundmass feldspars
 5 Chlorite infilling vesicle/pod
 6, 7 Fe - Cu sulphides inside vesicle/pod

M 49 - Hydrothermal vein from brecciated part of same lava

	1	2	3	4	5	6	7	8
SiO ₂	58.10	57.90	58.33	58.59	-	-	-	-
Al ₂ O ₃	15.04	14.73	14.68	14.70	-	-	-	-
Cr ₂ O ₃	-	-	-	-	-	-	-	-
FeO	-	-	-	-	-	-	-	-
MnO	-	-	-	-	-	-	.18	.26
MgO	-	-	-	-	-	-	-	-
NiO	-	-	-	-	-	-	-	-
CaO	7.83	7.77	7.81	7.87	58.68	57.27	55.23	54.82
Na ₂ O	-	-	-	-	-	-	-	-
K ₂ O	-	-	-	-	-	-	-	-
TiO ₂	-	-	-	-	-	-	-	-
V ₂ O ₃	-	-	-	-	-	-	-	-
<u>Total</u>	<u>80.97</u>	<u>80.40</u>	<u>80.81</u>	<u>81.16</u>	<u>58.68</u>	<u>57.27</u>	<u>55.41</u>	<u>55.08</u>

- 1 - 4 Zeolites probably stilbite
 5 - 8 Calcite

C 212 - Centre of plagioclase pyric flow
in lower half of drill core.

	1	2	3	4	5	6	7	8	9
SiO ₂	47.75	47.67	63.12	62.62	58.28	27.82	26.89	27.21	26.91
Al ₂ O ₃	4.03	4.13	19.29	21.56	17.48	18.16	18.85	17.96	18.85
Cr ₂ O ₃	-	-	-	-	-	-	-	-	-
FeO ³	11.35	12.02	.28	.15	.20	24.40	24.86	24.41	24.45
MnO	-	.18	-	-	-	.39	.43	.38	.39
MgO	10.81	10.33	-	-	-	16.18	16.08	16.55	16.18
NiO	-	-	-	-	-	-	-	-	-
CaO	21.20	20.82	.64	4.33	8.09	.20	.18	-	.14
Na ₂ O	.59	.62	.73	8.04	-	-	-	-	-
K ₂ O	-	-	14.57	-	.08	-	-	-	-
TiO ₂	2.84	2.76	.17	-	-	-	-	-	-
V ₂ O ₅	-	.16	-	-	-	-	-	-	-
Total	98.52	98.69	98.78	96.70	84.13	87.15	87.28	86.50	86.90

Cation proportions

Basis	1	2	3	4	5	6	7	8	9
	0 = 6	0 = 6	0 = 8	0 = 8		0 = 28	0 = 28	0 = 28	0 = 28
Si	1.839	1.839	2.944	2.848		5.865	5.685	5.790	5.700
Al	0.183	0.188	1.061	1.156		4.512	4.698	4.507	4.708
Cr	-	-	-	-		-	-	-	-
Fe	0.366	0.388	0.011	0.006		4.302	4.397	4.343	4.331
Mn	-	0.006	-	-		0.069	0.077	0.069	0.069
Mg	0.621	0.594	-	-		5.084	5.068	5.248	5.108
Ni	-	-	-	-		-	-	-	-
Ca	0.875	0.861	0.032	0.211		0.046	0.040	-	0.031
Na	0.044	0.046	0.066	0.709		-	-	-	-
K	-	-	0.867	-		-	-	-	-
Ti	0.082	0.080	0.006	-		-	-	-	-
V	-	0.005	-	-		-	-	-	-
Σ	4.009	4.007	4.986	4.929		19.878	19.965	19.956	19.946
Wo	44.96	Wo 44.44	An 3.30	An 22.94					
En	34.64	En 33.41	Ab 6.81	Ab 77.06					
Fs	20.41	Fs 22.15	Or 89.88	Or -					

	10	11	12	13	14	15	16	17	18
SiO ₂	62.93	64.58	54.98	48.63	54.45	48.38	37.71	.38	45.66
Al ₂ O ₃	21.38	18.76	28.27	25.45	23.04	21.49	24.41	-	14.08
Cr ₂ O ₃	-	-	-	-	-	-	-	-	-
FeO ³	.22	.11	.24	.40	-	-	11.25	-	.42
MnO	-	-	-	-	-	-	-	-	-
MgO	-	-	-	-	-	-	-	-	-
NiO	-	-	-	-	-	-	-	-	-
CaO	3.09	-	10.12	16.10	10.12	14.86	23.34	54.42	16.65
Na ₂ O	1.27	.51	5.44	5.10	1.49	-	-	-	1.11
K ₂ O	11.09	15.65	.22	.20	.69	.27	-	-	.59
TiO ₂	.12	.18	-	-	-	-	-	-	13.06
V ₂ O ₅	-	-	-	-	-	-	.15	-	-
Total	100.10	99.79	99.26	95.87	89.78	84.99	96.86	54.80	91.57

Cation proportions

Basis	10	11	12	13	16
	0 = 8	0 = 8	0 = 8	0 = 8	0 = 15
Si	2.866	2.983	2.494	2.359	.200
Al	1.148	1.022	1.511	1.455	2.442
Cr	-	-	-	-	-
Fe	0.008	0.004	0.009	0.016	0.799
Mn	-	-	-	-	-
Mg	-	-	-	-	-
Ni	-	-	-	-	-
Ca	0.151	-	0.492	0.837	2.123
Na	0.112	0.045	0.478	0.479	-
K	0.645	0.923	0.013	0.012	-
Ti	0.004	0.006	-	-	-
V	-	-	-	-	0.010
Σ	4.934	4.984	4.997	5.159	8.574

An	16.62	An -	An 50.04	An 62.99
Ab	12.34	Ab 4.70	Ab 48.66	Ab 36.08
Or	71.05	Or 95.30	Or 1.30	Or 0.93

- 1,2 Relict pyroxenes.
3-5 Altered groundmass feldspars
3 - orthoclase,
4 - partially zeolitised albite,
5 - Ca - zeolite probably stilbite.
6,7 Chlorite pseudomorphs after olivine.
8,9 Groundmass chlorite.
10 - 18 All from same altered feldspar phenocryst.
10,11 - alkali feldspar,
12 plagioclase
13,14 partly zeolitised plagioclase.
15 laumontite,
16 epidote,
17 calcite,

C 232 a/b Hydrothermally brecciated lava from lower flow in drill core

	1	2	3	4	5	6	7	8	9
SiO ₂	54.32	26.88	27.76	27.38	27.50	.36	52.75	52.85	52.40
Al ₂ O ₃	21.50	18.38	18.43	17.89	18.58	-	47.21	46.99	46.69
Cr ₂ O ₃	-	-	-	-	-	-	-	-	-
FeO*	.30	26.31	26.19	26.57	26.81	.17	.50	.50	.65
MnO	-	.27	.32	.33	.31	.80	-	-	-
MgO	-	15.29	15.91	14.65	14.85	-	.39	-	-
NiO	-	-	-	-	-	-	-	-	-
CaO	10.07	.21	.09	.18	.17	56.88	-	-	-
Na ₂ O	.85	-	-	-	-	-	-	-	-
K ₂ O	.44	-	-	-	-	-	-	-	-
TiO ₂	.16	-	-	-	.12	-	-	-	.13
V ₂ O ₃	-	-	-	-	-	-	-	-	-
<u>Total</u>	<u>87.62</u>	<u>87.34</u>	<u>88.70</u>	<u>86.99</u>	<u>88.33</u>	<u>58.21</u>	<u>100.84</u>	<u>100.34</u>	<u>99.86</u>

Cation proportions

	2	3	4	5
Basis	0 = 28	0 = 28	0 = 28	0 = 28
Si	5.723	5.797	5.855	5.788
Al	4.614	4.537	4.512	4.611
Cr	-	-	-	-
Fe	4.684	4.573	4.752	4.719
Mn	0.048	0.057	0.060	0.056
Mg	4.852	4.951	4.669	4.658
Ni	-	-	-	-
Ca	0.047	0.021	0.040	0.037
Na	-	-	-	-
K	-	-	-	-
Ti	-	-	-	0.019
V	-	-	-	-
Σ	<u>19,969</u>	<u>19,934</u>	<u>19,888</u>	<u>19,887</u>

- 1 Clouded groundmass feldspar altered to laumontite.
 2,3 Chlorite pseudomorphs after olivine.
 4 Groundmass chlorite.
 5 Chlorite from discordant vein filling hydrofracture.
 6 Calcite from same vein as 5.
 7,8,9 Large euhedral iron pyrites within groundmass.

1 - E CHEMICAL ANALYSES AND C.I.P.W. NORMS

Zeolitised lavas

Hydrothermally altered lavas

Alteration products

Other Mull and Hebridean rocks

Zr values used for Skye - Mull comparison

Note : n.d. is used as an abbreviation
for not detected in these tables.

XENOLITHISED LAVAS

	LA1	LA3	LA5	LA2	LA4	LA7	LA8	LA9	LA10	LA11	LA12
MAJOR ELEMENT (wt. %)											
SiO ₂	46.25	46.46	46.06	46.94	46.16	46.41	46.18	46.29	46.08	46.09	44.14
TiO ₂	2.09	2.05	2.04	2.09	2.04	1.87	1.82	1.82	1.81	1.86	1.53
Al ₂ O ₃	16.54	17.10	16.51	16.93	16.53	17.09	16.67	16.85	17.20	16.73	12.29
Fe ₂ O ₃	4.72	3.96	3.36	3.34	3.37	6.38	3.98	7.92	8.89	4.85	12.93
FeO	9.39	9.93	10.56	10.67	10.36	6.65	8.86	5.62	4.65	8.41	-
MnO	.23	.22	.21	.21	.21	.17	.19	.19	.17	.20	.17
MgO	6.30	6.65	6.44	6.82	6.46	5.94	6.98	6.91	6.60	7.10	9.04
CaO	8.44	8.43	8.71	8.64	8.73	9.25	8.62	8.85	8.95	8.88	7.54
Mn ₂ O	3.17	3.00	2.93	3.06	3.05	2.93	2.83	2.71	2.76	2.86	4.54
K ₂ O	.30	.34	.29	.31	.29	.24	.26	.26	.23	.24	.18
H ₂ O ⁺	2.54	2.22	2.61	1.87	2.34	2.53	2.81	2.44	2.50	2.92	5.92
P ₂ O ₅	.16	.17	.16	.17	.16	.15	.15	.14	.14	.14	.12
CO ₂	.13	.05	.08	.05	.03	.43	.21	.14	.19	.09	.06
TOTAL	100.26	100.58	99.96	101.10	99.75	100.04	99.56	100.14	100.17	100.37	98.46

TRACE ELEMENT (ppm)

Zr	114	114	111	117	112	102	96	96	100	103	89
Y	30	31	29	28	28	26	27	25	28	25	31
Rb	1	3	3	3	3	3	3	1	1	2	9
Nb	6	3	6	8	6	4	5	3	5	5	-
Sr	323	327	319	316	316	344	318	334	325	323	280
Zn	74	70	76	75	79	70	102	139	138	79	-
Cu	32	38	28	52	38	31	94	141	148	27	-
Ba	-	-	-	-	-	73	58	74	63	79	-
Cr	2	8	3	8	7	23	24	20	19	24	-
Ni	44	43	41	35	41	51	47	44	46	47	-
Ta	-	-	-	-	-	-	.26	-	-	-	-
Hf	-	-	-	-	-	-	3.13	-	-	-	-
Th	-	-	-	-	-	-	.32	-	-	-	-
La	-	-	-	-	-	-	4.80	-	-	-	-
Ce	-	-	-	-	-	-	15.07	-	-	-	-
Nd	-	-	-	-	-	-	14.69	-	-	-	-
Sm	-	-	-	-	-	-	4.50	-	-	-	-
Eu	-	-	-	-	-	-	1.68	-	-	-	-
Gd	-	-	-	-	-	-	5.19	-	-	-	-
Tb	-	-	-	-	-	-	.82	-	-	-	-
Tm	-	-	-	-	-	-	.35	-	-	-	-
Yb	-	-	-	-	-	-	2.19	-	-	-	-
Lu	-	-	-	-	-	-	.34	-	-	-	-

CIPW WEIGHT NORMS. (Standard State Fe₂O₃)

Qz	-	-	-	-	-	-	-	-	-	-	-
Or	1.77	2.01	1.71	1.83	1.71	1.42	1.54	1.54	1.36	1.42	1.06
Ab	26.82	25.39	24.79	25.89	25.81	24.79	23.95	22.93	23.35	24.20	25.78
An	30.02	32.19	31.04	31.54	30.61	32.77	32.01	33.04	33.86	32.10	12.62
Ne	-	-	-	-	-	-	-	-	-	-	6.85
Wo	4.17	3.43	4.43	4.13	4.79	3.93	3.53	3.78	3.52	4.37	9.86
En	1.91	1.62	2.05	1.96	2.24	1.85	1.77	1.87	1.71	2.18	5.91
Fe	2.23	1.77	2.34	2.12	2.49	2.04	1.68	1.85	1.75	2.10	3.44
Hy	2.83	3.79	3.77	3.42	2.69	5.66	6.23	6.28	5.71	4.07	-
Fe	3.30	4.13	4.29	3.70	2.99	6.23	5.90	6.21	5.84	3.92	-
Pl	7.76	7.82	7.16	8.13	7.82	5.11	6.58	6.36	6.32	8.01	11.64
Pa	9.87	9.40	8.97	9.68	9.58	6.18	6.87	6.94	7.14	8.51	7.49
Il	3.97	3.89	3.87	3.97	3.87	3.55	3.46	3.46	3.44	3.53	2.91
Mt	2.18	2.18	2.18	2.18	2.18	2.18	2.18	2.18	2.18	2.18	2.90
Ap	.37	.39	.37	.39	.37	.35	.35	.32	.32	.32	.28
H ₂ O	2.54	2.20	2.61	1.87	2.34	2.53	2.81	2.44	2.50	2.92	5.92
Co	.30	.11	.18	.11	.07	.98	.48	.32	.43	.21	.14
TOTAL	99.94	100.33	99.77	100.92	99.56	99.55	99.31	99.50	99.43	100.03	96.79
D.I. ^a	28.60	27.39	26.51	27.72	27.52	26.21	25.48	24.47	24.71	25.62	33.69
F/F _H ^b	.686	.672	.681	.670	.677	.679	.643	.651	.660	.627	.554

^aD.I. = Thornton Tuttle Differentiation Index.

ZEOLITISED LAVAS

	LA13	LA14	LA15	LA16	LA17	LA18	LA20	M1	M5	M6	M7
MAJOR ELEMENT (wt %)											
SiO ₂	45.48	46.08	46.42	45.96	46.26	46.18	45.54	45.76	46.63	46.67	46.94
TiO ₂	1.54	1.54	1.56	1.65	1.70	1.61	1.60	1.81	3.05	3.06	3.07
Al ₂ O ₃	13.45	14.00	13.80	13.97	14.05	13.94	14.31	16.49	16.89	16.67	16.53
Fe ₂ O ₃	3.76	2.43	2.20	3.60	3.21	2.36	1.40	3.21	4.23	3.04	4.08
FeO	7.71	9.02	9.20	7.90	8.39	9.02	10.27	9.25	9.86	11.12	10.18
MnO	.18	.19	.19	.18	.19	.19	.18	.18	.19	.19	.19
MgO	11.49	12.30	12.06	10.33	10.26	12.35	11.50	8.31	5.47	5.22	5.42
CaO	9.75	9.75	10.19	9.39	9.70	9.99	10.55	10.17	7.45	7.52	7.51
Na ₂ O	2.08	1.99	2.34	2.40	2.71	2.03	2.60	2.94	4.01	4.20	4.18
K ₂ O	.26	.25	.27	.36	.37	.29	.24	.20	.23	.24	.27
H ₂ O+	3.33	2.97	2.35	3.70	2.85	2.65	2.36	2.58	1.97	1.62	1.38
F ₂ O ₅	.14	.14	.14	.18	.18	.14	.14	.14	.28	.27	.30
CO ₂	.24	.08	.04	.05	.07	.02	.11	.05	.12	.01	.05
TOTAL	99.45	100.74	100.76	99.67	99.94	100.77	100.80	101.09	100.18	99.83	100.10

TRACE ELEMENT (ppm)

Zr	90	88	88	101	102	92	102	94	202	194	227
Y	24	23	21	24	24	21	25	27	29	28	35
Rb	4	1	2	4	3	4	nd	1	nd	3	3
Nb	6	1	4	4	6	4	3	3	8	8	8
Sr	231	241	293	332	309	296	292	276	575	589	560
Zn	112	108	110	127	159	97	74	78	80	79	128
Cu	195	194	189	213	264	159	117	90	45	47	148
Ba	101	63	121	-	-	-	-	-	20	90	44
Cr	785	738	783	517	501	720	747	68	12	9	11
Mn	354	337	328	234	223	292	304	124	42	38	40
Ta	-	.19	-	-	.24	-	-	.29	-	-	.51
Hf	-	2.72	-	-	3.04	-	3.22	3.23	-	-	6.07
Th	-	.41	-	-	-	-	-	-	-	-	.61
La	-	5.41	-	-	-	-	-	-	-	-	8.23
Ce	-	15.31	-	-	20.01	-	15.06	15.09	-	-	30.57
Bd	-	13.97	-	-	-	-	14.89	-	-	-	29.69
Sm	-	3.78	-	-	-	-	4.69	-	-	-	8.44
Eu	-	1.45	-	-	1.62	-	1.60	1.69	-	-	2.82
Gd	-	4.60	-	-	4.50	-	5.06	5.42	-	-	8.53
Tb	-	.73	-	-	.73	-	.82	.86	-	-	1.15
Tm	-	.27	-	-	.32	-	.33	.39	-	-	.38
Yb	-	1.99	-	-	2.00	-	1.99	2.85	-	-	2.37
In	-	.36	-	-	-	-	.33	-	-	-	.39

CIPW WEIGHT MORPHS (Standard State Fe₂O₃)

Qtz	-	-	-	-	-	-	-	-	-	-	-
Or	1.54	1.48	1.60	2.13	2.19	1.71	1.42	1.18	1.36	1.42	1.60
Ab	17.60	16.84	19.80	20.31	22.93	17.18	18.00	22.17	33.93	34.54	35.10
An	26.60	28.53	26.35	26.28	25.08	28.07	26.67	31.21	26.86	25.92	25.54
Ho	-	-	-	-	-	-	2.17	1.47	-	.54	.15
Wo	8.16	7.69	9.62	7.85	8.95	8.54	10.05	7.52	3.14	3.99	3.94
Di	En	5.10	4.87	6.07	4.76	5.40	5.44	6.19	4.10	1.45	1.79
Fe	2.57	2.33	2.95	2.66	3.07	2.55	3.27	3.15	1.65	2.18	2.11
Hy	En	6.56	6.73	1.52	5.18	.82	4.98	-	1.42	-	-
Fe	3.31	3.23	.74	2.89	.47	2.34	-	-	1.61	-	-
Ol	Fe	11.88	13.34	15.73	11.06	13.55	14.25	15.73	11.63	7.53	8.20
Fe	6.61	7.04	8.42	6.81	8.50	7.37	9.17	9.86	9.42	10.52	10.54
Il	2.92	2.92	2.96	3.13	3.23	3.06	3.04	3.44	5.79	5.81	5.83
Mt	2.18	2.18	2.18	2.18	2.18	2.18	2.18	2.18	2.90	2.90	2.90
Ap	.32	.32	.32	.42	.42	.32	.32	.32	.65	.65	.70
H ₂ O	3.33	2.97	2.35	3.70	2.85	2.65	2.36	2.58	1.97	1.62	1.38
Co	.55	.18	.09	.11	.16	.05	.25	.11	.27	.02	.11
TOTAL	99.22	100.65	100.69	99.47	99.77	100.68	100.81	100.92	99.96	99.73	99.89
D.I.	19.14	18.32	21.40	22.44	25.12	18.89	21.58	24.82	35.29	36.90	36.84
F/F+M	.534	.538	.526	.546	.541	.531	.525	.547	.517	.521	.522

F/F+M = (FeO + Fe₂O₃)/FeO + Fe₂O₃ + MgO, Standard state Fe₂O₃

ZEOLITISED LAVAS

	M8	M11	M12	M51	M52	M53	M54	M55
MAJOR ELEMENT (wt. %)								
SiO ₂	46.00	45.29	45.19	45.18	45.05	45.02	44.84	45.44
TiO ₂	3.06	2.73	2.68	2.05	2.05	2.04	2.00	2.05
Al ₂ O ₃	16.70	15.59	15.22	15.66	14.99	15.00	14.93	15.63
Fe ₂ O ₃	3.58	3.09	3.94	3.50	1.97	2.56	2.31	3.18
FeO	10.67	10.79	9.93	8.44	9.79	9.20	9.44	9.18
MnO	.19	.19	.19	.18	.19	.18	.18	.19
MgO	5.40	7.94	7.77	8.35	8.53	8.35	8.86	8.29
CaO	7.65	8.89	8.93	11.31	11.45	11.42	11.14	11.61
Na ₂ O	4.04	2.97	2.95	2.95	2.39	2.16	2.16	2.39
K ₂ O	.23	.37	.37	.18	.17	.17	.15	.16
H ₂ O ⁺	1.79	2.76	2.80	2.99	2.90	3.04	3.28	3.20
P ₂ O ₅	.27	.28	.25	.16	.17	.17	.16	.16
CO ₂	.01	.12	.15	.09	.06	.06	.05	.23
TOTAL	100.39	100.85	100.37	100.08	99.46	99.53	99.50	101.71

TRACE ELEMENT (ppm)

Zr	204	183	172	108	113	112	106	112
Y	30	23	26	27	24	26	22	24
Rb	1	3	5	nd	nd	nd	nd	nd
Nb	7	13	15	4	6	4	4	4
Sr	575	544	582	315	320	287	253	289
Zn	226	122	173	66	70	67	67	64
Cu	308	146	227	167	151	158	133	143
Ba	35	-	-	9	2	12	nd	14
Cr	11	-	-	244	274	253	260	271
Ni	39	100	99	145	149	140	165	161
Ta	-	-	-	.21	-	.20	-	-
Hf	-	-	-	3.23	-	3.31	-	-
Th	-	-	-	.29	-	.27	-	-
La	-	-	-	-	-	4.88	-	-
Ce	-	-	-	16.98	-	16.54	-	-
Nd	-	-	-	14.62	-	14.89	-	-
Sm	-	-	-	4.91	-	4.77	-	-
Eu	-	-	-	1.63	-	1.71	-	-
Gd	-	-	-	5.60	-	5.14	-	-
Tb	-	-	-	.79	-	.82	-	-
Tm	-	-	-	-	-	.31	-	-
Yb	-	-	-	1.99	-	2.12	-	-
In	-	-	-	.32	-	.37	-	-

CIPW WEIGHT NORMS. (Standard State Fe₂O₃)

Qz	-	-	-	-	-	-	-	-
Or	1.36	2.19	2.19	1.06	1.01	1.01	.89	.95
Ab	34.19	25.13	24.96	20.22	18.28	19.63	18.28	20.22
An	26.75	28.11	27.20	31.47	30.71	30.01	30.60	31.45
Ms	-	-	-	-	-	-	-	-
Wo	3.91	5.66	6.07	9.61	10.28	10.50	9.73	9.88
Di	En	1.78	2.52	3.14	5.43	5.84	5.95	5.61
Fe	2.10	2.92	2.76	3.79	3.99	4.11	3.68	4.05
En	.35	.55	1.02	.02	2.07	.59	2.31	.01
Hy	Fe	.41	.64	.90	.01	1.41	.41	1.52
Fo	7.93	10.80	10.64	10.76	9.34	9.99	9.91	10.64
Ol	Pa	10.30	11.37	10.28	8.27	7.03	7.61	8.72
Il	5.81	5.18	5.09	3.89	3.86	3.87	3.80	3.89
Mt	2.90	2.18	2.18	2.18	2.18	2.18	2.18	2.18
Ap	.63	.65	.58	.37	.39	.39	.37	.37
H ₂ O	1.79	2.76	2.80	2.99	2.90	3.04	3.28	3.20
Co	.02	.27	.34	.21	.14	.14	.11	.52
TOTAL	100.23	100.85	100.15	99.88	99.41	99.42	99.42	101.54
D.I.	35.54	27.32	27.15	21.29	19.28	20.64	19.16	21.17
F/T+H	723	633	636	584	579	583	568	595

HYDROTHERMALLY ALTERED LAVAS

	M13	M14	M15	M16	M17	M18	M19	M20	M21	M22	M26
MAJOR ELEMENT (wt. %)											
SiO ²	47.73	44.17	46.72	45.03	45.28	45.93	45.88	46.19	45.80	46.20	44.20
TiO ₂	1.59	1.52	1.43	1.38	1.34	1.38	1.32	1.36	1.38	1.38	3.09
Al ₂ O ₃	16.41	14.38	14.28	13.60	13.64	13.71	13.27	14.25	14.30	14.10	16.53
Fe ₂ O ₃	1.92	2.31	2.87	2.87	3.34	3.86	3.44	3.98	4.03	3.38	5.87
FeO	10.01	9.01	8.51	8.51	7.78	7.35	7.45	7.48	7.62	7.38	7.67
MnO	.20	.19	.18	.18	.17	.18	.17	.18	.18	.18	.20
MgO	10.32	11.06	11.90	11.50	10.96	10.59	10.49	11.92	11.76	10.60	4.84
CaO	2.11	6.84	6.91	8.20	9.13	9.60	9.67	9.36	9.32	9.47	6.20
Na ₂ O	5.21	3.43	3.33	2.46	1.91	1.91	1.89	1.85	1.97	1.97	3.99
K ₂ O	.24	.07	.11	.57	.66	.69	.53	.10	.39	.68	.51
H ₂ O ⁺	6.51	5.57	5.28	5.38	5.50	5.67	5.92	4.02	4.28	4.29	4.45
H ₂ O ⁻	.10	.17	.16	.15	.14	.16	.15	.15	.15	.15	.38
CO ₂	.03	1.59	.36	.62	.28	.27	.20	.09	.07	.32	.04
TOTAL	100.38	100.31	102.04	100.45	100.13	101.30	100.38	100.93	101.25	100.50	97.97

TRACE ELEMENT (ppm)

Zr	119	108	99	93	97	96	94	93	95	98	218
Y	28	24	22	20	20	21	21	21	21	24	33
Rb	5	1	nd	10	14	13	12	nd	10	12	8
Nb	7	9	6	5	6	7	7	6	6	7	13
Sr	247	377	296	427	331	314	274	264	275	294	619
Zn	78	74	70	72	73	76	70	70	71	75	123
Cu	79	67	64	92	73	91	95	85	101	93	130
Ba	61	5	34	276	178	164	142	106	151	316	-
Cr	745	634	573	539	594	624	586	589	602	610	20
Mn	411	365	381	399	397	378	375	405	409	383	49
Ta	.25	.28	.27	.27	.22	.23	.22	.24	.22	.23	-
Hf	3.15	3.14	3.22	3.05	2.75	2.76	2.77	2.76	2.73	2.75	-
Th	1.13	1.23	1.27	1.23	1.02	1.02	.99	1.10	1.04	1.05	-
La	8.16	-	7.22	6.99	-	-	7.86	7.71	7.66	-	-
Ce	23.64	22.53	23.28	22.56	19.93	19.96	20.20	20.23	20.25	19.51	-
Nd	17.32	16.70	16.98	15.96	14.25	14.94	14.14	15.50	14.24	14.97	-
Sm	4.77	4.49	4.50	4.43	4.04	4.23	4.05	3.83	4.01	4.04	-
Ba	1.90	1.56	1.63	1.51	1.37	1.41	1.40	1.43	1.29	1.43	-
Gd	5.02	5.08	5.14	4.49	3.90	3.97	3.88	4.53	3.55	4.35	-
Tb	.80	.78	.77	.71	.64	.66	.63	.69	.63	.67	-
Tm	.38	.29	.32	.30	.29	.24	.28	.31	.31	.30	-
Yb	2.29	2.01	2.08	1.99	1.71	1.73	1.69	1.88	1.71	1.80	-
Lu	.43	.31	.30	.31	.29	.29	.28	.26	.28	.24	-

CIPW WEIGHT NORMS

Qtz	1.98	-	-	-	-	-	-	-	-	-	-
Or	1.42	.41	.65	3.37	3.90	4.08	3.13	.59	2.31	4.02	3.01
Ab	27.16	29.02	28.18	20.82	16.16	16.16	15.99	15.65	16.67	16.17	33.76
An	9.63	22.77	23.69	24.38	26.70	26.80	26.16	30.28	29.02	27.62	25.69
Ms	-	-	-	-	-	-	-	-	-	-	-
Wo	-	-	3.04	4.76	6.65	7.55	8.17	6.10	6.59	6.83	.93
Di	-	-	2.03	3.16	4.53	5.26	5.60	4.32	4.65	4.69	.66
Fs	-	-	.77	1.25	1.60	1.67	1.92	1.24	1.38	1.60	.25
En	25.70	7.53	7.57	8.14	12.11	13.33	14.20	17.57	12.12	13.15	6.65
Hy	Fs	3.41	2.87	3.22	4.27	4.23	4.88	5.05	3.61	4.49	2.48
Fo	-	14.03	14.04	12.15	7.47	5.46	4.44	5.46	8.78	6.01	3.33
Ol	Fs	-	7.00	5.86	5.29	2.90	1.91	1.73	2.88	2.26	1.37
Il	3.02	2.89	2.72	2.62	2.55	2.62	2.51	2.58	2.62	2.62	3.87
Nt	2.78	3.35	4.16	4.16	4.84	5.60	4.99	5.77	5.84	5.19	8.51
Ap	.23	.39	.37	.35	.32	.37	.35	.35	.35	.35	.88
H ₂ O	6.51	5.57	5.28	5.38	5.50	5.67	5.92	4.02	4.28	4.29	4.45
Co	.07	3.62	.82	1.40	.64	.62	.46	.21	.16	.73	.09
Cor	7.34	.32	-	-	-	-	-	-	-	-	-
TOTAL	100.38	100.31	102.04	100.45	100.13	101.30	100.38	100.93	101.25	100.50	97.97

HYDROTHERMALLY ALTERED LAVAS

	N27	N28	N29	N30	N32	N34	N35	N36	N37	N38	N39
MAJOR ELEMENT (wt. %)											
SiO ₂	44.82	45.43	44.99	43.95	44.36	44.57	44.62	44.61	44.24	43.56	42.78
TiO ₂	3.09	3.04	1.68	1.80	1.62	1.81	1.74	1.80	1.52	1.49	1.26
Al ₂ O ₃	16.50	16.62	16.18	15.32	15.11	15.66	15.25	15.47	15.09	15.21	15.49
Fe ₂ O ₃	4.99	4.31	2.08	2.80	1.95	5.73	2.39	3.57	5.24	4.32	11.11
FeO	8.24	8.78	9.77	9.65	9.68	7.17	9.97	9.03	6.61	7.22	-
MnO	.16	.18	.18	.19	.18	.19	.18	.18	.19	.17	.20
MgO	5.11	4.75	7.63	7.57	8.73	8.65	9.02	8.16	9.18	9.60	6.15
CaO	7.98	8.06	8.92	8.15	9.08	8.67	9.06	9.46	9.60	9.30	15.40
Na ₂ O	3.57	3.66	3.20	3.75	2.96	2.63	2.34	2.60	2.18	2.01	1.97
K ₂ O	.20	.43	.30	.25	.29	.21	.21	.25	.27	.21	.13
H ₂ O ⁺	3.46	2.87	4.38	4.31	4.92	3.84	4.17	4.02	5.23	5.31	5.48
P ₂ O ₅	.39	.38	.17	.16	.17	.16	.16	.16	.14	.15	.15
CO ₂	.01	.01	.48	.69	.31	.06	.06	.07	.07	.10	.23
TOTAL	98.52	98.52	99.96	98.57	99.36	99.35	99.17	99.38	99.56	98.65	100.35

TRACE ELEMENTS (ppm)

Zr	216	213	100	101	94	101	97	101	87	80	192
Y	33	33	22	22	20	23	21	6	1	1	5
Rb	3	10	8	1	4	1	13	23	27	21	28
Sr	16	15	8	3	4	3	4	3	4	6	4
Sr	514	585	330	297	303	281	263	267	276	246	520
Zn	186	102	168	151	82	73	207	74	71	104	78
Cu	203	105	241	260	80	85	293	86	72	106	54
Ba	-	-	-	-	-	-	-	-	-	-	-
Cr	14	13	186	204	417	180	200	166	282	281	287
Bi	50	48	103	190	211	172	172	166	230	222	38
Ta	.80	-	-	.28	-	-	-	-	-	-	-
Hf	5.71	-	-	3.07	-	-	-	-	-	-	-
Th	1.05	-	-	.34	-	-	-	-	-	-	-
La	12.19	-	-	4.75	-	-	-	-	-	-	-
Ce	36.93	-	-	15.91	-	-	-	-	-	-	-
Nd	29.23	-	-	14.05	-	-	-	-	-	-	-
Sm	7.97	-	-	4.29	-	-	-	-	-	-	-
Eu	2.73	-	-	1.60	-	-	-	-	-	-	-
Gd	8.10	-	-	4.83	-	-	-	-	-	-	-
Tb	1.14	-	-	.78	-	-	-	-	-	-	-
Tm	.41	-	-	.34	-	-	-	-	-	-	-
Yb	2.75	-	-	2.00	-	-	-	-	-	-	-
In	.45	-	-	.32	-	-	-	-	-	-	-

CIPW WEIGHT MORPH

Qtz	-	-	-	-	-	-	-	-	-	-	-
Or	1.18	2.54	1.77	1.48	1.71	1.24	1.24	1.48	1.60	1.24	.77
Ab	30.21	30.97	27.08	28.88	24.73	22.25	19.80	22.00	18.45	17.01	7.43
An	28.41	27.65	28.90	24.32	27.09	30.30	30.49	29.80	30.59	31.86	33.04
Mo	-	-	-	1.45	.17	-	-	-	-	-	5.01
V ⁺	3.58	4.09	4.68	4.47	6.22	4.71	5.44	6.53	6.55	5.29	17.09
Di	En	2.26	2.35	2.61	2.55	3.62	3.38	3.21	4.00	4.76	3.69
Fe	1.10	1.56	1.89	1.73	2.30	.91	1.97	2.16	1.18	1.16	7.59
En	7.37	4.54	.63	-	-	10.98	6.72	4.75	11.55	11.66	-
Hy	Fe	3.59	3.02	.45	-	-	2.95	4.13	2.57	2.85	3.68
Fo	2.18	3.47	11.05	11.43	12.70	5.04	8.79	8.11	4.59	6.00	4.43
Ol	Fe	1.17	2.54	8.83	8.54	8.90	1.49	5.95	4.84	1.25	2.09
Il	5.87	5.77	3.19	3.42	3.08	3.44	3.30	3.42	2.89	2.83	2.39
Ht	7.23	6.25	3.02	4.06	2.83	8.31	3.47	5.18	7.60	6.26	2.18
Ap	.90	.88	.39	.37	.39	.37	.37	.37	.32	.35	.35
H ₂ O	3.46	2.87	4.38	4.31	4.92	3.80	4.17	4.02	5.23	5.31	5.48
Co	.02	.02	1.09	1.57	.71	.14	.14	.16	.16	.23	.52
Cor	-	-	-	-	-	-	-	-	-	-	-
TOTAL	98.52	98.52	99.96	98.57	99.36	99.35	99.17	99.38	99.56	98.65	99.39 ^o

^oStandard State Fe₂O₃

HYDROTHERMALLY ALTERED LAVAS (wt. %)

	M40	M41	M42	M43	M46	M45	M47	M48	M50	M59	C54	C84
MAJOR ELEMENT ANALYSES												
SiO ₂	44.91	45.03	45.14	44.89	45.23	43.66	45.98	44.14	44.56	47.14	43.89	46.10
TiO ₂	3.00	2.91	2.99	3.00	2.97	3.17	2.40	2.34	2.45	2.63	1.41	1.43
Al ₂ O ₃	16.60	16.30	16.39	16.36	16.20	15.04	16.19	15.87	17.01	14.68	14.75	13.90
Fe ₂ O ₃	4.16	3.68	4.98	6.49	4.69	8.16	3.14	4.20	2.50	6.35	4.34	3.83
FeO	9.86	9.86	8.96	7.33	9.07	8.06	10.04	8.87	11.19	7.04	7.70	8.03
MnO	.18	.18	.22	.17	.19	.20	.20	.20	.32	.26	.20	.18
MgO	5.39	5.15	5.34	4.65	5.24	3.95	7.17	7.23	7.81	3.28	11.06	10.31
CaO	7.55	7.65	7.58	7.93	7.67	3.50	9.35	8.42	7.97	6.99	7.73	8.15
Na ₂ O	3.60	3.40	3.43	3.66	3.30	5.01	2.16	2.94	2.11	4.69	2.72	3.06
K ₂ O	.29	.33	.30	.30	.25	.16	.32	.33	.42	1.49	.28	.40
H ₂ O ⁺	3.46	3.50	3.28	3.00	3.27	4.26	2.32	4.09	2.99	2.49	5.33	4.79
P ₂ O ₅	.33	.32	.33	.32	.31	.33	.24	.22	.24	1.68	.18	.16
CO ₂	.06	.08	.03	.02	.02	.21	.07	.09	.02	.09	.09	.16
TOTAL	99.39	98.39	99.17	98.14	98.41	97.71	99.58	98.94	99.39	98.81	99.68	100.50

TRACE ELEMENT ANALYSES (ppm)

Zr	195	189	193	198	190	189	132	133	138	349	105	113
Y	32	31	32	35	32	37	25	28	31	67	262	22
Hf	2	5	1	1	1	nd	11	9	12	21	6	8
Rb	12	11	11	11	11	10	5	6	5	16	3	4
Sr	532	533	551	549	526	563	353	365	308	584	362	242
Zn	69	134	.39	71	71	107	85	84	82	140	90	80
Cu	32	149	34	29	27	28	.59	50	107	-	78	65
Be	-	-	-	-	-	-	-	-	-	-	75	146
Cr	nd	nd	nd	nd	1	9	95	96	99	-	692	669
Bi	24	26	26	25	25	36	99	101	105	-	376	369
Ta	-	-	.63	-	-	-	-	-	-	-	-	-
Rf	-	-	5.18	-	-	-	-	-	-	-	-	-
Th	-	-	.90	-	-	-	-	-	-	-	-	-
La	-	-	10.29	-	-	-	-	-	-	-	-	-
Ce	-	-	30.21	-	-	-	-	-	-	-	-	-
Pr	-	-	25.06	-	-	-	-	-	-	-	-	-
Sm	-	-	6.94	-	-	-	-	-	-	-	-	-
Eu	-	-	2.50	-	-	-	-	-	-	-	-	-
Gd	-	-	7.28	-	-	-	-	-	-	-	-	-
Tb	-	-	1.07	-	-	-	-	-	-	-	-	-
Dm	-	-	.44	-	-	-	-	-	-	-	-	-
Yb	-	-	2.65	-	-	-	-	-	-	-	-	-
Lu	-	-	.41	-	-	-	-	-	-	-	-	-

CIPW WEIGHT NORMS

Qz	-	-	-	.01	-	-	-	-	-	-	-	-
Or	1.71	1.95	1.77	1.77	1.48	.95	1.89	1.95	2.48	8.81	1.66	2.36
Ab	30.46	28.77	29.02	30.97	27.92	42.39	18.28	24.88	17.85	39.69	23.02	25.89
An	28.28	28.24	28.99	27.33	28.65	18.08	33.54	29.13	35.70	14.60	27.21	23.01
Ms	-	-	-	-	-	-	-	-	-	-	-	-
Wo	2.77	2.97	2.62	4.09	3.03	2.39	4.53	4.44	.90	3.56	3.92	6.42
Il	En	1.53	1.58	1.57	2.88	.77	1.66	2.57	.49	2.27	2.74	4.32
	Fs	1.14	1.30	.92	.87	1.11	.54	1.76	1.43	.38	1.06	1.61
	Ed	4.66	6.64	8.62	8.71	10.33	1.53	13.31	5.36	11.20	4.37	5.19
Hy	Fs	3.49	5.49	5.06	2.63	6.32	.50	9.13	2.78	8.65	2.04	1.93
	Fo	5.07	3.23	2.19	-	.67	4.66	1.39	6.93	5.44	1.07	13.60
Ol	Fs	4.18	2.94	1.41	-	.46	1.67	1.05	3.96	4.64	.55	4.68
	Il	5.70	5.53	5.68	5.70	5.64	6.02	4.55	4.44	4.65	4.99	2.68
	Ht	6.03	5.34	7.22	9.41	6.80	11.83	4.55	6.09	3.62	9.21	6.29
	Ap	.77	.74	.77	.74	.72	.77	.56	.51	.56	3.89	.42
	H ₂ O	3.46	3.50	3.28	3.00	3.27	4.26	2.32	4.09	2.99	2.49	5.33
	Co	.14	.18	.07	.05	.05	.48	.16	.21	.05	.21	.36
	Cor	-	-	-	-	-	-	-	-	-	-	-
TOTAL	99.39	98.39	99.17	98.14	98.41	97.71	99.58	98.94	99.39	98.81	99.68	100.50

HYDROTHERMALLY ALTERED LAVAS

	C90	C130	C136	C142	C145	C149	C153	C153V	C154	C158
MAJOR ELEMENT (wt. %)										
SiO ₂	44.58	46.20	44.56	47.75	43.53	46.05	44.62	47.27	44.37	42.97
TiO ₂	1.48	1.34	1.40	1.46	1.31	1.36	1.39	1.67	1.40	1.46
Al ₂ O ₃	13.95	14.01	13.87	12.74	13.73	13.48	13.77	11.84	13.96	14.34
Fe ₂ O ₃	3.88	5.54	4.42	3.38	3.43	3.65	3.89	3.08	3.97	3.73
FeO	8.39	7.53	7.19	8.24	7.89	7.58	7.49	8.41	7.67	8.28
MnO	.19	.16	.16	.17	.17	.17	.17	.20	.18	.18
MgO	11.09	9.57	9.88	10.32	11.14	10.95	10.80	10.90	11.24	11.66
CaO	6.59	8.25	9.46	7.86	8.76	9.88	9.12	9.29	9.65	8.83
Na ₂ O	3.27	3.36	2.90	2.77	1.51	1.77	1.96	2.11	1.78	1.90
K ₂ O	.25	.47	.04	1.22	1.03	.28	.26	.80	.12	.10
H ₂ O ⁺	5.20	4.91	4.63	4.60	6.95	3.95	4.88	4.25	4.57	5.57
P ₂ O ₅	.19	.18	.19	.21	.18	.18	.19	.21	.18	.19
CO ₂	.11	.08	.16	.06	.11	.10	.18	.15	.13	.09
TOTAL	99.17	99.60	98.86	100.76	99.72	99.40	98.72	100.18	99.22	99.30

TRACE ELEMENT (ppm)

Zr	114	102	107	118	99	95	100	112	102	111
Y	26	20	24	26	21	21	23	21	22	22
Rb	6	12	1	25	25	6	6	13	2	1
Nb	7	2	3	9	3	3	2	4	5	5
Sr	249	174	331	294	196	230	247	257	243	230
Zn	86	78	78	87	85	81	82	88	84	83
Cu	76	67	54	72	75	87	55	223	103	90
Ba	108	196	-	340	329	161	119	799	79	77
Cr	644	571	604	593	550	537	593	452	580	613
Ni	369	339	362	369	345	340	366	278	370	374
Ta	-	-	-	-	-	-	-	-	-	-
Hf	-	-	-	-	-	-	-	-	-	-
Tb	-	-	-	-	-	-	-	-	-	-
La	-	-	-	-	-	-	-	-	-	-
Ce	-	-	-	-	-	-	-	-	-	-
Md	-	-	-	-	-	-	-	-	-	-
Sm	-	-	-	-	-	-	-	-	-	-
Eu	-	-	-	-	-	-	-	-	-	-
Gd	-	-	-	-	-	-	-	-	-	-
Tm	-	-	-	-	-	-	-	-	-	-
Yb	-	-	-	-	-	-	-	-	-	-
Lu	-	-	-	-	-	-	-	-	-	-

CIPW WEIGHT NORMS

Qz	-	-	-	-	-	-	-	-	-	-
Or	1.48	2.78	.24	7.21	6.09	1.66	1.54	4.73	.71	.59
Ab	27.67	28.43	24.54	23.44	12.78	14.98	16.59	17.85	15.06	16.08
An	22.65	21.76	24.71	18.73	27.64	28.01	28.01	20.47	29.75	30.30
Ms	-	-	-	-	-	-	-	-	-	-
Wo	3.39	7.30	8.34	7.73	5.82	8.02	6.20	9.73	6.73	4.88
Di	En	2.29	4.90	5.84	5.13	3.97	5.54	4.32	6.49	3.34
Fe	.84	1.85	1.79	2.04	1.40	1.82	1.37	2.51	1.48	1.16
En	4.25	1.60	3.57	7.28	10.04	16.47	14.30	12.98	13.74	9.74
Hy	Fe	1.56	.60	1.09	2.90	3.55	5.42	4.55	5.03	3.37
Fe	14.77	12.15	10.65	9.32	9.63	3.69	5.80	5.38	6.70	11.19
Ol	Fe	5.96	5.05	3.59	4.09	3.75	1.34	2.04	2.30	4.26
Il	2.81	2.55	2.66	2.77	2.49	2.58	2.64	3.17	2.66	2.77
Mt	5.63	5.13	6.41	4.90	4.97	5.29	5.64	4.67	5.76	5.41
Ap	.44	.42	.44	.49	.42	.42	.44	.49	.42	.44
H ₂ O	5.20	4.91	4.63	4.60	6.93	3.95	4.88	4.25	4.57	5.57
Co	.25	.18	.36	.14	.25	.23	.41	.34	.30	.23
Cor	-	-	-	-	-	-	-	-	-	-
TOTAL	99.17	99.60	98.86	100.76	99.72	99.40	98.72	100.18	99.22	99.30

HYDROTHERMALLY ALTERED LAVAS

	C176	C191	C193	C199	C205	C212	C219	C225	C232AB	C246
MAJOR ELEMENTS (wt. %)										
SiO ₂	40.74	43.62	37.33	42.22	44.27	44.37	44.41	45.31	39.90	55.15
TiO ₂	2.56	2.65	2.85	2.81	2.65	2.62	2.68	2.64	2.72	1.74
Al ₂ O ₃	16.39	16.60	15.73	15.50	16.02	15.42	15.86	15.41	13.59	12.20
Fe ₂ O ₃	6.28	8.82	7.06	7.27	6.58	7.76	6.90	6.56	5.04	6.09
FeO	8.66	6.38	9.00	8.68	8.66	7.36	8.35	8.48	10.38	8.07
MnO	.27	.18	.24	.22	.21	.20	.21	.21	.21	.23
MgO	7.06	4.18	6.28	5.91	5.29	5.12	5.33	5.10	5.00	2.29
CaO	6.11	6.99	9.75	7.29	7.23	6.29	6.84	6.51	7.64	3.85
Na ₂ O	1.87	5.33	.40	3.47	3.47	3.84	3.38	3.18	4.05	2.51
K ₂ O	.47	.28	.25	.68	.65	.95	.79	.67	.57	3.02
H ₂ O ⁺	8.87	4.19	10.28	5.50	4.45	4.52	4.14	4.45	4.78	3.10
P ₂ O ₅	.38	.45	.49	.47	.44	.45	.45	.44	.45	.58
CO ₂	.11	.45	.41	.60	.19	.45	.72	.77	3.90	.10
TOTAL	99.77	100.12	100.07	100.62	100.09	99.33	100.04	99.73	98.23	98.93

TRACE ELEMENTS (ppm)

Zr	151	213	223	209	194	193	202	199	216	267
Y	38	43	45	41	39	40	40	38	42	79
Rb	10	6	4	12	10	18	14	12	11	71
Sr	6	14	14	13	11	10	13	10	10	10
Br	523	427	348	473	554	562	499	477	207	224
Eu	117	125	114	124	115	119	117	109	118	-
Ce	48	26	31	39	38	35	30	55	33	9
Ba	367	226	63	456	440	466	469	383	185	-
Cr	39	16	21	15	9	18	10	10	10	-
Hf	69	36	46	43	41	42	44	42	43	-
Ta	-	.80	.74	-	.70	-	-	.62	.61	-
Hf	-	5.78	5.81	-	5.28	-	-	5.01	5.41	-
Tb	-	1.07	.98	-	.96	-	-	.87	.79	-
La	-	-	-	-	-	-	-	-	-	-
Co	-	51.48	50.88	-	45.99	-	-	44.26	49.33	-
Ni	-	37.16	38.12	-	34.53	-	-	32.76	36.43	-
Sm	-	6.87	9.87	-	8.77	-	-	8.07	9.26	-
Rn	-	3.07	5.09	-	2.84	-	-	2.73	3.07	-
Gd	-	10.44	8.42	-	8.94	-	-	8.39	7.87	-
Tb	-	1.38	1.40	-	1.22	-	-	1.15	1.37	-
Th	-	-	.54	-	.48	-	-	-	-	-
Yb	-	3.19	3.48	-	2.99	-	-	2.82	3.24	-
Lu	-	.48	.56	-	.51	-	-	.45	.54	-

CIPW WEIGHT NORMS

Qz	2.64	-	3.84	-	-	-	-	3.23	-	16.24
Or	2.78	1.66	1.48	4.02	3.72	5.61	4.67	3.96	3.37	17.85
Ab	15.82	37.89	3.39	29.36	29.36	32.49	28.60	26.91	34.27	21.24
An	27.13	20.45	40.39	24.71	26.28	22.03	25.77	24.55	10.31	13.10
Ms	-	4.00	-	-	-	-	-	-	-	-
Wo	-	3.58	.91	1.92	2.30	1.47	.34	-	-	.66
Di	En	-	3.01	.60	1.28	1.45	1.07	.22	-	.29
Fe	-	.11	.25	.50	.71	.26	.09	-	-	.37
Rn	17.58	-	15.04	4.05	7.59	9.03	12.87	12.70	7.10	5.42
Hy	Fe	6.99	-	6.19	1.57	3.73	2.23	5.43	6.18	6.97
Fe	-	5.19	-	6.58	2.90	1.86	.13	-	3.75	-
Ol	Fe	-	.21	-	2.81	1.57	.51	.06	-	3.59
Il	4.86	5.03	5.41	5.34	3.03	4.98	5.09	5.01	5.17	3.30
Ht	9.10	12.79	10.24	10.54	9.54	11.25	10.00	9.51	7.31	8.83
Ap	.88	1.04	1.14	1.09	1.02	1.00	1.00	1.02	1.04	1.34
H ₂ O	8.87	4.19	10.28	5.50	4.45	4.52	4.14	4.45	4.78	3.10
Co	.25	.98	.93	1.37	.43	1.02	1.64	1.75	8.87	.23
Cor	2.86	-	-	-	-	-	-	.46	2.53	-
TOTAL	99.77	100.12	100.07	100.62	100.09	99.33	100.04	99.73	98.23	98.93

ALTERATION PRODUCTS

	M56R	M56Z	M56Z ^d	LA19R	LA19Z	LA19Z ^d	M24 ^d	M64 ^d
MAJOR ELEMENTS (wt. %)								
SiO ₂	42.20	41.73	51.32	45.00	46.40	51.12	32.22	53.11
TiO ₂	2.09	2.27	.04	1.72	2.20	.04	.06	.01
Al ₂ O ₃	14.05	13.57	3.36	14.36	13.36	2.63	11.97	21.20
Fe ₂ O ₃	4.85	5.48	.16	4.98	5.71	.12	.29	.06
FeO	8.68	8.49	.09	7.08	6.23	.16	.27	.05
MnO	.17	.18	.01	.17	.23	.09	.03	.00
MgO	9.01	9.32	.80	9.68	8.80	.37	.50	.04
CaO	10.11	10.32	29.85	9.80	9.05	29.58	28.58	11.75
Na ₂ O	2.13	1.90	.83	2.36	3.10	.74	.09	.04
K ₂ O	.12	.11	.11	.33	.66	.11	.04	.17
H ₂ O ⁺	6.38	5.90	11.96	3.68	3.86	11.38	7.91	13.72
P ₂ O ₅	.21	.23	.01	.20	.39	.01	.02	.02
CO ₂	.11	.33	2.06	.15	.21	3.12	18.91	.03
TOTAL	100.11	99.83	100.80	99.53	100.20	99.27	100.89	100.20

TRACE ELEMENT (ppm)

Kr	134	144	3	111	217	nd	-	-
Y	29	32	nd	27	47	nd	-	-
Rb	1	nd	nd	3	9	nd	2	2
Fb	4	4	2	3	7	nd	1	3
Sr	230	207	22	321	241	68	169	359
Zn	86	93	-	84	84	-	-	-
Cu	134	128	-	66	93	-	13	10
Ba	nd	nd	-	-	-	-	-	-
Cr	316	321	-	545	347	-	-	-
Bi	185	176	-	244	180	-	-	-
Ta	-	.14	-	-	-	-	-	-
Hf	-	3.95	-	-	-	-	-	-
Th	-	-	-	-	-	-	-	-
La	-	-	-	-	-	-	-	-
Ce	-	19.80	-	-	-	-	-	-
Pr	-	18.87	-	-	-	-	-	-
Sm	-	5.85	-	-	-	-	-	-
Eu	-	1.95	-	-	-	-	-	-
Gd	-	5.40	-	-	-	-	-	-
Tb	-	1.02	-	-	-	-	-	-
Tm	-	.45	-	-	-	-	-	-
Yb	-	2.39	-	-	-	-	-	-
Lu	-	.39	-	-	-	-	-	-

CIPW WEIGHT MORPHS (Standard State Fe₂O₃)

Qtz	-	-	-	-	-	-	-	-
Or	.71	.65	-	2.07	3.90	-	-	-
Ab	18.19	16.08	-	19.97	26.23	-	-	-
An	28.28	28.17	-	27.36	20.59	-	-	-
Wo	.01	-	-	-	-	-	-	-
Di	8.27	8.12	-	7.85	8.51	-	-	-
Hn	4.53	4.46	-	4.61	4.71	-	-	-
Fs	3.45	3.36	-	2.86	3.52	-	-	-
Hs	-	1.82	-	2.98	.06	-	-	-
Hy	-	1.38	-	1.85	.05	-	-	-
Fs	12.55	11.87	-	11.58	12.02	-	-	-
Ol	10.54	9.86	-	7.93	9.94	-	-	-
Fs	3.97	4.31	-	3.27	4.18	-	-	-
Ht	2.18	2.18	-	2.18	2.18	-	-	-
Ap	.49	.53	-	.46	.90	-	-	-
H ₂ O	6.38	5.90	-	3.68	3.86	-	-	-
Co	.25	.75	-	.34	.48	-	-	-
TOTAL	99.77	99.43	-	99.18	101.13	-	-	-
D.I.	18.90	16.73	-	22.04	30.13	-	-	-

^dMajor elements analysed by P. Watkins.

OTHER MULL AND BERRIDIAN ROCKS

	MS8	MS1	MS0	MS183	MS184	MS185	MS209 ^a	MS144 ^d
MAJOR ELEMENT (wt. %)								
SiO ₂	48.21	50.74	47.57	51.44	50.78	54.29	43.97	44.04
TiO ₂	1.54	1.74	1.61	1.91	1.97	1.44	2.03	3.49
Al ₂ O ₃	14.82	15.15	14.60	14.00	13.94	16.52	15.71	13.27
Fe ₂ O ₃	3.28	3.90	12.06	3.06	3.57	4.88	13.14	3.32
FeO	8.96	7.45	.00	9.37	9.81	6.25	.00	8.72
MnO	.21	.19	.20	.22	.26	.15	.17	.16
MgO	6.28	5.38	7.45	3.88	4.43	3.14	5.70	7.68
CaO	10.35	9.98	11.90	8.30	9.39	7.53	7.51	9.43
Na ₂ O	2.29	3.24	2.36	2.98	3.32	2.93	5.14	1.48
K ₂ O	.65	.81	.44	.73	.38	1.70	.36	2.49
K ₂ O+	2.43	2.09	2.18	4.80	2.86	2.14	5.11	3.91
P ₂ O ₅	.14	.23	.18	.41	.33	.22	.26	.94
CO ₂	.01	.06	.06	.05	.04	.05	.76	1.32
TOTAL	99.17	100.96	100.61	101.13	100.88	101.24	99.86	100.25

TRACE ELEMENT (ppm)

Zr	106	125	108	225	191	178	175	362
Y	54	30	23	61	56	36	31	30
Rb	31	11	2	22	9	50	6	49
Sr	8	7	2	14	13	10	4	67
Er	211	485	160	294	248	272	416	1293
Zn	180	98	79	-	-	-	-	-
Cu	-	31	143	-	-	-	-	-
Ba	-	523	-	-	-	-	-	1005
Cr	-	40	175	-	-	-	-	-
Mn	-	29	316	-	-	-	-	-
Ta	.40	-	-	-	-	-	-	5.22
Hf	3.21	4.05	-	-	-	-	-	9.30
Th	2.84	2.29	-	-	-	-	-	8.22
La	10.34	-	-	-	-	-	-	-
Ce	25.58	40.52	-	-	-	-	-	150.51
Pr	15.64	26.51	-	-	-	-	-	81.32
Sm	4.41	6.84	-	-	-	-	-	16.12
Eu	1.58	2.16	-	-	-	-	-	4.53
Gd	5.56	6.22	-	-	-	-	-	9.61
Tb	1.01	1.12	-	-	-	-	-	1.55
Tm	.59	.49	-	-	-	-	-	.41
Yb	3.72	3.39	-	-	-	-	-	2.54
Lu	.56	.53	-	-	-	-	-	.30

CIPW WEIGHT NORMS (Standard State Fe₂O₃)

Qz	-	-	-	5.20	1.33	6.88	-	-
Or	3.84	4.79	2.60	4.31	2.25	10.05	2.13	14.71
Ab	19.38	27.42	19.97	25.22	28.09	24.79	28.96	12.52
An	28.24	24.40	27.94	22.67	22.01	26.90	18.73	22.21
Ms	-	-	-	-	-	-	7.87	-
no	9.24	9.70	12.33	6.48	9.25	3.63	5.02	4.21
Ml	En	4.49	4.88	6.79	2.50	3.67	1.42	2.50
	Fe	4.59	4.60	5.09	4.08	5.69	2.26	1.57
	Mn	8.86	7.47	3.83	7.17	7.36	6.40	10.12
Hy	Fe	9.06	7.05	2.87	11.72	11.40	10.22	6.52
	Fe	1.61	0.74	5.57	-	-	-	8.20
O1	Fe	1.81	0.77	4.60	-	-	-	8.72
Il		2.92	3.30	3.06	3.63	3.74	3.86	6.63
Nt		2.18	2.90	2.18	2.18	2.18	2.90	2.18
Ap		.32	.53	.42	.95	.77	.60	2.18
H ₂ O		2.43	2.09	2.18	4.80	2.86	2.14	5.11
Co		.02	.14	.14	.11	.09	.11	1.73
TOTAL		98.99	100.77	99.55	100.99	100.69	98.74	100.07
D.I. ^a		23.22	32.20	22.57	34.73	31.67	41.72	38.96
F/F+H ^b		.658	.675	.596	.759	.746	.775	.678

^aTrace elements by G. Mariner

Zr values determined at Bedford College and used for
Skye - Mull comparisons in chapter 6.

<u>Sample Zr</u>		<u>Sample Zr</u>		<u>Sample Zr</u>	
LA 1	128	M 7	230	M 27	222
LA 3	119	M 8	210	M 28	220
LA 5	121	M 11	201	M 29	109
LA 2	119	M 12	176	M 30	109
LA 4	118	M 51	121	M 32	97
LA 7	112	M 52	126	M 34	101
LA 8	111	M 53	120	M 35	103
LA 9	108	M 54	118	M 36	105
LA 10	117	M 55	112	M 37	99
LA 11	108	M 13	129	M 38	105
LA 13	103	M 14	130	M 40	197
LA 14	97	M 15	105	M 41	192
LA 15	92	M 16	100	M 42	190
LA 16	112	M 17	105	M 43	200
LA 17	110	M 18	112	M 46	196
LA 18	96	M 19	104	M 45	187
LA 20	94	M 20	96	M 47	135
M 1	97	M 21	112	M 48	135
M 5	210	M 22	99	M 50	145
M 6	204	M 26	215	M 61	123

I-F Density data

<u>Sple</u>	<u>density</u>	<u>Sple</u>	<u>density</u>
LA 13	2.96	M 13	2.76
LA 14	2.92	M 14	2.83
LA 15	2.97	M 15	2.88
LA 16	2.87	M 16	2.88
LA 17	2.91	M 17	2.86
LA 18	2.96	M 18	2.80
		M 19	2.83
LA 20	2.94	M 20	2.87
		M 21	2.84
		M 22	2.90

APPENDIX II

ANALYTICAL TECHNIQUES.

Sampling and sample preparation.

In order to investigate various scales of element mobility a wide variety of different sized samples were crushed for geochemical work. Initially, 2 - 3 kg specimens were collected from all the outcrops sampled. No attempt was made to separate small secondary mineral pods or the light and dark patches within the mottled lavas from the epidote zone, instead 2 kg portions of these rocks were crushed to homogenise all such features and assess any bulk changes in composition across the lava flows. Similar sized pieces of the zeolitised lavas were crushed to ensure comparability of the data.

This collection was supplemented by the drill core (2.5 cms diameter) which was obtained using a N.E.R.C. petroleum powered diamond drill shown in fig. 1 - 11. The drill string consisted of a diamond drill bit followed by a reaming shell to maintain the gauge of the hole, a steel core barrel and lightweight magnesium-zirconium drill rods. The base plate of the machine was anchored to the rock surface using a 10 inch split bolt so as to be able to maintain a downwards leverage on the bit which was cooled by pumping water down the drill string at a pressure of 200 psi. The top few metres of rock transected by the drilling were intensely shattered as a result of quarrying and water loss occurred through the sides of the hole making it necessary to grease the drill rods to prevent sticking and abrasion. Core recovery from this part of the hole was low as small shattered lava pieces tend to move into it and block the core barrel, causing grinding of the core. Below the quarry floor the rocks appeared to be unfractured and relatively impermeable. A constant flow of water back up the drill hole was maintained and core recovery of nearly 100% was achieved.

Pieces of the drill core 4 cms in length were removed for geochemical work and thin sections made of the material on either side of these. The positions of these are indicated on the log of the drill core. They were selected so as to be able to relate any chemical variation between them to features such as marked changes in colour and texture and the presence or absence of vesicles, secondary mineral pods or veins.

The altered vesicle surrounds from the zeolitised lavas (LA 19, M 56) were removed by sawing these two samples across perpendicular to the vesicle margins. Thin sections that transected the amygdale/lava boundary were taken from these slices which were sawn into centimetre - wide strips parallel to the vesicle margin. The concentric zones of the secondary mineral pods in the Upper lava flow from Pennygown Quarry were similarly removed by sawing them into thin strips parallel to the pod margins. The material obtained was used only for XRD studies as it was insufficient for chemical work. Only the smaller pods 3 - 4 cms. in diameter could be treated in this way as the larger zeolite and calcite - filled ones were extremely friable and tended to disintegrate on collection.

All the vein and vesicle samples were crushed by hand using an agate pestle and mortar; the other specimens were treated as follows. A steel rock splitter was used to remove any weathered surfaces and split them into approximately one inch cubes. These were then reduced to a grain size of 1200 mesh or less with a steel jaw crusher. 40 gm splits of this material were then ground to a 200 mesh grain size in a tema using 20 second grinding times. Approximately half of the samples were done in an agate tema and half in a tungsten - carbide one and no meaningful chemical differences between these two groups in ratios such as Ta/Nb (see fig.AII - 1) could be detected, indicating that the use of small sample portions and low grinding times prevented significant Ta contamination of the powders. Similarly, the adherence of both the hammer collected and drill - core samples from the same lava flow in Pennygown quarry to the same geochemical trends, demonstrates that contamination during drilling was insignificant for the elements considered in this study.

Major element analyses

H_2O^- was not determined as replicate measurements of this on several samples produced results that varied considerably; by up to 50% in some cases. No correlation could be found between mineralogy and H_2O^- . The values of H_2O^- for zeolite - rich samples showed the same range as samples virtually devoid of secondary minerals, suggesting that most of the water determined as H_2O^- was atmospheric water adsorbed by the rock powders. Accordingly, all the samples were dried at $110^\circ C$ for 24 hours before analysis. Zeolite - rich samples were dried by raising the oven temperature to $100^\circ C$ over a period of several hours.

The major element oxides SiO_2 , TiO_2 , Al_2O_3 , $Fe_2O_3^*$, MnO , MgO , CaO , K_2O and P_2O_5 were obtained using the Phillips 1212 X-ray spectrometer at Imperial College. The powders were ignited to constant weight at $850^\circ C$ and then fused with lithium tetraborate in a 1 : 7 ratio at $1100^\circ C$ in platinum crucibles. After quenching, the resulting glass was ground and pressed into briquettes using polyvinyl alcohol solution as an internal binder. A two - in - three duplication ratio was used and both sides of the non - duplicated sample briquettes were analysed. Various aspects of this method have been discussed by Borley (1977) and Parker (1977a). The major potential source of error is differential water absorption by the standard and sample briquettes and to eliminate this they were dried together at $110^\circ C$ for 24 hours and stored in a dessicator immediately before analysis.

All XRF data was corrected for dead - time and machine drift. The sample concentrations were calculated from calibration lines, erected from standards run both before and after the samples, using the procedures of Parker and Willis (1977) and Parker (1977b). U.S.G.S. standard rocks and I.C. internal standards covering the compositional range $38\% < SiO_2 < 60\%$ were used and the results checked by running standard briquettes as 'unknowns' with the samples (Table AII - 1). In addition, replicate analyses of some of the samples were made by wet-chemical techniques and two other XRF methods (Table AII - 2).

Na_2O was determined by flame photometry using a radiation buffer solution with both the samples and the standards (Maxwell 1968). FeO was determined titrimetrically and subtracted from the total Fe_2O_3 value obtained by XRF, assuming that $Fe_2O_3^* - (FeO \times 1.1113) = Fe_2O_3$.

The samples were decomposed in the presence of NH_4 , VO_3 and excess Fe determined by titrating against ferrous ammonium sulphate (Whipple 1974).

Table A II - 1 Analyses of U.S.G.S. Standard rocks
on a volatile - free basis.

	AGV		recommended value (Abbey 1973)	BCR	recommended value (Abbey 1973)
SiO_2	60.37	60.30	60.21	54.88	54.85
TiO_2	1.06	1.05	1.06	2.23	2.22
Al_2O_3	17.37	17.39	17.36	13.65	13.68
Fe_2O_3^*	6.87	6.92	6.94	13.60	13.54
MnO	.10	.10	.10	.19	.19
MgO	1.44	1.59	1.56	3.65	3.49
CaO	4.96	4.98	5.04	6.98	6.98
Na_2O	4.42	4.42	4.31	3.29	3.29
K_2O	3.02	3.01	2.95	1.74	1.68
P_2O_5	.50	.50	.50	.37	.33
Total	100.11	100.26	100.08	100.58	100.25

Table AII - 2 Replicate major analyses of samples by different analytical methods

	M 7 ^a	M 7 ^b	M 7 ^c	M 7 ^d	M 8 ^a	M 8 ^c
SiO ₂	46.94	46.63	46.93	46.46	46.80	46.48
TiO ₂	3.07	3.09	3.19	3.03	3.06	3.17
Al ₂ O ₃	16.53	16.50	17.12	16.54	16.70	17.11
Fe ₂ O ₃ *	15.39	15.39	15.85	15.40	15.44	15.71
MnO	.19	.19	.18	.18	.19	.18
MgO	5.42	5.32	5.34	5.52	5.40	5.40
CaO	7.51	7.51	7.49	7.59	7.65	7.50
Na ₂ O	4.18	4.33	4.69	4.18	4.04	4.40
K ₂ O	.27	.24	.28	.26	.23	.23
P ₂ O ₅	.30	.30	.31	.34	.27	.28
	M 37 ^a	M 37 ^b	M 59 ^a	M 59 ^b		
SiO ₂	44.24	44.61	47.14	47.75		
TiO ₂	1.52	1.52	2.63	2.68		
Al ₂ O ₃	15.09	15.29	14.68	14.78		
Fe ₂ O ₃ *	12.59	12.90	14.17	14.05		
MnO	.19	.19	.26	.27		
MgO	9.18	9.52	3.28	3.32		
CaO	9.60	9.68	6.99	7.09		
Na ₂ O	2.18	2.27	4.69	4.70		
K ₂ O	.27	.28	1.49	1.49		
P ₂ O ₅	.14	.15	1.68	1.34		

a - this study

b - wet chemical analysis by H.Lloyd, Bedford College

c - XRF determination at Bedford College using mixed lithium tetraborate and lithium carbonate flux (Wood 1977)

d - XRF analysis using flux mixture of Norrish and Hutton (1969)

- analyst R.Parker, Imperial College

Table AII - 3 Multiple analyses for major element oxides of sample M 39

	1	2	3	4	5	6	7	8	9	10	Mean	Standard Deviation
SiO ₂	42.78	42.72	42.78	42.61	42.60	42.77	42.76	42.88	42.74	43.16	42.78	.157
TiO ₂	1.26	1.26	1.26	1.26	1.27	1.25	1.25	1.25	1.26	1.27	1.26	.007
Al ₂ O ₃	15.63	15.52	15.64	15.41	15.41	15.53	15.34	15.42	15.44	15.51	15.49	.099
Fe ₂ O ₃ *	11.14	11.18	11.24	11.00	11.05	11.05	11.10	11.06	11.15	11.15	11.11	.073
MnO	.20	.20	.20	.20	.19	.19	.20	.19	.20	.20	.20	.055
MgO	6.09	6.19	6.21	6.26	6.05	6.09	6.09	6.19	6.11	6.27	6.16	.078
CaO	15.44	15.40	15.50	15.30	15.39	15.28	15.40	15.33	15.46	15.45	15.40	.072
Na ₂ O ^(a)	1.97	1.97	1.97	1.97	1.97	1.97	1.97	1.97	1.97	1.97	-	-
K ₂ O	.14	.13	.14	.14	.14	.14	.13	.15	.13	.14	.14	.006
H ₂ O ^(b)	5.48	5.48	5.48	5.48	5.48	5.48	5.48	5.48	5.48	5.48	-	-
P ₂ O ₅	.15	.15	.15	.15	.15	.15	.15	.15	.16	.15	.15	.003
CO ₂ ^(b)	.23	.23	.23	.23	.23	.23	.23	.23	.23	.23	-	-
Total	100.51	100.43	100.80	100.01	99.93	100.13	100.10	100.30	100.33	100.98		
(a) Na ₂ O average of flame photometry values table AII - 5												
(b) CHN analysis												

Table AII - 4 FeO, Na₂O Determinations Standard Rocks.

	FeO		Na ₂ O	
	this study	recommended Abbey(1973)	this study	recommended Abbey(1973)
NIMN	7.34 7.36	7.44	2.39 2.39 2.46	2.47
91	1.32	1.38	-	-
DR	-	-	2.87	3.00

Table AII - 5 Multiple determinations of Na₂O in M39.

1	2	3	4	5	6	7
1.99	1.94	1.90	2.04	1.99	1.99	1.99
8	9	10	Mean	Standard Deviation		
1.94	1.99	1.94	1.97	.040		

Volatiles determinations.

Loss on ignition was determined for all the samples to give an estimate of the total volatile content. The powders were weighed into previously dried crucibles and ignited to constant weight at 850°C. The percent weight loss, corrected for the oxidation of FeO to Fe₂O₃, was then calculated. Eight samples (LA 8, LA 14, M 7, M 51, M 53, M 13, M 24, M 27) were analysed for F and Cl using the method of Sen Gupta (1968) but no detectable amounts of these elements could be found. H₂O⁺ and CO₂ were determined using a Perkin and Elmer model 240 CHN analyser. All the analyses were done in duplicate. Spec - pure organic compounds containing known amounts of hydrogen and carbon were used to check the sensitivity as standard rocks with a similar range of H₂O and CO₂ contents to the Mull lavas were not available. H₂O⁺ was also determined in duplicate for several samples using the rapid method of Shapiro and Brannock (1975) for comparison (Table AII - 6).

Table A II - 6 Volatile determinations.

Sample.	Loss on ignition	H ₂ O ⁺	CHN analysis.		
			H ₂ O	CO ₂	Total
LA 2	2.21	1.86	1.87	.05	1.93
LA 3	2.31	2.14	2.22	.05	2.27
LA 15	2.12	1.78	2.35	.04	2.39
M 5	1.78	1.61	1.97	.12	2.09
M 6	1.67	1.14	1.62	.01	1.63
M 7	1.31	.91	1.38	.05	1.43
M 8	1.67	1.19	1.79	.01	1.80
M 51	2.51	2.58	2.59	.09	2.68
M 13	6.12	5.48	6.51	.03	6.54
M 14	6.47	4.79	5.57	1.59	7.16
M 17	5.69	5.11	5.50	.28	5.78
M 18	5.73	5.19	5.67	.27	5.94
M 28	2.85	2.73	2.87	.01	2.88
M 42	3.32	2.99	3.28	.05	3.33

The values determined with the CHN analyser agree well with the LOI values for most of the samples whilst, the H_2O^+ values determined by the method of Shapiro and Brannock tended to be lower than the values obtained by both the other methods. This discrepancy is most marked for the extensively altered samples (e.g. M 13) and the H_2O^+ values measured for these rocks using the CHN analyser were higher than those obtained by both the other methods. This is almost certainly due to the fact that contained water is not released from minerals such as epidote and amphibole on heating in air until temperatures in excess of $1000^\circ C$ are reached. The ignition of the powders in a stream of pure oxygen in the CHN analyser avoids this problem and ensures that more complete dehydration is achieved. Hence, the slightly higher totals obtained with the CHN analyser were used in this study.

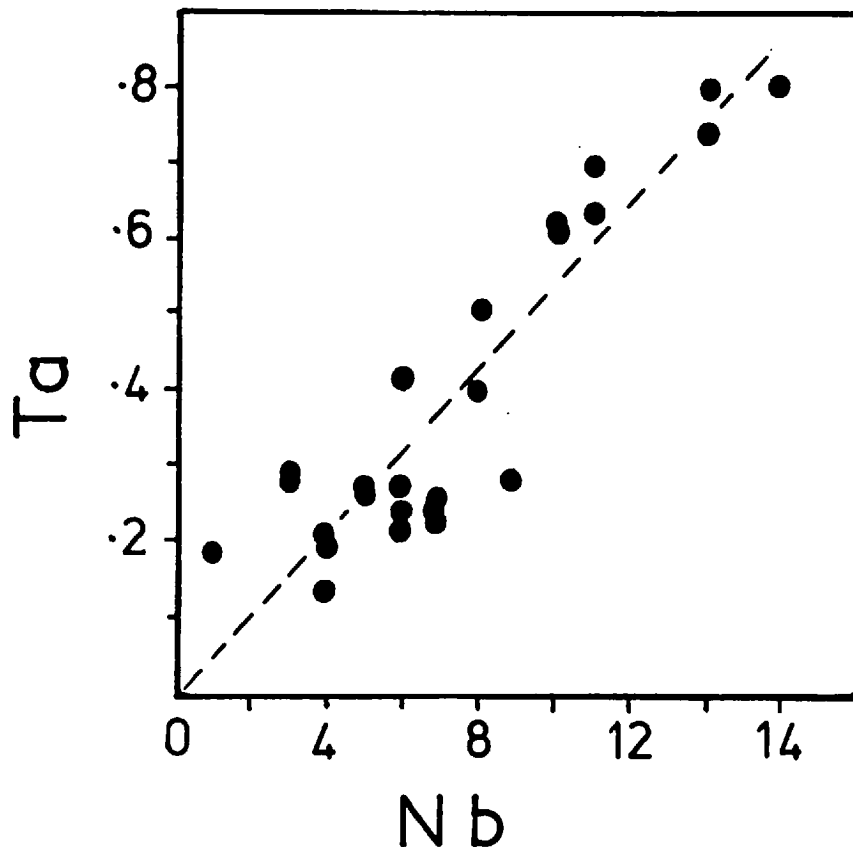


Figure AII-1.
Ta versus Nb in
the Mull lavas.

Trace element analyses.

The elements Zr, Y, Rb, Nb, Sr, Zn, Cu, Cr, Ni and Ba were determined using XRF methods. Two different procedures were used. In chapter 6 the Mull lavas are compared with lavas and dykes from the other Tertiary centres. The Skye Main Lava Series (Thompson et. al. 1979), Skye and Mull dykes (Mattey et.al. 1977) and the samples from the Blackstones centre (Mitchell et.al. 1976) were all analysed at Bedford College. Accordingly, Zr, Y, Rb, Nb, Sr and Zn for the Mull lavas were determined by the same method at Bedford College, to ensure that any differences detected between these groups were real and not a function of analytical procedure. The Skye and Mull lavas were analysed at the same time using the same calibration lines and so the accuracy and precision data listed in Tables AII - 7 and 8 apply to both these groups.

The analyses were made on pressed powder pellets made from 6 gm of rock powder and 1 gm of binding resin. The pellets were strengthened by baking in an oven at 108°C for 20 minutes. The elements were analysed as a group using the silver X-ray tube. Calibrations were erected using international and internal standard rocks. The intensity of reflected silver X-rays were recorded during the analyses, from which the Sr mass absorption of each sample could be calculated using the calibration of the U.S.G.S. standards. Fuller descriptions of the analytical and computing procedures are given by Wood (1977).

Zr, Y, Rb, Nb, Sr and Zn for the drill core samples (C 54 - C 246), the vesicle surrounds (IA 19, M 56) and the veins (M 24, M 64), and Ba, Cu, Cr and Ni on all the samples were determined at Imperial College. Pressed powder pellets were made from 5 gm rock powder mixed with 10 drops of polyvinyl alcohol solution as an internal binder. These were backed with boric acid and pressed in a steel die at a pressure of 6 tons/sq. inch. Standard trace element discs were run with the samples and the results determined by comparison with a spiked reference sample. Blanks were run to enable tube background factors to be measured and mass absorption corrections, calculated from the major element analyses, were applied. The results were calculated using an Imperial College programme described by Parker (1979) who also gives details of the analytical methods.

Standard rock analyses and precision data are given in tables AII - 9 and 10.

Zr, Y, Rb, Nb, Sr and Zn were also redetermined at Imperial College on several of the samples analysed at Bedford College. No significant differences between the results obtained using these two different methods were detected, other than for Zr. A 5% relative difference existed between the two data sets for this element. Both accuracy and precision were better for the Imperial College data and so Zr was redetermined for all the samples. The difference is probably due to the choice of X-ray peak. The Bedford College Zr analyses were made using the K_{β} peak whilst, the Imperial College determinations were made using the K_{α} peak and corrected for Sr interference. The use of the K_{β} peak avoids the problem of Sr interference but results in lower count rates and a reduction in accuracy and precision for samples with relatively low concentrations. Since absolute accuracy is less important than relative accuracy in this particular study, the Imperial College Zr determinations were used in the studies of intra - lava variation described in chapters 2 and 3 whilst the Bedford College data was used in chapter 6 for the reasons described above. Both sets of Zr data are listed in Appendix I.

Instrumental Neutron Activation Analysis (I.N.A.A.)

The trace elements Ta, Th, Hf and the REE (Ce, Nd, Sm, Eu, Gd, Tb, Tm, Yb and Lu) were determined by this method (Gordon et.al. 1968) using a Ge(Li) 1 cm³ low energy photon detector with a resolution of approximately 640 eV at 122 keV. La was determined using a Ge(Li) 30 cm³ (large volume) detector with high resolution in the 1000 to 2000 keV energy range. The gamma spectra were recorded on a 1024 channel multi - channel analyser and the data reduced using the photopeak method of Routi. (1969). All the analyses were performed at Bedford College and the sample preparation, counting procedures and computer programmes used were the same as those described by Wood (1977) with one exception- longer count times were used. All the samples were counted for a minimum of twelve hours and those collected from the same lava flows were counted for a minimum of 24 hours. In addition these samples (M 13 - 22, M 51, M 53, M 56 Zr, C 191 - C232 a/b) were packed for irradiation in a random order so that they occupied different positions in the reactor core. They were similarly counted in a

random order rather than in any particular sequence so as to eliminate systematic errors during analysis. The results obtained on U.S.G.S. standard rocks at Bedford College by this method are listed in Table AII - 12 and again the accuracy and precision data apply to both the Mull lavas and the Skye lavas discussed in chapter 6.

Table AII - 7 Trace element analyses of U.S.G.S. Standard rocks made at Bedford College.

	G - 2	GSP	AG V	W - 1	BCR	
Zr	1	309,314	500,495	208,205	79,89	171,164
	2	300	500	225	105	190
	3	300	500	220	105	185
Y	1	10	29	22	19	38
	2	12	30	21	25	37
	3	12	32	26	25	46
Rb	1	168	247	64	19	38
	2	168	254	67	21	37
	3	170	250	67	21	46
Sr	1	490	239,230	652,641	187,180	317,318
	2	479	233	657	190	330
	3	480	230	660	190	330
Nb	1	12	20	13	8	14
	2	13.5	29	15	9.5	13.5
	3	14	29	15	9.5	14
Zn	1	76	100	81	75	102
	2	85	98	84	86	120
	3	85	98	84	86	120
1 - measured values						
2 - recommended values Flanagan (1973, 1976)						
3 - recommended values Abbey (1973, 1975)						

Table AII - 8 Multiple trace element analyses of sample M 17
made at Bedford College

	Zr	Y	Rb	Nb	Sr	Zn
1	107	21	16	4	333	70
2	102	19	15	6	322	74
3	109	23	13	5	328	72
4	109	18	13	6	334	74
5	100	18	15	6	331	74
6	105	17	16	7	329	74
7	112	21	12	6	338	73
8	99	21	12	6	332	73
9	94	17	16	6	332	75
10	112	22	13	6	326	75
Mean	104.9	19.7	14.1	5.8	330.5	73.4
Standard deviation	6.01	2.16	1.66	0.79	4.48	1.51

Table AII - 5 Trace element analyses of standard rocks made at Imperial College. 1, 2, 3 as for Table AII - 7.

		Zr	Y	Rb	Nb	Sr
G1	1	224,224	14,13	216,216	23,23	253,255
	2	210	13	220	23.5	250
	3	-	-	-	-	-
G-2	1	322,320	11,8	168,169	14	460,478
	2	300	12	168	13.5	479
	3	300	12	170	14	480
GSP	1	514,511	29,29	254,257	26,23	230,236
	2	500	30	254	29	233
	3	500	32	250	29	230
NIMS	1	10,9	4,nd	521,539	nd,nd	62,62
	2	30	5	550	3	76
	3	-	-	560	-	76
AGV	1	216,216	24,22	69,67	16,16	683,663
	2	225	21	67	15	657
	3	220	26	67	15	660
W-1	1	91,91	27,25	21,21	6,7	185,188
	2	105	25	21	9.5	190
	3	105	25	21	9.5	190
BCR	1	187,186	45,45	51,48	12,14	342,344
	2	190	37	47	13.5	330
	3	185	46	47	14	330
		Cr	Ni	Cu	Zn	Ba
G1	1	-	-	16,16	71	-
	2	-	-	13	45	-
	3	-	-	-	-	-
G-2	1	-	6,5	19,15	85	1842
	2	-	5	12	85	1870
	3	-	6	11	85	1850
GSP	1	17	11,13	33,37	100	1259
	2	13	13	33	98	1300
	3	13	9	35	98	1300
NIMS	1	-	6,3	22,20	-	2500
	2	-	8	23	-	2590
	3	-	8	19	-	2400
AGV	1	9	18,17	56,55	83	1214
	2	12	19	60	84	1208
	3	12	17	63	84	1200
W-1	1	117	74,66	104,104	83	-
	2	114	76	110	86	-
	3	120	78	110	86	-
BCR	1	14	15,12	19,19	123	720
	2	18	16	18	120	675
	3	16	13	19	120	680

Table AII - 10 Repeat trace element analyses on LA 18
made at Imperial College.

	1	2	3	4	5	Mean	Standard deviation
Zn	111	119	105	106	112	110.6	5.59
Cr	713	731	714	725	718	720.2	7.66
Nb	4	5	1	4	5	3.8	1.64
Ni	294	295	288	297	286	292	4.74
Cu	161	155	161	152	165	158.8	5.22
Zr	90	91	92	93	93	91.8	1.30

Table AII - 11 Comparison of trace element determinations on the
same samples made at Imperial College(1) and Bedford College(2).

	LA 18	M 7	M 54	M 55	M 17	M 24
Zr 1	92	227	106	112	97	nd
2	96	230	118	112	105	nd
Y 1	24	32	23	29	21	nd
2	21	35	22	24	20	nd
Rb 1	4	2	nd	nd	14	2
2	4	3	nd	nd	14	2
Nb 1	4	3	5	3	6	1
2	4	8	4	4	7	1
Sr 1	298	554	250	295	335	169
2	296	560	253	289	331	163

Table AII - 12 Neutron Activation analysis, Bedford College figures for accuracy and precision.

<u>Sample</u>	BCR - 1									W-1			
	<u>5.4.05</u>	<u>11.3.08</u>	<u>15.3.01</u>	<u>20.1.07</u>	<u>21.2.08</u>	<u>Mean</u>	<u>Standard Devi- ation</u>	<u>No. of Samples</u>	<u>Flanagan 1973</u>	<u>5.4.07</u>	<u>21.3.08</u>	<u>Mean</u>	<u>Flanagan 1973</u>
La	25.04	-	23.80	-	23.80	24.21	0.716	3	26	11.55	-	11.55	9.8
Ce	50.92	50.92	57.78	52.82	52.05	52.90	2.845	5	53.9	22.57	22.69	22.63	23
Nd	28.62	28.60	30.06	29.67	30.01	29.39	0.730	5	29	13.32	14.06	13.69	15
Sm	7.22	-	7.33	-	7.30	7.28	0.057	3	6.61	3.67	3.71	3.69	3.6
Eu	2.08	2.05	2.17	2.07	2.10	2.09	0.046	5	1.94	1.18	1.19	1.19	1.11
Gd	-	6.86	-	6.57	6.82	6.75	0.157	3	6.6	3.67	3.75	3.72	4
Tb	1.07	1.03	1.14	1.05	0.96	1.05	0.065	5	1.0	0.63	0.65	0.64	0.65
Tm	0.54	0.58	0.52	0.54	0.52	0.54	0.024	5	0.6	0.36	0.32	0.34	0.30
Yb	3.51	3.44	3.60	3.50	3.42	3.49	0.071	5	3.36	2.14	2.18	2.16	2.1
Lu	0.54	0.52	0.56	0.42	0.52	0.51	0.540	5	0.55	0.34	0.34	0.34	0.35
Ta	0.92	0.85	0.87	0.81	0.87	0.86	0.040	5	0.91	0.53	0.48	0.51	0.50
Th	6.45	6.48	7.02	6.33	7.02	6.66	0.333	5	6.0	2.51	2.54	2.53	2.42
Hf	4.90	4.69	5.19	4.77	4.92	4.89	0.191	5	4.7	2.58	2.60	2.59	2.67

Microprobe analyses.

Mineral analyses were made using the Microprobe at the Department of Mineralogy and Petrology, Cambridge University which is fitted with an energy - dispersive X-ray spectrometer (Statham 1976). Analytical precision, detection limits and comparison of the method with that of the conventional 'Bragg angle' microprobe spectrometry have been given by Reed and Ware (1975). The operating conditions used were: accelerating voltage 20 kV, specimen current 0.3 A., counting times 80 secs., beam focused to minimum spot. No measureable loss of Na during analysis of feldspars was detected. Zeolites and carbonates did nevertheless lose volatiles (and possibly alkalis) during analysis and the minerals could be seen to contain large pits caused by the surface loss of material under the beam. A defocussed beam and reduced count times were both tried in an attempt to reduce the effects of this but some surface disintegration could always be subsequently observed in reflected light.

When analysing the secondary minerals, or the altered plagioclases in the greenschist - facies lavas, either olivine or jadeite standards were determined every fifth analysis. Only those analyses bracketed by good standard determinations with totals close to 100% were accepted. As a further check Dr. N.J. Charnley also made several analyses of the altered minerals in the samples and produced similar low totals and 'mixed' analyses for the Fe:Ti oxides in the zeolitised lavas and altered primary minerals in the greenschist - facies lavas. Hence, these are thought to be the result of oxidation, hydration and secondary mineral growth as discussed in chapters 2 and 3.

Table AII - 13 Analyses of olivine probe Standard.

	1	2	3	4	5	6	7	8	9	10
SiO ₂	40.30	40.16	39.75	40.43	40.03	40.48	40.83	40.21	40.60	40.24
FeO	9.75	9.72	9.62	9.59	9.64	9.81	9.72	9.79	9.62	9.74
MnO	0.14	-	-	0.15	-	0.12	0.16	-	0.12	-
MgO	49.51	48.80	49.13	48.89	49.43	49.70	49.49	48.96	49.83	49.20
NiO	0.31	0.27	0.26	0.34	0.22	0.30	0.28	0.33	0.32	0.34
Total	<u>100.01</u>	<u>98.95</u>	<u>98.76</u>	<u>99.39</u>	<u>99.32</u>	<u>100.41</u>	<u>100.49</u>	<u>99.28</u>	<u>100.49</u>	<u>99.52</u>
	11	12	13	14	15	16	17	18	19	20
SiO ₂	40.33	40.68	40.08	40.51	40.99	40.32	40.84	40.51	40.57	40.42
FeO	9.44	9.69	9.64	9.56	9.65	9.57	9.45	9.77	9.46	9.40
MnO	-	0.12	0.11	0.12	-	-	0.15	0.12	-	0.14
MgO	49.09	49.89	49.38	49.34	49.46	49.28	50.09	49.58	49.39	49.43
NiO	0.24	0.23	0.25	0.26	0.26	0.32	0.30	0.31	0.28	0.19
Total	<u>99.09</u>	<u>100.61</u>	<u>99.46</u>	<u>99.80</u>	<u>100.36</u>	<u>99.48</u>	<u>100.81</u>	<u>100.30</u>	<u>99.70</u>	<u>99.59</u>
	21	22	23	24	25	Mean	Standard Deviation	Recommended value		
SiO ₂	40.41	40.50	40.67	40.56	40.53	40.44	0.274	40.82		
FeO	9.76	9.62	9.74	9.62	9.78	9.65	0.117	9.55		
MnO	0.11	0.14	0.14	0.15	-	.08	0.067	.12		
MgO	49.56	49.66	49.66	49.70	49.52	49.43	0.311	49.20		
NiO	0.31	0.32	0.25	0.24	0.22	.28	0.042	.30		
Total	<u>100.15</u>	<u>100.23</u>	<u>100.45</u>	<u>100.27</u>	<u>100.06</u>	<u>99.88</u>		<u>99.99</u>		

Table AII - 14 Analyses of Jadeite probe standard.

	1	2	3	4	5	6	7	8	9
SiO ₂	59.22	59.50	58.90	59.40	58.53	59.17	58.58	59.66	59.57
Al ₂ O ₃	26.02	26.15	25.99	25.80	25.59	25.71	25.79	25.98	25.89
FeO	-	-	-	-	-	-	0.12	-	-
CaO	-	-	-	-	-	0.09	-	-	-
Na ₂ O	15.20	15.21	15.28	14.75	14.95	14.77	14.71	15.11	15.37
Total	100.44	100.85	100.17	99.95	99.07	99.74	99.21	100.75	100.83
	10	11	12	13	14	15	16	17	18
SiO ₂	58.95	59.70	58.93	58.86	59.17	59.06	58.82	59.87	58.87
Al ₂ O ₃	25.82	25.88	25.67	25.59	25.79	25.70	25.55	24.78	25.65
FeO	-	-	-	0.18	0.15	-	0.13	0.53	-
CaO	-	0.28	-	-	-	-	0.09	0.23	-
Na ₂ O	14.54	14.86	14.57	15.18	14.97	14.97	15.15	14.63	15.04
Total	99.32	100.73	99.17	99.81	100.07	99.73	99.73	100.03	99.56
	19	20	21	22	Mean	Standard Deviation	Recommended value		
SiO ₂	58.49	58.61	59.05	58.87	59.08	0.396	59.43		
Al ₂ O ₃	25.61	25.53	25.39	25.46	25.70	0.281	25.00		
FeO	0.23	-	-	-	0.06	0.127	0.22		
CaO	-	-	0.11	-	0.08	0.217	-		
Na ₂ O	14.97	14.98	15.17	14.74	14.96	0.237	15.29		
Total	99.30	99.11	99.72	99.07	99.88		99.94		

Table AII - 15 Analyses of Elba pyrite probe standard.

	1	2	3	4	5	6	Mean	Standard Deviation	Recommended value
S	52.25	52.70	51.84	52.09	52.50	51.93	52.22	0.333	53.48
Fe	46.44	46.95	46.29	46.56	46.83	46.33	46.57	0.270	46.53
Co	0.54	0.36	0.52	0.56	0.55	0.46	0.50	0.077	-
Cu	0.45	0.32	0.32	0.51	0.26	0.45	0.39	0.098	-
Zn	0.32	0.39	0.52	0.51	0.46	0.51	0.45	0.081	-
Total	100.00	100.73	99.49	100.23	100.58	99.68	100.13		100.01

Density determinations

The density measurements were made using a 50 cm³ density-bottle. The weight of rock powder used was between 0.8 and 1.0 gm., and the weight of fluid of known density (detergent solution) that was displaced, was measured.

The standard used was pure quartz and the values obtained given in Table AII - 16. The low precision is due to the small volume changes involved.

Table AII - 16 Density determinations on pure quartz.

1	2	3	4	5	6	7	8
2.639	2.642	2.623	2.633	2.657	2.629	2.639	2.674

Mean 2.642

Standard deviation 0.016

Recommended value 2.65

[5]

THE USE OF "IMMOBILE" TRACE ELEMENTS TO DISTINGUISH THE PALAEOTECTONIC AFFINITIES OF METABASALTS: APPLICATIONS TO THE PALEOCENE BASALTS OF MULL AND SKYE, NORTHWEST SCOTLAND

M. ANN MORRISON

Department of Geology, Imperial College of Science and Technology, London, SW7 2BP (Great Britain)

Received September 14, 1977

Revised version received February 15, 1978

The regional zeolitisation in the British Tertiary Volcanic Province causes little change in K and Sr in transitional basalts but mobilises these elements in the tholeiites. In contrast, local greenschist-facies hydrothermal alteration affects K and Sr in both basalt types and also P in tholeiites. Titanium, Nb, Zr and Y appear to be unaffected by low-grade metamorphism in all the basalts. Plots involving these elements cannot distinguish between Hebridean tholeiitic and alkalic basalts but demonstrate the occurrence of several distinct basaltic magma types on a regional scale within the Tertiary Province. Such magma types are not merely a feature of individual centres. Similar spatial chemical variation appears to occur within other extensional igneous provinces.

Attempts to deduce the palaeotectonic regime of the British Tertiary Volcanic Province from published "diagnostic" diagrams produce conflicting results, even for the same magma type. The range of settings derived for the area as a whole is clearly at variance with its known relation to the opening of the North Atlantic. The results suggest that the use of trace elements alone to diagnose the tectonic setting of ancient metabasic sequences could lead to erroneous results.

1. Introduction

Several classifications relating basic volcanics to their magma type and tectonic setting by means of trace element content have recently been proposed. Cann [1] and J.A. Pearce and Cann [2,3] suggested a scheme based on Ti, Zr and Y and, for less altered rocks, Hf, Zr and Sm. T.H. Pearce et al. [4] distinguished between oceanic and non-oceanic basalts using TiO₂, K₂O and P₂O₅. Floyd and Winchester [5] proposed a scheme based on Ti, Nb, Y, P and Zr to discriminate between tholeiitic and alkalic basalts but "obtained no meaningful separation between continental and oceanic analogues of any one type".

The nature and diversity of the igneous activity within the British Tertiary Province is well documented. Three distinct basaltic magma types have been recognised in Skye: (1) the Skye Main Lava Series, (2) low-alkali tholeiites, now renamed the

Preshal Mhor type, and (3) a third Fairy Bridge Magma type [6,7]. Equivalents of the first two have been noted elsewhere in the Province, in Antrim [8] and Mull [9]. The exact relationship between the different magma types is not clear, but in Skye they cannot be linked by the accumulation or fractionation of any of the observed phenocryst phases. Matley et al. [6] suggested that other Tertiary igneous centres might contain a similar range of basaltic magma types to that observed in Skye. Floyd and Winchester [5] classified the British Tertiary rocks as continental tholeiites. The same view was taken by Carmichael et al. [10] who summarised previous work in the region and described it as a mixed tholeiitic and alkali continental basalt province.

In this paper analyses of Mull basalts and new trace element analyses of the Skye Main Lava Series are combined with published data to assess both the persistence of the different magma types within the

province and the effectiveness of the various "diagnostic" trace element diagrams.

2. Analytical procedure

Samples of the Mull lavas 2 kg in weight were crushed for analysis to eliminate small-scale variations. Major element compositions were determined using a Philips 1212 X-ray spectrometer with lithium tetraborate fusions [11]. Na₂O, FeO, H₂O* and H₂O⁺ were determined using flame photometric, titration and gravimetric methods respectively. A two-in-three duplication ratio was used and the results further checked against wet chemical analyses of six of the samples. The trace elements Nb, Y, Rb, Sr and Zr were also determined by X-ray fluorescence methods [12]. As data obtained in three different laboratories are combined in this paper, repeat analyses were made of several of these rocks to ensure that any differences in trace element content are not a function of laboratory procedure.

3. Geological setting and petrography

Fourteen of the lavas analysed (Table 1) belong to the Mull Plateau Group of Bailey et al. [13]. These

TABLE 1

Specimen No.	TiO ₂ (wt.%)	K ₂ O (wt.%)	P ₂ O ₅ (wt.%)	Nb (ppm)	Y (ppm)	Sr (ppm)	Zr (ppm)
<i>Zeolitized lavas</i>							
LA7	1.86	0.24	0.15	4	26	344	128
LA8	1.82	0.26	0.15	5	27	318	127
LA9	1.81	0.26	0.14	3	25	334	123
LA10	1.79	0.23	0.14	5	28	325	133
LA11	1.86	0.24	0.14	5	27	323	123
LA13	1.53	0.26	0.14	6	21	231	117
LA14	1.54	0.25	0.14	1	23	241	111
LA15	1.56	0.27	0.14	4	21	293	105
MS1	2.03	0.18	0.16	4	27	315	138
MS2	2.02	0.17	0.17	6	24	320	144
MS3	2.03	0.17	0.17	4	26	287	137
MS4	1.99	0.15	0.16	4	22	253	135
MS5	2.05	0.16	0.16	4	24	289	128
<i>Hydrothermally altered lava flow</i>							
M13	1.61	0.24	0.10	7	28	247	147
M14	1.54	0.07	0.17	9	24	377	148

form the lower half of the lava pile in Mull. Individual flows contain phenocrysts of olivine and less common plagioclase in a matrix of olivine, plagioclase, titaniferous augite, titanomagnetite, traces of biotite, apatite, chlorite and zeolites. They are transitional basalts and chemically very similar to the Skye Main Lava Series of Thompson et al. [7,14], who give a fuller description of this type.

Three representatives of the Non-Porphyrific Central type are included (Table 1: MS183, MS184, MS185). These tholeiites occur mainly in the down-faulted central calderas of Mull [13]. The analysed samples contain very rare phenocrysts of plagioclase, augite and magnetite in a fine groundmass of abundant plagioclases, granules of augite, magnetite and chloritic material. Bailey et al. [13] found these lavas to be easily recognisable, both in thin section and hand specimen, and estimated a total thickness for the group even greater than that of the Plateau Group.

The lava enclosing Macculloch's tree (Table 1: M61) belongs to the Staffa type, a sub-group of the Non-Porphyrific Central type [13]. Basalts of this type occur in limited numbers at the base of the lava pile, interdigitated with the Plateau Group lavas. M61 consists of plagioclase and augite phenocrysts in a groundmass of plagioclase, augite, minor olivine and magnetite. An originally glassy matrix is now repre-

TABLE 1 (continued)

Specimen No.	TiO ₂ (wt.%)	K ₂ O (wt.%)	P ₂ O ₅ (wt.%)	Nb (ppm)	Y (ppm)	Sr (ppm)	Zr (ppm)
M15	1.45	0.11	0.16	6	22	296	120
M16	1.39	0.58	0.15	5	20	427	114
M17	1.34	0.66	0.14	6	20	331	120
M18	1.39	0.69	0.16	7	21	314	128
M19	1.34	0.54	0.15	7	21	274	119
M20	1.35	0.10	0.15	6	21	264	109
M21	1.38	0.39	0.15	6	21	275	128
M22	1.40	0.69	0.15	7	24	294	113
<i>Mull Plateau Group</i>							
LA2 (z)	2.07	0.31	0.17	8	28	316	154
LA17 (z)	1.68	0.37	0.18	6	24	309	125
LA20 (z)	1.60	0.24	0.14	3	25	292	111
M1 (z)	1.81	0.20	0.14	3	27	276	107
M12 (z)	2.66	0.37	0.25	15	26	582	176
M32 (h)	1.64	0.25	0.16	4	20	303	111
M36 (h)	1.81	0.25	0.16	3	23	267	120
M37 (h)	1.50	0.27	0.14	4	27	276	113
M47 (h)	2.39	0.32	0.24	5	25	353	154
<i>Other Mull basalts</i>							
M61 (z)	1.74	0.81	0.23	7	30	485	140
MS183 (h)	1.90	0.73	0.41	14	61	294	257
MS184 (h)	1.97	0.38	0.33	13	56	248	218
MS185 (h)	1.44	1.70	0.22	10	36	272	203
MS133 (z)	1.25	0.14	0.12	5	46	124	89
AV* (z)	0.87	0.13	0.07	5	26	129	48
<i>Skye Main Lava Series</i>							
SK894 (z)	1.42	0.55	0.19	7	15	382	98
J1286 (z)	2.07	0.39	0.26	9	20	455	156
SK918 (z)	2.15	0.52	0.26	6	25	313	146
SK901 (z)	1.56	0.94	0.22	6	22	359	125
SK947 (z)	1.68	0.65	0.25	4	24	582	149
JF278 (z)	2.30	0.42	0.27	6	24	568	172
JF291 (z)	1.73	0.31	0.20	3	22	558	133
SK961 (z)	1.42	0.43	0.18	6	25	376	111
SK906 (z)	2.51	0.18	0.25	10	31	449	179
SK940 (z)	2.49	0.29	0.27	8	28	583	201
SK956 (z)	1.39	0.58	0.22	7	27	418	123
SK976 (z)	1.66	0.47	0.18	4	21	304	96
SK925 (z)	2.03	0.37	0.22	9	21	548	143
SK891 (z)	1.65	0.40	0.19	8	18	379	145
SK921 (z)	2.15	0.35	0.23	8	19	443	153
SK949 (z)	2.63	0.41	0.28	10	31	395	182
SK892 (z)	1.27	0.62	0.17	6	23	358	129
SK928 (z)	1.60	0.38	0.16	6	33	505	140
SK929 (z)	1.44	0.44	0.17	9	20	1210	114
SK932 (z)	2.05	0.22	0.20	6	26	332	152
<i>Skye basal tholeiite pillow</i>							
SK965 (z)	1.11	0.23	0.09	6	18	293	119

* AV = average of sixteen low-alkali tholeiite dykes [9].

z = zeolitized, h = hydrothermally altered.

TiO₂, K₂O, P₂O₅ for Skye Main Lava Series from Thompson et al. [7].

sented by chlorite-rich material. For comparison SK965, a petrographically similar pillow lava from the base of the Skye lava pile is included. Chemically, they are both olivine tholeiites [15].

Also included in Table 1 is a low-alkali tholeiite lava from Mull (MS133), an average of sixteen low-alkali tholeiite Mull dykes [9] and new trace element data for the Skye Main Lava Series [14]. Data for the Skye Preshal Mhor and Fairy Bridge magma types were provided by D.P. Matney.

4. Effects of hydrothermal alteration

Two distinct types of low-grade metamorphism occur in both Skye and Mull. Flat-lying regional zeolite-facies zones lie outside ^{18}O -depleted regions of steeply dipping greenschist-facies zones that constitute hydrothermal aureoles around the central intrusive complexes [16–18]. With the exception of some of the Skye dykes from the northern and southern extremities of that regional swarm, *all* of the basalts discussed here have been subjected to one or other of these metamorphisms.

To estimate the metasomatic effects of these processes, four lavas from the Mull Plateau Group were studied in detail. All of them appear to have been originally homogeneous in composition and texture. Three (Table 1: LA7–11, LA13–15, MS1–55) come from the *highest-grade* zeolite zone of Walker [16]. The thin sections of these flows show little petrographic evidence of zeolitisation, other than some serpentinisation of the olivines and the growth of material rich in serpentine, chlorite and zeolites in the groundmass. The fourth lava (Table 1: M13–22) is a hydrothermally altered flow from the epidote zone. In the least-altered part of the section only olivine has decomposed, with the consequent formation of serpentine, chlorite and iron oxides. As the alteration proceeded, plagioclases were albited and patches of calcite and/or epidote formed. The titanomagnetites are replaced by Fe-Ti oxides and sphene. Only at the margins of the flow has pyroxene completely broken down and a quartz-chlorite-albite-amphibole-sphene-epidote assemblage (M13) has been formed in which none of the original igneous mineralogy is preserved.

Titanium, Zr, Nb and Y preserve constant ratios in all the lavas studied and therefore appear to have

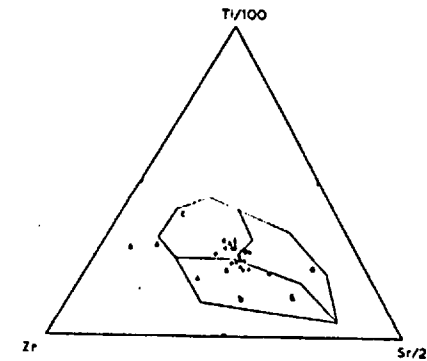


Fig. 1. Ti/100-Zr-Sr/2 diagram of J.A. Pearce and Cann [3] showing effects of low-grade alteration on basalt compositions. Fields: *a* = low-alkali tholeiites, *b* = calc-alkali basalts, *c* = ocean-floor basalts. Symbols: \circ = LA7–11, $+$ = LA13–15, Δ = M51–55, \bullet = M13–22, \blacktriangle = spilitised Deccan basalt [19].

been unaffected during alteration. The zeolitised lavas show slight variability in Sr content but not in K_2O or P_2O_5 as shown by the clustering of the data for each of these lava flows in Fig. 2. Flows M51–55, and LA13–15 exhibit internal differences of 60 ppm in Sr, causing variations of up to 7% in the Sr component in Fig. 1. M13–22, the hydrothermally altered

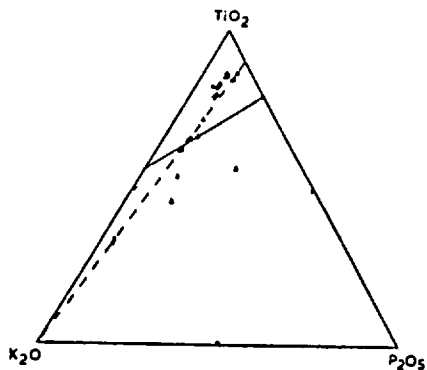


Fig. 2. TiO_2 - K_2O - P_2O_5 diagram of T.H. Pearce et al. [4] showing effects of low-grade alteration on basalt compositions. Symbols as Fig. 1.

flow, shows 18% and 26% variation in the Sr and K_2O components in Figs. 1 and 2, respectively. This is just sufficient to cause the points to plot across the dividing line between the oceanic and non-oceanic regions of the TiO_2 - K_2O - P_2O_5 diagram (Fig. 2). M13 is the only specimen in this flow to show loss of P_2O_5 . However, as this is also the only sample in which the igneous mineralogy has been totally destroyed, loss of P_2O_5 is not thought to occur in other less-altered rocks of this chemical type. King [17] found similar patterns of alteration zones within the Skye lavas, and also comparable chemical changes within single zeolitised lava flows. The Skye Main Lava Series should therefore show a similar degree of element mobility to the Mull Plateau Group.

No further results concerning the effects of these alteration processes on the other Scottish Tertiary magma types are available. There is, however, a wealth of published data describing the chemistry of low-grade metamorphic processes affecting tholeiites. Wood et al. [12] demonstrated in eastern Icelandic tholeiites that a *lower grade* of zeolitisation than that encountered in the Hebrides caused significant mobilisation of Sr and K_2O , but not Ti, Zr, Nb, Y or P, throughout the lava pile. Vallance [19] has described the transformation of a Deccan tholeiite to spilitite which, from his description, is analogous to the prod-

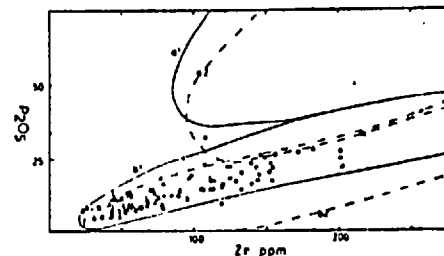


Fig. 3. Distribution of the various Skye/Mull basalt types on the P_2O_5 -Zr diagram of Floyd and Winchester [5]. Fields: a_1 = continental alkali basalts, b_1 = continental tholeiites, a_2 = oceanic alkali basalts, b_2 = oceanic tholeiites. Symbols, Skye basalts: Δ = Preshal Mhor type, \circ = Skye Main Lava Series, $+$ = Fairy Bridge type, \bullet = SK965; Mull basalts: \blacktriangle = low-alkali tholeiites, \bullet = Mull Plateau Group, \times = Non-Porphyrilite Central type, \bullet = M61.

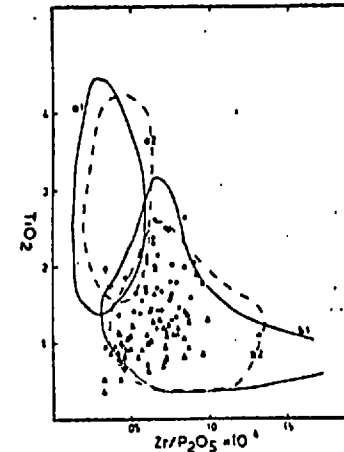


Fig. 4. Distribution of the various Skye/Mull basalts on the TiO_2 -Zr/ P_2O_5 diagram of Floyd and Winchester [5]. Fields and symbols as Fig. 3.

ucts of hydrothermal alteration around central intrusive complexes seen in the Hebrides. In the Deccan flow Sr varies from 55 to 600 ppm, K_2O from 0.34 to 2.22 wt.% and P_2O_5 from 0.10 to 0.75 wt.%. The Ti-Zr-Y ratios for both spilitite and tholeiite are

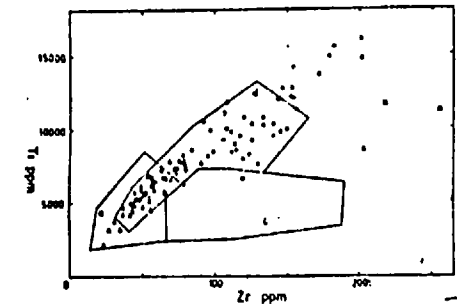


Fig. 5. Distribution of the various Skye/Mull basalts on the Ti-Zr diagram of J.A. Pearce and Cann [3]. Fields: *a* + *b* = low-alkali tholeiites, *c* + *b* = calc-alkali basalts, *d* + *b* = ocean-floor basalts. Symbols as Fig. 3.

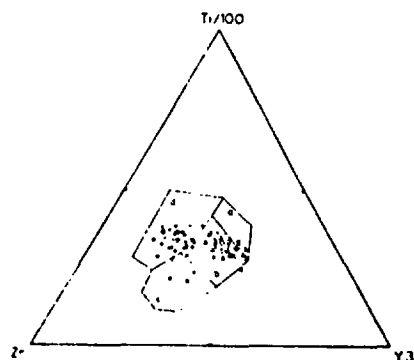


Fig. 6. Distribution of the various Skye/Mull basalts on the Ti/100-Zr-Y.3 diagram of J.A. Pearce and Cann [3]. Fields: *a* + *b* = low-alkali tholeiites, *c* + *d* = calc-alkali basalts, *d* = within-plate basalts. Symbols as Fig. 3.

constant. Tholeiites thus, appear to be far more susceptible to low-grade metamorphism than transitional basalts (see also Smith and Smith [20]). They can be expected to show a wider spread of results on diagrams involving Sr, K_2O or P_2O_5 , both within single lava flows (Figs. 1, 2) and for the groups as a whole (Figs. 7, 9), than the other Skye/Mull basalts. This is prob-

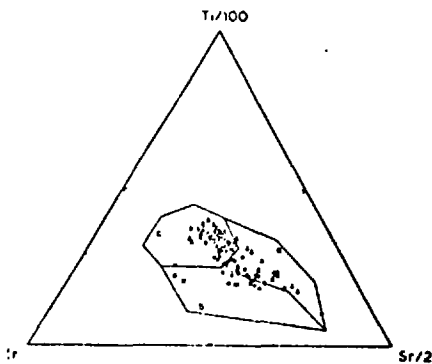


Fig. 7. Distribution of the various Skye/Mull basalts on the Ti/100-Zr-Sr/2 diagram of J.A. Pearce and Cann [3]. Fields as Fig. 2, symbols as Fig. 3.

ably due to the location of incompatible elements in interstitial glasses [21].

5. Distribution of the magma types on trace element diagrams

Recent studies in Iceland [22-24], Timolus [25], Skye [6] and from the Deep Sea Drilling Projects [26], suggest that many basaltic provinces contain a variety of magma types. Gibson et al. [27] suggested that this may be a general feature of extensional tectonic situations. In this section, plots of the Skye and Mull basalts on the different trace element diagrams proposed by various authors [1-5] are used to assess whether or not the basic magmas supplying these two centres were identical.

Skye Main Lava Series and Mull Plateau Group. These are indistinguishable from each other on all the diagrams. In each of Figs. 3-7 they occupy different regions from the low-alkali tholeiites. The Mull Plateau Group show a smaller scatter than the Skye lavas. This is thought to be a function of the larger hand specimen size taken for the former; eliminating small-scale inhomogeneities. The petro-tectonic interpretation of these lavas, as derived from the diagrams, is confused. They plot in the "ocean-floor", "within-plate" and straddle all three fields of Figs. 5-7 respectively.

Skye Preshal Mhor type and Mull low-alkali tholeiites. Again identical distributions are shown by the Mull and Skye rocks in Figs. 3-7. They lie in the "low-alkali tholeiite" region of the Ti/100-Zr-Y.3 diagram (Fig. 6) and between the "low-alkali tholeiite" and "ocean-floor" fields of Figs. 5 and 7. The greater degree of elemental mobility shown by slightly metamorphosed tholeiites is demonstrated by their spread in Figs. 7 and 9.

Skye Fairy Bridge type. These form a tight cluster on each of Figs. 3-7. On the Ti-Zr diagram (Fig. 5) they fall within the "ocean-floor" field, but the within-group variation on this and the P_2O_5 -Zr diagram (Fig. 3) exhibits a greater slope than is seen in any of the other basalt types, emphasising their distinctive chemistry. On the Ti/100-Zr-Y.3 (Fig. 6),

they fall mainly within the "ocean-floor" field, overlapping the Preshal Mhor and low-alkali basalts but totally separate from the Skye Main Lava Series and Mull Plateau Group. On the Ti/100-Zr-Sr/2 diagram (Fig. 7) they fall in the "low-alkali tholeiite" field, completely distinct from the Preshal Mhor type. The tight clustering of the data for this group in Fig. 9 suggests that these particular basalts have been relatively unaffected by alteration.

Mull Non-Porphyrific Central lavas. These again form a distinct group and they plot in totally different areas of Figs. 3, 5, 6 and 7 from any of the other basalt types. On the Ti-Zr diagram (Fig. 5) they occupy none of the fields delineated by J.A. Pearce and Cann. On the Ti/100-Zr-Y.3 and Ti/100-Zr-Sr/2 diagrams (Figs. 6, 7) they fall in the "calc-alkali" regions. M61 belongs to the group proposed by Bailey et al. [13] as suitable parental magma for the Central suite of lavas in Mull. This plots well away from the Central lavas in all the diagrams except Fig. 4 and is clearly unrelated to them. The Non-Porphyrific Central lavas would thus appear from these diagrams to belong to yet another distinct Hebridean magma type.

M61 and SK965. M61 is inseparable from the Skye Main Lava Series and the Mull Plateau Group on all the diagrams, despite its tholeiitic nature. SK965 plots close to these in Figs. 3-6 and separate from all the groups in Figs. 7 and 9. Both these lavas have the major element chemistry of typical ocean-floor tholeiitic basalts and the trace element chemistry, excepting P_2O_5 , of more alkalic types. It appears that in both Mull and Skye slightly anomalous lavas were produced at the base of the lava piles, during the initiation of the mantle melting cycles.

6. Discussion

The combined use of the various trace element diagrams, except the TiO_2 - K_2O - P_2O_5 and Nb/Y-Zr/ P_2O_5 plots (Figs. 8, 9), will successfully separate most Hebridean magma types. The immobility of Ti, Zr, Nb and Y during low-grade metamorphism suggests that these elements can be used with a high degree of confidence to similarly distinguish between meta-

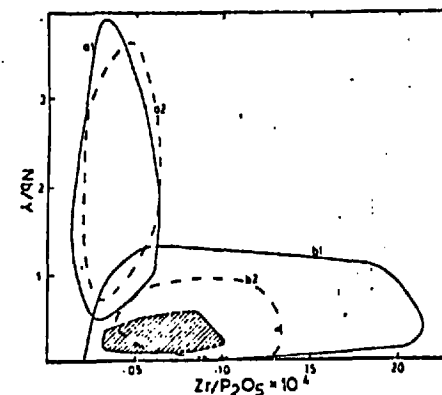


Fig. 8. Nb/Y-Zr/ P_2O_5 diagram of Floyd and Winchester [5]. Fields as Fig. 3. All the basalts plot in the shaded region with the exception of SK965 (a).

basalt varieties. It should be stressed that this conclusion is contingent upon the use of hand specimens large enough to eliminate small-scale metasomatically-produced inhomogeneities (cf. Smith and Smith [20]).

The overlapping chemistry of the Skye Main Lava Series and the Mull Plateau Group, and also of the Preshal Mhor magma type in Skye with the low-alkali tholeiites in Mull, shows that the generation of both magma types is a major regional feature of igneous activity within the British Tertiary Province. The similarity between these two centres is emphasised by the presence at the base of both lava piles of limited amounts of tholeiite with anomalous trace element concentrations (M61 and SK965).

The tholeiite/alkali basalt discriminant diagrams of Floyd and Winchester [5] fail to separate these basalt types in the Hebrides. It should be emphasised however, that the Skye Main Lava Series, the Mull Plateau Group and the Skye Fairy Bridge basalts all contain both nepheline- and hypersthene-normative varieties and are best described as transitional basalts. A slight repositioning of the field boundaries in Figs. 3 and 4 would bring many of them into the "alkaline" region. This would, however, cause a similar reclassification of the Non-Porphyrific Central type (quartz-norma-

tive) and M61 (14% normative hypersthene). This discrepancy between the normative and trace-element-based classifications of magma types cannot be attributed to low-grade metamorphic processes as, with the exception of possibly Sr, the compositions of all the transitional basalts affected by the regional zeolitisation appear to be pyrogenic [28]. In Fig. 8 the basalts all have low Nb/Y ratios and none of them plot in the "alkaline" field. As Thompson [29] points out, Tertiary Hebridean alkalic lavas possess lower incompatible-element abundances than those from many other regions, although the reasons for this are not yet fully understood. Other alkaline basalt suites with similar "anomalously low" trace element contents have been reported in the literature [30,31].

The trace element contents of basaltic magmas are a function of initial mantle concentration, the melt fraction and subsequent crystallisation processes. In contrast, the position of the normative join Ol-Cpx-Plag in compositional space is a function of pressure and hence depth of origin [32]. Thus chemical criteria used to distinguish between hypersthene- and nepheline-normative varieties will vary, not only from region to region but probably between different magma types within the same province. In metabasalts the immobile elements can undergo changes in concentration, due to the addition or leaching of more easily mobilised elements (see M13-22, Table 1). Despite the minor effects of this process, relative to the differences between basalt magma types, it will augment the problem of uniquely assigning altered basalts to one or other variety. The diagrams in Figs. 3, 4 and 8 could be improved, if a similar procedure was adopted to that of Schwarzer and Rogers [33] who defined an *area* on their alkali-silica diagram which represented the boundary between the alkali olivine basalt series and the subalkaline series.

All the diagrams purporting to distinguish palaeotectonic relationships (Figs. 5, 6, 7 and 9) largely fail to confirm the known setting of Hebridean Tertiary igneous rocks. The Skye Main Lava Series and the Mull Plateau Group plot in three distinct fields of Figs. 5-7. The data as a whole give results requiring the postulation of every single type of tectonic setting distinguished by the authors of the various diagrams [1-5]. The interpretation of the Non-Porphyrific Central lavas in Figs. 6 and 7 require an island arc situation, which is totally at variance with

all that is known of the region. The transitional basalts and SK965 and M61 also transgress this boundary in Fig. 7.

The reason the Non-Porphyrific Central lavas plot in the "calc-alkali" fields is they possess higher Zr and only slightly higher TiO_2 contents than the other Hebridean magma types. A high Zr/ TiO_2 ratio is often an indicator of magmatic differentiation. These lavas do possess occasional titanomagnetite phenocrysts and their inclusion in Figs. 5-7 may be criticised on such grounds. Nevertheless, all previous workers, notably Wager who allowed for the effects of fractional crystallisation on their chemistry, classified the Mull Non-Porphyrific Central lavas as *basalts* [13,34-36]. This highlights an inherent weakness in such diagrams: as crystal-liquid processes can cause data to plot in the "wrong" field. Floyd and Winchester [5] allowed for the effects of differentiation when formulating their diagrams. J.A. Pearce and Cann [3] used only rocks with 20% $> MgO + CaO$ > 12%. T.H. Pearce et al. [4] confined their attention to analyses with total alkalis below 20% on a $MgO \cdot (Na_2O + K_2O) \cdot (FeO + Fe_2O_3)$ diagram. These chemical screens use elements which are easily mobilised during alteration processes, making them unreliable in metabasalts.

Like the Hebrides, the Deccan basalts were erupted in an extensional regime, related to an active mid-oceanic ridge. Vallance [19] noted that rocks from Bhoiwada and another Deccan basalt, on the basis of their Ti-Zr-Y contents, "fall into the suite of island arc andesites, a suite to which they manifestly do not belong." Deccan basalt types include tholeiites and transitional alkali basalts [37]. This range of trace element distributions may not therefore be a unique feature of the British Tertiary but general to other regions of similar tectonic setting [27].

The petrotectonic status of the British Tertiary Province has already presented problems to the compilers of the "diagnostic" trace element diagrams discussed in this paper. Only Floyd and Winchester [5] used data for the region when formulating their diagrams. They classified both the British Tertiary and Deccan rocks as *continental tholeiites*. J.A. Pearce and Cann [3] stated that it was not possible to distinguish between ocean island and continental basalts by means of their trace element compositions alone, and

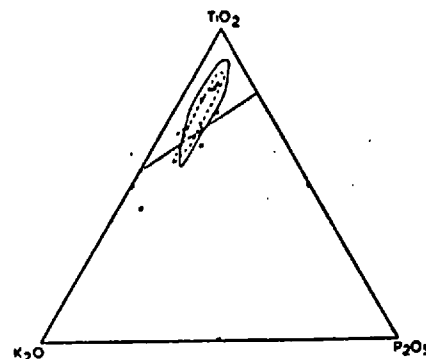


Fig. 9. Distribution of the various Skye/Mull basalts on the TiO_2 - K_2O - P_2O_5 diagram of T.H. Pearce et al. [4]. \circ = Predial Mhor magma type, \bullet = Skye Main Lava Series and Mull Plateau Group, \square = Skye Fairy Bridge magma type, \blacktriangle = SK965, \blacktriangle = Mull low-alkali tholeiites, \times = Mull Non-Porphyrific Central type, \blacksquare = M61.

placed the Deccan rocks in their "within-plate" division. T.H. Pearce et al. [4] in their compilation stated that the Deccan rocks show a "strongly oceanic character".

In Fig. 9 all the groups straddle the oceanic/non-oceanic division, with 89% of the data lying in the "oceanic" field. The failure of the TiO_2 - K_2O - P_2O_5 diagram to separate two major basalt provinces erupted upon continental crust from the lavas of ocean basins casts doubts on its validity. Also, the varying responses of K_2O and P_2O_5 in different basalt types to low-grade metamorphic processes suggest that this diagram may only be applied with impunity to fresh basalts: in which case their provenance is rarely in doubt. T.H. Pearce et al. [38] have also devised a diagram, based on major elements, to relate basic and intermediate rocks to tectonic setting. This plot uses only rocks with 51-56 wt.% SiO_2 . All except two of the 75 analyses used in the present study have $SiO_2 < 51$ wt.%, this diagram therefore cannot be applied to the Hebridean province.

Mattey et al. [6] compared the Preshal Mhor magma type of Skye with Mid-Ocean Ridge and Icelandic basalts and suggested that the British Tertiary Province may represent an abortive constructive plate margin. Thompson et al. [14] have shown that the

short-time-span mantle melting cycle beneath Skye is analogous to the long-time-span process proposed in recent models for ocean ridge basalt genesis. Future regional metamorphism of a Hebridean (or Deccan) type of igneous province would lead to the formation of a complex with many of the features of currently exposed amphibolite complexes, greenstone belts or ophiolite suites. After incurring added complications due to deformation, alteration and erosion, the trace-element petrotectonic analysis of such a complex, if taken in isolation from other geological data, could clearly lead to any one of a number of possible plate-tectonic interpretations. For these reasons, it is suggested that plots such as Figs. 1-9 be treated merely as a species of variation diagram: useful in identifying magma types and their evolutionary trends, but not as indicators of palaeotectonic environment.

Acknowledgements

Grateful thanks are due to Dr. R.N. Thompson, Dr. I.L. Gibson and K. Brodie for discussion and comments on the text, to Dr. I.L. Gibson, Miss G.F. Marriner and Mr. H. Lloyd of Bedford College for assistance with the analytical work and finally, to NERC for financial support.

References

- J.R. Cann, Rb, Sr, Y, Zr and Nb in some ocean floor basalt rocks, *Earth Planet. Sci. Lett.* 10 (1970) 7.
- J.A. Pearce and J.R. Cann, Ophiolite origin investigated by discriminant analysis using Ti, Y and Zr, *Earth Planet. Sci. Lett.* 12 (1971) 339.
- J.A. Pearce and J.R. Cann, Tectonic setting of basic volcanic rocks determined using trace element analysis, *Earth Planet. Sci. Lett.* 19 (1973) 290.
- T.H. Pearce, H.E. Gorman and T.C. Birkett, The TiO_2 - K_2O - P_2O_5 diagram: a method of discriminating between oceanic and non-oceanic basalts, *Earth Planet. Sci. Lett.* 24 (1975) 419.
- P.A. Floyd and J.A. Winchester, Magma type and tectonic setting discrimination using immobile elements, *Earth Planet. Sci. Lett.* 27 (1975) 211.
- D.P. Mattey, I.L. Gibson, G.F. Marriner and R.N. Thompson, The diagnostic geochemistry, relative abundance and spatial distribution of high-calcium, low-alkali tholeiite dykes in the Lower Tertiary regional swarm of the Isle of Sky, N.W. Scotland, *Mineral. Mag.* 77 (1977) 273.

- 7 R.N. Thompson, J. Esson and A.C. Dunham, Major element variation in the Eocene lavas of the Isle of Skye, Scotland, *J. Petrol.* 13 (1972) 219.
- 8 I.M. Patterson, The Tertiary lava succession in the western part of the Antrim Plateau, *Proc. R. Ir. Acad., Sect. B*, 57 (1955) 155.
- 9 H. Lamacraft, The geochemistry of the Mull, Jura and Islay dyke swarms, M. Phil. Thesis, University of London (1977).
- 10 I.S.I. Carmichael, F.J. Turner and J. Verthogen, *Igneous Petrology* (McGraw-Hill, New York, N.Y., 1974) 739 pp.
- 11 R.J. Parker, Factors affecting the quality of major element rock analysis by X-ray fluorescence combined with fusion sample preparation, Tech. Rep. No. XRF-2II, Dep. of Geology, Imperial College, University of London (1977).
- 12 D.A. Wood, I.L. Gibson and R.N. Thompson, Elemental mobility during zeolite-facies metamorphism of the Tertiary basalts of eastern Iceland, *Contrib. Mineral. Petrol.* 55 (1976) 241.
- 13 E.B. Bailey, T.C. Clough, W.B. Wright, J.E. Riehey and G.V. Wilson, Tertiary and post-Tertiary geology of Mull, Loch Aline and Oban, *Mem. Geol. Surv. Scotl.* (1924).
- 14 R.N. Thompson, I.L. Gibson, G.F. Marriner, D.P. Matthey and M.A. Morrison, Trace element evidence of multistage mantle fusion and polybaric fractional crystallisation in the Paleocene lavas of Skye, N.W. Scotland, *Contrib. Mineral. Petrol.* (1978) in press.
- 15 H.S. Yoder and C.L. Tilley, Origin of basaltic magmas: an experimental study of natural and synthetic rock systems, *J. Petrol.* 3 (1962) 342.
- 16 G.P.L. Walker, The distribution of amygdale minerals in Mull and Morvern (Western Scotland), *West Connem. Volume* (1970) 181.
- 17 P. King, The secondary minerals of the Tertiary lavas of Northern and Central Skye - zeolite zonation patterns, their origin and formation. Unpublished Ph.D. Thesis, University of Aberdeen (1977).
- 18 H.P. Taylor Jr. and R.W. Forester, Low ^{18}O rocks from the intrusive complexes of Skye, Mull and Ardnamurchan, *J. Petrol.* 12 (1971) 465.
- 19 T.G. Vallance, Spilitic degradation of a tholeiite basalt, *J. Petrol.* 15 (1974) 79.
- 20 R.L. Smith and S.E. Smith, Comments on the use of Ti, Zr, Y, Sr, K, P and Nb in the classification of basaltic magmas, *Earth Planet. Sci. Lett.* 32 (1976) 114.
- 21 S.F. Humphris, M.A. Morrison and R.N. Thompson, Influence of rock crystallisation history upon subsequent lanthanide mobility during hydrothermal alteration of basalts, *Chem. Geol.* (1978) in press.
- 22 G.E. Sigvaldason, S. Steinthorsson, N. Oskarsson and P. Inslund, Compositional variation in recent Icelandic tholeiites and the Kverkfjöll hot spot, *Nature* 251 (1974) 579.
- 23 G.E. Sigvaldason, S. Steinthorsson, N. Oskarsson and P. Inslund, The simultaneous production of basalts, enriched and depleted in large ion lithophile (LIL) elements within the same fissure swarm in Iceland, *Bull. Soc. Geol. Fr.* 7 (1976) 863.
- 24 D.A. Wood, Spatial and temporal variation in the trace element geochemistry of the eastern Iceland flood basalt succession, *J. Geophys. Res.* 81 (1976) 1353.
- 25 J.D. Stuewing, K.O. Simonsen and I.G. Gies, Metabasalts from the Troodos massif, Cyprus, granitic high-alumina deduced from petrography and trace element geochemistry, *Contrib. Mineral. Petrol.* 51 (1975) 49.
- 26 M.F.J. Flower, P.T. Robinson, H.U. Schminke and W. Ohmacht, Deep-Sea Drilling Project, Leg 37: geochemical evidence for processes of crustal construction, *Bull. Soc. Géol. Fr.* 7 (1976) 819.
- 27 I.L. Gibson, G. Marriner, D.P. Matthey, R.N. Thompson and D.A. Wood, Is the extrusive portion of the oceanic crust vertically compositionally zoned?, *Bull. Géol. Soc. Fr.* 7 (1976) 897.
- 28 M.A. Morrison, Interactions between water and Paleocene basalt, Mull, N.W. Scotland, *Abstr. IASPEI/IAVCEI Meet., Durbam* (1977) 250.
- 29 R.N. Thompson, in: *Igneous Rocks of the British Isles*, D.S. Sutherland, ed. (John Wiley and Sons, New York, N.Y., 1979).
- 30 A.R. McBirney, K. Aoki and H. Williams, *Geology and Petrology of the Galapagos Islands*, *Geol. Soc. Am. Mem.* 118 (1969) 197 pp.
- 31 A.N. Baxter, Geochemistry and petrogenesis of primitive alkali basalts from Mauritius, Indian Ocean, *Geol. Soc. Am. Bull.* 87 (1976) 1028.
- 32 M.J. O'Hara, The bearing of phase equilibria studies in natural and synthetic systems on the evolution and origin of basic and ultrabasic rocks, *Earth-Sci. Rev.* 4 (1968) 69.
- 33 R.R. Schwarzer and J.J.W. Rogers, A world-wide comparison of alkali olivine basalts and their differentiation trends, *Earth Planet. Sci. Lett.* 23 (1974) 286.
- 34 W.Q. Kennedy, The parental magma of the British Tertiary Province, *Geol. Surv. G.B., Summary of Progress II* (1930) 61.
- 35 C.E. Tilley, Some aspects of magmatic evolution, *Q. J. Geol. Soc.* 106 (1950) 37.
- 36 L.R. Wager, A chemical definition of fractionation stages as a basis for comparison of Hawaiian, Hebridean and other basic lavas, *Geochim. Cosmochim. Acta* 9 (1956) 217.
- 37 N.C. Ghose, Composition and origin of Deccan basalts, *Lithos* 9 (1976) 65.
- 38 T.H. Pearce, B.E. Gorman and T.C. Birkett, The relationship between major element chemistry and tectonic environment of basic and intermediate volcanic rocks, *Earth Planet. Sci. Lett.* 36 (1977) 121.

INFLUENCE OF ROCK CRYSTALLISATION HISTORY UPON SUBSEQUENT LANTHANIDE MOBILITY DURING HYDROTHERMAL ALTERATION OF BASALTS*

SUSAN E. HUMPHRIS, M. ANN MORRISON and R.N. THOMPSON

Department of Geology, Imperial College of Science and Technology, London SW7 2BP (Great Britain)

(Accepted for publication March 7, 1978)

ABSTRACT

Humphris, S.E., Morrison, M.A. and Thompson, R.N., 1978. Influence of rock crystallisation history upon subsequent lanthanide mobility during hydrothermal alteration of basalts. *Chem. Geol.*, 23: 125–137.

Rare-earth element (REE) distributions in individual eruptive basaltic units from eastern Iceland, Mull and the Mid-Atlantic Ridge are presented in order to determine the mobility of these elements during hydrothermal alteration. The factors that cause the light REE (La, Ce and Nd) to be mobile in some cases and not in others are considered. It is postulated that the main control on potential lanthanide mobility is the igneous crystallisation history of the individual lavas, because this affects the sites of concentration, and hence availability, of the REE during hydrothermal alteration. The subsequent importance of the nature of the secondary minerals which form in determining which elements remain in the system is also discussed.

INTRODUCTION

The high geothermal gradients and permeabilities which characterise active eruptive centres provide ideal conditions for the circulation of hot fluids through fresh basalts. Such a process results in metamorphism of the lavas shortly after eruption, and the circulating solutions provide optimum conditions for element transport. Examples of interaction between basalts and hot fluids have been described from mid-ocean ridges (e.g., Miyashiro et al., 1971; Humphris and G. Thompson, 1978 a, b), ophiolites (e.g., Gass and Smewing, 1973; Spooner and Fyfe, 1973), fissure-erupted subaerial lava fields (e.g., Walker, 1970, 1974), and volcanoes (e.g., Fujishima and Fan, 1977). The mineral assemblages developed are, in most cases, typical of the

*Presented at Symposium V6 "New Concepts in Volcanology" of the IASPEI/IAVCEI Joint General Assemblies in Durham, August 15, 1977.

zeolite and greenschist metamorphic facies. Data from currently active geothermal areas indicate that alteration takes place at temperatures of up to about 300°C. (e.g., White and Sigvaldason, 1962; Brown and Ellis, 1970; Tomasson and Kristmannsdottir, 1972), which is consistent with the reaction temperatures obtained from metamorphosed oceanic rocks (Muehlenbachs and Clayton, 1972; Wenner and Taylor, 1973). The fluid/rock ratios in these geothermal systems are extremely variable (e.g., Mottl et al., 1975; Spooner et al., 1977 a, b), but intense hydration and carbonation of the rocks is generally observed.

In recent years, the chemical changes in basaltic rocks subjected to hydrothermal metamorphism have been much studied. Interest has focussed upon element mobility and its role in geochemical mass balances (e.g., Humphris and G. Thompson, 1978a) and ore genesis (e.g., Graf, 1977), and on attempts to decipher the pre-metamorphic chemistry of the basalts (e.g., Condie and Baragar, 1974). Certain elements, such as Ti, P, Zr, Hf, Nb, Ta and Y have been shown to be comparatively immobile, except during extreme metasomatism (e.g., Herrmann et al., 1974; Smith and Smith, 1976). Other elements, such as Li, K, Rb, Sr, Ba and U appear to be mobile (e.g., Vallance, 1974; Gunn and Roobol, 1976; Wood et al., 1976).

In this paper we concentrate on the rare-earth elements (REE) for which evidence of mobility during hydrothermal alteration is controversial (e.g., Herrmann and Wedepohl, 1970; Haskin et al., 1971; Frey et al., 1974; Tanaka, 1975; Ferrara et al., 1976; Menzies, 1976; Wood et al., 1976; Floyd, 1977; Hellman and Henderson, 1977). Using the published results of Wood et al. (1976) for eastern Iceland, and new data, obtained by the same method (Wood et al., 1976, p. 242), for Mid-Atlantic Ridge pillow basalts and Mull lavas, we shall compare the REE mobility in these three hydrothermal systems, and attempt to elucidate the reasons why the light REE (La, Ce and Nd) are mobile in some instances and not in others.

It is essential to emphasize that the three examples to be discussed are all concerned with chemical changes within *individual eruptive units* (flows or pillows) of basalt. Recent geochemical studies of unmetamorphosed basaltic suites, which are based on abundant analytical data, show considerable unit-by-unit diversity in chondrite-normalised REE pattern slopes (Sun and Hanson, 1975; O'Nions et al., 1976; Puchelt and Emmermann, 1977). It therefore seems improbable that attempts to study possible large-scale lanthanide mobility by comparing sets of analyses from unmetamorphosed and metamorphosed lava successions will be able to separate pyrogenic from subsequent variation.

EASTERN ICELAND

A 10 km thickness of predominantly basaltic flows is exposed in eastern Iceland. These have formed mainly by subaerial fissure eruptions during the separation of the European and North American lithospheric plates since approximately 14 Ma. The flows dip gently westwards and are cross-cut by

sub-horizontal zeolite facies metamorphic zones. Local greenschist hydrothermal aureoles surround several buried Tertiary centres of abundant acid/intermediate volcanism — analogues of the currently active central volcanoes in the Neovolcanic Zone (Walker, 1974). Wood et al. (1976) studied element mobility resulting from the zeolite facies regional metamorphism. They compared chemical variations across a post-glacial basalt on the Reykjanes peninsula, SW Iceland, with a zeolitised Tertiary flow from Reydarfjordur, eastern Iceland.

Reykjanes flow

This 4.5 m thick basalt flow lacks a soil cover and is therefore probably no more than a few hundred years old. It contains several percent of subhedral olivine, augite and plagioclase phenocrysts with variable distributions. The groundmass consists mainly of equant granular augite intergrown with plagioclase laths, sparse subhedral Fe—Ti oxides, and rare olivine. The abundant spaces between the groundmass grains are filled with pale brown glass, which contains numerous, indeterminate $< 2 \mu\text{m}$ opaque and translucent crystals.

Chemically, this lava is a typical Icelandic *hy*-normative olivine tholeiite with 7.6–8.0% MgO. A suite of twelve specimens from a vertical section through the flow revealed little variability for any elements (Wood et al., 1976, table 3). Moreover, such variation as was observed could be attributed entirely to varying concentrations of the three phenocryst phases. REE data are summarised in Fig. 1, which shows the chondrite-normalised patterns with the highest and lowest values of ΣREE and $(\text{Ce}/\text{Yb})_N$ ratios. It is apparent that the light rare-earth elements (LREE) display no greater variability than the heavy rare-earth elements (HREE).

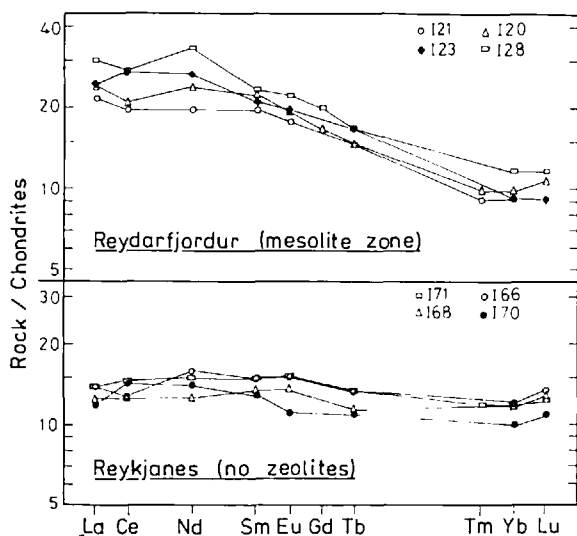


Fig. 1. Chondrite-normalised REE patterns for basalts from a Recent flow from the Reykjanes peninsula, and from a zeolitised flow, Reydarfjordur, eastern Iceland. (Data from Wood et al., 1976.)

Reydarfjordur flow

This 20.5 m thick basalt flow is about 12 Ma old. It lies within the meso-lite zeolite zone of Walker (1974) and contains this mineral, together with abundant stilbite, infilling prominent vesicles at the top and bottom of the flow. Zeolites and submicroscopic green and brown ferromagnesian minerals also fill the small vesicles throughout the lava and are disseminated within the rock. Sufficient of the pre-metamorphic mineralogy of the lava is preserved to see that it closely resembled the Reykjanes basalt petrographically. A few percent olivine, augite and plagioclase phenocrysts were present, with abundances varying little throughout the flow. The groundmass is rich in granular augite but the interstitial glass patches have all been converted to fine-grained assemblages of zeolites and hydrated ferromagnesian minerals.

The intensity of hydrothermal alteration depends on the original vesicularity of the lava. Thus it is greatest at the flow margins but also varies considerably in the interior. Zones with maximum alteration show, in addition to recrystallisation of the glass, complete replacement of olivine and incipient conversion of plagioclase to hydrous minerals. The augite, however, remains intact.

Chemically, this lava is a *hy*-normative olivine tholeiite with 6.0–7.2% MgO. Wood et al. (1976) compared the chemical variation of twelve samples from a vertical section through this flow with that of the Reykjanes lava. Variability greater than could be explained by phenocryst distribution or analytical error was recorded for Si, Mg, K, Rb, Sr and the LREE. As most of this variation occurred near the vesicular margins of the flow, Wood et al. (1976) attributed it to different elemental mobility during zeolite facies metamorphism. REE data, represented by the patterns with highest and lowest values of Σ REE and (Ce/Yb)_N ratios, are summarised in Fig. 1.

MULL, NW SCOTLAND

In Mull, Tertiary lavas reaching a thickness of up to 1850 m cover an area of about 840 km². The lower part of the pile consists mainly of basalts which are chemically and petrographically similar to the Skye Main Lava Series (R.N. Thompson et al., 1972; Morrison, 1978). They are transitional basalts that straddle the critical plane of silica saturation — the normative “join” olivine—clinopyroxene—plagioclase — and vary from nepheline to hypersthene normative varieties.

Two distinct types of alteration occur in the basalts. A hydrothermal aureole, consisting of an inner epidote and outer prehnite zone, surrounds the central intrusive complex in south and east Mull. Everywhere within this region, $\delta^{18}\text{O}$ whole-rock values decrease radially towards the intrusive complex (from about +5‰ to about -5‰) demonstrating that interaction with heated meteoric water has occurred at temperatures up to about 300°C (Forrester and Taylor, 1976). Outside the central aureole, flat-lying zeolite facies zones, that essentially parallel the base of the lava pile, occur.

Most of the basalts lie in the laumontite zone, only the top 200 m of which is exposed in Iceland (Walker, 1970). These Mull basalts have "normal" igneous $\delta^{18}\text{O}$ values (+9‰ to +5‰), indicating temperatures sufficiently low for the water to have $\delta^{18}\text{O}$ values required for isotopic equilibrium between plagioclase and water — between 100 and 150°C (Forrester and Taylor, 1976).

To estimate the metasomatic effects of these two types of alteration on the REE contents, two lava flows have been studied — one from the laumontite zone, and one from the epidote zone within the central aureole.

Zeolitised lava

This lava is exposed in a quarry in SW Mull and contains olivine, large poikilitic titanaugites, subpoikilitic titanomagnetites, chlorite, and zeolites. Rare apatites are enclosed in the pyroxenes. The secondary alteration is concentrated mainly at the base of the flow where an amygdaloidal layer lies immediately above the bole, and zeolite-filled vesicle pipes, up to 1 m in length, penetrate vertically into the flow. Petrographically, these can be seen to cause some serpentinisation of the olivine, partial replacement of plagioclase by hydrous minerals and the growth of small patches of chlorite and zeolites in the groundmass.

Little chemical change is seen across this flow, other than slight variations in Sr content and variable ferrous/ferric ratios. REE patterns for two examples are shown in Fig. 2. Sample *M53* is from the non-vesicular flow cen-

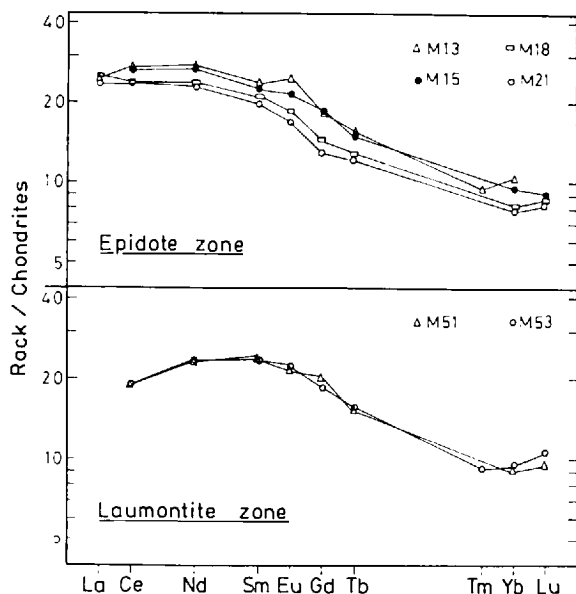


Fig. 2. Chondrite-normalised REE patterns for altered basalts from Mull. (*M53* and *M51* are from the zeolitised lava; *M13*, *M15*, *M18* and *M21* are from a flow in the epidote zone.)

tre, and *M51* is from the pipe vesicle zone. These two patterns are virtually indistinguishable.

Epidote zone

This lava flow is exposed in a quarry 3.5 km E of Salem, and shows a gradual transition for dark rock in the centre of the flow to green "spilitic" rock at the margin. Originally, it consisted of olivine phenocrysts in a matrix of olivine, plagioclase, titanomagnetite and poikilitic augite. In the dark centre of the flow, only olivine has broken down. This is pseudomorphed by chlorite and Fe-oxides, and the groundmass is rich in chlorite. As the margin of the flow is approached, plagioclase is albitised and growth of calcite and epidote occurs. Only at the margin of the flow is pyroxene broken down and an assemblage of chlorite, albite, quartz, carbonate, epidote, Fe-oxides, and amphibole has formed. Within this flow, Ti, Zr, Y, Nb and P preserve constant ratios, except at the margin where slight loss of P occurs (Morrison, 1978). This is accompanied by variations in Na₂O, K₂O, MgO, SiO₂, Rb, and Sr, and drastic leaching of CaO as the margin is approached.

Four REE patterns from the flow are shown in Fig. 2, and summarised data are given in Table I. Sample *M13* is from the green flow margin, and samples *M19*–*M21* are from the dark flow interior. The slopes of the patterns, as expressed by (Ce/Yb)_N, are constant, and there is no change in abundance of the LREE relative to the HREE, except in sample *M13*. There is, however, an apparent increase in total abundance of most of the REE progressively from the least altered to the most altered parts of the flow.

TABLE I

Selected rare-earth and trace element data from the altered lava flow in the epidote zone, Mull

Sample *	Ce (ppm)	Yb (ppm)	(Ce/Yb) _N	TiO ₂ (wt.%)	Y (ppm)
<i>M13</i>	23.64	2.29	2.63 ± 0.11	1.61	28
<i>M14</i>	22.53	2.01	2.86 ± 0.07	1.54	24
<i>M15</i>	23.28	2.08	2.83 ± 0.06	1.45	22
<i>M16</i>	22.56	1.99	2.87 ± 0.07	1.39	20
<i>M17</i>	19.93	1.71	2.95 ± 0.06	1.34	20
<i>M18</i>	19.96	1.73	2.92 ± 0.07	1.39	21
<i>M19</i>	20.20	1.69	3.02 ± 0.06	1.34	21
<i>M20</i>	20.23	1.88	2.72 ± 0.08	1.35	21
<i>M21</i>	20.25	1.71	3.00 ± 0.09	1.38	21
<i>M22</i>	19.51	1.80	2.76 ± 0.09	1.40	24

* Sample numbers increase progressively towards the dark flow interior (*M19*–*M21*). *M22* shows the beginning of changes approaching the lower margin, which lies below the quarry floor, as has been proved by drilling.

MID-ATLANTIC RIDGE BASALTS

The basalts analysed in this study were dredged from the median valley of the Mid-Atlantic Ridge at 22°S. The four samples discussed here are pillow basalts that show zoning due to partial greenschist facies metamorphism of the outer pillow margins during reaction with a circulating, seawater-derived fluid. The distinct zoning displayed by these rocks allowed portions of the altered rims and the relatively fresh interiors of the same pillows to be separated for analysis.

The mineralogy and the mineral conversions during alteration of these basalts have been extensively discussed previously (Humphris and G. Thompson, 1978a). The interiors of these pillows have the typical mineralogy and textures of oceanic tholeiites. Briefly, they are composed dominantly of glass (generally 60–70% by modal analysis) containing microphenocrysts and microlites of plagioclase (An_{60-70}), and rare olivine. Fe-oxides are extremely fine-grained and are scattered throughout the groundmass. The altered rims show the characteristic greenschist facies mineralogy of albite—actinolite—chlorite—epidote, with the dominant mineral being a ripidolitic chlorite (up to 60% by modal analysis). However, the outer rim of the most highly altered sample (*AII-42 1-96*) is composed dominantly of quartz and chlorite with no actinolite and only 15% modal albite. In all the samples, the glass is replaced by chlorite which is sometimes intergrown with actinolite. Chlorite also forms pseudomorphs after olivine, which are commonly associated with euhedral pyrite. The plagioclase is albitised and, in some cases, altered to chlorite. The vesicles are generally filled with chlorite although, in the more altered samples, they are lined with quartz and then subsequently filled with chlorite.

Considerable mobility of many of the major and trace elements during hydrothermal alteration has been observed (Humphris and G. Thompson, 1978a, b). In particular, Ca, Si, Cu, and Sr are leached from the rock, while Mg and H₂O are taken up. Mobilisation of Fe, Mn, B, Li, Ba, Ni, and Co is also indicated, but Ti, V, Y, Zr and Cr do not appear to be affected by hydrothermal alteration.

REE data for the fresh and altered zones of each pillow are summarised in Table II, and the chondrite-normalised patterns are shown in Fig. 3. Within the analytical error, the HREE display no variability during alteration. However, some small, but significant, variation is observed in the concentrations of the LREE. In particular, higher concentrations of La are observed in the altered zones of *AII-42 1-96*.

DISCUSSION

In discussing the variation in REE abundance within individual eruptive units, it is necessary to distinguish between *real* changes in concentration and *apparent* differences due to leaching or addition of other elements.

TABLE II

Selected rare-earth and trace element data from partially altered pillow basalts from the Mid-Atlantic Ridge (22° S).

Sample*	Ce (ppm)	Yb (ppm)	(Ce/Yb) _N	TiO ₂ (wt.%)	Y (ppm)
AII-42 1-96A	8.77	3.27	0.68 ± 0.03	1.40	35
	8.02	2.89	0.71 ± 0.03	1.33	30
	8.57	2.96	0.73 ± 0.02	1.26	39
AII-42 1-97A	10.47	3.53	0.76 ± 0.03	1.46	40
	9.58	3.34	0.73 ± 0.04	1.37	35
AII-42 1-108A	8.88	3.42	0.66 ± 0.04	1.98	45
	9.88	3.02	0.83 ± 0.04	1.43	39
AII-42 1-118A	8.61	3.21	0.68 ± 0.04	1.53	39
	8.60	2.91	0.75 ± 0.04	1.35	38

* A, B, C: zones from a single pillow basalt, from the altered rim (A) towards the relatively fresh interior (B or C).

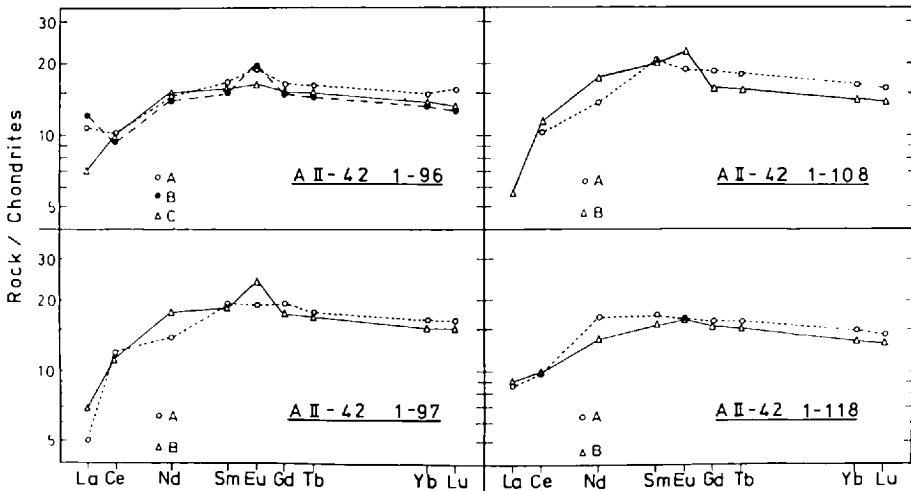


Fig. 3. Chondrite-normalised REE patterns for four partially hydrothermally altered pillow basalts from the Mid-Atlantic Ridge. [A, B, C: zones from a single pillow basalt, from the altered rim (A) towards the relatively fresh interior (B or C).]

Tables I and II illustrate the proportionality between the changes in REE abundances and those of other immobile elements. This suggests that the parallel shifts of the REE patterns that can be seen in Fig. 2, and of the HREE patterns in Fig. 3, can be ascribed to such leaching processes, which

will result in apparent enrichments of the immobile elements. However, taking this into account, we wish to emphasize that the maximum relative LREE movement recorded in the examples of hydrothermal metamorphism considered in this paper is small. This contrasts with the very large alterations to basaltic REE distributions postulated to occur during spilitisation by Hellman and Henderson (1977). Furthermore, it is apparent that the degree of mobility or immobility shown by the REE cannot be related to metamorphic grade.

Solution chemistry also seem unlikely to be the key to the problem. The three areas of study include interaction of basalt with either meteoric or seawater, and yet no obvious distinction in the REE behaviour that can be attributed to solution chemistry can be observed.

We postulate that the *main control on potential lanthanide mobility is the igneous crystallisation history of the individual lavas*, insofar as this affects the sites of concentration and relative distribution of the REE *before* subsequent metamorphism.

The Iceland and Mull lavas may first be contrasted. The presence of augite among the sparse phenocrysts in the Iceland basalts used in this study indicates that this phase precipitated at liquidus or near-liquidus temperatures. In a basalt devoid of hydrous minerals, all the early-crystallising phases — olivine, plagioclase, and pyroxene — have partition coefficients for the REE of <1.0 . Of these phases, augite has the highest partition coefficients [averaging 0.62 for Yb (Arth, 1976)] for the HREE, but low coefficients [averaging 0.15 (Arth, 1976)] for the LREE. An eastern Icelandic basalt crystallising abundant augite throughout its consolidation will therefore contain a residuum, chilled to glass, which is rich in total REE, and has a high LREE/HREE ratio. The two Icelandic basalts that we have discussed are both comparatively impoverished in P and Zr (Wood et al., 1976), so that the REE-rich phases, apatite and zircon, would, if at all, precipitate very late in their consolidation. We can find no apatite or zircon within the groundmass minerals or interstitial glass patches of these flows. The composition of the interstitial glass patches is, in most cases, rhyolitic (D.A. Wood, pers. commun., 1977) but they are too small to extract for REE analysis. O'Nions and Grönvold (1973) have, however, analysed several Recent Icelandic acid lavas and found them to have $(\text{Ce}/\text{Yb})_N$ from 3.2 to 7.4, compared with 0.9–1.9 for associated basalts. The phase in the eastern Icelandic basalts most readily attacked by circulating fluids during hydrothermal metamorphism is the interstitial glass; hence the preferential mobilisation of the LREE.

The zeolitised transitional basalts of Mull and Morvern never contain augite phenocrysts. It occurs only as a comparatively late-stage groundmass phase, usually in relatively large poikilitic crystals enclosing large numbers of small plagioclase subhedra. The restricted precipitation of augite during consolidation greatly reduces the potential of this phase to fractionate the REE in the residuum. Furthermore, the comparatively small number of large augite and occasional Ti-magnetite poikilocrysts in the groundmass of a

given volume of ophitic basalt leave fewer intergranular spaces where residual glass pools can collect than occur in a comparable volume of typical Icelandic basalt. Fresh glass is not uncommon in acid intrusions, basaltic hyaloclastites and dyke selvages in the Hebridean Province (e.g., Bailey et al., 1924). Nevertheless, we know of no examples of fresh interstitial glass within the transitional basalts, and from petrographic studies of the least metamorphosed basalts ($H_2O < 1.0\%$), it appears that these lavas were almost entirely holocrystalline. In the absence of abundant glass, the hydrothermal fluids attacked first the olivine and then the plagioclase; hence the REE immobility. In sample *M13* the breakdown of the poikilitic augite allowed alteration of the enclosed apatite, as is indicated by loss of P (Morrison, 1978), which results in a slight decrease in the LREE abundances.

In contrast to this, the oceanic pillow basalts discussed contain no augite and are composed of up to 80% glass with a very high glass/crystal ratio. The microphenocrysts are dominantly plagioclase, with rare olivine. In comparison with Iceland, this glass is therefore basaltic and will not have been relatively enriched in the LREE during its crystallisation history. Hydrothermal alteration of the pillow basalts has resulted in almost complete replacement of the original mineralogy, and hence any variation in the overall REE pattern will be dominantly controlled by the secondary mineralogy.

This leads into our final point which is that, although rock crystallisation history may largely control relative REE availability during hydrothermal metamorphism, the nature of the metamorphic minerals that form must also influence the extent to which the elements, once in solution, are reprecipitated nearby or pass out of the system. Wood et al. (1976) gave chemical data for thirteen minerals common in the amygdales of zeolite facies metamorphosed eastern Iceland lavas. They comprised nine zeolites, plus apophyllite, aragonite, celadonite, and chalcedony. Only the celadonite contained detectable La (>1.0 ppm) and even in this phase the REE were in concentrations too low to be measured accurately by the techniques available to these authors. In addition, one of us (M.A.M.) has attempted to measure the REE contents of Mull secondary calcite, but 2.5-day counts resulted in no resolvable peaks.

In contrast, there are suggestions in the literature that albite, epidote, and chlorite, which are all characteristic products of greenschist facies metamorphism, can affect the distribution of selected REE. The conditions under which alteration occurred may affect the distribution of Eu, since it is the only REE that will be stabilised in the divalent state if conditions are mildly reducing. The extent of alteration of the plagioclase may also affect the Eu abundance. Weill and Drake (1973) observed a positive correlation between the Eu concentration and the Ab content of the plagioclase. The Eu contents of the altered rims of the oceanic pillows show small variations relative to the interiors, some of which may be due to variations in the original distribution of plagioclase within the pillow. However, these rocks all contain pyrite, indicating that reducing conditions were prevalent at some time dur-

ing alteration, and this, together with the variable degree of albitisation of the plagioclase, may result in changes in the Eu content of the altered rims relative to the interiors. Similarly, the margin of the Mull flow from the epidote zone (sample *M13*), which is highly reduced, shows a small change in the Eu content.

Although not found in basaltic rocks, the existence of allanite indicates that LREE can enter the Ca^{2+} sites in members of the epidote group. The uptake of substantial amounts of La by adsorption has been described in Quaternary clay—chlorite mixtures of Norway (Roaldset and Rosenquist, 1971). There is a suggestion that this process may have operated during alteration of the ocean-floor basalts. The outer margin of sample *AII-42 1-96* contains the most chlorite (60%) and also shows enrichment of La relative to its concentration in the interior (Fig. 3). The REE abundances in chlorites from greenschist facies metabasalts are currently being investigated (M.A.M.).

ACKNOWLEDGEMENTS

We should like to thank Bedford College and particularly Dr. I. Gibson for making analytical facilities available to us, and Miss. G. Marriner for much helpful advice and assistance in the laboratory.

This work was funded by NERC grant number GR3/2946, and was reported at the IASPEI/IAVCEI Assembly in Durham, August 1977.

REFERENCES

- Arth, J.G., 1976. Behavior of trace elements during magmatic processes — a summary of theoretical models and their applications. *J. Res. U.S. Geol. Surv.*, 4: 41–47.
- Bailey, E.B., Clough, C.T., Wright, W.B., Richey, J.E. and Wilson, G.V., 1924. Tertiary and post-Tertiary geology of Mull, Loch Aline and Oban. *Mem. Geol. Surv. Scotl.*
- Brown, P.R.L. and Ellis, A.J., 1970. The Ohaki—Broadlands geothermal area, New Zealand: mineralogy and related geochemistry. *Am. J. Sci.*, 269: 97–131.
- Condie, K.C. and Baragar, W.R.A., 1974. Rare-earth element distributions in volcanic rocks from Archaean greenstone belts. *Contrib. Mineral. Petrol.*, 45: 237–246.
- Ferrara, G., Innocenti, F., Ricci, C.A. and Serri, G., 1976. Ocean-floor affinity of basalts from north Apennine ophiolites: geochemical evidence. *Chem. Geol.*, 17: 101–111.
- Floyd, P.A., 1977. Rare earth element mobility and geochemical characteristics of spilitic rocks. *Nature (London)*, 269: 134–137.
- Forrester, R.W. and Taylor, Jr., H.P., 1976. ^{18}O -depleted rocks from the Tertiary complex of the Isle of Mull, Scotland. *Earth Planet. Sci. Lett.*, 32: 11–17.
- Frey, F.A., Bryan, W.B. and Thompson, G., 1974. Atlantic ocean floor: geochemistry and petrology of basalts from Legs 2 and 3 of the Deep Sea Drilling Project. *J. Geophys. Res.*, 79: 5507–5527.
- Fujishima, K.Y. and Fan, P.-F., 1977. Hydrothermal mineralogy of Keolu Hills, Oahu, Hawaii. *Am. Mineral.*, 62: 574–582.
- Gass, I.G. and Smewing, J.D., 1973. Intrusion, extrusion and metamorphism at constructive margins: evidence from the Troodos Massif, Cyprus. *Nature (London)*, 242: 26–29.

- Graf, J.L., 1977. Rare earth elements as hydrothermal tracers during the formation of massive sulfide deposits in volcanic rocks. *Econ. Geol.*, 72: 527–548.
- Gunn, B.M. and Roobol, M.J., 1976. Metasomatic alteration of the predominantly island arc igneous suite of the Limestone Caribbees (E. Caribbean). *Geol. Rundsch.*, 65: 1078–1108.
- Haskin, L.A., Heinke, P.A., Paster, T.P. and Allen, R.O., 1971. Rare earths in meteoric, terrestrial and lunar matter. In: A.O. Brunfelt and E. Steinnes (Editors): *Activation Analysis in Geochemistry and Cosmochemistry*. Universitetsforlaget, Oslo, pp. 201–218.
- Hellman, P.L. and Henderson, P., 1977. Are rare earth elements mobile during spilitisation? *Nature (London)*, 267: 38–40.
- Herrmann, A.G. and Wedepohl, K.H., 1970. Untersuchungen an spilitischen gesteinen der Variskischen Geosynkline in Nordwestdeutschland. *Contrib. Mineral. Petrol.*, 29: 255–274.
- Herrmann, A.G., Potts, M.J. and Knake, D., 1974. Geochemistry of the rare earth elements in spilites from oceanic and continental crust. *Contrib. Mineral. Petrol.*, 44: 1–16.
- Humphris, S.E. and Thompson, G., 1978a. Hydrothermal alteration of oceanic basalts by seawater. *Geochim. Cosmochim. Acta*, 42: 107–125.
- Humphris, S.E. and Thompson, G., 1978b. Trace element mobility during hydrothermal alteration of oceanic basalts. *Geochim. Cosmochim. Acta*, 42: 127–136.
- Menzies, M., 1976. Rifting of a Tethyan continent — rare earth evidence of an accreting plate margin. *Earth Planet. Sci. Lett.*, 28: 427–438.
- Miyashiro, A., Shido, F. and Ewing, M., 1971. Metamorphism on the Mid-Atlantic Ridge near 24 and 30° N. *Philos. Trans. R. Soc. London, Ser. A*, 268: 589–603.
- Morrison, M.A., 1978. The use of “immobile” trace elements to distinguish palaeotectonic affinities of metabasalts: applications to the Paleocene basalts of Mull and Skye, north-west Scotland. *Earth Planet. Sci. Lett.*, 39: 407–416.
- Mottl, M.J., Corr, R. and Holland, H.D., 1975. Trace element content of the Reykjanes and Svartsengi thermal brines, Iceland. *Geol. Soc. Am., Progr. Abstr.*, 7: 1206 (abstract).
- Muehlenbachs, K. and Clayton, R., 1972. Oxygen isotope geochemistry of submarine greenstones, Mid-Atlantic Ridge. *Can. J. Earth Sci.*, 9: 471–478.
- O’Nions, R.K. and Grönvold, K., 1973. Petrogenetic relationships of acid and basic rocks in Iceland: Sr-isotopes and rare earth elements in Late and Postglacial volcanics. *Earth Planet. Sci. Lett.*, 19: 397–409.
- O’Nions, R.K., Pankhurst, R.J. and Grönvold, K., 1976. Nature and development of basalt magma sources beneath Iceland and the Reykjanes Ridge. *J. Petrol.*, 17: 315–338.
- Puchelt, H. and Emmermann, R., 1977. REE characteristics of ocean floor basalts from the Mid-Atlantic Ridge 37° N (Leg 37 DSDP). *Contrib. Mineral. Petrol.*, 62: 43–52.
- Roadset, E. and Rosenquist, I. Th., 1971. Unusual lanthanide distribution. *Nature (London)*, *Phys. Sci.*, 231: 153–154.
- Smith, R.E. and Smith, S.E., 1976. Comments on the use of Ti, Zr, Y, Sr, K, P and Nb in classification of basaltic magmas. *Earth Planet. Sci. Lett.*, 32: 114–125.
- Spooner, E.T.C. and Fyfe, W.S., 1973. Sub-sea floor metamorphism, heat and mass transfer. *Contrib. Mineral. Petrol.*, 42: 287–304.
- Spooner, E.T.C., Chapman, H.J. and Smewing, J.D., 1977a. Sr-isotopic contamination and oxidation during ocean floor hydrothermal metamorphism of the ophiolitic rocks from the Troodos Massif, Cyprus. *Geochim. Cosmochim. Acta*, 41: 873–890.
- Spooner, E.T.C., Beckinsale, R.D., England, P.C. and Senior, A., 1977b. Hydration, ¹⁸O enrichment and oxidation during ocean floor hydrothermal metamorphism of ophiolitic metabasic rocks from E. Liguria, Italy. *Geochim. Cosmochim. Acta*, 41: 857–871.

- Sun, S.S. and Hanson, G.N., 1975. Origin of Ross Island basanitoids and limitations upon the heterogeneity of mantle sources for alkali basalts and nephelinites. *Contrib. Mineral. Petrol.*, 52: 77–106.
- Tanaka, T., 1975. Geological significance of rare earth elements in Japanese geosynclinal basalts. *Contrib. Mineral. Petrol.*, 52: 233–246.
- Thompson, R.N., Esson, J. and Dunham, A.C., 1972. Major element variation in the Eocene lavas of the Isle of Skye, Scotland. *J. Petrol.*, 13: 219–253.
- Tomasson, J. and Kristmannsdottir, H., 1972. High temperature alteration minerals and thermal brines, Reykjanes, Iceland. *Contrib. Mineral. Petrol.*, 36: 123–134.
- Vallance, T.G., 1974. Spilitic degradation of a tholeiitic basalt. *J. Petrol.*, 15: 79–96.
- Walker, G.P.L., 1970. The distribution of amygdale minerals in Mull and Morvern (western Scotland). *West Commem. Vol.*, pp. 181–194.
- Walker, G.P.L., 1974. The structure of Eastern Iceland. In: L. Kristjansson (Editor): *Geodynamics of Iceland and the North Atlantic Area*. D. Reidel, Dordrecht, pp. 177–188.
- Weill, D.F. and Drake, M.J., 1973. Europium anomaly in plagioclase feldspar: experimental results and semi-quantitative model. *Science*, 180: 1059–1060.
- Wenner, D.B. and Taylor, H.P., 1973. Oxygen and hydrogen isotope studies of the serpentinisation of ultramafic rocks in oceanic environments and continental ophiolite complexes. *Am. J. Sci.*, 273: 207–239.
- White, D.E. and Sigvaldason, G.E., 1962. Epidote in hot-spring systems, and depth of formation of propylitic epidote in epithermal ore deposits. *U.S. Geol. Surv., Prof. Pap.*, 450-E: 80–84.
- Wood, D.A., Gibson, I.L. and Thompson, R.N., 1976. Elemental mobility during zeolite facies metamorphism of the Tertiary basalts of eastern Iceland. *Contrib. Mineral. Petrol.*, 55: 241–254.

A reduction in $^{87}\text{Sr}/^{86}\text{Sr}$ during basalt alteration

HYDROTHERMAL alteration of basalts on the ocean floor has been reported to cause a general increase in the $^{87}\text{Sr}/^{86}\text{Sr}$ ratio of the basalts^{1,2}. Results are presented here from Mull in the British Tertiary province which suggest strongly that hydrothermal alteration in such discrete magmatic centres may actually cause a reduction in the $^{87}\text{Sr}/^{86}\text{Sr}$ ratios of some basalts. Preliminary data indicate that the $^{143}\text{Nd}/^{144}\text{Nd}$ ratios are unaffected.

Oxygen isotope studies^{3,4} of Tertiary igneous rocks from Skye, Mull and Ardnamurchan have demonstrated that large scale hydrothermal systems were established in these areas at the time of igneous intrusion. On both Skye and Mull hydrothermal aureoles extend for up to 6 km from the central intrusive complexes into the surrounding basalts. Within these regions greenschist-facies mineral assemblages have been formed and the rocks are depleted in ^{18}O due to interaction with hot meteoric waters.

The samples selected for this study are from a quarry 3.5 km east of Salen, which lies within the epidote zone of the central aureole on Mull. A hydrothermally altered lava flow is exposed which shows a gradual transition from dark basalt in the massive flow interior to green 'spilitic' material at the margin. In the centre of the flow only olivine has broken down; it is pseudomorphed by chlorite and oxides and the groundmass is rich in chlorite. With increasing alteration plagioclase and the titanomagnetites are replaced by albite, sphene, and calcite and/or epidote. Only at the margin of the flow is pyroxene completely broken down (Fig. 1) and an assemblage of chlorite, albite, quartz, amphibole, epidote, and sphene occurs in which none of the original mineralogy is preserved. Within this flow Al, Ti, Zr, Nb, Y, P, and the rare earth elements preserve almost constant ratios except at the margin where slight loss of P and the light rare earths (La, Ce) is observed⁵⁻⁷. This is accompanied by variations in the other major and trace elements; particularly, drastic leaching of Ca. Sr isotope analyses were carried out on 10 whole rock samples across the lava flow and on leached pyroxene separated from the flow centre. A secondary mineral pod consisting of zeolite, calcite, and albite surrounded by

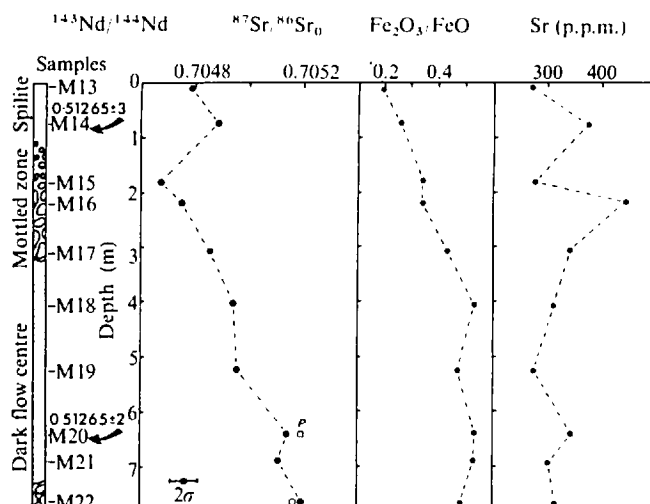


Fig. 1 Variations in $^{87}\text{Sr}/^{86}\text{Sr}_0$, $\text{Fe}_2\text{O}_3/\text{FeO}$, and Sr p.p.m. across 7.5 m of an individual lava flow, near Salen, Mull. The degree of hydrothermal alteration is illustrated and M22 shows the onset of increased alteration approaching the base of the flow. Open symbols denote samples leached in 6M HCl; □, pyroxene; ○, whole rock.

chlorite which formed immediately above the base of the overlying lava flow, and two discordant veins were also analysed to determine the $^{87}\text{Sr}/^{86}\text{Sr}$ ratio of at least some of the hydrothermal fluids.

The results are presented in Table 1. Within the lava flow the age-corrected initial $^{87}\text{Sr}/^{86}\text{Sr}$ ratios range from 0.70467 near the top of the flow to 0.70519 at the base of the sampled section (Fig. 1). The decrease in $^{87}\text{Sr}/^{86}\text{Sr}$ towards the top of the flow is accompanied by an increase in the degree of visible alteration and a decrease in $\text{Fe}^{3+}/\text{Fe}^{2+}$. Sr contents range between 270 and 440 p.p.m. in the more altered samples but seem to be much less variable near the centre of the flow.

$^{143}\text{Nd}/^{144}\text{Nd}$ ratios were determined on two samples using the technique described in ref. 8. The two samples show very

Table 1 Rb-Sr results

Sample	Lithology/mineralogy	Rb*	Sr*	Rb/Sr	$^{87}\text{Sr}/^{86}\text{Sr} \dagger$	$(^{87}\text{Sr}/^{86}\text{Sr})_0 \ddagger$
M13	Altered basalt, chl-plag-qtz-sph	7.17	271	0.026	0.70486 ± 3	0.70479
M14	Altered basalt, some relict cpx	1.76	375	0.005	0.70489 ± 3	0.70488
M15	Altered basalt, increasing growth of secondary minerals	2.51	279	0.009	0.70469 ± 3	0.70467
M16	16-19% relict cpx	11.8	443	0.027	0.70482 ± 3	0.70475
M17	Similar to M15, M16	14.5	338	0.043	0.70496 ± 3	0.70485
M18	Less altered basalt; mainly chl pseudomorphs after ol	15.4	310	0.050	0.70506 ± 4 (0.70519 ± 2)	0.70494
M19	Some growth of sphene and albite	11.6	274	0.042	0.70505 ± 5 (0.70514 ± 4)	0.70495
M20	Similar to M18	2.62	340	0.008	0.70515 ± 2 (0.70525 ± 6)	0.70513
M20	Pyroxene	(0.26)	(51.9)	(0.005)	(0.70520 ± 2)	(0.70519)
M21	Similar to M18	9.08	299	0.030	0.70519 ± 3	0.70511
M22	Similar to M15, M16	14.6 (11.6)	311 (129)	0.047 (0.090)	0.70531 ± 3 (0.70538 ± 4)	0.70519 (0.70516)
M24	Calcite and laumontite vein	2*	169*	0.012	0.70521 ± 6	0.70519
M64	Laumontite vein	2*	359*	0.006	0.70467 ± 3	0.70466
M65	Altered basalt adjacent to M64				0.70505 ± 4	
M75A	Alteration pod: chl-laumontite-cc				0.70421 ± 6	
M75B	Alteration pod: cc, laumontite				0.70427 ± 4	

Rb and Sr contents determined by isotope dilution (±1%) unless postscripted* which denotes XRF analysis. chl, chlorite; plag, plagioclase; qtz, quartz; sph, shene; cpx, clinopyroxene; cc, calcereous; ol, olivine.

† present day $^{87}\text{Sr}/^{86}\text{Sr}$ ratio ± 2 s.e.m. E-A = 0.70807 ± 3 and NBS 987 = 0.71029 ± 3 during this study.

‡ Initial Sr composition calculated assuming an age of 60 Myr and $\lambda = 1.39 \times 10^{-11} \text{ yr}^{-1}$ for ^{87}Rb decay.

Results in brackets indicate that they were determined on samples which had been leached in 6M HCl (see text).

different degrees of alteration but in sharp contrast to their variable $^{87}\text{Sr}/^{86}\text{Sr}$ ratios (Fig. 1) their Nd compositions are indistinguishable analytically (M14, 0.51265 ± 3 ; M20, 0.51265 ± 2 ; 2σ errors).

To investigate further the Sr isotope geochemistry, pyroxene was separated from M20 and it and some whole rock powders were subjected to leaching experiments. Leaching was carried out with 6M HCl in sealed Teflon bombs for 14 h at 130°C (ref. 9). X-ray analysis of the whole rock powders before and after leaching showed a marked increase in the concentration of pyroxene and to a lesser extent plagioclase, due to the dissolution of secondary minerals such as chlorite. Analysis of the residue after leaching should therefore provide $^{87}\text{Sr}/^{86}\text{Sr}$ ratios close to the pre-alteration composition of the lava flow.

The pyroxene has an age-corrected initial $^{87}\text{Sr}/^{86}\text{Sr}$ ratio of 0.70519 while that of the leached whole rock sample M22 is 0.70516 (Fig. 1). Rb and Sr concentrations for the leached residues from M18, M19, and M20 are not available but they all have significantly higher present-day $^{87}\text{Sr}/^{86}\text{Sr}$ ratios than the unleached samples. This indicates that the altered material tends to have lower $^{87}\text{Sr}/^{86}\text{Sr}$ ratios than the fresh basalts.

The leaching experiments and the observed decrease of $^{87}\text{Sr}/^{86}\text{Sr}$ with increasing bulk rock alteration and decreasing $\text{Fe}^{3+}/\text{Fe}^{2+}$ (Fig. 1), all suggest that hydrothermal alteration of this lava flow resulted in a general reduction in $^{87}\text{Sr}/^{86}\text{Sr}$. The composition of the separated leached pyroxene provides the best estimate of the primary composition of the magma (~ 0.7052). The two $^{143}\text{Nd}/^{144}\text{Nd}$ results, however, indicate that the lava was isotopically homogeneous when it crystallised, and that Nd was not affected significantly by the hydrothermal alteration (see also ref. 7).

Evidence that the fluids responsible for the hydrothermal alteration did have low $^{87}\text{Sr}/^{86}\text{Sr}$ ratios is provided by the results on secondary minerals (Table 1). The secondary pod from the overlying flow gave values of 0.70421 and 0.70427. The two vein samples M64 and M24 which cut the flow and therefore represent later stage fluids have $^{87}\text{Sr}/^{86}\text{Sr}$ ratios of 0.70467 and 0.70521. This may also indicate a rise in the value of the $^{87}\text{Sr}/^{86}\text{Sr}$ ratio of the fluids with time at this locality.

Forester and Taylor⁴ have suggested that the alteration within the hydrothermal aureole on Mull was caused by interaction with fluids having $\delta^{18}\text{O}$ values of about -11 to -12 . Such depleted oxygen compositions are suggestive of meteoric water in high latitudes, but at least in the area of this study the fluids are also apparently characterised by low $^{87}\text{Sr}/^{86}\text{Sr}$ ratios (< 0.7048). This clearly rules out interaction with Moian basement¹⁰, or Tertiary intrusives such as the Glen Cannel and Loch Usig

granophyres which have initial $^{87}\text{Sr}/^{86}\text{Sr}$ ratios of 0.7094 ± 3 and $0.7135-0.7162$ (refs 11 and 10) respectively. Sources of the unradiogenic Sr in the fluids are either unconfirmed but possible granulite facies basement, or, much more likely, the basalts themselves.

We envisage that interaction of meteoric water with hot volcanic rocks caused the chemistry of the resultant fluids to be buffered by that of the basalts. As 70% of the fresh volcanic rocks from Mull analysed by Beckinsale *et al.*¹¹ have $^{87}\text{Sr}/^{86}\text{Sr}$ ratios < 0.7043 , the fluids in this area are likely to have similar $^{87}\text{Sr}/^{86}\text{Sr}$ ratios. Their interaction with basalt of Sr composition 0.7052 will therefore result in a reduction in $^{87}\text{Sr}/^{86}\text{Sr}$ in the more altered material (see Fig. 1). Moreover as no systematic variation in Sr content in the altered rocks was observed (Fig. 1) it seems that Sr isotope exchange took place without net addition or removal of Sr. Finally these results may provide some constraints on our models for the size of water circulation 'cells'. They suggest that the Sr composition of the fluids in this area was not affected significantly by interaction with either 'old' basement (perhaps 0.5 km beneath the present erosion surface) or Tertiary intrusive rocks which crop out only 1.5 km to the south.

Isotope research at Leeds is funded by NERC. We thank the NERC for research fellowships and NERC studentships during this work, and J. Kramers for his review of this article.

C. J. HAWKESWORTH

*Department of Earth Sciences,
Leeds University,
Leeds, UK*

M. A. MORRISON

*Department of Geology,
Imperial College,
Prince Consort Road,
London SW7, UK*

Received 24 August; accepted 3 October 1978.

1. Hart, S. R., Erlank, A. J. & Kable, E. J. D. *Contr. Miner. Petrol.* **44**, 219-230 (1974).
2. O'Nions, R. K., Carter, S. R., Cohen, R. S., Evenson, N. M. & Hamilton, P. J. *Nature* **273**, 435-438 (1978).
3. Forester, R. W. & Taylor, H. P. *Am. J. Sci.* **277**, 136-177 (1977).
4. Forester, R. W. & Taylor, H. P. *Earth planet. Sci. Lett.* **32**, 11-17 (1976).
5. Morrison, M. A. *Earth planet. Sci. Lett.* **39**, 407-416 (1978).
6. Morrison, M. A. thesis Univ. London (1978).
7. Humphris, S. E., Morrison, M. A. & Thompson, R. N. *Chem. Geol.* **23**, 125-137 (1978).
8. Hawkesworth, C. J. *et al. Earth planet. Sci. Lett.* (in the press).
9. O'Nions, R. K. & Pankhurst, R. J. *Earth planet. Sci. Lett.* **31**, 255-261 (1976).
10. Pankhurst, R. J., Walsh, J. N., Beckinsale, R. D. & Skelhorn, R. R. *Earth planet. Sci. Lett.* **38**, 355-363 (1978).
11. Beckinsale, R. D., Pankhurst, R. J., Skelhorn, R. R. & Walsh, J. N. *Contr. Mineral. Petrol.* **66**, 415-428 (1978).